

Technical Report Documentation Page

1. Report No. 1993-1 FHWA/TX-03/1993-1 (Volume 1)		2. Government Accession No.		3. Recipient's Catalog No.	
4. Title and Subtitle AN ANALYSIS OF THE MECHANISMS AND EFFICACY OF THREE LIQUID CHEMICAL SOIL STABILIZERS: VOLUME 1				5. Report Date May 2003	
7. Author(s) Alan F. Rauch, Lynn E. Katz, and Howard M. Liljestrand				6. Performing Organization Code	
9. Performing Organization Name and Address Center for Transportation Research The University of Texas at Austin 3208 Red River, Suite 200 Austin, TX 78705-2650				8. Performing Organization Report No. 1993-1	
				10. Work Unit No. (TRAIS)	
12. Sponsoring Agency Name and Address Texas Department of Transportation Research and Technology Implementation Office P.O. Box 5080 Austin, TX 78763-5080				11. Contract or Grant No. Research Project 7-1993	
				13. Type of Report and Period Covered Research Report	
				14. Sponsoring Agency Code	
15. Supplementary Notes Project conducted in cooperation with the Texas Department of Transportation and the U.S. Department of Transportation, Federal Highway Administration.					
16. Abstract Liquid chemical products are marketed by a number of companies for stabilizing pavement base and subgrade soils. If effective, these products could be used as alternatives for treating sulfate-rich soils, which are susceptible to excessive heaving when treated with traditional, calcium-based stabilizers like lime, cement, and fly ash. However, the chemical composition, stabilizing mechanisms, and performance of these liquid products are not well understood. The primary objective of this study was to investigate and identify the mechanisms by which clay soils are modified or altered by these liquid chemical agents. Three representative, commercial products were selected for study: an ionic product, an enzyme product, and a polymer product. The chemical composition of each was characterized using standard chemical test methods. The three products were then reacted with three reference clays (kaolinite, illite, and montmorillonite) and several native Texas soils. In the "micro-characterization" study, the mechanisms of soil modification at the particle level were studied using physical-chemical analyses of untreated and treated soil samples. Very high product application rates were used so that possible soil modifications could be observed. In a paired "macro-characterization" study, standard geotechnical laboratory tests were performed on untreated and treated compacted soil specimens. The products were mixed at the suppliers' recommended application rates and at ten times the recommended application rates. These tests failed to show significant, consistent changes in the engineering properties of the test soils following treatment with the three selected products at the application rates used. The findings of this study clearly point to the need to conduct standard laboratory tests, prior to specifying the use of these products in field applications, to prove the effectiveness of the treatment on a particular soil type at a given chemical application rate.					
17. Key Words soil stabilization, soil modification, liquid stabilizers, nontraditional soil stabilizers, high-sulfate soils			18. Distribution Statement No restrictions. This document is available to the public through the National Technical Information Service, Springfield, Virginia 22161.		
19. Security Classif. (of report) Unclassified	20. Security Classif. (of this page) Unclassified		21. No. of pages 204	22. Price	

An Analysis of the Mechanisms and Efficacy of Three Liquid Chemical Soil Stabilizers

Volume 1

Alan F. Rauch
Lynn E. Katz
Howard M. Liljestrand

Research Report 1993-1

Research Project 7-1993
Evaluation of Nontraditional Soil and Aggregate Stabilizers

Conducted for the
Texas Department of Transportation
in cooperation with the
U.S. Department Of Transportation
Federal Highway Administration
by the
Center for Transportation Research
Bureau of Engineering Research
The University of Texas at Austin

May 2003

Disclaimers

The contents of this report reflect the views of the authors, who are responsible for the facts and the accuracy of the data presented herein. The contents do not necessarily reflect the official views or policies of the Federal Highway Administration or the Texas Department of Transportation. This report does not constitute a standard, specification, or regulation.

There was no invention or discovery conceived or first actually reduced to practice in the course of or under this contract, including any art, method, process, machine, manufacture, design or composition of matter, or any new and useful improvement thereof, or any variety of plant, which is or may be patentable under the patent laws of the United States of America or any foreign country.

NOT INTENDED FOR CONSTRUCTION,
BIDDING, OR PERMIT PURPOSES

Alan F. Rauch
Research Supervisor

Acknowledgments

The researchers acknowledge the assistance provided by following TxDOT personnel: Joe Thompson (DAL, program coordinator), John Rantz (LBB, program coordinator), Moon Won (CST, project director), Darren Hazlett (CST, project director), Harold Albers (CST, project monitoring committee), Tom Yarbrough (CST), and Kenneth Cline (Smith County, project monitoring committee).

The hard work and dedication of the following graduate research assistants at the University of Texas at Austin is also acknowledged: Jacqueline S. Harmon, Kristine S. Shaw, John A. Thomas, and Adriano Vieira. Undergraduate research assistants included Lee Austin and Michael Welfel. Additional thanks go to Nadine Gordon, Kitty Milliken, Jeffrey Cook Michael Schmerling, and John Swinnea for their assistance in conducting various tests for this study.

Research performed in cooperation with the Texas Department of Transportation and the U.S. Department of Transportation, Federal Highway Administration.

Table of Contents

Volume 1

List of Tables	xiii
List of Figures	xvii
Chapter 1. Background and Project Objectives	1
1.1. Overview	1
1.2. Liquid Soil Stabilizers	1
1.3. Project Objectives and Work Plan	4
1.4. Report Organization	6
Chapter 2. Selection of Test Materials	7
2.1. Liquid Stabilizer Products	7
2.2. Product Application Rates	8
2.3. Test Soils	9
2.4. Reference Clays	10
2.5. Native Texas Soils	11
Chapter 3. Chemical Characterization of Principal Product Constituents	15
3.1. Overview	15
3.2. Review of Manufacturers' Literature	15
3.3. Chemical Characterization Methods	16
3.4. Characterization of The Ionic Stabilizer	21
3.5. Characterization of The Polymer Stabilizer	25
3.6. Characterization of The Enzyme Stabilizer	26
Chapter 4. Methods for Micro-Characterization of Stabilizer Mechanisms	43
4.1. Overview	43
4.2. Preparation of Clay Materials	43
4.3. Clay Mineral Characterization Procedures	44
4.4. Clay Mineral/Stabilizer Characterization Procedures	49
Chapter 5. Methods for Macro-Characterization of Stabilizer Effectiveness	53
5.1. Introduction	53
5.2. Preparation of Soil Test Specimens	53
5.3. Sample Preparation Protocol	54
5.4. Measurement of Grain Size Distribution	59
5.5. Measurement of Atterberg Limits	60
5.6. Measurement of Compaction Characteristics	60
5.7. Measurement of Undrained Shear Strength	61
5.8. Measurement of Free Swell Potential	63

Chapter 6. Ionic Stabilizer: Results from Study of Stabilizer Mechanisms	69
6.1. Overview	69
6.2. Results of Stabilizer/Clay Experiments Conducted in the Range of the Manufacturer's Suggested Application Ratios.....	69
6.3. Overview of Tests at High Application Rates.....	71
6.4. XRD Results of Treated and Untreated Clay and Soil Samples	72
6.5. BET Analysis of Treated and Untreated Clay and Soil Samples.....	73
6.6. ESEM and SEM/EDS Analyses of Treated and Untreated Clay and Soil Samples.....	74
6.7. CEC Analysis of Treated and Untreated Montmorillonite.....	77
6.8. Summary.....	77
Chapter 7. Ionic Stabilizer: Results from Study of Stabilizer Effectiveness	101
7.1. Overview.....	101
7.2. Effect of the Ionic Stabilizer on Atterberg Limits	101
7.3. Effect of the Ionic Stabilizer on Compacted Density	101
7.4. Effect of the Ionic Stabilizer on Shear Strength	102
7.5. Effect of the Ionic Stabilizer on Swell Potential.....	102
Chapter 8. Enzyme Stabilizer: Results from Study of Stabilizer Mechanisms.....	109
8.1. Overview	109
8.2. XRD Results of Treated and Untreated Clay and Soil Samples	109
8.3. BET Analysis of Treated and Untreated Clay and Soil Samples.....	110
8.4. ESEM and SEM/EDS Analyses of Treated and Untreated Clay and Soil Samples.....	111
8.5. CEC Analysis of Treated and Untreated Montmorillonite.....	111
8.6. Summary.....	111
Chapter 9. Enzyme Stabilizer: Results from Study of Stabilizer Effectiveness	123
9.1. Overview.....	123
9.2. Effect of the Enzyme Stabilizer on Atterberg Limits	123
9.3. Effect of the Enzyme Stabilizer on Compacted Density	123
9.4. Effect of the Enzyme Stabilizer on Shear Strength	124
9.5. Effect of the Enzyme Stabilizer on Swell Potential.....	124
Chapter 10. Polymer Stabilizer: Results from Study of Stabilizer Mechanisms.....	131
10.1. Overview.....	131
10.2. XRD Results of Treated and Untreated Clay and Soil Samples.....	131
10.3. BET Analysis of Treated and Untreated Clay and Soil Samples	131
10.4. ESEM and SEM/EDS Analyses of Treated and Untreated Clay and Soil Samples.....	132
10.5. CEC Analysis of Treated and Untreated Montmorillonite	132
10.6. Summary	132
Chapter 11. Polymer Stabilizer: Results from Study of Stabilizer Effectiveness	145

11.1. Overview.....	145
11.2. Effect of the Polymer Stabilizer on Atterberg Limits.....	145
11.3. Effect of the Polymer Stabilizer on Compacted Density.....	146
11.4. Effect of the Polymer Stabilizer on Shear Strength.....	146
11.5. Effect of the Polymer Stabilizer on Swell Potential	146
Chapter 12. Follow-up Study: Effectiveness of Stabilizers at High Application Rates.....	153
12.1. Overview.....	153
12.2. Test Soils.....	153
12.3. Product Application Rates	154
12.4. Treatment with Hydrated Lime.....	154
12.5. Preparation of Test Specimens	155
12.6. Stabilizer Effects on Atterberg Limits	157
12.7. Stabilizer Effects on Compaction Characteristics	157
12.8. Stabilizer Effects on Shear Strength	158
12.9. Stabilizer Effects on Swell Potential	159
Chapter 13. Summary and Conclusions	171
13.1. Overview of Study	171
13.2. Micro-Characterization of Stabilizer Mechanisms.....	172
13.3. Macro-Characterization of Stabilizer Efficacy	173
Chapter 14. Recommendations.....	175
References.....	177

Volume 2

Appendix A. Supplier Recommended Field Application Rates.....	A-1
Appendix B. Results from Tests to Characterize Chemical Composition of Stabilizer Products	A-5
Appendix C. BET Pore Size Distribution Comparisons	A-11
Appendix D. ESEM Images	A-13
Appendix D.1. ESEM images of kaolinite.....	A-15
Appendix D.2. ESEM images of illite	A-23
Appendix D.3. ESEM images of sodium montmorillonite.....	A-31
Appendix D.4. ESEM images of Bryan soil	A-39
Appendix D.5. ESEM images of Mesquite soil.....	A-46

Appendix E. SEM/EDS Results	A-53
Appendix E.1. SEM/EDS images of kaolinite.....	A-55
Appendix E.2. SEM/EDS images of illite	A-63
Appendix E.3. SEM/EDS images of sodium montmorillonite	A-71
Appendix E.4. SEM/EDS images of Bryan soil	A-79
Appendix E.5. SEM/EDS images of Mesquite soil	A-84
Appendix E.6. SEM/EDS spectra of kaolinite.....	A-91
Appendix E.7. SEM/EDS spectra of illite	A-142
Appendix E.8. SEM/EDS spectra of sodium montmorillonite	A-202
Appendix E.9. SEM/EDS spectra of Bryan soil	A-259
Appendix E.10. SEM/EDS spectra of Mesquite soil	A-298
 Appendix F. Raw Data for pH, Conductivity, Total Organic Carbon (TOC), UV/Vis Spectroscopy, Potentiometric Titrations, and Mass Spectrometry	 A-343
 Appendix G. XRD Results for Oriented and Glycolated Samples.....	 A-369
 Appendix H. Results from Hydrometer Analysis of Grain Size Distributions of Bulk Test Soils.....	 A-373
 Appendix I. Measured Atterberg Limits of Untreated and Treated Bulk Test Soils	 A-377
 Appendix J. Results from Compaction Tests on Untreated Bulk Test Soils	 A-381
 Appendix K. Index Properties of Triaxial and Free Swell Bulk Test Specimens	 A-385
 Appendix L. Results from Unconsolidated-Undrained Triaxial Compression Tests on Untreated and Treated Bulk Test Soils.....	 A-391
 Appendix M. Shear Strength Envelopes Fit to UU Triaxial Test Data.....	 A-399
 Appendix N. Results from One-Dimensional Free Swell Tests on Untreated and Treated Bulk Test Soils.....	 A-403
 Appendix O. Test Results from Follow-up Study using Stabilizers at High Application Rates and Lime	 A-409
 Appendix P. Protocol for Preparing Laboratory Test Specimens of Soils Treated with Liquid Chemical Soil Stabilizers: Summary of Comments from TxDOT and Industry Representatives.....	 A-419

Appendix Q. Recommended Protocol for Preparing Laboratory Test Specimens of Soils Treated with Liquid Chemical Soil Stabilizers	A-435
Appendix R. Application Guidelines for Nontraditional Liquid Chemical Soil Stabilizers.....	A-441

List of Tables

Table 2-1.	Liquid stabilizer products considered for study.....	12
Table 2-2.	Dilution and application rates of the stabilizer products evaluated.....	13
Table 2-3.	Test soils used in evaluating the liquid stabilizers.....	13
Table 2-4.	Chemical-physical properties of reference clay minerals.....	14
Table 2-5.	Index properties of test soils	14
Table 3-1.	Analytical techniques used to characterize the stabilizers.....	28
Table 3-2.	pH and conductivity measurements for sulfuric acid, sulfonated limonene, and ionic stabilizer	28
Table 3-3.	Hydrogen ion concentrations in ionic stabilizer, sulfonated limonene, and sulfuric acid samples.....	28
Table 3-4.	Results of sulfate analysis by ion chromatography	29
Table 3-5.	Results of TOC analysis for the sulfonated limonene and ionic stabilizer.....	29
Table 3-6.	pH and conductivity measurements for the polymer stabilizer and sodium silicate	29
Table 3-7.	Interpretation of peaks in FTIR spectra for the polymer stabilizer	29
Table 3-8.	Interpretation of peaks in FTIR spectra for the enzyme stabilizer	30
Table 5-1.	Summary of compaction test results from tests on untreated bulk soil samples.....	65
Table 6-1.	XRD results of composite and montmorillonite fraction samples.....	78
Table 6-2.	Summary of d-spacings and values of 2q for the 001 peak for untreated and ionic stabilizer and sulfuric acid treated samples of clay minerals and native soils	79
Table 6-3.	BET results for ionic stabilizer treated samples of montmorillonite, kaolinite, illite, Bryan soil and Mesquite soil	80
Table 6-4.	Al:Si ratios and hypothesis testing of EDS results obtained for untreated and ionic stabilizer and sulfuric acid treated samples of clay minerals and native soils	81
Table 6-5.	Cation exchange capacity results for the untreated and ionic treated montmorillonite.....	82
Table 7-1.	Atterberg limits of the untreated test soils and of those treated with the ionic stabilizer product.....	104
Table 7-2.	Shear strength parameters for envelopes that were fit to UU triaxial data in Figure 7-3	104
Table 8-1.	Summary of d-spacings and values of 2q for the 001 peak for untreated and enzyme treated samples of clay minerals and native soils	113
Table 8-2.	BET results for enzyme stabilizer treated samples of montmorillonite, kaolinite, illite, Bryan soil, and Mesquite soil	114
Table 8-3.	Al:Si ratios and hypothesis testing of EDS results obtained for untreated and enzyme stabilizer treated samples of clay minerals and native soils	115

Table 8-4.	Cation exchange capacity results for the untreated and enzyme treated montmorillonite.....	116
Table 9-1.	Atterberg limits of the untreated test soils and of those treated with the enzyme stabilizer product	125
Table 9-2.	Shear strength parameters for envelopes that were fit to UU triaxial data in Figure 9-3	126
Table 10-1.	Summary of d-spacings and values of 2q for the 001 peak for untreated and polymer treated samples of clay minerals and native soils	133
Table 10-2.	BET results for polymer stabilizer treated samples of montmorillonite, kaolinite, illite, Bryan soil, and Mesquite soil	134
Table 10-3.	Al:Si ratios determined from EDS results for polymer stabilizer treated samples of montmorillonite, kaolinite, illite, Bryan soil, and Mesquite soil.....	135
Table 10-4.	Cation exchange capacity results for the untreated and polymer treated montmorillonite.....	136
Table 11-1.	Atterberg limits of the untreated test soils and of those treated with the polymer stabilizer product	148
Table 11-2.	Shear strength parameters for envelopes that were fit to UU triaxial data in Figure 11-3	148
Table 12-1.	Index properties of soils used in the follow-up study	160
Table 12-2.	Dilution and application rates used in the follow-up study	161
Table 12-3.	Atterberg limits of the untreated and treated test soils from the follow-up study	162
Table 12-4.	Results from standard Proctor compaction tests (ASTM D 698) on the untreated and treated test soils in the follow-up study.....	162
Table 12-5.	Shear strength parameters for envelopes fitted to UU triaxial data on the untreated and treated test soils in the follow-up study.....	163
Table F-1.	Raw data from pH and conductivity replicates.....	A-343
Table F-2.	Raw data from TOC autosampler	A-344
Table F-3.	Raw data from TOC boat sampler	A-345
Table F-4.	Raw data from sulfate analysis	A-345
Table F-5.	UV/Visible spectrometer results for sulfonated limonene.....	A-346
Table F-6.	UV/Visible spectrometer results for the ionic stabilizer.....	A-348
Table F-7.	UV/Visible spectrometer results for the polymer stabilizer	A-350
Table F-8.	UV/Visible spectrometer results for the enzyme stabilizer (1:10,000) from wavelengths 190-750 nm	A-352
Table F-9.	UV/Visible spectrometer results for the enzyme stabilizer (1:5,000) from wavelengths 190-600 nm	A-354
Table F-10.	UV/Visible spectrometer results for the enzyme stabilizer (1:1,000) from wavelengths 190-305 nm	A-356
Table F-11.	Raw data from titration of the ionic stabilizer	A-357
Table F-12.	Raw data from titration of sulfuric acid.....	A-358
Table F-13.	Raw data from titration of sulfonated limonene	A-359
Table F-14.	Raw data from titration of the polymer stabilizer.....	A-360
Table F-15.	Raw data from titration of the enzyme stabilizer.....	A-365

Table F-16.	FAB analysis of the enzyme stabilizer	A-368
Table I-1.	Summary of measured Atterberg limits for all untreated and treated bulk soils	A-377
Table J-1.	Summary of compaction test results from tests on untreated bulk soil samples	A-381
Table K-1.	Properties of kaolinite test specimens	A-385
Table K-2.	Properties of illite test specimens	A-386
Table K-3.	Properties of montmorillonite test specimens	A-387
Table K-4.	Properties of TX Bryan HP test specimens	A-388
Table K-5.	Properties of TX Mesquite HS HP test specimens	A-389
Table M-1.	Shear strength parameters for envelopes fitted to the UU triaxial data in Figures M-1 through M-5	A-399

List of Figures

Figure 3-1. Chemical shifts of the proton in organic compounds (from Klute 1986)	30
Figure 3-2. GC/MS results for sulfonated limonene and limonene samples	31
Figure 3-3. Results of potentiometric titration of the ionic stabilizer and its components	32
Figure 3-4. UV/Vis spectroscopy results for sulfonated limonene and the ionic stabilizer	32
Figure 3-5. FTIR results for sulfonated limonene and ionic stabilizer	33
Figure 3-6. Proton (1H) NMR results for sulfonated limonene and ionic stabilizer	34
Figure 3-7. HPLC/MS results for the (a) ionic stabilizer and (b) sulfonated limonene prepared in the laboratory	35
Figure 3-8. FTIR results for the polymer stabilizer	36
Figure 3-9. HPLC/MS results for the polymer stabilizer (the top portion of the corresponds to the LC chromatogram and the bottom portion to the mass spectra)	36
Figure 3-10. ²⁹ Si NMR results for (a) sodium silicate and (b) the polymer stabilizer	37
Figure 3-11. Potentiometric titration of enzyme stabilizer	38
Figure 3-12. FTIR results for the enzyme stabilizer	38
Figure 3-13. 1H NMR results for the enzyme stabilizer	39
Figure 3-14. GPC results for the enzyme stabilizer	39
Figure 3-15. HPLC/MS results for enzyme stabilizer	40
Figure 3-16. Enzyme stabilizer UV/Vis absorption spectra obtained at 1:10,000 dilution	40
Figure 3-17. Polyethylene glycol UV/Vis absorbance spectra (from Journal of American Ceramic Society, Vol. 82, 1999)	41
Figure 4-1. Diffraction from crystal planes according to Bragg's Law (from Whittig and Allardice 1986)	51
Figure 4-2. Comparison of XRD results for air dried and freeze-dried sodium montmorillonite	51
Figure 5-1. Phase diagrams for the untreated soil, diluted stabilizer, and chemically treated soil after mixing to the optimum water content	66
Figure 5-2. Determination of grain size distribution using the hydrometer test method, and determination of liquid limits using a hand-operated liquid limit device	67
Figure 5-3. Apparatus used for conducting the unconsolidated-undrained triaxial compression tests	67
Figure 5-4. Apparatus used for conducting the one-dimensional free swell tests	68
Figure 6-1. SEM images at a magnification of 5,000× for (a) untreated and (b) ionic stabilizer (AMR 1:6,000) treated composite samples	83

Figure 6-2. Reference SEM images of (a) sodium montmorillonite coating another mineral (adapted from www.glossary.oilfield.slb.com/Files/OGL98037.jpg) and (b) pure montmorillonite (adapted from Keller 1989)	83
Figure 6-3. Comparison of EDS results for an untreated composite sample and AN ionic stabilizer treated sample (AMR 1:6,000)	84
Figure 6-4. Reference XRD pattern for montmorillonite and XRD patterns for montmorillonite composite samples that were untreated and treated with the ionic stabilizer at AMRs of 1:1,000, 1:6,000, and 1:9,000	84
Figure 6-5. X-ray diffraction patterns for (a) composite sample and (b) montmorillonite fraction treated with the ionic stabilizer at the recommended AMR of 1:6,000	85
Figure 6-6. X-ray diffraction patterns for freeze-dried composite samples treated at an AMR of 1:6,000 with the ionic stabilizer, sulfonated limonene, and sulfuric acid	86
Figure 6-7. X-ray diffraction patterns for untreated and ionic stabilizer and sulfuric acid treated samples of illite, kaolinite, and montmorillonite (reference spectra from Mineral Powder Diffraction File Data Book, 1980)	87
Figure 6-8. X-ray diffraction patterns for untreated and ionic stabilizer and sulfuric acid treated samples of Mesquite and Bryan soils	88
Figure 6-9. Pore size distributions for untreated and ionic stabilizer treated samples of illite, kaolinite, and montmorillonite	89
Figure 6-10. Pore size distributions for untreated and ionic stabilizer treated samples of Mesquite and Bryan soil	90
Figure 6-11. Pore size distributions for untreated and sulfuric acid treated samples of illite, kaolinite, and montmorillonite	91
Figure 6-12. Pore size distributions for untreated and sulfuric acid treated samples of Bryan and Mesquite soils	92
Figure 6-13. Pore size distributions of untreated montmorillonite and of montmorillonite samples treated with an excess of sulfuric acid (weathered)	93
Figure 6-14. ESEM images for ionic stabilizer treated clay minerals at a magnification of 7,000× for (a) untreated montmorillonite, (b) ionic stabilizer/montmorillonite treatment, (c) untreated kaolinite, (d) ionic stabilizer/kaolinite treatment, (e) untreated illite sample, and (f) ionic stabilizer/illite treatment	94
Figure 6-15. Reference SEM images of (a) illite (adapted from Mitchell, 1993) and (b) kaolinite (adapted from Keller, 1989)	95
Figure 6-16. ESEM images for ionic stabilizer treated clay minerals at a magnification of 7,000× for (a) untreated Mesquite soil, (b) ionic stabilizer/Mesquite soil treatment, (c) untreated Bryan soil, and (d) ionic stabilizer/Bryan soil treatment	96
Figure 6-17. SEM image of gypsum (The Gypsum Project, Wilhelms University, 1996)	97

Figure 6-18. SEM/EDS results for untreated and ionic stabilizer treated Bryan soil at a magnification of 11,500× including (a) SEM image of untreated Bryan soil with EDS point identified, (b) SEM image of ionic stabilizer treated Bryan soil with EDS point identified, and (c) corresponding EDS spectra for the untreated and treated samples.....	98
Figure 6-19. EDS results for ionic stabilizer, untreated Mesquite soil, and Mesquite soil treated with the ionic stabilizer	99
Figure 7-1. Atterberg limits of the untreated test soils and of those treated with the ionic stabilizer product.....	105
Figure 7-2. Water contents and dry unit weights of the triaxial and swell test soil specimens, both untreated and treated with the ionic stabilizer product	106
Figure 7-3. Fitted shear strength envelopes from UU triaxial tests on the untreated soils and on the soils treated with the ionic stabilizer product	107
Figure 7-4. Reference shear strengths of the untreated test soils and of those treated with the ionic stabilizer product.....	108
Figure 7-5. One-dimensional free swell of the untreated test soils and of those treated with the ionic stabilizer product.....	108
Figure 8-1. XRD patterns of enzyme treated and untreated samples of montmorillonite, illite, and kaolinite	117
Figure 8-2. XRD patterns of enzyme treated and untreated samples of Bryan and Mesquite soil samples.....	118
Figure 8-3. Pore size distributions for untreated and enzyme stabilizer treated samples of illite, kaolinite, and montmorillonite	119
Figure 8-4. Pore size distributions for untreated and enzyme stabilizer treated samples of Bryan and Mesquite soils	120
Figure 8-5. ESEM images for enzyme stabilizer treated clay minerals at a magnification of 7,000× for (a) untreated montmorillonite, (b) enzyme stabilizer/montmorillonite treatment, (c) untreated kaolinite, (d) enzyme stabilizer/kaolinite treatment, (e) untreated illite sample, and (f) enzyme stabilizer/illite treatment	121
Figure 8-6. ESEM images for enzyme stabilizer treated clay minerals at a magnification of 7,000× for (a) untreated Mesquite soil, (b) enzyme stabilizer/Mesquite soil treatment, (c) untreated Bryan soil, and (d) enzyme stabilizer/Bryan soil treatment.....	122
Figure 9-1. Atterberg limits of the untreated test soils and of those treated with the enzyme stabilizer product	127
Figure 9-2. Water contents and dry unit weights of the triaxial and swell test soil specimens, both untreated and treated with the enzyme stabilizer product	128
Figure 9-3. Fitted shear strength envelopes from UU triaxial tests on the untreated soils and on the soils treated with the enzyme stabilizer product	129
Figure 9-4. Reference shear strengths of the untreated test soils and of those treated with the enzyme stabilizer product	130

Figure 9-5. One-dimensional free swell of the untreated test soils and of those treated with the enzyme stabilizer product	130
Figure 10-1. XRD patterns of polymer treated and untreated samples of montmorillonite, illite, and kaolinite	137
Figure 10-2. XRD patterns of enzyme treated and untreated samples of Bryan and Mesquite soil samples	138
Figure 10-3. Pore size distributions for untreated and polymer stabilizer treated samples of illite, kaolinite, and montmorillonite	139
Figure 10-4. Pore size distributions for untreated and polymer stabilizer treated samples of Bryan and Mesquite soils	140
Figure 10-5. ESEM images for polymer stabilizer treated clay minerals at a magnification of 7,000× for (a) untreated montmorillonite, (b) polymer stabilizer/montmorillonite treatment, (c) untreated kaolinite, (d) polymer stabilizer/kaolinite treatment, (e) untreated illite sample, and (f) polymer stabilizer/illite treatment	141
Figure 10-6. ESEM images for polymer stabilizer treated clay minerals at a magnification of 7,000× for (a) untreated Mesquite soil, (b) polymer stabilizer/Mesquite soil treatment, (c) untreated Bryan soil, and (d) polymer stabilizer/Bryan soil treatment	142
Figure 10-7. SEM/EDS results for untreated and polymer stabilizer treated Bryan soil at a magnification of 11,500× including (a) SEM image of untreated Bryan soil with EDS point identified, (b) SEM image of polymer stabilizer treated Bryan soil with EDS point identified, and (c) corresponding EDS spectra for the untreated and treated samples	143
Figure 11-1. Atterberg limits of the untreated test soils and of those treated with the polymer stabilizer product	149
Figure 11-2. Water contents and dry unit weights of the triaxial and swell test soil specimens, both untreated and treated with the polymer stabilizer product	150
Figure 11-3. Fitted shear strength envelopes from UU triaxial tests on the untreated soils and on the soils treated with the polymer stabilizer product	151
Figure 11-4. Reference shear strengths of the untreated test soils and of those treated with the polymer stabilizer product	152
Figure 11-5. One-dimensional free swell of the untreated test soils and of those treated with the polymer stabilizer product	152
Figure 12-1. Grain size distribution of the untreated test soils, as determined by the hydrometer test method	163
Figure 12-2. Results from pH-lime series tests (ASTM C 977, 1995) on the three test soils	164
Figure 12-3. Results from trial tests with a pneumatic tamper on untreated Fire clay	164
Figure 12-4. Atterberg limits for the untreated and treated test soils in the follow-up study	165
Figure 12-5. Moisture contents and dry unit weights of all compacted test specimens prepared for the follow-up study	166

Figure 12-6. Shear strengths of untreated and treated specimens measured in UU triaxial tests in the follow-up study.....	167
Figure 12-7. Comparison of reference shear strengths, as determined from fitted strength envelopes, for untreated and treated soils in the follow-up study.....	168
Figure 12-8. Results from 1-D free swell tests on the untreated and treated soils in the follow-up study	169
Figure B-1. HPLC/MS results for limonene	A-5
Figure B-2. Infrared absorbance for organic functional groups (from Klute 1986)	A-6
Figure B-3. FAB results for the enzyme stabilizer.....	A-7
Figure B-4. FTIR results for polymer stabilizer.....	A-7
Figure B-5. UV/Vis spectroscopy results for enzyme stabilizer at 1:5000 dilution	A-8
Figure B-6. Titration replicates for ionic stabilizer.....	A-8
Figure B-7. Titration replicates for sulfuric acid.....	A-9
Figure B-8. Titration replicates for sulfonated limonene.....	A-9
Figure B-9. Titration replicates for polymer stabilizer	A-10
Figure B-10. Titration replicates for enzyme stabilizer	A-10
Figure C-1. Pore size distribution comparison for washed/untreated and unwashed/untreated samples of sodium montmorillonite.....	A-11
Figure C-2. Pore size distribution comparison for washed/untreated and unwashed/untreated samples of Bryan soil.....	A-12
Figure C-3. Pore size distribution comparison for washed/untreated and unwashed/untreated samples of Mesquite soil.....	A-12
Figure G-1. Oriented results for sodium montmorillonite.....	A-369
Figure G-2. Glycolated results for sodium montmorillonite	A-369
Figure G-3. Oriented results for illite	A-370
Figure G-4. Glycolated results for illite	A-370
Figure G-5. Oriented results for Bryan soil.....	A-371
Figure G-6. Glycolated results for Bryan soil	A-371
Figure H-1. Grain size distribution of untreated and treated bulk kaolinite.....	A-373
Figure H-2. Grain size distribution of untreated and treated bulk illite	A-373
Figure H-3. Grain size distribution of untreated and treated bulk montmorillonite.....	A-374
Figure H-4. Grain size distribution of untreated and treated TX Bryan HP.....	A-374
Figure H-5. Grain size distribution of untreated and treated bulk TX Mesquite HS HP	A-375
Figure I-1. Summary of measured Atterberg limits for all untreated and treated soils	A-378
Figure I-2. Liquid limit test results on bulk kaolinite	A-378
Figure I-3. Liquid limit test results on bulk illite.....	A-379
Figure I-4. Liquid limit test results on bulk montmorillonite	A-379
Figure I-5. Liquid limit test results on TX Bryan HP	A-380
Figure I-6. Liquid limit test results on TX Mesquite HS HP	A-380
Figure J-1. Compaction test results on bulk kaolinite.....	A-381
Figure J-2. Compaction test results on bulk illite	A-382
Figure J-3. Compaction test results on bulk montmorillonite.....	A-382
Figure J-4. Compaction test results on TX Bryan HP.....	A-383

Figure J-5.	Compaction test results on TX Mesquite HS HP	A-383
Figure K-1.	Summary of the water content, dry unit weight, and void ratio of all triaxial and swell test specimens.....	A-390
Figure L-1.	Results from unconsolidated-undrained triaxial compression tests on untreated and treated bulk kaolinite.....	A-393
Figure L-2.	Results from unconsolidated-undrained triaxial compression tests on untreated and treated bulk illite	A-394
Figure L-3.	Results from unconsolidated-undrained triaxial compression tests on untreated and treated bulk montmorillonite.....	A-395
Figure L-4.	Results from unconsolidated-undrained triaxial compression tests on untreated and treated TX Bryan HP	A-396
Figure L-5.	Results from unconsolidated-undrained triaxial compression tests on untreated and treated TX Mesquite HS HP	A-397
Figure M-1.	Fitted shear strength envelopes from UU triaxial tests on untreated and treated bulk kaolinite.....	A-400
Figure M-2.	Fitted shear strength envelopes from UU triaxial tests on untreated and treated bulk illite	A-400
Figure M-3.	Fitted shear strength envelopes from UU triaxial tests on untreated and treated bulk montmorillonite.....	A-401
Figure M-4.	Fitted shear strength envelopes from UU triaxial tests on untreated and treated TX Bryan HP.....	A-401
Figure M-5.	Fitted shear strength envelopes from UU triaxial tests on untreated and treated TX Mesquite HS HP.	A-402
Figure M-6.	Comparison of the reference shear strengths measured for all soils and all treatments	A-402
Figure N-1.	Results from 1-D free swell tests on untreated and treated bulk kaolinite	A-403
Figure N-2.	Results from 1-D free swell tests on untreated and treated bulk illite.....	A-404
Figure N-3.	Results from 1-D free swell tests on untreated and treated bulk montmorillonite (initial sample height = 0.40 inch).....	A-405
Figure N-4.	Results from 1-D free swell tests on untreated and treated TX Bryan HP	A-406
Figure N-5.	Results from 1-D free swell tests on untreated and treated TX Mesquite HS HP	A-407
Figure N-6.	Comparison of the 1-D free swell measured for all soils and all treatments	A-408
Figure O-1.	Compaction test results on Fire clay.....	A-409
Figure O-2.	Compaction test results on DG Taylor clay.....	A-410
Figure O-3.	Compaction test results on TG Taylor clay	A-410
Figure O-4.	Results from unconsolidated-undrained triaxial compression tests on the untreated soil in the follow-up study	A-411
Figure O-5.	Results from unconsolidated-undrained triaxial compression tests on treated Fire clay in the follow-up study.....	A-412
Figure O-6.	Results from unconsolidated-undrained triaxial compression tests on treated DG Taylor clay in the follow-up study	A-413

Figure O-7. Results from unconsolidated-undrained triaxial compression tests on treated TG Taylor clay in the follow-up study	A-414
Figure O-8. Results from 1-D free swell tests on Fire clay in the follow-up study	A-415
Figure O-9. Results from 1-D free swell tests on DG Taylor clay in the follow-up study	A-416
Figure O-10. Results from 1-D free swell tests on TG Taylor clay in the follow-up study	A-417
Figure Q-1. Phase diagrams for the untreated soil, diluted stabilizer, and chemically treated soil after mixing to the optimum water content	A-436

CHAPTER 1

BACKGROUND AND PROJECT OBJECTIVES

1.1. OVERVIEW

Pavement subgrade and base soil stabilization has traditionally been accomplished using lime, cement, and fly ash. The stabilization mechanisms of cement and lime are well understood, and rational application guidelines and laboratory testing methods have been developed for these conventional materials. However, calcium-based additives can cause excessive pavement heaving when used to treat sulfate-rich soils; alternatives thus need to be investigated. Various non-calcium-based soil and aggregate stabilizers (in liquid form) are actively marketed by a number of companies. The stabilizing mechanisms of these products are not fully understood, and their proprietary chemical composition makes it very difficult to evaluate the stabilizing mechanisms and predict their long-term performance. The primary objective of this study was to investigate and identify the mechanisms by which clay soils are modified or altered by these liquid chemical agents. The chemical composition of three commercially available, non-calcium-based liquid soil stabilizers was characterized using a variety of standard chemical test methods. In what will be called the "micro-characterization" study, the mechanisms of soil modification at the particle level were studied using physical-chemical analyses of untreated and treated soil samples. A paired "macro-characterization" study was also undertaken, wherein standard geotechnical laboratory tests were performed on untreated and treated compacted soil specimens to determine whether the chemical treatments lead to significant changes in the engineering properties of the test soils. The findings of this study clearly point to the need to conduct standard laboratory tests, prior to specifying the use of these products in field applications, to prove the effectiveness of the treatment on a particular soil type at a given chemical application rate.

1.2. LIQUID SOIL STABILIZERS

Chemical treatment of pavement base, subbase, and subgrade materials is undertaken to improve workability during compaction, to create a firm working surface for paving equipment, to increase the strength and stiffness of a foundation layer, to reduce potential shrink and swell due to moisture changes and/or frost action, or to control dust on unpaved roads. Stabilization is most commonly accomplished with bulk powder materials such as lime, Portland cement, and fly ash. Supported by a good understanding of the underlying mechanisms of soil modification, technical guidelines for treating highway soils with these materials have been developed by a number of state and national agencies (e.g., Meyers et al. 1976; TRB Committee 1987; ACI Committee 230 1990; Joint Depts. of the Army and Air Force 1994). Criteria for the appropriate field application rates are derived from years of demonstrated field experience with these materials. To determine the mix proportions needed to obtain the desired engineering properties in the treated soil, different laboratory test procedures are used by various agencies. Testing of the untreated and treated soils may include measurement of the Atterberg limits, California bearing ratio (CBR), swell potential, unconfined compressive strength, or durability in wet-dry or freeze-thaw cycles.

In some cases involving soils with high sulfate contents, stabilization with conventional, calcium-rich chemicals has lead to excessive swelling and heaving (Sherwood 1962; Mitchell 1986; Hunter 1988; Mitchell and Dermatas 1992; Dermatas 1995; Kota et al. 1996; Rollings et al. 1999). Such failures apparently occur when the added calcium reacts with sulfates and alumina present in the soil to form a series of calcium-aluminum-sulfate hydrates leading to ettringite and thaumasite, a reaction that causes significant volume expansion (Hunter 1988; Mitchell and Dermatas 1992; Rollings et al. 1999). Concentrated liquid products that do not contain calcium can be used on sulfate-rich soils without causing excessive expansion due to this mechanism.

Numerous proprietary, liquid chemical products are actively marketed for stabilizing soils on highway projects. Usually supplied as concentrated liquids, these products are diluted in water on the project site and sprayed on the soil to be treated prior to mixing and compaction. In addition to being cheaper to transport than traditional bulk stabilizer materials, these products are a potentially attractive alternative for treating high-sulfate soils. However, there are a number of technical barriers to routine application of these products. First, supplier claims of product effectiveness are often not well substantiated with independent field or laboratory evaluations performed under controlled conditions. The chemical composition of these products is usually considered proprietary, and the suppliers often give minimal or incomprehensible information regarding the mechanisms of soil modification. In addition, rational guidelines for the use of these products, including accepted test methods for evaluating their effectiveness in stabilizing particular soils, have not been adequately developed and evaluated. The lack of a mechanistic understanding of the stabilization processes makes assessing their limitations and appropriate applications speculative at best.

Scholen (1992) lists some of these liquid chemical products, which he classified as electrolytes, enzymes, acrylic polymers, and mineral pitches. Based on a review of the most readily available products, liquid soil stabilizers were classified for this study as being one of three broad types: ionic, polymer, or enzyme. Liquid chemical stabilizers may work through a variety of mechanisms including encapsulation of clay minerals, exchange of interlayer cations, breakdown of clay mineral with expulsion of water from the double layer, or interlayer expansion with subsequent moisture entrapment (Scholen 1992; Petry and Das 2001). With some products, improved engineering properties may result from obtaining higher compacted soil densities (Randolph 1997). Recent physical-chemical studies have shown limited evidence for possible changes in the structure of some clays when treated with one ionic stabilizer (Sarkar et al. 2000).

Twelve nontraditional soil stabilizers of several different types were recently evaluated by the U.S. Army Engineer Research and Development Center (Santoni et al. 2002). These products were screened for their potential effectiveness in treating silty sand subgrade materials. Unconfined compressive strength was used as an index of performance, with some samples being subjected to wetting following different curing periods. Most stabilizers did not exhibit significant soil improvements in that study. Some polymer stabilizers showed promising results, but only when applied to the silty sand at much higher rates (25 to 50 times) than those recommended by the product suppliers.

Despite the potential advantages offered by various nontraditional soil stabilizers, especially for treating sulfate-rich soils, most engineers are reluctant to specify the use of these products. This lack of acceptance can be traced to a number of issues:

- A principal concern is the lack of published, independent studies of non-calcium-based stabilizers (Kota et al. 1996). Test results provided by product suppliers are not necessarily unbiased (Petry 1997; Santoni et al. 2002) and are appropriately viewed with skepticism.
- Field performance data is particularly lacking. Scholen (1992; 1995) surveyed a number of projects undertaken by the U.S. Forest Service where several of these products were used, mostly to stabilize unpaved roads. While there were some notable failures, usually attributed to misapplication of the product, there were a number of reported successes. However, most of the field case studies promoted to demonstrate the benefits of these commercial products, which are typically given without data on untreated control sections, are often little more than poorly documented testimonials.
- There is a lack of standard laboratory test methods that can be used effectively to predict performance in the field (Scholen 1992). Well-established testing protocols are needed to quantify how much a particular stabilizer product may improve the properties of specific project soils. Laboratory testing programs of this kind must include untreated control specimens prepared in the same manner, including water content, as the chemically treated samples (Petry and Das 2001; Petry 1997).
- Positive or negative results obtained in the laboratory are sometimes questioned as predictors of field performance, because laboratory sample preparation may not completely simulate field conditions. For example, it is possible to achieve more complete mixing of the chemical agent with pulverized laboratory soil samples than is possible in the field (Petry 1997). However, if a chemical does not exhibit positive results in the laboratory when mixed with a well-pulverized soil, it is difficult to see how better results would be obtained from less complete mixing in the field.
- The information provided by stabilizer suppliers is often inadequate. Many manufacturers understandably consider the chemical composition of their products to be proprietary, but this makes it difficult to independently assess the stabilizing mechanisms and forecast potential field benefits. In some cases, application rates recommended in the product literature are poorly defined or inconsistent. In general, the reluctance to implement nontraditional soil stabilizers can be attributed somewhat to the lack of appropriate engineering expertise within some supplier companies (Scholen 1992).
- Very little, if any, independent testing has been conducted to identify and describe the mechanisms by which these stabilizers work. There is a dearth of published experimental data that can substantiate stabilizing mechanisms reported by the product suppliers.
- Suppliers and products seem to appear, disappear, or change names with some regularity, making it difficult for an agency to develop confidence with a given product through long-term experience.

To take better advantage of these products, a rational first step is to develop a clear understanding of the underlying mechanisms by which a soil is modified by these nontraditional, liquid chemical stabilizers. Secondly, standard laboratory tests on untreated and treated soil samples, prepared under controlled conditions, are needed to evaluate the potential effectiveness of these products in modifying the engineering properties of various soils. Implementation of these products is likely to require the development of standardized test methods that can be used to predict field performance of a treated soil from a given project site, as well as to select appropriate field application rates.

1.3. PROJECT OBJECTIVES AND WORK PLAN

The primary objective of this project was to evaluate selected, representative liquid chemical stabilizers and to elucidate the modes of reactivity of the products with different clay soils. A secondary objective was to assess how much the chemical treatment changed the relevant engineering properties of the test soils, as an indicator of the potential effectiveness of selected products. This required work in three areas:

- chemical analyses to identify the principal chemical constituents of each stabilizer product
- a detailed physical-chemical study of the untreated and treated soils to characterize the modes of product reactivity at the soil particle level (micro-characterization study)
- conventional geotechnical laboratory tests conducted to assess how much the engineering properties of the soils were altered by treatment with these products (macro-characterization study)

The project was carried out in the six work tasks briefly described below.

Task 1. Select non-calcium-based soil stabilizers and soils to be evaluated.

Three commercial products, representing three major classes of liquid chemical soil stabilizers, were selected for study. These products are referred to as the ionic, enzyme, and polymer stabilizers; the trade name of each product is not identified in this report. Five test soils were also selected. Three of the soils are well characterized "reference clays," each composed primarily of one clay mineral: kaolinite, illite, and sodium montmorillonite. The other two soils are high-plasticity, native Texas soils provided by TxDOT. One of the Texas soils was reported to have a high sulfate content.

Task 2. Perform laboratory tests on candidate stabilizers.

In this task the chemical properties and composition of the selected stabilizers were characterized. While the major constituents were determined, the exact chemical formulation of these proprietary products was not resolved. The tests employed included potentiometric titrations, high-performance liquid chromatography-mass spectroscopy (HPLC-MS), Fourier transform infrared spectroscopy (FTIR), nuclear magnetic resonance (NMR) spectroscopy, and UV/visible absorption spectroscopy.

Task 3. Soil characterization.

Work accomplished under this task established the baseline properties of the selected soils prior to reaction with the stabilizers. Tests were conducted to measure both physical and chemical properties. The macro-characterization study included measurement of grain size distribution, Atterberg limits and plasticity index, compacted density, undrained shear strength, and free swell potential, all performed using standard ASTM test methods. The micro-characterization study involved scanning electron microscopy (SEM), environmental scanning electron microscopy (ESEM), SEM coupled with energy dispersive x-ray spectroscopy (EDS),

and x-ray diffraction (XRD), as well as analyses of surface area, pore size distribution, and cation exchange capacity.

Task 4. Identify mechanisms of reaction between the soils and the stabilizers.

The approach to identifying the mechanisms of soil modification involved reacting the soils and stabilizers, then identifying changes in the treated soil properties using the same test procedures described in Task 3. In the "micro-characterization" phase, the stabilizing mechanisms of the three representative products were identified from changes in the physical-chemical soil properties observed at the particle level. In most of these tests, very high product application rates were used to increase the likelihood of discerning the underlying mechanism. In many cases, tests were repeated to characterize test variability and the significance of observed changes.

In the "macro-characterization" phase under this task, the physical properties of the treated soil were assessed to determine whether the mechanisms observed at the particle level translated into beneficial changes in the properties of the compacted soil samples. The same standard ASTM geotechnical test methods used in Task 3 were used to measure the properties of the treated samples. Multiple tests on identically prepared samples were conducted to allow characterization of experimental variability. Here, the soils were mixed with each product at the suppliers' recommended application rates, then compacted and cured following a specified ten-step sample preparation protocol. A concerted effort was made to clearly define a rational protocol for preparing laboratory test specimens of compacted, untreated and treated soils.

Task 5. Evaluate laboratory findings to assist in the development of rational guidelines for the use of non-calcium-based soil stabilizers.

This study was successful in describing the mechanisms by which these products alter a soil. However, given the normal variability between different test specimens, the measured engineering properties of the test soils were not consistently and substantially improved by treatment with these products at the suppliers' recommended application rates. Therefore, it is recommended that the potential application of these products on highway projects in Texas should be preceded by carefully conducted laboratory tests to evaluate the effectiveness, as well as the appropriate application rate, of a given product on the soils encountered at a particular project site. A specific protocol for preparing soil test specimens for such evaluation tests is recommended.

Task 6. Prepare reports.

The results of this study are presented in three project deliverables:

- Research Report (this report), which gives a comprehensive documentation of the project, including laboratory analyses of the stabilizer products and test soils
- Project Summary Report, which summarizes the work accomplished, findings, and gives a list of discretely numbered recommendations for implementation
- Application Guidelines, for the use of non-calcium-based soil stabilizers

Follow-up study.

The tests conducted under the above work plan failed to show a consistent, significant improvement in the engineering properties of the five test soils following treatment with the selected products at the recommended application rates. It was thus decided to conduct an additional, follow-up study with the same stabilizer products and three different clay soils (all natural soils from the Austin, Texas, area). In an effort to determine whether higher application rates were needed to improve the soil, the stabilizers were used at application rates *ten* times that recommended by the product suppliers. For comparison, the same test soils were also treated with 6% hydrated lime. As before, no consistent, significant improvement in the engineering properties of these soils was observed, even with the high application rates used.

1.4. REPORT ORGANIZATION

Following this introductory chapter, the selection of representative stabilizer products and test soils is discussed in Chapter 2. Chemical characterization of the selected products is described in Chapter 3. In Chapters 4 and 5, the test methods used in the micro-characterization and macro-characterization studies, respectively, are described. Results from the tests on the untreated and treated test soils are presented in Chapters 6 through 11. The micro-characterization of the ionic stabilizer mechanism is covered in Chapter 6, while the macro-characterization of the ionic stabilizer effectiveness is covered in Chapter 7. Similarly, the results from tests with the enzyme stabilizer are given in Chapters 8 and 9, while the results from tests with the polymer product are covered in Chapters 10 and 11. The follow-up macro-characterization study, involving three different soils from the Austin area, lime-treated specimens, and the three stabilizer products applied at ten times the recommended application rates, is discussed in Chapter 12. Project conclusions and recommendations are given in Chapters 13 and 14, respectively. Detailed test data from all of the tests conducted in this study, as well as other supporting data and information, are given in Appendices A through P. A recommended protocol for preparing laboratory test specimens and guidelines for potential application of these products are given in Appendices Q and R, respectively.

CHAPTER 2

SELECTION OF TEST MATERIALS

2.1. LIQUID STABILIZER PRODUCTS

Three commercially available, liquid soil stabilizer products were selected for evaluation in this study. All of the products that were identified and considered in this selection are listed in Table 2-1. TxDOT personnel provided information, including literature from the manufacturers, for several of the products listed. Other listed products were identified in published articles, found in Internet searches, and gathered from other sources. However, no effort was made to assemble a comprehensive list of available products and suppliers. Because many of the product suppliers listed in Table 2-1 were not contacted, several of the listed products may no longer be available or are distributed by different companies. Hence, the information in Table 2-1 should not be viewed as a complete or accurate listing of soil stabilizer products currently on the market.

Considering the most readily available liquid soil stabilizers, it appears that most of the identified products can be classified as one of three types:

- (1.) ionic stabilizers, reported to work through cation exchange within the clay mineral
- (2.) enzyme stabilizers, described as consisting of various organic catalysts
- (3.) polymer stabilizers, comprised of various organic and inorganic polymers

This simple classification is not intended to provide a comprehensive scheme for categorizing the many different products sold for stabilizing soils. Rather, an attempt was made to simply group the most widely available products and facilitate the selection of representative products for further study.

Three products, representative of the three types of liquid stabilizers, were chosen from those listed in Table 2-1. The manufacturers were then contacted by TxDOT personnel and asked to provide product samples for evaluation in this study. Throughout this report, the selected products are identified simply as the “ionic stabilizer,” “enzyme stabilizer,” or “polymer stabilizer.” Specific product names are not identified to avoid endorsement of particular products and to avert disclosure of the chemical components of proprietary products.

Ionic Stabilizer

The chosen ionic product has a patented formulation (U.S. Patent Nos. 4,941,924 and 5,000,789) and reportedly contains sulfuric acid, d-limonene (citrus stripper oil), a surfactant, and a corrosion inhibitor. The supplier claims the product can be used to improve soil strength, reduce the potential swell of clay subgrade soils, achieve greater compacted soil density, and to enhance the effectiveness of conventional stabilizers like Portland cement and fly ash. The product is said to be most effective in treating soils having a significant concentration of clay, limestone, or other natural minerals. It is least effective in soils with very high sand concentrations or a plasticity index less than 10.

Enzyme Stabilizer

The selected enzyme stabilizer product is a proprietary, concentrated, biodegradable, nonbacterial, multi-enzymatic formulation. The product is advertised to increase soil density, reduce compaction effort, improve bearing capacity, and lower soil permeability. The supplier recommends the product for treating road base materials that contain between 18% and 30% cohesive fines (finer than the No. 200 mesh size) at a moisture content of 2% to 3% below optimum.

Polymer Stabilizer

While many stabilizer products of this type contain organic polymers, the selected polymer stabilizer is an inorganic, sodium silicate based product. The supplier advertises the polymer stabilizer as effective in reducing permeability and plasticity index, while increasing soil bearing capacity. The product is recommended for use in conjunction with Portland cement, lime, or fly ash to treat semi-cohesive and cohesive soils.

2.2. PRODUCT APPLICATION RATES

The suppliers' recommendations for product dilution and application rates in the field are summarized in Appendix A for each of the three selected stabilizer products. While slightly different dilution and application rates are sometimes mentioned in the product literature, the suppliers' recommendations are general and unrelated to the particular characteristics of the soils to be treated. It does not appear that optimal application rates are typically determined for different projects or soil types. In contrast, the application rates for traditional bulk stabilizers are usually selected by the project engineers based on the soil characteristics and project requirements. Typical recommended dilution and application rates for the three evaluated products are listed in Table 2-2. Throughout this study, these values are referred to as the suppliers' recommended dilution and application rates.

Because various suppliers express the recommended application rates using different terminology and units, it is advantageous to define the following terms:

- *Dilution Mass Ratio* (DMR) is the mass ratio of concentrated chemical product to water, used to express the product dilution in water prior to soil application.
- *Application Mass Ratio* (AMR) is the mass ratio of concentrated chemical product to oven-dry material in the treated soil.

These terms clearly distinguish dilution rate (how much concentrated product is mixed with water) from the application rate (how much product is mixed with a given quantity of soil). These definitions also reduce possible confusion in determining equivalent application rates for field operations and laboratory test specimens. Both the DMR and AMR were expressed as mass ratios for convenience in preparing laboratory test specimens, where materials were proportioned on a mass balance. Converting the suppliers' recommended application rates, in terms of volume of product per volume of soil, to an equivalent AMR requires an estimate of the treated soil unit weight; here, a soil dry unit weight of 100 pcf (16 kN/m³) was assumed, as indicated in Table 2-2.

The AMR is a key parameter, as it expresses the concentration of stabilizer chemical in the treated soil. Recommended application rates for the liquid products under study are fairly low, making it convenient to express the AMR as a ratio (last row of Table 2-2). The AMR is equivalent, however, to an application rate expressed as the percentage by weight of stabilizer to dry soil, as traditionally used with bulk soil stabilizers like lime. The recommended AMRs expressed as a percentage (Table 2-2) can be compared with the much higher application rates generally used for lime (1.5% to 8%) and cement (3% to 16%) (TRB Committee 1987; ACI Committee 230 1990).

2.3. TEST SOILS

The clay soils selected for the testing program are listed in Table 2-3. The soils include three *reference clays* (kaolinite, illite, and montmorillonite) and two *native Texas clays* (from Bryan and Mesquite, Texas). Samples of each reference clay were obtained from two different sources: *repository samples* were used in the micro-characterization study, and *bulk samples* were used in the macro-characterization study.

Natural soils encountered in the field typically contain a mixture of many different mineral constituents. To increase the likelihood of observing subtle physical-chemical changes induced by the stabilizer products, less complex, “pure” clay soils were needed. Accordingly, the three reference clays were chosen to represent the most commonly encountered clay constituents found in natural soils: kaolinite, illite, and montmorillonite. Typical properties of these three minerals are given in Table 2-4 (Juma 1998). Illite and kaolinite are generally considered to possess little to no swell potential, while montmorillonite exhibits considerable expansion upon wetting.

Well-characterized samples of each reference clay were purchased from the Source Clays Repository at the University of Missouri. The purity and consistency of these repository samples were needed for the physical-chemical analyses undertaken in the micro-characterization study. Only a few grams of soil were generally required for these laboratory tests. Much larger quantities of material were needed for conducting tests for compaction, strength, and swell potential in the macro-characterization study. Because the Source Clays Repository could not supply more than a few pounds of each clay, alternate sources for bulk samples of these clays were identified (Table 2-3). While the bulk sample of each reference clay is not chemically identical to the repository sample, the soils obtained from both sources are predominantly one clay mineral. Hence, valid comparisons can be drawn between the results of the physical-chemical tests on the repository samples (micro-characterization study) and the engineering properties of the bulk samples (macro-characterization study).

The two native Texas soils are both high-plasticity, natural clay soils of mixed mineralogy that classify as fat clays (Table 2-3). Samples of these clays were obtained by TxDOT from locations near Bryan and Mesquite, Texas. The Mesquite clay had a high sulfate content, as described in section 2.5.

Index properties for the untreated bulk reference clays and the native Texas clays are summarized in Table 2-5. This data includes the classification and Atterberg limits, as well as the optimum water content for compaction and maximum dry unit weight determined using the modified Proctor compaction energy.

2.4. REFERENCE CLAYS

Repository and Bulk Kaolinite

The repository kaolinite sample was “KGa-1b Kaolinite” excavated from Washington County, Georgia. Kaolinite, classified as a 1:1 layered dioctahedral clay, is comprised of sheets of silica atoms arranged in tetrahedral coordination and aluminum atoms arranged in octahedral coordination. It is one of the most widespread aluminosilicate minerals, forming either as a residual weathering product, or sometimes by hydrothermal alteration of other aluminosilicates, especially feldspars.

The bulk kaolinite was purchased in 50-lb bags from the Dry Branch Kaolin Company of Dry Branch, Georgia. The material is sold under the name “Hydrite R” and is used commercially in the production of paints, plastics, inks, and adhesives. As delivered, the bulk kaolinite is a white, odorless, dry powder. The material safety data sheet (MSDS) describes Hydrite R kaolinite as pulverized hydrous aluminum silicate (CAS No. 1332-58-7) with a chemical formula of $\text{Al}_2\text{O}_3 \cdot 2\text{SiO}_2 \cdot 2\text{H}_2\text{O}$. It has a specific gravity of 2.62, a pH of 4.2 to 5.2 in a 20% aqueous solution, and a median particle size of 0.77 microns (μm).

Repository and Bulk Illite

The repository illite sample was “IMt-2 Illite” excavated from Silver Hill, Montana. Illite is a 2:1 aluminosilicate in which substitution of some Al for Si in the tetrahedral layer yields a net negative charge on the particles. However, the interlayer charge is balanced by potassium ions that become trapped in the interlayer and are unavailable for exchange. As a result, the clay is not expansive.

The bulk illite is a dry, pulverized gray clay with no noticeable sand component. Dr. Roy E. Olson of the University of Texas at Austin excavated this soil in the 1960s from a hillside near Fithian, Illinois. The illite was previously ground and sieved through a No. 40 sieve. The behavior of this soil was studied by Olson and Mesri (1970) and Olson (1974). The specific gravity of this soil is assumed to be 2.80, based on values reported by Grim (1968) and Olson and Mesri (1970).

Repository and Bulk Montmorillonite

The repository montmorillonite sample was “SWy-2 Sodium Montmorillonite” excavated from the Newcastle formation in Crook County, Wyoming. Montmorillonite is classified as a 2:1 dioctahedral layered clay comprised of sheets of silica atoms arranged in tetrahedral coordination and aluminum atoms arranged in octahedral coordination. Isomorphic substitution of Mg (2+ charge) for Al (3+ charge) in the octahedral layers provides the montmorillonite with a net negative charge, which is counterbalanced by cations occupying the interlayer regions between the octahedral sheets of adjacent layers. The spacing between layers is variable (10Å to 18Å), depending on the size of the interlayer cation, the hydration energy of the cation (which is a function of ion properties such as size and valence), and the relative humidity. Because the interlayer is expansible, montmorillonite-containing soils can undergo as much as a 30% volume change due to wetting and drying. Given its expansive properties, montmorillonite is an ideal candidate for examining the effects of treatment with various stabilizer chemicals.

The bulk montmorillonite was purchased in 50-lb bags from Baroid Drilling Fluids, Inc., of Houston, Texas. The material is an odorless, dry, grayish-tan powder sold under the name of “Quik Gel.” The soil, predominantly sodium montmorillonite, is a finely ground, high-yield bentonite excavated in Wyoming (CAS No. 1302-78-9). The MSDS states that the soil contains 2% to 6% crystalline quartz or silica, has a specific gravity of 2.5, and has a pH of 8.9 in a 3% solution. Compaction test results indicated that a higher specific gravity would be more appropriate, so a value of 2.77 was assumed, based on values reported by Grim (1968) and Olson and Mesri (1970).

2.5. NATIVE TEXAS SOILS

TX Bryan HP

The TX Bryan HP soil was supplied in November 1999 by the Bryan District of TxDOT. This natural soil was excavated along State Highway 21 (limits BS6-R to FM 158) in Brazos County, Texas. The TX Bryan HP is a dark brown, sandy clay. Very fine, clear sand particles are present with occasional larger pink sand particles. The clay was dried and pulverized for testing, but was not sieved to remove the larger sand fraction. A specific gravity of 2.70 was assumed. Because a limited quantity of this soil was available, some of the untreated clay used in the initial tests was dried and reused in preparing treated specimens for later tests.

TX Mesquite HS HP

The TX Mesquite HS HP was supplied in November 1999 by the Dallas District of TxDOT. This natural soil was excavated from a slope failure on the west side of FM 1382 in Dallas County, Texas. The TX Mesquite HS HP is a yellowish-brown, sandy clay with fine sand grains and has a high sulfate content. A specific gravity of 2.75 was assumed. The clay was dried and pulverized for testing, but was not sieved to remove the larger sand fraction.

Sulfate Content

The sulfate contents of the Bryan and Mesquite soils were determined by the Nutrient and Elemental Analysis Laboratory at Cornell University. The measurements involved microwave digestion in hydrofluoric acid (HF), to dissolve all solid materials (USEPA 2002, Standard Method 3052), then measuring the sulfur in the remaining aqueous solution using an Inductively Coupled Plasma (ICP) Atomic Emission Spectrometer.

The results showed that the Bryan clay had a sulfate content of 281 microgram S per gram of soil (843 µg sulfate/g soil). The Mesquite clay had a much higher sulfate content of 40,810 µg sulfate/g soil (4.081% sulfate by weight).

Table 2-1. Liquid stabilizer products considered for study

<i>Product Name</i>	<i>Stabilizer Type</i>	<i>Supplier</i>
<i>ABS-65</i>	Polymer	Southwest Envirotech Services, Inc.
<i>Base Seal</i>	Polymer	Base-Seal International Houston, Texas
<i>Bio-Cat</i>	Enzyme	Soil Stabilization Products Co. (<i>Product no longer available</i>)
<i>Chemical Injection Stabilization (CIS)</i>	Potassium	Hayward Baker, Inc. Fort Worth, Texas
<i>ClayPack DuraPack (?)</i>	Enzyme	Soil Bond International Texas
<i>Condor SS</i>	Ionic (Sulfonated Oil)	Earth Science Products Corp. (manufacturer) Pro Chemical Stabilization Co. (distributor)
<i>Consolid 444</i>	Ammonium Chloride	American Consolid, Inc. Iowa
<i>EcSS 3000</i>	Ionic	Environmental Soil Stabilization, LLC Arlington, Texas
<i>EMC²</i>	Enzyme	Soil Stabilization Products Co. Merced, California
<i>Perma-Zyme 11X</i>	Enzyme	ENFRA, LLC Anaheim, California (previously The Charbon Group, LLC)
<i>Polybuilt 4178</i>	Polymer	Exxon (<i>Product no longer available</i>)
<i>PSCS-320</i>	Enzyme	Alpha Omega Enterprises
<i>Road King</i>	Ionic?	Jeff Brink, Victoria, Texas (<i>Product no longer available</i>)
<i>Road Oyl</i>	Mineral Pitch	Road Products Corp (manufacturer) Soil Stabilization Products (distributor)
<i>Roadbond EN-1</i>	Ionic (Sulfonated Oil)	Roadbond International Arkansas (previously CSS Technology, Inc)
<i>SA44-LS40</i>	Ionic	Dallas Roadway Products Dallas, Texas
<i>Soil Seal</i>	Polymer	Soil Stabilization Products Co. Merced, California
<i>SS-13/WA-13</i>	Polymer + Enzyme	Soil Science International Arkansas
<i>Top Seal</i>	Polymer	Soils Control International Killeen, Texas
<i>Top Shield</i>	Polymer	Base-Seal International Houston, Texas

Table 2-2. Dilution and application rates of the stabilizer products evaluated

<i>Stabilizer Type</i>	<i>Ionic</i>	<i>Enzyme</i>	<i>Polymer</i>
Specific gravity of concentrated product	1.70	1.07	1.15
Supplier's recommended dilution (volume of concentrated product per volume of water)	$\frac{1}{300}$	$\frac{1}{1,000}$	$\frac{1}{30}$
Equivalent Dilution Mass Ratio (DMR)	$\frac{1}{176}$	$\frac{1}{935}$	$\frac{1}{26}$
Supplier's recommended application rate	1 gallon of product, when diluted, treats 30 yd ³ of soil	1 gallon of product treats 165 yd ³ of material	1.0 to 1.75 fluid ounces per cubic foot of soil
Equivalent Application Rate (% per dry weight of soil) ^a	0.02%	0.002%	0.1%
Equivalent Application Mass Ratio (AMR) ^a	$\frac{1}{6,000}$	$\frac{1}{50,000}$	$\frac{1}{1,000}$

^a Computed assuming a typical soil dry unit weight of 100 pcf (16 kN/m³).

Table 2-3. Test soils used in evaluating the liquid stabilizers

<i>Soil</i>			<i>Source</i>
<i>Reference Clays</i>	<i>Repository Samples</i>	Kaolinite	"KGa-1b Kaolinite" from Washington County, Georgia
		Illite	"IMt-2 Illite" from Silver Hill, Montana
		Montmorillonite	"SWy-2 Na-Montmorillonite" from the Newcastle formation, Crook County, Wyoming
	<i>Bulk Samples</i>	Kaolinite	"Hydrite R" from Dry Branch Kaolin Co.
		Illite	Natural deposit acquired near Fithian, Illinois
		Montmorillonite	"Quik-Gel Bentonite" from Baroid Drilling Fluids, Inc.
<i>Native Texas Soils</i>	TX Bryan HP		Natural, mixed clay acquired from Bryan, Texas
	TX Mesquite HS HP		Natural, mixed clay acquired from Mesquite, Texas

Table 2-4. Chemical-physical properties of reference clay minerals

<i>Property</i>	<i>Kaolinite</i>	<i>Illite</i>	<i>Montmorillonite</i>
Size (μm)	0.5–5.0	0.02–2.0	0.01–1.0
Shape	Hexagonal crystals	Irregular flakes	Flakes
External surface area (m^2/g)	10–30	70–100	70–120
Internal surface area (m^2/g)	–	–	550–650
Plasticity	Low	Medium	High
Cohesiveness	Low	Medium	High
Swelling capacity	Low	Low to none	High
Unit-layer charge	0	1.0–1.5	0.5–0.9
Interlayer (C) spacing (nm)	0.7	1.0	1.0–2.0
Bonding	Hydrogen	Potassium ions	Van der Waal's bonds (weak attractive force)
Net negative charge (cmol/kg)	2–5	15–40	80–120

Source: Juma 1998.

Table 2-5. Index properties of test soils

Soil	USCS Classification ^a	Atterberg Limits ^b			Compaction ^c	
		PL	LL	PI	OWC (%)	γ_{dmax} (pcf)
Bulk kaolinite	Elastic silt (MH)	32	51	19	24	98.7
Bulk illite	Lean clay (CL)	24	44	20	12	124.5
Bulk montmorillonite	Fat clay (CH)	32	567	535	24	96.8
TX Bryan HP	Fat clay (CH)	20	68	48	16	115.0
TX Mesquite HS HP	Fat clay (CH)	23	60	37	17	112.0

^a Unified Soil Classification System (ASTM D 2487, 1998c).

^b Plastic Limit, Liquid Limit, and Plasticity Index (ASTM D 4318, 1998e).

^c Optimum water content (OWC) and maximum dry unit weight (γ_{dmax}) for compaction with a modified Proctor effort (ASTM D 1557, 1998b).

CHAPTER 3

CHEMICAL CHARACTERIZATION OF PRINCIPAL PRODUCT CONSTITUENTS

3.1. OVERVIEW

The chemical stabilizers selected for this study were tested using various analytical techniques to identify the primary (or active) ingredients and to evaluate both physical and chemical characteristics of the stabilizers. Samples of the stabilizers were obtained from their respective commercial manufacturers. Due to the range of stabilizers used in this research, a number of analytical techniques were used to help identify the properties and composition of the stabilizers. The analytical techniques included pH, conductivity, ion chromatography (IC), potentiometric titrations, total organic carbon (TOC) analysis, Fourier transform infrared (FTIR) spectroscopy, gas chromatography/mass spectrometry (GC/MS), high performance liquid chromatography/mass spectrometry (HPLC/MS), gel permeation chromatography (GPC), UV/Vis Spectroscopy, and nuclear magnetic resonance (NMR) spectroscopy, as appropriate. In addition, proposed stabilizer components were either synthesized in the laboratory or purchased from chemical suppliers and analyzed using the appropriate techniques identified above to confirm the proposed composition of each stabilizer. Results from the analyses of the stabilizers and the stabilizer components are presented in this chapter.

3.2. REVIEW OF MANUFACTURERS' LITERATURE

The first step in selecting the appropriate analytical techniques for characterizing each of the stabilizers was to review manufacturers' literature, Material Safety Data Sheets (MSDS), and previous research reports to identify potential active ingredients. For example, review of the available information for the ionic stabilizer indicates that it is produced by reacting sulfuric acid with d-limonene, an aromatic oil that is a by-product of citrus processing. A patent search provided a recipe for a sulfonated limonene-based stabilizer of 3% limonene to 97% sulfuric acid, by volume (U.S. Patent #4,941,924). This product, also referred to as sulfonated limonene, was synthesized in the laboratory because no primary standard was commercially available. The analytical techniques used to characterize the ionic stabilizer were also applied to sulfonated limonene. Sulfuric acid was also tested to assist in characterizing the commercial stabilizer product.

The manufacturer-supplied literature for the selected polymer stabilizer indicated that the stabilizer contained sodium silicate components. Sodium silicate solution 42° Baume (The Chemistry Store, Pompano Beach, Florida) was evaluated using the same analytical procedures used to test the polymer stabilizer. The same dilution ratio used to prepare the polymer stabilizer was also used for the sodium silicate samples.

The manufacturer's literature for the selected enzyme stabilizer indicated that it was a "non-toxic, non-hazardous, non-flammable, organic product with an enzyme base and dispersant in a water base solution." Specific information regarding the stabilizer contents was unavailable. However, the results of the chemical characterization suggested that one of the major components of the enzyme stabilizer was polyethylene glycol. A sample of polyethylene glycol

(average molecular weight = 570 to 630) was obtained from EM Science (Gibbstown, New Jersey) and analyzed to verify these findings.

The selection of the specific chemical analyses used to characterize each of the stabilizers was based on the information described above. Table 3-1 presents the matrix of analyses performed on each of the stabilizers. In addition, substances that were suspected to be major components based on review of the literature (sulfonated limonene and sulfuric acid for the ionic stabilizer and sodium silicate for the polymer stabilizer) or determined to be major components during the analytical testing (polyethylene glycol for the enzyme stabilizer) were analyzed using the appropriate techniques identified in Table 3-1.

3.3. CHEMICAL CHARACTERIZATION METHODS

pH and Conductivity

An Orion model 720A pH meter and Orion Sure-flow Ross® semi-micro pH Model 8175 BN pH probe were used to measure pH for this study. The pH meter was standardized using commercially available pH buffers. Three pH buffers (pH 4, pH 7, and pH 10) were used to standardize the instrument prior to each use. The pH of the enzyme stabilizer and the polymer stabilizer were measured at the manufacturer's recommended dilution ratio (see Chapter 2, Table 2-2). The pH measurement taken for the ionic stabilizer at the recommended dilution ratio (1:300) would have been outside the range of reliable pH measurement for the instrument. The pH electrode specifications indicate incompatibility with solutions more than 1M in strong acid. As a result, 1:500 dilutions were made for the ionic stabilizer and its components.

Conductivity readings were obtained using a Radiometer Copenhagen Meter Lab™ CDM230 Conductivity Meter. The instrument was calibrated using a standard KCl solution. Samples were diluted using the same ratios used for pH measurement.

Potentiometric Titrations

Potentiometric titrations were conducted for the ionic, polymer, and enzyme-based stabilizers, as well as for the components, to determine the acid/base characteristics of the samples. The ionic stabilizer, sulfuric acid, and sulfonated limonene samples were diluted using carbon dioxide-free ultrapure water and the same dilution ratio as for the pH measurements (1:500). Ultrapure water was prepared by passing distilled water through a Millipore (Millipore Corp., Bedford, Massachusetts) water treatment system containing a combination of ion exchange and reverse osmosis columns and Millipore's patented electrodeionization technology. Carbon dioxide-free water was used to reduce the formation of carbonic acid that may affect the titration results. The carbon dioxide-free water was obtained by boiling ultrapure water.

Although there were no visible precipitates, the ionic stabilizer and sulfonated limonene samples were then filtered through a 0.07 μm cellulose filter to remove any precipitates that may have formed. The sulfuric acid, sulfonated limonene, and ionic stabilizer samples were placed on mechanical stirrers overnight in a nitrogen glove box. The remainder of the titration procedure was conducted under a nitrogen blanket to minimize carbon dioxide contamination. Titrations were conducted on 50 mL samples of each diluted stabilizer by adding aliquots (30 μL to 0.5 mL) of acid or base and recording the pH. The titration was carried out using either standardized

sodium hydroxide (DILUT-IT® Analytical Concentrate, Baker Scientific), or hydrochloric acid (DILUT-IT® Analytical Concentrate, Baker Scientific).

Ion Chromatography

Based on the pH results and manufacturer's literature for the ionic stabilizer, ion chromatography was employed to analyze sulfate in the ionic stabilizer, the synthetically prepared sulfonated limonene sample, and sulfuric acid. Sulfate analysis was performed using a Waters Millenium HPLC system, a Waters IC-PAK™ Anion column (Part #WAT026765, Waters Corporation, Bedford, Massachusetts) and a Waters 432 Conductivity Detector. The amount of sulfate in the samples was determined by comparing the conductivity detector response of the samples to a series of standards prepared using reagent-grade sodium sulfate. Sulfate analysis of the samples was performed using dilutions of 1:10,000, and all of the results were well within the standard calibration curve.

Total Organic Carbon

Total organic carbon (TOC) analysis was selected for stabilizer characterization to identify and determine the amount of carbon in the stabilizers and was measured for all three stabilizers as well as the sulfonated limonene sample prepared in the laboratory. The method used to analyze organic carbon involves oxidizing the organic carbon in the sample to carbon dioxide (CO₂) and determining the amount of CO₂ in the oxidized sample using an infrared spectrophotometer. The oxidation of the organic carbon was performed by high-temperature (680°C) combustion using a Tekmar-Dohrman Apollo 9000 TOC Combustion Analyzer (Tekmar-Dohrman, Cincinnati, Ohio) with an autosampler and a boat sampler (which allows for analysis of solid samples). In order to distinguish inorganic carbon from organic carbon in the sample, the instrument runs two analyses of the sample. The total amount of carbon (organic and inorganic) in the sample is measured in the first analysis. The pH of the sample is then reduced using phosphoric acid and purged with inert gas to convert all inorganic carbon to carbon dioxide and strip the carbon dioxide from the sample, respectively. Total organic carbon is then calculated from the difference between total and inorganic carbon.

Aliquots (200 µL) of the ionic stabilizer and sulfonated limonene samples (each diluted at 1:500) were injected into the instrument through an autosampler. The polymer stabilizer was analyzed in concentrated form. The polymer and enzyme stabilizers were both analyzed for TOC using the boat sampler with a sample volume of 40 µL. The boat method was used for the polymer stabilizer to avoid plugging the syringe and for the enzyme stabilizer to avoid foaming of the sample. Separate calibration curves for the boat sampler and the autosampler were prepared using potassium hydrogen phthalate (Alfa Aesar, Ward Hill, Massachusetts) standard solutions at concentrations ranging from 25 to 200 mg/L. The resulting curves showed good linearity at $R^2 = 0.9997$ or better for the autosampler and $R^2 = 0.9995$ or better for the boat sampler.

Fourier Transform Infrared Spectroscopy (FTIR)

Fourier transform infrared spectroscopy (FTIR) is a technique used to identify organic functional groups by measuring the absorption at characteristic wavelengths of bonds and

functional groups that vibrate independently of one another. FTIR was performed for all three stabilizers (ionic, polymer, and enzyme) and sulfonated limonene using a Perkin Elmer Spectrum 2000 instrument. The instrument was operated with a resolution element of 8 cm^{-1} and a J-Stop resolution of 6.48 cm^{-1} . The concentrated, undiluted stabilizers were extracted with chloroform and applied to polytetrafluoroethylene (PTFE) IR cards furnished by West Georgia Laboratories (Willis, Texas). The card was inserted in the instrument and analyzed with absorbance measured at characteristic wavenumbers between 450 and $6,500\text{ cm}^{-1}$. For the polymer stabilizer, the procedure was slightly different than that used for the other stabilizers to enable evaluation of a more concentrated sample. The polymer was allowed to harden by exposing it to the air and evaporating the water for one week under a vent hood to avoid contamination. The hardened polymer stabilizer was then pulverized and affixed to the IR card with chloroform.

Gas Chromatography/Mass Spectroscopy (GC/MS) and High-Performance Liquid Chromatography/Mass Spectroscopy (HPLC/MS)

Chromatography is a common technique employed for separating complex mixtures. In this process a sample is transported in a mobile phase (gas or liquid) in contact with an immiscible stationary phase fixed in a column. The mobile and stationary phases are selected based on the properties of the sample being evaluated, so that the components of the sample distribute between both phases with different affinities for the immobile phase. The mobile phase is transported through the column under pressure. The components that exhibit an affinity towards the stationary phase move at a slower rate through the column. As a result of differences in mobility, the sample components separate into discrete bands by the time they exit from the column. A detector residing downstream of the column responds to effluent concentrations from the column and provides a signal that can be calibrated for each species and used to quantify concentrations. The plot of the detector signal, typically referred to as a chromatogram, includes a series of peaks associated with the various sample components as a function of elution volume (or elution time for constant flowrate). The peak positions on the time axis are used to identify sample constituents, and the peak areas provide a quantitative measurement of each sample component.

A variety of detectors are available for liquid and gas chromatographs. However, in this research both liquid chromatography and gas chromatography procedures employed a mass spectrometer (MS) as the detector. In a mass spectrometer compounds are fragmented, and the fragmented ions are transferred into a mass analyzer (e.g., a quadrupole or ion trap mass analyzer) that separates charged molecules according to their mass-to-charge ratio (m/z). Ions of the various m/z values exit the analyzer and are “counted” by the detector, producing a mass spectrum. A mass spectrum displays the relative abundance of ions of different m/z produced by the fragmentation process. The spectrum for a particular molecule is unique and represents a “chemical fingerprint” of the compound. Thus, the detector can be used to provide molecular weight, and structural and quantitative information for compounds that have been separated by the gas chromatograph. The mass spectrometer used in conjunction with the gas chromatograph (Hewlett-Packard Model 5890) was a quadrupole mass spectrometer (Hewlett-Packard 5972 MSD). In the HPLC/MS tests, the mass spectrometer measurements were made by electron ionization.

Samples of the ionic stabilizer, sulfuric acid, and sulfonated limonene were analyzed using GC/MS to determine the presence (or absence) of limonene and other organic solutes. (R)

(+) limonene obtained from Aldrich Chemical (Sigma-Aldrich Corp., St. Louis, Missouri) was analyzed as a primary standard. The sulfuric acid was tested as a control. A sample of the synthetically prepared sulfonated limonene was also analyzed using GC/MS to ensure that all limonene was converted to the sulfonated product.

Prior to injection into the GC/MS, samples were extracted with methylene chloride, which is appropriate for analysis of hydrophobic compounds such as limonene. A sample of the extract was injected into the GC (Hewlett Packard Model 5890) containing an SGE 30m x 0.35mm ID BPX5 (nonpolar) column. The helium carrier gas was set at 35.1 psi. The injector temperature was ramped from 50°C to 310°C. The oven was initially set at 35°C, ramped at 15°C/min to 175°C, 20°C/min to 250°C, 30°C/min to 310°C, and then held at 310°C for 11.5 minutes. The MS (Hewlett Packard Model 5972) detector temperature was set at 280°C. Mass spectrograms were compared to Hewlett Packard NB S75K spectra library and to the sample of (R) (+) limonene purchased from Aldrich.

All three stabilizers and the sulfonated limonene sample were analyzed using HPLC/MS at the Mass Spectrometer Facility at the University of Texas at Austin. To enable better detection results, the samples were analyzed in concentrated form. The HPLC/MS instrument used was a Varian 9000 Series HPLC Interface 2 with Finnigan MAT (San Jose, California) LCQ Mass Spectrometer. In chromatography the average rate at which a solute migrates down the column depends upon the relative affinity of the solute for the mobile phase compared to the stationary phase. To maximize separation on a particular column, the composition of the mobile phase can be varied during the course of the analysis. Separation efficiency in this study was enhanced by dual solvent gradient elution, which involves combining two solvent systems that differ in polarity. Solvent A contained 99% water, 1% acetonitrile, and 0.1% trifluoroacetic acid (TFA), and solvent B contained 90% acetonitrile, 10% water, and 0.1% TFA. The mobile phase gradient consisted of initiating the analysis with 99% solvent A, reducing the proportion of solvent A to 10% over 25 minutes, holding this composition of the mobile phase for 10 minutes, then ramping back up to 99% solvent A over a one-minute time period.

This study used a C18 column with an eluent flow of 100 μ L/min. Results were provided for full MS and chemical ionization mass spectrometry (CI/MS). Chemical ionization employed an electron beam to ionize methane at a pressure of 3 torr. The ionized methane in turn collided with the sample eluent, ionizing the sample species for MS. This approach results in less fragmentation of the sample species than direct ionization with the electron beam.

The enzyme stabilizer was fragmented using fast atom bombardment (FAB) at the Mass Spectrometer Facility to confirm the CI/MS results. In FAB the enzyme constituents were ionized by bombardment with energetic argon atoms releasing positive and negative analyte ions. FAB treatment provides rapid sample heating and desorption and reduces sample fragmentation. This feature enables the analysis of high-molecular-weight, polar species, if present.

Gel Permeation Chromatography (GPC)

Gel permeation chromatography (GPC) is a size-exclusion chromatography technique that uses nonpolar organic solvents and hydrophobic packings to separate higher molecular weight molecules from lower molecular weight molecules. This technique was used in this research to determine the molecular weight distribution of the enzyme stabilizer. In particular, if

the enzyme stabilizer contained high molecular weight proteins, then a high molecular weight peak would be apparent in the GPC chromatogram.

The GPC system consisted of two Polymer Laboratories Plgel 10 μ m Mixed B columns connected in series with a Visotek Model 250 Dual Refractometer/Viscometer as the detector. The enzyme sample was diluted in 10 mL tetrahydrofuran and injected in the system. Tetrahydrofuran was used as the mobile phase, and the samples were run for 25 minutes at a flow of 1 mL/min. The results were presented as retention volume versus detector response. The dual detector responds to changes in the fluid density/refractive index and viscosity as the sample species elute from the column.

UV/Vis Spectroscopy

UV/Vis spectroscopy was employed to characterize inorganic and organic stabilizer constituents of the stabilizers by comparing absorption spectra (plots of absorbance vs. wavelength) to known spectra or absorbance wavelengths for specific chromophoric functional groups. UV/Vis spectroscopy was conducted for all three stabilizers and the synthetically prepared sulfonated limonene. For UV/Vis spectroscopy analysis of sulfonated limonene and the ionic stabilizer, it was necessary to remove the chemical constituents causing the dark black color of the ionic stabilizer. This was accomplished by increasing the pH of the sample to 10 with 1N NH_3 , followed by extracting one mL of the sample with 10 mL methylene chloride. The methylene chloride layer was retained and one mL of this methylene chloride extract was diluted in 10 mL of methylene chloride, which resulted in 1:100 dilution of the ionic stabilizer, after pH adjustment. In all of the analyses, ultrapure water was used as a blank, and the samples were analyzed on a Perkin-Elmer Lambda 3B UV/Vis spectrophotometer. Wavelengths were scanned from 190 nm to 500 nm using 2 to 5 nm increments where absorbance was above baseline and 10 nm increments for the remainder of analysis.

Nuclear Magnetic Resonance (NMR) Spectroscopy

Nuclear magnetic resonance (NMR) spectroscopy is used to identify functional groups of chemical species by evaluating a sample's magnetic properties. A spinning charged nucleus behaves as a magnet, and nuclei with nonzero spin can be caused to switch energy levels between quantized spin numbers. In NMR the sample is exposed to a magnetic field that allows the atomic nuclei with nonzero spin to absorb electromagnetic radiation, causing the nuclei to switch spin states. This is useful for species containing protons, carbon, or silica and corresponding to ^1H NMR, ^{13}C NMR, or ^{29}Si NMR. The observed NMR frequency of a given nucleus in different parts of a molecule shifts as a result of interactions with fields produced by electrons and other neighboring nuclei. These chemical shifts allow the types of bonds to be identified (McBride 1995). Based on the bonding structure of chemical species in a sample, constituents containing magnetic nuclei can be identified according to σ (screening constant), which is a function of magnetic resonance. Common chemical shifts of ^1H in organic compounds are presented in Figure 3-1.

NMR was used to identify functional groups for all three stabilizers, sulfonated limonene, and sodium silicate. Each sample was extracted using deuterated water (D_2O) prior to analysis. For the ionic stabilizer, enzyme stabilizer and sulfonated limonene, ^1H and ^{13}C NMR analyses were performed using a Varian Unity Inova 500 instrument. The operating frequency was 499.35

MHz. For characterization of the polymer stabilizer and sodium silicate, a Bruker AMX500 Series instrument was employed in performing a ^{29}Si NMR analysis. The operating frequency was 99.3 MHz with a 2-centimeter slice from the center of the sample being analyzed by the instrument.

3.4. CHARACTERIZATION OF THE IONIC STABILIZER

The analytical experiments used to characterize the ionic stabilizer were pH, potentiometric titrations, sulfate analysis, TOC, UV/VIS, FTIR, HPLC/MS, GC/MS, and NMR. The results for the characterization of the ionic stabilizer were compared to a synthetically prepared sulfonated limonene sample and sulfuric acid. The synthesized sample was prepared at 3% limonene and 97% sulfuric acid (by volume). This represents the same total-sulfur:total-carbon ratio as that reported in the patent for the ionic stabilizer.

Gas Chromatography/Mass Spectroscopy (GC/MS) Results for the Ionic Stabilizer

The synthesized sulfonated limonene was initially analyzed using GC/MS, and the results were compared to a sample of (R) (+) limonene obtained from Aldrich (Milwaukee, Wisconsin). The results presented in Figure 3-2b confirmed that the first major peak located in the GC chromatogram of the limonene sample in Figure 3-2a (at a retention time of 8.19 minutes) was limonene. The absence of the limonene peak in the GC chromatogram of the synthesized sulfonated limonene sample in Figure 3-2a verified complete sulfonation of limonene species. GC/MS analyses were also performed on the ionic stabilizer. No limonene was detected in the sample; however, the presence of hexamethylcyclotrisiloxane ($(\text{C}_6\text{H}_{18})_3\text{Si}_3$) and its derivatives were detected in the second and subsequent rounds of GC/MS analyses of the sulfonated limonene and the stabilizer.

Results indicating the presence of a siloxane component in both the sulfonated limonene and the ionic stabilizer were unexpected. The first round of analyses of the ionic stabilizer, polymer stabilizer, and limonene did not identify siloxane in the GC/MS results. It was hypothesized that the source of the siloxanes was the GC column. Indeed, strong acids can catalyze the breaking of Si-O bonds associated with the stationary phase of the column and lead to column bleed. However, to be certain that the presence of the siloxanes was attributable to column deterioration rather than a stabilizer component, proton NMR results were reviewed. Eighteen protons are attached to the chemical configuration of hexamethylcyclotrisiloxane, and the proton NMR peak for this chemical is located between 0 and 0.1 ppm. Evaluation of the ionic, polymer, and enzyme stabilizers indicated that none of the proton NMR spectra exhibited a peak in the range of 0 to 0.1 ppm. Thus, it could be reasonably concluded that the stabilizers did not contain hexamethylcyclotrisiloxane, and its detection in samples was associated with column deterioration.

pH and Conductivity Results for the Ionic Stabilizer

Conductivity and pH were measured for sulfuric acid, sulfonated limonene, and the ionic stabilizer. The pH of the samples was measured prior to and after filtration. The conductivity of the samples was measured prior to filtering. The measurements were obtained in triplicate, and

the average pH and conductivity results are reported in Table 3-2. The low pH and high conductivity are consistent with the presence of strong acid in the system (Kota 1996).

The results indicate a decrease in pH after filtering. A possible explanation for this is that the acid dissolved some of the cellulose filter, which then adsorbed some of the protons. As a result, post filtration pH measurements were not considered reliable.

Potentiometric titrations were performed in order to determine the concentration of acid in the system and to identify the acid. Triplicate experiments were conducted and are presented in Appendix F. Figure 3-3 presents the potentiometric titration results for one experiment for a sample of ionic stabilizer, sulfonated limonene, and 2 normal (2N = 1 molar = 1M) sulfuric acid. The amount of base required to reach the equivalence point (located at the vertical inflection point in Figure 3-3) can be used to determine the concentration of acid in the system. The titration was carried out using 1 N NaOH. The initial volume for each of the samples was 50 mL of a 1:500 diluted solution. A single inflection (equivalence) point of the titration data occurs at pH 7 for all of the samples, indicating the presence of a strong acid. The volume of 1N NaOH titrant required to reach the equivalence point for the samples varied between 3.02 ml for the ionic stabilizer to 3.34 ml for the concentrated sulfuric acid. The hydrogen ion concentrations corresponding to these volumes of 1N NaOH for the samples are presented in units of equivalent acid normality and molarity in Table 3-3. The following equation was used to calculate the acid concentration of the diluted samples:

$$\text{Normality}_{\text{Sample}} = \text{Volume}_{\text{Titrant}} \times 1\text{N}_{\text{NaOH}} / \text{Volume}_{\text{Sample}}$$

The results indicate that the acidity of the stabilizer (and the sulfonated limonene) is lower than concentrated sulfuric acid, and the acidity of the sulfonated limonene prepared in the laboratory and the ionic stabilizer are similar. However, sulfonated limonene contains a slightly higher concentration of acid. This observation was confirmed by sulfate analysis.

Ion Chromatography Results for the Ionic Stabilizer

Sulfate analysis by ion chromatography was conducted for the ionic stabilizer and the sulfonated limonene. Sulfate analysis was conducted in triplicate for each sample, and the average and standard deviation of these measurements are reported in Table 3-4. The ion chromatography method used for sulfate analysis detects sulfate, but compounds in which sulfate is bound to organics (such as those attached to limonene) are not detected. The results indicate that sulfate is a significant component of the ionic stabilizer. The sulfonated limonene sample prepared in the University of Texas Environmental and Water Resources Engineering (EWRE) laboratory contained a higher concentration of sulfate even though the same ratio of sulfuric acid to limonene was used in the preparation as that reported in the patent for the ionic stabilizer. Only 35% of the sulfate added in the form of H₂SO₄ was incorporated into limonene for the sample prepared in the EWRE laboratory. The remainder of the sulfuric acid (65%) that was added during the preparation of the sulfonated limonene sample was detected and quantified with sulfate analysis. However, the difference between the sulfate concentration for sulfonated limonene and the ionic stabilizer was less than 5%.

Total Organic Carbon Analysis Results for the Ionic Stabilizer

The chemical analyses conducted support the hypothesis that sulfonated limonene was a major component of the ionic stabilizer. Since sulfonated limonene is an organic compound, total organic carbon (TOC) analyses were conducted on filtered and unfiltered samples for both sulfonated limonene and the ionic stabilizer. Three replicates were analyzed for the ionic stabilizer (unfiltered) and filtered and unfiltered sulfonated limonene samples. Average values of TOC for each are presented in Table 3-5. Three samples were also analyzed for the ionic stabilizer (filtered). However, one of the results differed by 14%. The remaining two sample results were averaged, and the result is reported in Table 3-5.

After correcting for the dilution factors to determine the TOC values for the original concentrated solutions, the TOC results for unfiltered and filtered ionic stabilizer were approximately 42,000 mg/L and 41,000 mg/L, respectively. These results suggest that there was minimal carbon loss for the ionic stabilizer due to filtration. The TOC results for the sulfonated limonene unfiltered and filtered sample were determined to be approximately 16,000 and 7,000 mg/L, respectively. Hypothesis testing was conducted to determine whether the means of the unfiltered sample results were statistically different from the filtered sample results. A 95% confidence level was selected as the criteria for significance, and the results of the hypothesis test indicated that the filtered and unfiltered means for the ionic stabilizer were not statistically different. In contrast, the hypothesis that the filtered and unfiltered samples were the same was rejected at the 95% confidence level for the sulfonated limonene.

Thus, it was determined that significant carbon loss occurred upon filtration of the sulfonated limonene samples. The number of sulfate groups attached to the limonene or polymerization after sulfonation may explain these results. The formation of larger molecules due to either polymerization or addition of multiple sulfate groups may render the chemical less soluble in water. If these less soluble chemical species precipitated, then they would be removed by filtration, thus removing some of the organic fraction from the sulfonated limonene samples. Overall, the sulfonated limonene sample exhibits a much lower organic carbon content than the ionic stabilizer. This is supported by comparing the carbon:sulfur ratio based on molarity of sulfonated limonene (1.3:13.6) with the ionic stabilizer (3.5:12.9). According to the calculated carbon:sulfur ratios, it can be inferred that the sulfonated limonene sample contains more sulfate per mole of sulfonated limonene.

UV/Visible and Fourier Transform Infrared Spectroscopy Results for the Ionic Stabilizer

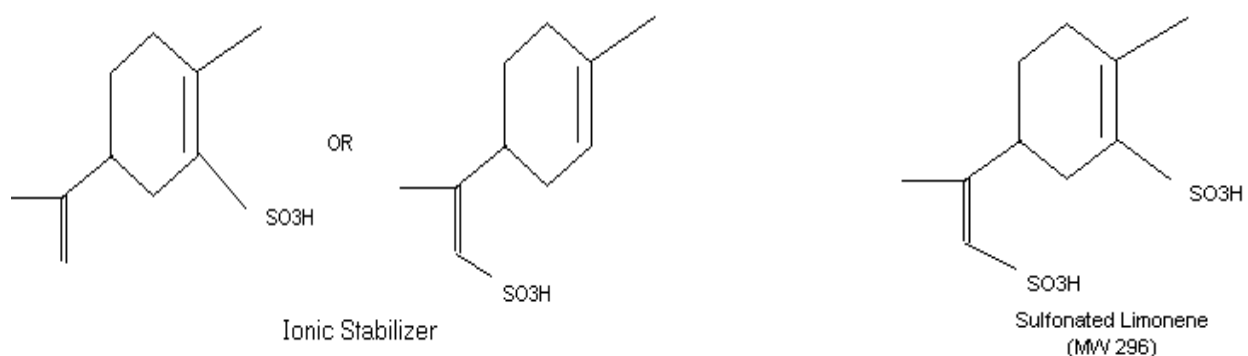
UV/Vis spectroscopy was used to evaluate the sulfonated limonene sample and the ionic stabilizer. As mentioned above, it was necessary to modify the ionic stabilizer solution by adding ammonium hydroxide and extracting with methylene chloride. Care was taken to ensure that the dilution rates were consistent. The UV/Vis spectroscopy results, presented in Figure 3-4, show that sulfonated limonene and the ionic stabilizer share similar chemical species that absorb in the UV/Vis range of 260 to 270 nm and at 330 nm. However, there are differences that could not be explained by UV/Vis spectroscopy, such as the absence of the peak from the sulfonated limonene at 240 nm and the slight shift in the 270 nm peak identified for sulfonated limonene to 280 nm for the ionic stabilizer. Due to these differences, a more sophisticated analysis using FTIR was employed to further characterize organic components in the ionic stabilizer and sulfonated limonene sample.

The FTIR results for sulfonated limonene and the ionic stabilizer were very similar, as shown in Figure 3-5. The sharp peaks at 1150 cm^{-1} and 1200 cm^{-1} and a broad peak at 3400 cm^{-1} indicate the presence of a sulfonic acid functional group ($\text{R-SO}_2\text{H}$). Thus, it was still not clear why there were differences in the UV/Vis spectra.

Proton NMR and HPLC/MS Results for the Ionic Stabilizer and Sulfonated Limonene

Proton (^1H) NMR spectroscopy was conducted for the sulfonated limonene and the ionic stabilizer to confirm the FTIR results and identify additional functional groups. Several functional groups were identified, as presented on the NMR spectrum in Figure 3-6.

Based on the ^1H NMR analysis, the following chemical structures were proposed for the major component of the ionic stabilizer and sulfonated limonene:



HPLC/MS was then performed to validate the hypothesized chemical structures. Limonene (MW 137) was used as a standard in this analysis. The molecular weight of 137 g/mole was confirmed using HPLC/MS. The MS results confirmed the ionic stabilizer molecular weight of the major component to be 215 g/mole, as in Figure 3-7a. The HPLC/MS results for sulfonated limonene similarly confirmed a molecular weight of 296 g/mole as indicated in Figure 3-7b. The sulfonated limonene sample that was evaluated using HPLC/MS was unfiltered. Thus, the results suggest that the differences observed in the UV/Vis spectra for the sulfonated limonene and the ionic stabilizer are due to the differences in the chemical structure of the compounds. In the sulfonated limonene sample prepared in the EWRE laboratory, two sulfate groups are present, whereas only one sulfate group is present on the ionic stabilizer sulfonated limonene molecules.

Summary of Results for the Ionic Stabilizer

The above analytical techniques were successful in characterizing the ionic stabilizer. The ionic stabilizer is a sulfonated limonene species with one sulfate substitution, rather than the two sulfate-substituted sulfonated limonene that was synthesized in the EWRE laboratory. The sulfate analysis and potentiometric titrations confirm that the ionic stabilizer contains less sulfate than sulfonated limonene. Both proton NMR and FTIR results confirm the presence of sulfur group species attached to an organic chemical for both sulfonated limonene and the ionic stabilizer. The HPLC/MS results provided the molecular weight of sulfonated limonene and the ionic stabilizer, which confirmed the significant organic fraction as determined by TOC results.

It is reasonable that since the ionic stabilizer has only one sulfate substitution, it has more detectable carbon groups. On the other hand, the sulfonated limonene with two sulfate substitutions has a lower volatility and is more difficult to oxidize to release the TOC (Sawyer and McCarty 1978).

3.5. CHARACTERIZATION OF THE POLYMER STABILIZER

pH, Conductivity, and Potentiometric Titration Results for the Polymer Stabilizer

The analytical procedures used to characterize the polymer stabilizer were pH, TOC, FTIR, HPLC/MS, and NMR. Three replicate pH and conductivity measurements were obtained for the polymer stabilizer and sodium silicate. The results were averaged and are presented in Table 3-6. The sodium silicate standard was similarly evaluated and compared with the polymer stabilizer. Sodium silicate was chosen as a standard based on the manufacturer's literature that identified the polymer stabilizer as a sodium silicate solution.

The results of the pH measurements are consistent with the presence of a base such as silicate. Potentiometric titrations were attempted by adding 0.5 mL to 30 μ L increments of 1N HCL and recording the pH. However, the sample crystallized around pH 6, which prevented accurate pH measurements from being taken.

Total Organic Carbon Analysis Results for the Polymer Stabilizer

TOC analysis was used to determine if the polymer stabilizer contained a significant carbon fraction. If the predominant chemical species in the polymer stabilizer was sodium silicate, then the carbon fraction would be very small. As expected, the results indicated that the concentrated polymer stabilizer had a very small organic fraction and contained only 238 mg TOC/L.

Fourier Transform Infrared Spectroscopy, HPLC/MS and ^{29}Si NMR Spectroscopy Results for the Polymer Stabilizer

FTIR spectroscopy was conducted on the polymer stabilizer, and results (Figure 3-8) showed the presence of a number of characteristic functional groups. The functional groups identified from the peaks in the FTIR spectra of the polymer stabilizer are presented in Table 3-7.

FTIR was not conducted on sodium silicate, due to an inability to affix the sodium silicate to the IR card. The sodium silicate beaded up on the IR card and did not show any signs of drying after four days.

HPLC/MS results confirmed an m/z pattern of 136, as presented in Figure 3-9. This was identified as sodium silicate ($\text{Na}_2(\text{SiO}_4)^{-2}$) (MW 136). The repetitive peaks indicate polymeric chains comprised of sodium silicate groups. This analytical technique was successful in characterizing the polymer stabilizer as containing a significant component of sodium silicate (Na_4SiO_4).

Detection of the silicate species for both sodium silicate and the polymer stabilizer was enabled by ^{29}Si NMR, as shown in Figure 3-10. The chemical shifts of both the polymer stabilizer and sodium silicate were similar (± 0.4 ppm) and occurred at -69 ppm, -78 ppm, -86

ppm, and -95 ppm. The background peak, accounting for the sample container, was removed in an attempt to integrate the silicate peaks without background interference. Once removed, the integration was standardized to the largest area peak at -95 ppm by applying a value of 100 to this peak. The other peak areas were integrated as a fraction of the largest area peak (e.g., -85 ppm peak at 53.9, -78 ppm peak at 18.6). The integrated results for sodium silicate and the polymer stabilizer were similar.

3.6. CHARACTERIZATION OF THE ENZYME STABILIZER

pH, Conductivity, and Potentiometric Titration Results for the Enzyme Stabilizer

The analytical experiments used to characterize the enzyme stabilizer were pH, potentiometric titration, TOC, FTIR, NMR, HPLC/MS, FAB, and UV/Vis spectroscopy. The pH and conductivity measurements obtained for the enzyme stabilizer diluted 1:10,000 were 3.26 and 0.791 mS/m, respectively. This value of conductivity is in the range of high purity water.

The acidic characteristics of the enzyme stabilizer were explored further by conducting potentiometric titrations. Potentiometric titrations were conducted for the enzyme stabilizer (diluted 1:100). The sample was prepared in a volumetric flask using carbon-dioxide-free, high-purity water, filtered through a 0.7 μm cellulose filter and placed on a mechanical stirrer in a nitrogen filled glove box overnight. Next, a 50 mL aliquot was titrated using 1.0 N HCl until the pH decreased below 2. Then, 1.0 N NaOH was used to titrate the sample to high pH values. The results are presented in Figure 3-11.

The enzyme stabilizer behaved like a weak acid with an acidity constant greater than $K_a = 10^{-5}$. An inflection (equalization) point at approximately pH 8 corresponded to the addition of approximately 0.13 ml 1N NaOH. The enzyme sample thus consisted of a 0.26N acid.

Total Organic Carbon Analysis Results for the Enzyme Stabilizer

In an attempt to quantify the organic content of the enzyme stabilizer, total organic carbon analysis was performed on a diluted sample. The TOC results were attained using the boat sampling method (rather than liquid autosampler) due to difficulties controlling foaming of this sample. The TOC of the enzyme stabilizer was found to be 37 mg/L at the 1:10000 dilution. Thus, the TOC of the concentrated enzyme stabilizer was 370,000 mg/L. This result suggests a very large organic carbon fraction in the enzyme stabilizer.

Fourier Transform Infrared Spectroscopy and ^1H NMR Results for the Enzyme Stabilizer

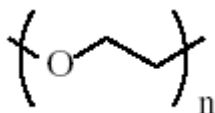
FTIR and ^1H NMR were conducted to identify organic carbon functional groups present in the enzyme stabilizer. The FTIR results shown in Figure 3-12 show a number of characteristic infrared absorption bands for common functional groups. Based on the *Journal of Optical Society* (1988), a number of functional groups were identified, as indicated in Table 3-8.

Similar results were obtained using ^1H NMR. Peaks attributable to -COH and -CH₃ were identified at 3.5 ppm and 1.1 ppm, respectively, as shown in Figure 3-13.

Gel Permeation Chromatography, HPLC/MS, and UV/Visible Spectroscopy Results for the Enzyme Stabilizer

The next step was to determine if the enzyme stabilizer contained low molecular weight species or high molecular weight species by employing gel permeation chromatography. The GPC results shown in Figure 3-14 are consistent with the presence of a large fraction of low molecular weight species. The high molecular weight species eluted earlier, while the low molecular weight species reached the detector between 18 and 20 minutes, as presented in the chromatogram (Figure 3-14). This figure shows the appearance of sample components as a function of retention volume or time. Integration of the area under each peak in the chromatogram indicated that less than 1% of the chemical species found in the enzyme stabilizer were high molecular weight species. Furthermore, the peak at a retention volume of approximately 19 mL corresponds to an average molecular weight of 590 g/mole. Due to the predominance of low molecular weight species, HPLC/MS was performed to further identify these species. The lack of high molecular weight species made protein analysis unnecessary.

HPLC/MS was conducted for the enzyme stabilizer with the results shown in Figure 3-15. The HPLC/MS results show a repetitive m/z pattern of 44. Based on the fact that the enzyme stabilizer contains a significant carbon component, polyethylene glycol (C_2H_4O) (MW 44) was suggested. The FTIR and proton NMR results indicate the chemical structure of polyethylene glycol to be:



To verify this hypothesis, FAB was performed, and the results confirmed the presence of polyethylene glycol (C_2H_4O). In addition, a UV/Vis spectra of the sample (Figure 3-16) was consistent with previously published spectra for polyethylene glycol. Polyethylene glycol has two absorbance peaks in the ultraviolet region at 220 and 276 nm, as shown in Figure 3-17.

Summary of Results for the Enzyme Stabilizer

Although the above analytical techniques were successful in characterizing a component of the enzyme stabilizer, it is unlikely that polyethylene glycol is the activating ingredient. Polyethylene glycol has been used as a protein/enzyme deactivator (Inada 1995). However, literature is not available that identifies polyethylene glycol as a surfactant that reduces clay expansion or induces soil stabilization.

Table 3-1. Analytical techniques used to characterize the stabilizers

<i>Analytical Technique</i>	<i>Ionic Stabilizer</i>	<i>Polymer Stabilizer</i>	<i>Enzyme Stabilizer</i>
pH	X	X	X
Potentiometric titration	X		X
Conductivity	X	X	X
Ion chromatography	X		
Total organic carbon	X	X	X
Fourier transform infrared spectroscopy	X	X	X
UV/Vis spectroscopy,	X		X
Gas chromatography/mass spectrometry	X		
High-performance liquid chromatography/mass spectrometry	X	X	
Gel permeation chromatography			X
Nuclear magnetic resonance spectroscopy	X	X	X

Table 3-2. pH and conductivity measurements for sulfuric acid, sulfonated limonene, and ionic stabilizer

	<i>pH</i>	<i>St Dev (+/-)</i>	<i>Conductivity ($\mu\text{S/cm}$)</i>	<i>St Dev (+/-)</i>
Sulfuric acid				
1:500 unfiltered	1.365	0.008	15.52	0.206
1:500 filtered	1.92	0.004		
Sulfonated limonene				
1:500 unfiltered	1.391	0.002	14.74	0.386
1:500 filtered	1.79	0.002		
Ionic stabilizer				
1:500 unfiltered	1.437	0.005	13.63	0.119
1:500 filtered	1.83	0.003		

Table 3-3. Hydrogen ion concentrations in ionic stabilizer, sulfonated limonene, and sulfuric acid samples

<i>Samples</i>	<i>Normality (equivalents/L)</i>	<i>Molarity (moles/L)</i>
Ionic stabilizer	30.2	15.1
Sulfonated limonene	31.1	15.6
Concentrated sulfuric acid (H_2SO_4)	33.4	16.7

Table 3-4. Results of sulfate analysis by ion chromatography

<i>Samples</i>	<i>Avg. Sulfate Conc. (g/L)</i>	<i>Molarity (moles/L)</i>	<i>St. Dev. (+/- g/L)</i>
Sulfuric acid	2081.33	21.7	25.97
Ionic stabilizer	1242.54	12.9	9.44
Sulfonated limonene	1311.24	13.6	23.46

Table 3-5. Results of TOC analysis for the sulfonated limonene and ionic stabilizer

<i>Samples</i>	<i>Unfiltered/ Filtered</i>	<i>TOC (g/L)</i>	<i>TOC (moles C/L)</i>	<i>St. Dev (+/- g/L)</i>
Sulfonated limonene	Unfiltered	16.37	1.3	0.42
Sulfonated limonene	Filtered	7.35	0.58	0.05
Ionic stabilizer	Unfiltered	42.08	3.5	0.34
Ionic stabilizer	Filtered	41.35	3.4	—

Table 3-6. pH and conductivity measurements for the polymer stabilizer and sodium silicate

	<i>pH</i>	<i>St. Dev (+/-)</i>	<i>Conductivity (mS/cm)</i>	<i>St. Dev (+/-)</i>
Polymer stabilizer 1:10 Dilution	11.42	0.018	12.08	0.645
Sodium silicate 1:10 Dilution	11.32	0.035	11.99	0.179

Table 3-7. Interpretation of peaks in FTIR spectra for the polymer stabilizer

<i>Wavelength (cm⁻¹)</i>	<i>Functional Group</i>
870	Si-O (Si-OH stretching; Si-OH bending)
950–970	Si-O
1100	Si-O-Si
1650	Water
2,200–3,600	Stretching Si-OH

Source: *Journal of American Ceramic Society* (1998).

Table 3-8. Interpretation of peaks in FTIR spectra for the enzyme stabilizer

<i>Wavelength (cm^{-1})</i>	<i>Functional Group</i>
1,120	C-O
1,220	tertiary butyls
1,350	C-OH
1,300	$\text{CH}_2=\text{CH}$, CH-OH
1,460	C-H bend

Source: *Journal of Optical Society* (1988).

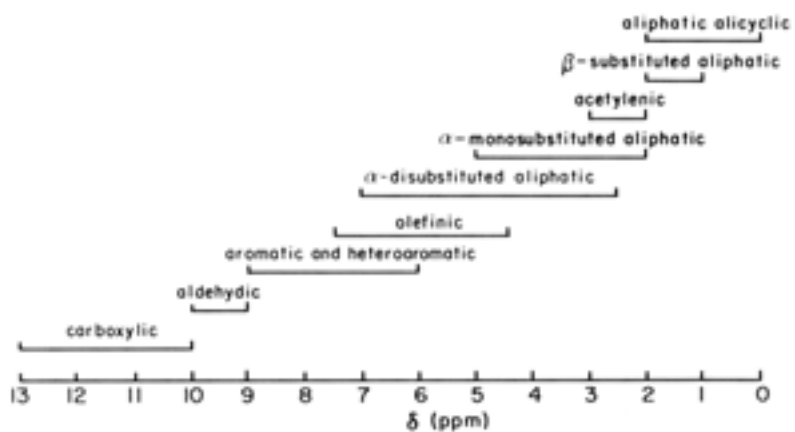


Figure 3-1. Chemical shifts of the proton in organic compounds (from Klute 1986)

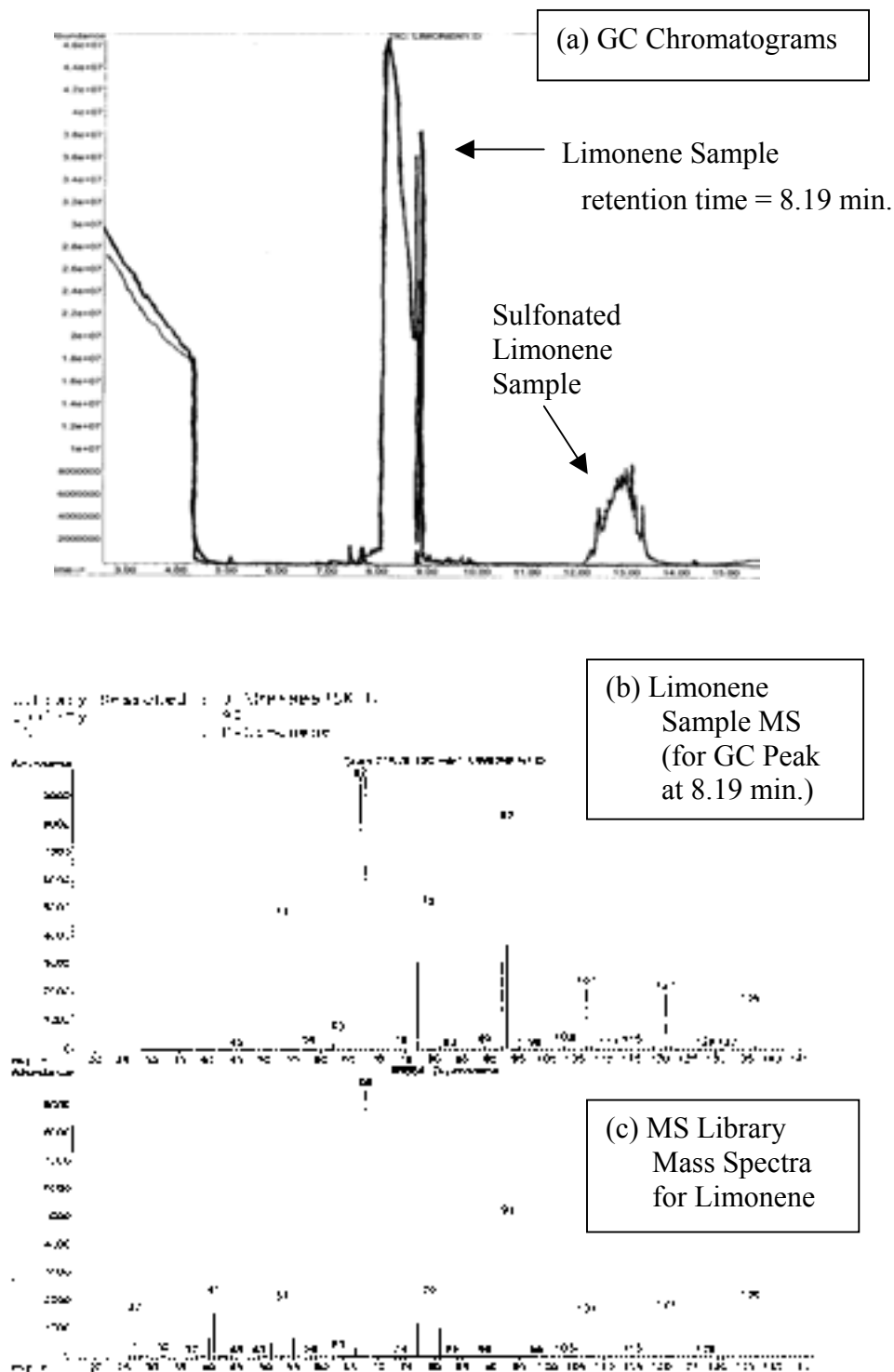


Figure 3-2. GC/MS results for sulfonated limonene and limonene samples

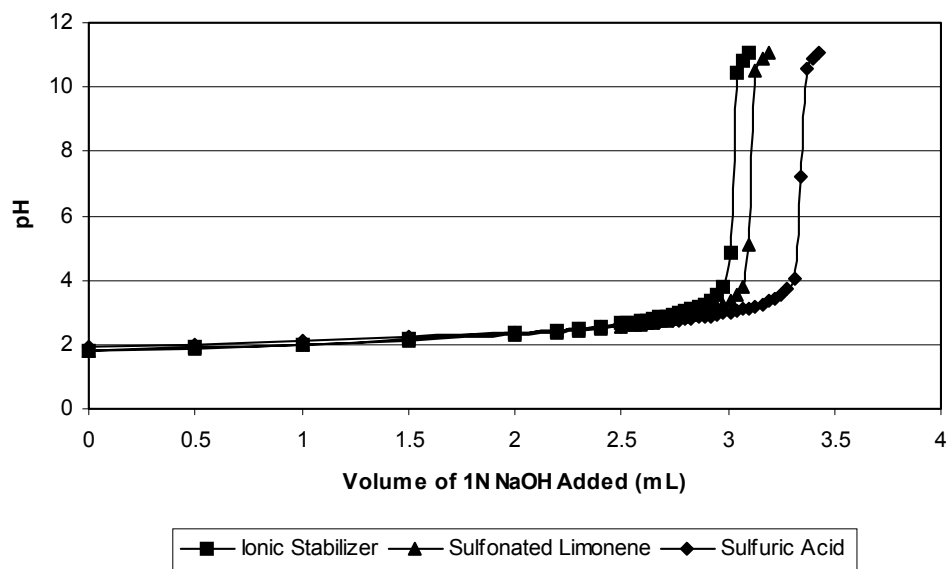


Figure 3-3. Results of potentiometric titration of the ionic stabilizer and its components

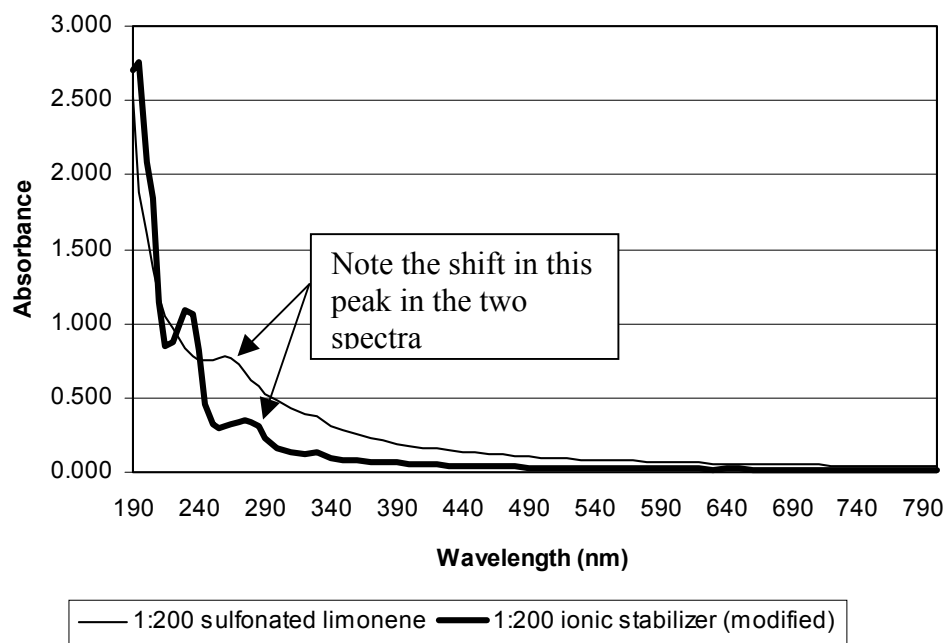


Figure 3-4. UV/Vis spectroscopy results for sulfonated limonene and the ionic stabilizer

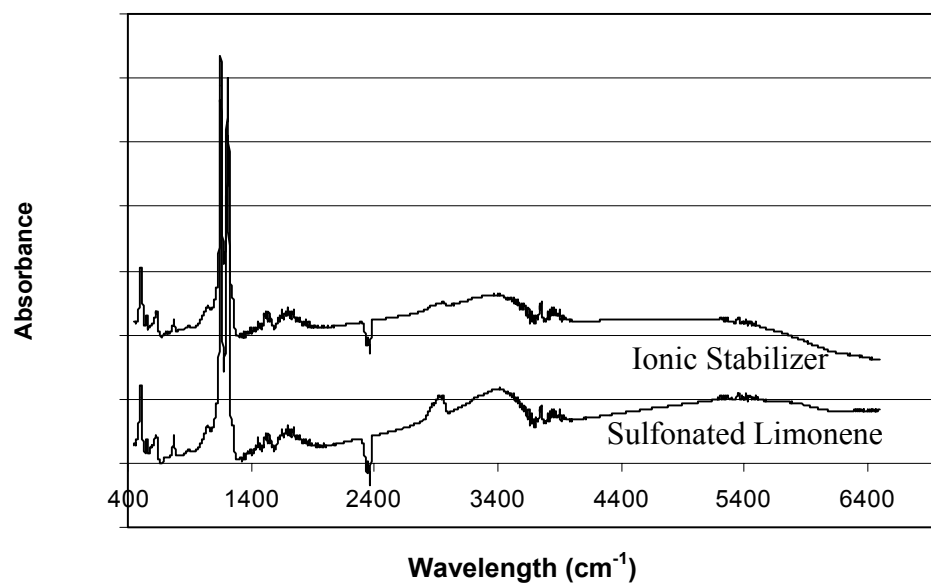


Figure 3-5. FTIR results for sulfonated limonene and ionic stabilizer

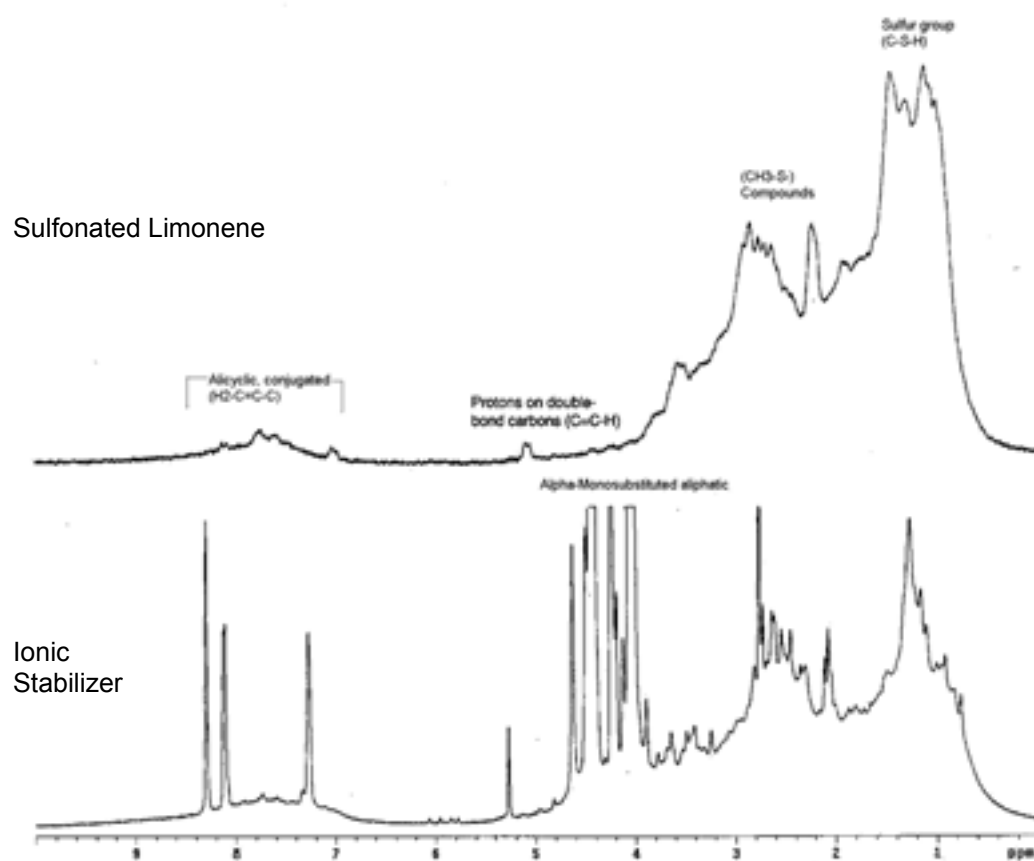


Figure 3-6. Proton (1H) NMR results for sulfonated limonene and ionic stabilizer

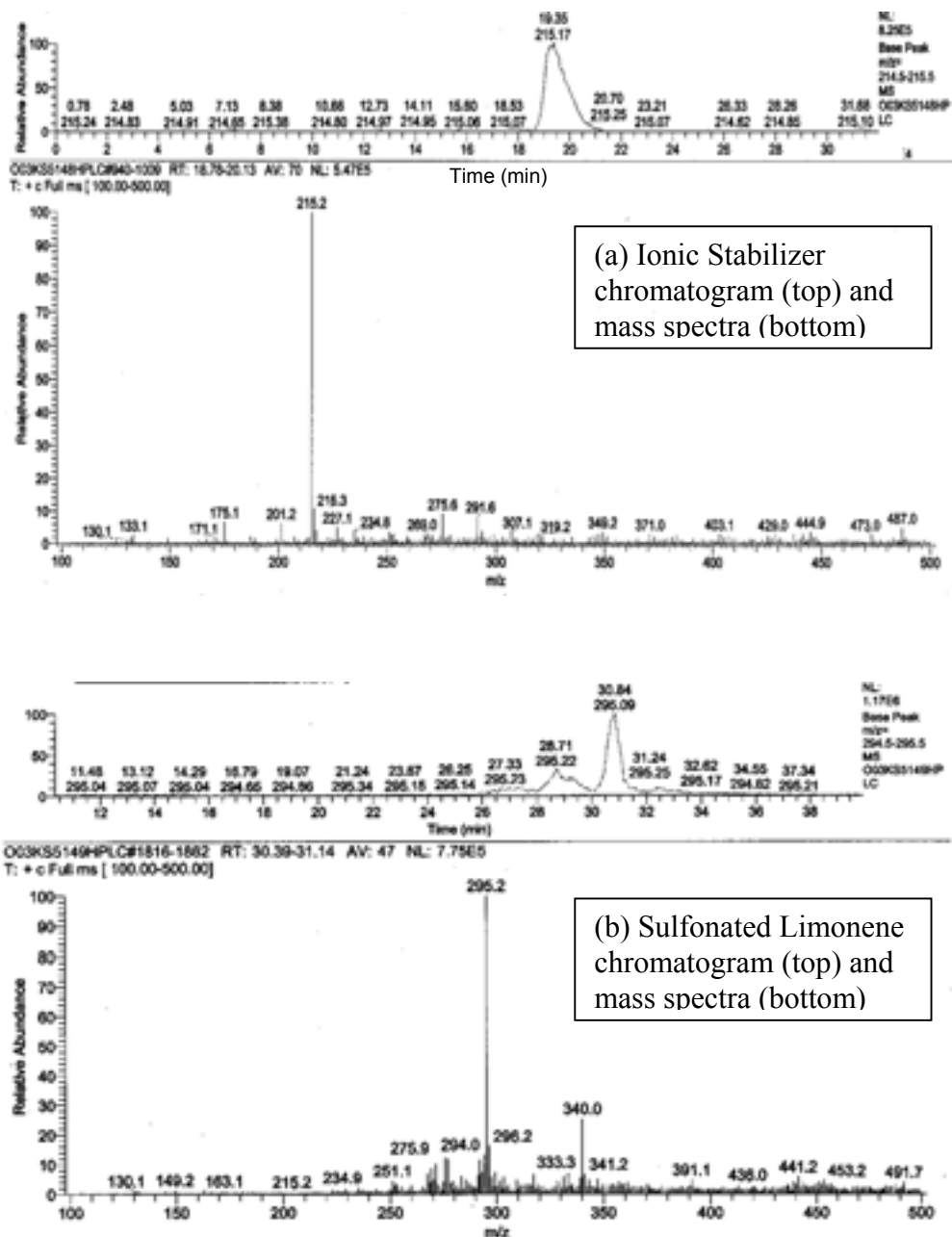


Figure 3-7. HPLC/MS results for the (a) ionic stabilizer and (b) sulfonated limonene prepared in the laboratory

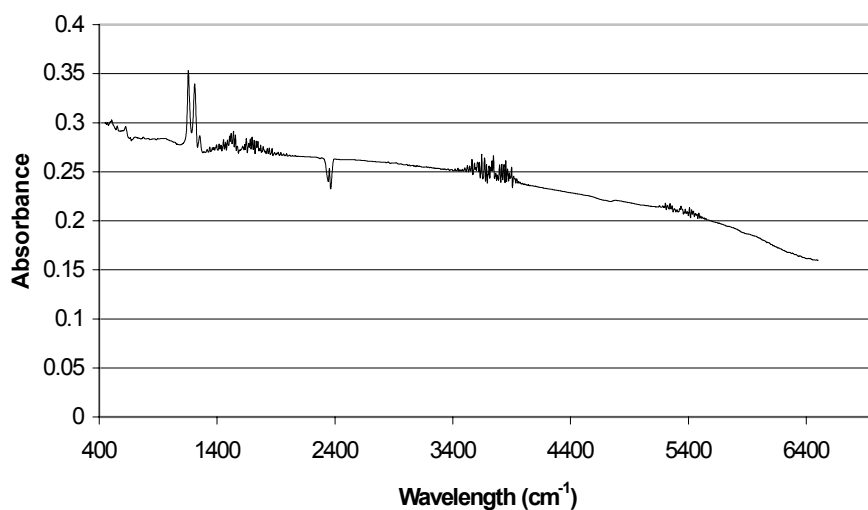


Figure 3-8. FTIR results for the polymer stabilizer

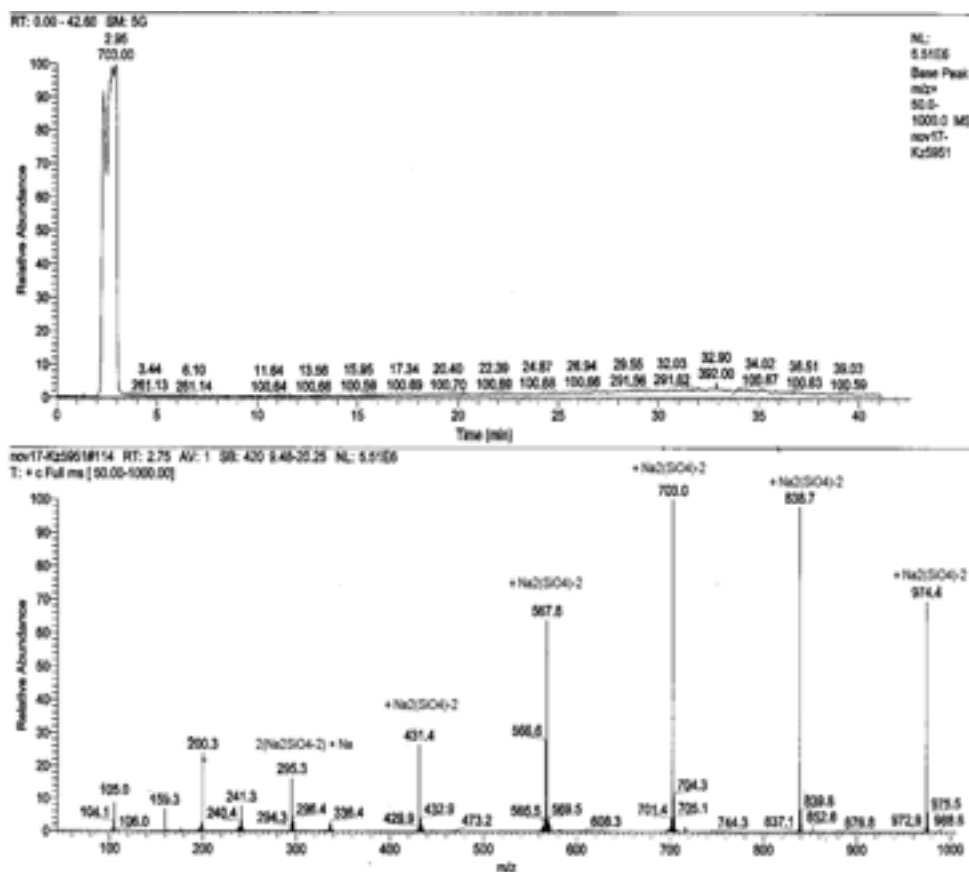
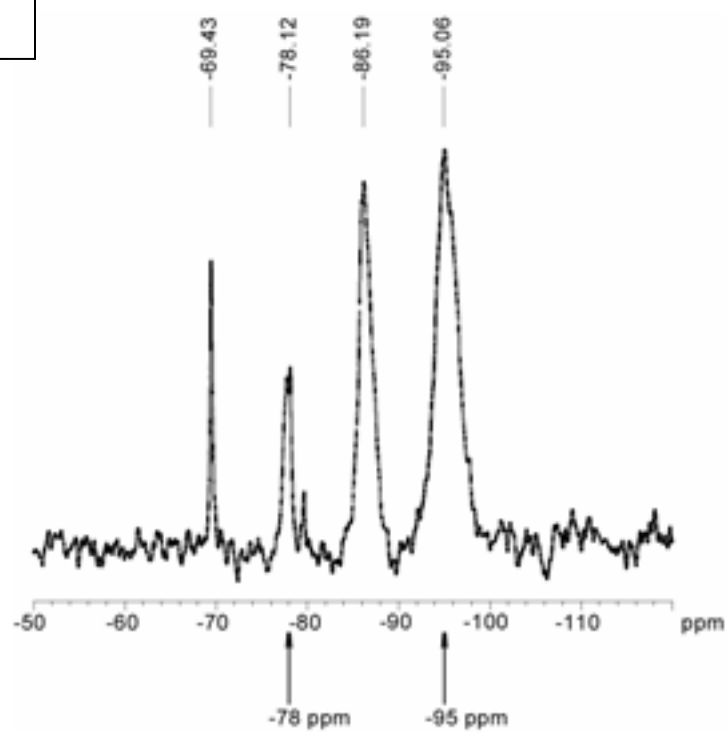


Figure 3-9. HPLC/MS results for the polymer stabilizer (the top portion of the corresponds to the LC chromatogram and the bottom portion to the mass spectra)

(a) Sodium Silicate



(b) Polymer Stabilizer

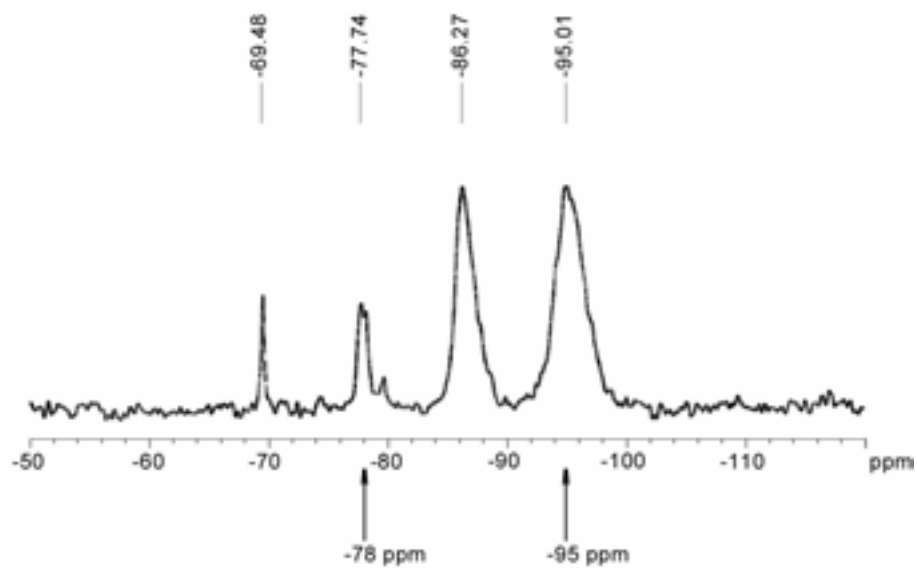


Figure 3-10. ^{29}Si NMR results for (a) sodium silicate and (b) the polymer stabilizer

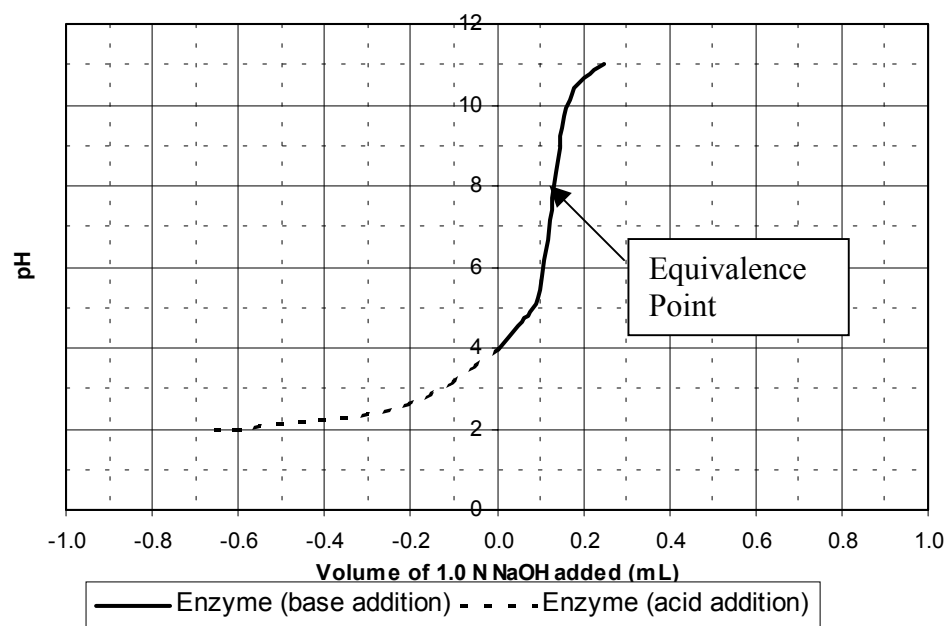


Figure 3-11. Potentiometric titration of enzyme stabilizer

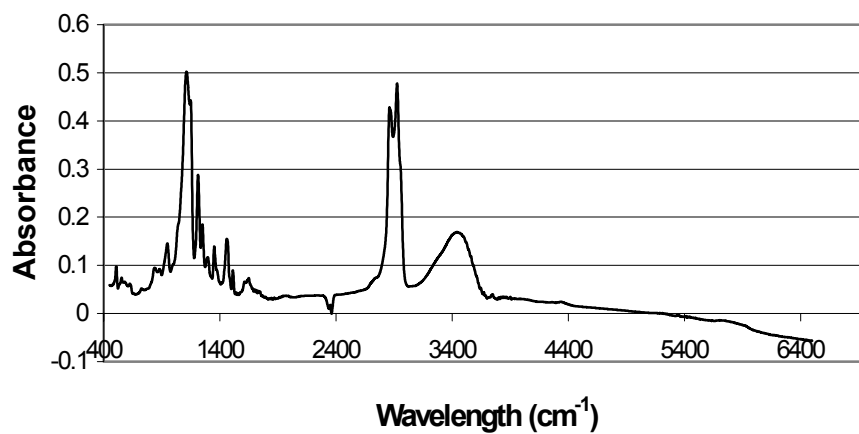


Figure 3-12. FTIR results for the enzyme stabilizer

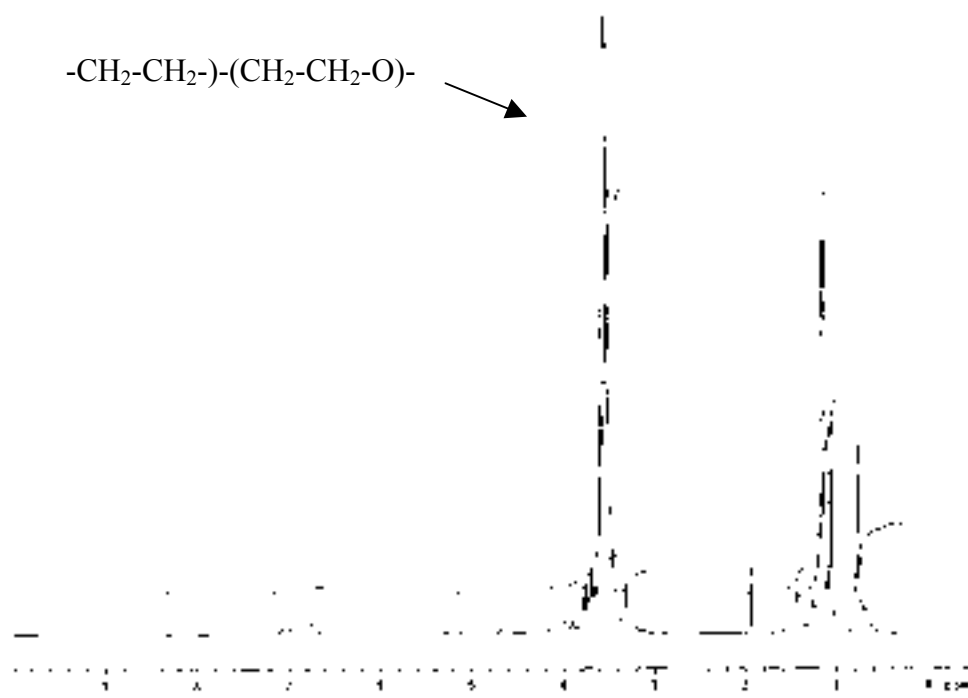


Figure 3-13. ^1H NMR results for the enzyme stabilizer

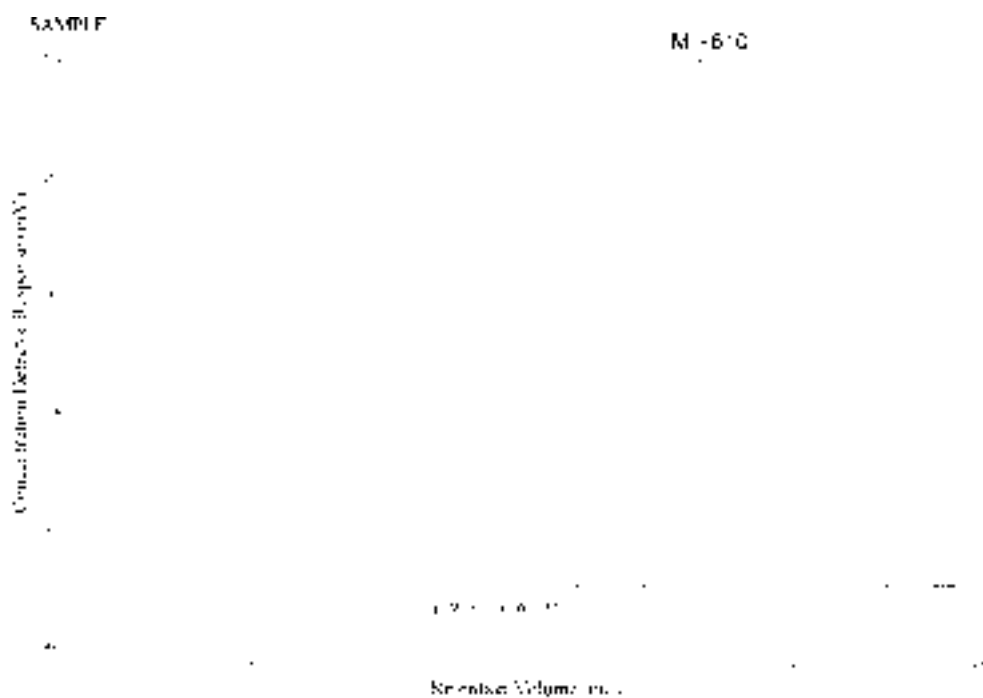


Figure 3-14. GPC results for the enzyme stabilizer

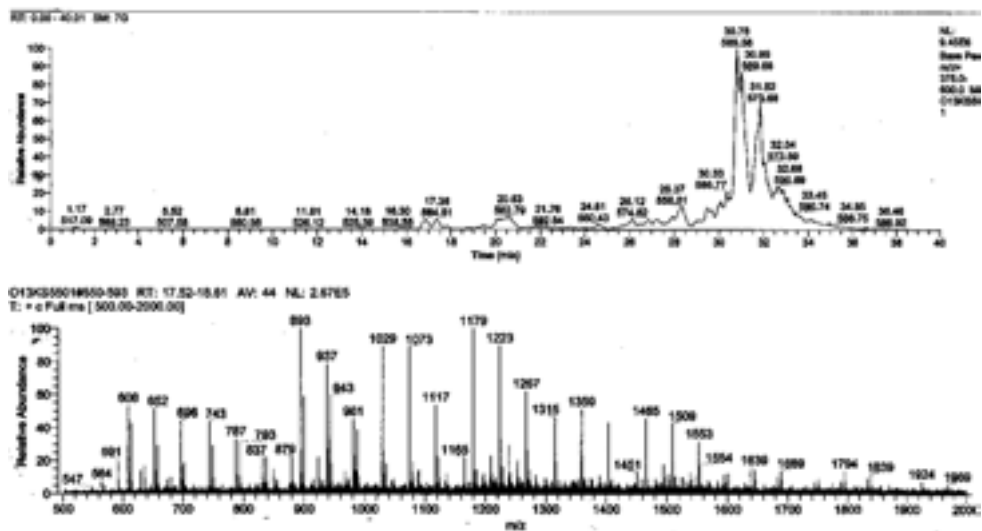


Figure 3-15. HPLC/MS results for enzyme stabilizer

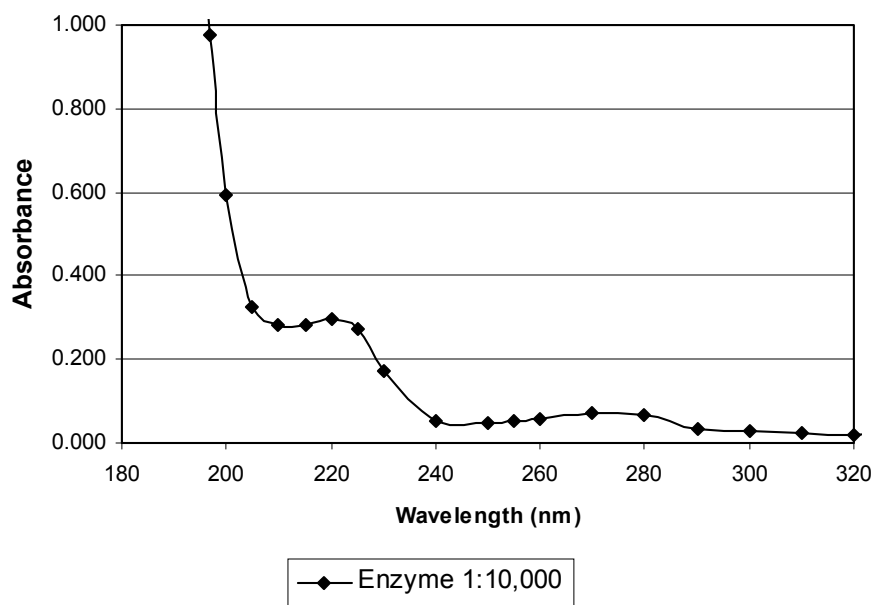


Figure 3-16. Enzyme stabilizer UV/Vis absorption spectra obtained at 1:10,000 dilution

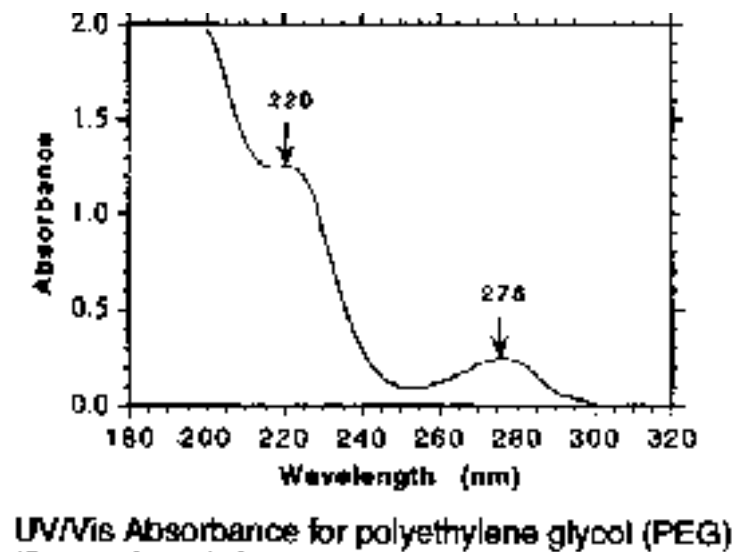


Figure 3-17. Polyethylene glycol UV/Vis absorbance spectra (from *Journal of American Ceramic Society*, Vol. 82, 1999)

CHAPTER 4

METHODS FOR MICRO-CHARACTERIZATION OF STABILIZER MECHANISMS

4.1. OVERVIEW

The clay materials were prepared and characterized before and after treatment with chemical stabilizers to evaluate the clay/stabilizer interaction. The clay materials were characterized using BET surface area analysis, cation exchange capacity (CEC), environmental scanning electron microscopy (ESEM), scanning electron microscopy (SEM), energy dispersive X-ray spectroscopy (EDX), and X-ray diffraction (XRD). Following initial characterization of the clay using these techniques, each of the clay minerals was treated with each of the stabilizers. To study the interaction and changes to the clay structure due to the addition of each stabilizer, a basis for the dilution rates was established. An application mass ratio of 1:2 (mass of concentrated stabilizer:mass of dry soil) was selected for the majority of the laboratory procedures. This ratio is much higher than application ratios suggested by the manufacturers; however, the goal was to maximize any chemical changes in the structure and morphology of the clay minerals. In this chapter the methods used to characterize the clays and the procedures for treating the clay minerals with the stabilizers are described.

4.2. PREPARATION OF CLAY MATERIALS

Field soils almost always contain quartz minerals, salts, and impurities in addition to typical clay particles. In an attempt to evaluate the direct response of the chemical stabilization to clay particles without interference of other materials that may be present in the samples, the repository clays were washed and the clay fraction was retained. Size fractionation of the illite and kaolinite clays was achieved by placing a pre-weighed sample of soil (50 grams of illite or kaolinite or 10 grams of montmorillonite) in ultrapure water and dispersing the particles using an ultrasonic probe. The suspension was transferred to a polyethylene container. The Fisher Scientific 550 Sonic Dismembrator was tuned and programmed for a 3-minute duration with 3-second pulse on and 1-second pulse off. The clay suspension was then decanted into a beaker and stirred for 30 minutes.

The ASTM D 422-63 settling procedure was used to separate particles larger than 2 μm . The procedure is based on Stokes' Law, which determines the time required for particles to settle. This settling procedure (which includes all steps after sonic dismembrator dispersion) was repeated until a homogeneous suspension was produced. The time required to remove particles of diameter D is a function of the specific gravity of the particles and the solution, the depth of the container, and temperature. Kaolinite quickly settled after being removed from the stirrer. An initial pH of 5.56 was measured for the kaolinite and water mixture. Due to the low pH, the kaolinite settled quickly and thus prevented the separation of the larger particles using Stokes' Law settling procedure (ASTM D 422-63). In order to disperse the clay, 1 mL of 10 N NaOH was added to reach a basic pH of 10.4. With this modification, the kaolinite settled more slowly, allowing its separation from the larger particles. No modifications for settling were necessary for the sodium montmorillonite or illite.

Based on Stokes' Law, 15 to 20 hours, depending on the type of clay, were required for all particles larger than 2 µm to settle out and leave the clay fraction in the supernatant. After the calculated time had passed, the clay suspension was siphoned, and the volume of the suspension was reduced by centrifugation. The clay suspension was poured into a 250 mL high-density polyethylene (HDPE) bottle, allowing a 2-inch headspace to avoid breakage, and was centrifuged using a Beckman Model J2-21 Centrifuge equipped with a JA-10 rotor at 4,000 rpm (1,750g) for one hour. The clay fraction was captured on the bottom and placed in a Spectra-Por™ MWCO:1000 dialysis membrane stored in 0.1% sodium azide.

For montmorillonite the supernatant was captured and centrifuged using a JA-20 Rotor at 17,000 rpm (29,100g) for 30 minutes to separate the montmorillonite from the quartz fraction, which has a specific gravity of 2.65. Since the specific gravity of quartz is less than that of montmorillonite and the particle size is roughly comparable (less than 2 µm), the time needed to settle quartz would be greater than that for montmorillonite, and quartz would thus be present in the clay suspension.

The dialysis membrane packed with clay was placed in a 2-liter HDPE container filled with ultrapure water and without headspace. The water was replaced with ultrapure water until the specific conductance reached 2 µmhos/cm or less. Finally, the washed clay was removed from the dialysis tubing, placed in a -70°C refrigerator (Kelvinator Series 100, Kelvinator Commercial Products, Manitowoc, Wisconsin) for 24 hours, and freeze dried using a Virtis (Virtis Company, Inc., Gardiner, New York) freeze drier equipped with a Labconco Model 195 pump. After 5 to 7 days, the clay fraction was sufficiently dry to conduct experiments.

In addition to the three clay minerals, the two natural soils (Bryan and Mesquite) were also studied. The soils were not washed in an attempt to study the soils as field specimens.

4.3. CLAY MINERAL CHARACTERIZATION PROCEDURES

BET Surface Area

BET surface area analysis can be used to quantify external surface area and pore size distribution. In this research the technique was used to determine changes in surface area and pore size distribution attributable to the various stabilizer treatments for each of the clay minerals and soils. The method is based on collecting isotherm data for the physical adsorption of an inert gas and modeling the adsorption data using the following BET isotherm equation:

$$\frac{v}{v_m} = \frac{c\left(\frac{P}{P_0}\right)}{\left(1 - \frac{P}{P_0}\right)\left[1 + (c - 1)\frac{P}{P_0}\right]}$$

where:

- v = volume of gas measured at standard temperature (298K) and pressure (1 atmosphere) adsorbed per unit weight of clay at a pressure, P
- v_m = volume of gas adsorbed for monolayer coverage
- P/P_0 = partial pressure of the gaseous adsorbate
- c = constant

Rearranged, the BET equation can be transformed to a linear form from which v_m and c can be obtained:

$$\frac{\frac{P}{P_0}}{v(1 - \frac{P}{P_0})} = \frac{1}{cv_m} + \frac{(c-1)(\frac{P}{P_0})}{cv_m}$$

A Micromeritics BET Model 2010 was employed for the BET surface area analyses to measure the external surface area of both treated and untreated samples for each type of clay and soil. Nitrogen was used as the adsorbing gas at a temperature of 77°K, and data was collected for partial pressures (P/P_0) ranging from 0.02 to 0.3. Surface area (A) was calculated and presented in units of m²/g using:

$$A = \left(\frac{v_m}{v_0}\right)N_0a$$

where:

$$\begin{aligned} N_0 &= \text{Avogadro's number (6.023 x 10}^{23}\text{)} \\ a &= \text{area of a nitrogen molecule} \end{aligned}$$

For BET analysis pore size distributions were observed to relate pore size trends among stabilizer treatments to assist in confirming (or disproving) the hypothesized mechanisms of interaction with clay and soil particles. The pore size distributions were provided for mesopores, which are pores between 2 and 50 nm. The size of pores measured corresponds to characteristic adsorption effects, which for mesopores occurs by capillary condensation with a characteristic hysteresis loop (Gregg and Sing 1982). The hysteresis loop includes a lower branch representing measurements obtained by progressive addition of liquid nitrogen to the system and the upper branch by progressive withdrawal (Gregg and Sing 1982). During surface area analysis the relative pressure (P/P°) is measured with the assumption that adsorption is restricted until inception of the hysteresis loop, which then prompts capillary condensation in the finest pores (Gregg and Sing 1982). As the pressure increases, wider and wider pores are filled until the system is filled with condensate at the saturation pressure. Using the relative pressure at the lower limit of the hysteresis loop, the minimum radius of pores in which capillary condensation takes place can be measured (Gregg and Sing 1982). This range of pores is determined as a function of relative pressure and amount of gas (nitrogen) adsorbed on the solid (clay). Then, the pore volume is calculated by dividing the incremental pore volume by the difference in the range of pore radii. The pore size distribution curve relates the pore volume to the average pore radius and yields information about the stabilizer mechanisms.

Scanning Electron Microscopy with Energy Dispersive X-ray Spectrometry

Scanning electron microscopy (SEM) was employed to study morphological variations in clay particles for treated and untreated specimens. A LEO 1530 scanning electron microscope equipped with IXRF Systems Model 500 energy dispersive X-ray spectrometer (EDS) was used to obtain images ranging in magnification from 200× to 11,500× at 15 kV. The SEM images for each clay and soil were obtained at 200×, 7000×, and 11,500× magnification for untreated and treated samples (ionic, polymer, enzyme stabilizers, and sulfuric acid treatments). Using a point analysis and line scan across clay particles, EDS was conducted to determine elemental changes in the surface chemical composition of clay particles for untreated and treated samples. The EDS results were displayed at 10 kV. The locations of the EDS analysis points are indicated on the SEM images. The SEM images and EDS results are presented in Appendix E.

The SEM images obtained for treated and untreated samples were compared to assess changes in morphological and topographic features associated with stabilizer treatment and to determine the appropriateness of using this technique for natural soil samples. Sample preparation involved freeze-drying the clay, grinding the freeze-dried sample into a homogeneous mixture, placing the clay onto an aluminum stub covered with double-sided carbon tape, and coating the specimen with chromium using a vacuum sputter coater. Since samples that conduct electricity are preferred for SEM analysis, the surfaces of treated and untreated clay samples were coated with chromium by vacuum sputtering. A Varian Model 9699834 vacuum sputterer was used. Chromium deposition time was set to 30 seconds. Argon was used to maintain the pressure at 0.01 torr and the power was set to 100 Watts.

In the SEM analysis the clay surface is scanned by a beam of energetic electrons in a raster pattern that produces signals including backscattered and secondary electrons. The electrons project an image of the sample showing crystal structure and layering. Secondary electrons, which offer the best imaging resolution, are typically low-energy and are ejected by interactions with the primary electrons of the beam. Alternatively, backscattered electrons (BSE) are high-energy electrons that are scattered from the sample by elastic collisions. Due to their high energy, backscattered electrons result in a larger volume of interaction but degraded image resolution. Two pairs of electromagnetic coils located within the objective lens control the scanning procedure; the x coil moves in a straight line as a function of time, and the y coil deflects the beam. By rapidly moving the beam, the clay samples are irradiated with electrons, and digital signals sent to the scan coils, reflecting differences in the sample, are then encoded to produce the SEM images. The sample chamber requires a high vacuum to generate and focus the electron beam.

The EDS emission feature of the SEM system allows detection and qualitative analysis of the major chemical elements. An X-ray is emitted as a result of inner shell electrons being scattered by an energetic electron. Because energy differences between shells are well-defined and specific to each element, the energy emitted from the X-ray is characteristic of the element. EDS collects, counts, and sorts X-rays, displaying results according to elemental intensities (counts/sec) versus energy (KeV). The energy levels are used to identify the elements present in the sample. The intensity is determined as a function of the element's concentration and matrix being examined. X-rays of different energies are emitted for each of the energy shells (primarily K, L, or M).

An IXRF-EDS internal algorithm was executed to convert the elemental intensities to weight percentage. Each element exhibiting noticeable peak intensity was selected to participate

in the algorithmic computation. Aluminum-to-silica ratios were evaluated for each sample using the weight percentage results. These ratios were selected to be an indicator of chemical structure changes as a result of treatment with chemical stabilizers. If a decrease in aluminum-to-silica ratios was observed, this could mean a decrease in aluminum due to a transfer of Al^{3+} cations to the stabilizer and/or an increase in silica. Silica-to-oxygen ratios were not used to compare treatments, because a change in Si/O ratios would not necessarily represent clay chemical structure alterations. That is, oxygen transfer or changes in oxidation state were not associated with any of the hypothesized mechanisms. In addition, there was considerable variability in the EDS results for oxygen due to the low atomic number, resulting in low-energy X-ray emissions (Electroscan 1996). Therefore, the reproducibility of oxygen in the EDS results was poor.

There are a number of limitations to EDS that need to be presented to qualify sample results. Topography can have a significant impact on EDS results, and clay clumping can provide misleading results if applied to a single clay particle. Also, lower atomic numbers emit low-energy X-rays and decrease the reliability of results (Electroscan 1996). Finally, the maximum X-ray penetration for EDS is 3 μm , which should not affect clay particles with diameters smaller than 2 μm . Therefore, the assumption that the elemental intensities are representative of the clay particles even after stabilizer treatment is reasonable. However, this method is very sensitive to topography and thickness of stabilizer coating. Any conclusions regarding Al/Si ratios must take this factor into account. For this study, all samples were handled similarly, and it is therefore assumed that untreated and treated samples have similar topography. As an additional quality assurance measure, multiple samples were analyzed in all cases (seven or more) to determine Al:Si ratios, and Al:Si ratios of untreated clay were compared to values reported in the literature.

Environmental Scanning Electron Microscopy

Environmental scanning electron microscopy (ESEM) was selected to evaluate untreated and treated specimens in-situ without having to freeze-dry and/or chromium-plate the sample. The ESEM contains multiple pressure limiting apertures (PLAs) that separate the sample chamber from the column and can therefore tolerate pressure differences more easily. Thus, it does not require high vacuum conditions, as do conventional SEMs. A gaseous secondary electron detector (GSED) was used for all sample analyses to discriminate between backscattered and secondary electrons to improve resolution and image quality. An ENVIROSCAN Philips Electroscan 2020 environmental scanning electron microscope was used to obtain images ranging in magnification from 200 \times to 14,500 \times at 20 kV.

X-Ray Diffraction

Powder X-ray Diffraction (XRD) is a procedure used to determine the arrangement and spacing of atoms in crystalline materials. XRD was employed in this study to provide qualitative verification of clay minerals of well-characterized clays, identification of clay minerals in the natural soils, and assessment of changes in clay mineralogy due to treatment by ionic, polymeric, and enzyme stabilizers. The strongest peaks in the sample recorded by XRD were compared to known mineral powder diffractograms for montmorillonite, illite, and kaolinite.

With x-ray diffraction, scattering of the electrons around an atom forms diffracted beams. When the reflected x-rays interact by constructive interference, the intensity of the diffraction beams is measured. These scattering beam measurements are adjusted according to phase

differences, which are dependent on the arrangement of atoms and the physical distance between atoms, determining how much the scattered rays will be out of phase. For diffraction to occur, the reflected beams must be perpendicular to the planes of atoms responsible for the scattering and are identified as 001 planes for clay materials (Moore 1997). The intensities of the 001 planes are controlled by the position of atoms and chemical composition.

Diffraction from equally spaced, parallel lattice planes results in a maximum peak detection with sufficient intensity to be recorded (Whittig and Allardice 1986). The distance of the separation of atomic planes (such as for the 001 plane) is also known as d-spacing. For a given d-spacing, a critical angle exists at which scattered rays will be in phase with one another, resulting in an intensity that can be recorded by XRD, which is designated by θ . XRD patterns are identified based on the position of a diffraction line response (represented by 2θ) and the relative intensities. Since the interatomic distances are unique to each mineral, the angle of incidence will be distinct for each mineral. The change of d-spacing can serve as an indicator of mineralogical alteration and is determined using Bragg's Law:

$$n\lambda = 2d \sin \theta$$

where:

- d = distance of interplanar spacing (as function of θ)
- n = order of diffraction
- θ = critical angle of incidence of the x-ray beam on the crystal plane
- λ = wavelength of the x-rays

A pictorial representation of Bragg's Law is presented in Figure 4-1 in which the d-spacing between crystal planes is clearly indicated.

Samples for XRD were prepared by grinding with a mortar and pestle to a fine homogeneous powder and were initially randomly oriented. An aluminum holder with an elliptical center was affixed to a petrographic microslide. The clay was placed in the elliptical opening and filled to the top. A microscope slide placed at a slight angle was used to evenly distribute the clay, but the clay was not packed to allow for random orientation. A Siemens D500 diffractometer was used to perform scans with the following parameters: an angle scan (2θ) between 3° and 50° using a 0.02° step size and dwelling time of one second at each step.

Most samples were freeze-dried prior to analysis. For sodium montmorillonite, samples that were oven dried at 25°C were analyzed, and the d-spacing results were not noticeably different from the results obtained with freeze dried samples. Since presumably any differences associated with drying procedures would be evident in results for the most expansive clay, it was determined that the freeze drying procedure did not alter the clay and soil samples.

Even within the 001 plane, not all reflections are the same intensity, and systematic absences and variations can often be informative of the positions of atoms in the unit cell (Moore and Reynolds 1997). By orienting the samples for XRD analysis, an attempt is made to limit the analysis to one dimension of the unit cell, so that the diffraction patterns only contain contributions from 001 spacings. A suspension was made by adding 0.5 grams of the clay to 50 mL of distilled deionized water. The suspension was dispersed with a W-370 Sonicator/cell disruptor (Heat Systems Ultrasonic, Inc.) for one minute. A transfer pipette was used to apply 2-3 mLs to a petrographic microslide, and the sample was allowed to dry for 24 hours. The

samples were scanned by XRD using the following parameters: an angle scan (2θ) between 2° and 15° dwelling for one second at each step. The reduction in angle scan was appropriate to evaluate the primary 001 peak, used to determine d-spacing.

The oriented samples were subsequently exposed to ethylene glycol according to the methods described in Moore and Reynolds (1997). Ethylene glycol solution invades the interlayer of expandable clays and causes them to swell, resulting in an increase in the d-spacing of the 001 lattice plane of the mineral (Sarkar 2000). Glycolation was performed to determine whether expansiveness of the clay was altered by treatment and to evaluate changes in d-spacing between treated and untreated samples. The oriented sample was placed in a 69°C closed container with ethylene glycol for 24 hours. The samples were analyzed immediately after being removed from the ethylene glycol environment. XRD analysis was employed using the same parameters that were used for the oriented samples. The ethylene glycol treatment was expected to maximize the inner layer spacing for expandable clays and to have no effect on the non-expanding clays.

Cation Exchange Capacity

Cation exchange capacity (CEC) can be defined as the total amount of cations required to balance the net negative charge associated with a soil or clay sample. It was utilized to verify the effects of different stabilizers. For example, reduction of the exchange capacity of an expanding clay implies that either the accessibility to exchange sites has been limited or the mineralogy of the clay has changed. CEC analyses were performed following a procedure slightly modified from the Soil Science Society of America (SSSA 1996), which allows the determination of the CEC of a sample at its natural pH. Five grams of the clay sample were placed into a 250-mL Nalgene PC centrifuge bottle. Next, 50 mL of 0.2 M NH_4Cl was added, and the bottle was shaken for 5 min. Then, the sample was centrifuged at 5,000 rpm for 20 min using a Beckman J2-21 centrifuge, and the supernatant was discarded very carefully to avoid loss of solids. This procedure, called the saturation step, was repeated four more times. After the clay material had been saturated with NH_4^+ ions, the sample was washed three times with ultrapure water to remove non-exchanged NH_4^+ ions. The next step, the extraction step, was performed using 0.2 M KNO_3 . After the addition of 50 mL of the extraction solution to each bottle, the samples were resuspended, shaken for 5 min, centrifuged, and the supernatants were collected in 250-mL Nalgene FEP bottles. The extraction step was performed four more times. In some of the steps, more than 50 mL of extraction solution was added in order to achieve balance among the centrifuge bottles. All the extra volume was recorded and considered in the final calculations. Finally, the total extracted solution was analyzed for NH_4^+ using the Phenate Method (Standard Methods 1989), and the CEC value for each sample was determined from the results.

4.4. CLAY MINERAL/STABILIZER CHARACTERIZATION PROCEDURES

Samples of the three mineral clays and two soils were reacted with the three stabilizers and allowed to equilibrate for seven days. All stabilizer characterization tests were performed in triplicate to assure reliability of the results. Average values of the results were reported for each of the tests conducted. Dilution rates were established to investigate changes in clay structure resulting from chemical stabilization. Initially, an application mass ratio (AMR) based on manufacturer recommendations was selected to be the appropriate method for stabilizer

application to the clay materials. The manufacturer-suggested application ratios were applied to the soil, and ultrapure water was added to achieve optimal water content (OWC). The OWC is defined as the mass ratio of water to oven-dry soil that yields the maximum dry density of untreated soil when compacted using modified Proctor effort (ASTM D-1557). The OWC determined for each clay and soil is listed in Table 2-5.

After the predetermined amount of the stabilizer was added according to the AMR and ultrapure water was added to achieve OWC, the samples were mixed manually with a spatula and mechanically with a Vortex Genie Mixer (Scientific Industries, Inc., Bohemia, New York) until the stabilizer was uniformly mixed with the soil based on visual observation. The samples were then cured undisturbed for seven days at 20°C. After a seven-day cure time, most samples were rinsed with ultrapure water through a 0.45 µm filter to remove excess salts, and a portion of each sample was removed for ESEM. The curing time before ESEM analysis varied from 7 to 9 days, according to ESEM equipment availability. The remainder of the sample was freeze-dried and analyzed using XRD, SEM, and surface area using the methods described above. Some of the samples were unwashed and air-dried. A comparison shows that no effects on d-spacing were observed between rinsed and unrinsed specimens or air-dried and freeze-dried samples. An example is shown in Figure 4-2 for sodium montmorillonite.

After curing for 7 to 9 days, the samples were characterized using the methods described in section 4-3 of this chapter. The results were inconclusive, presumably due to such low application rates. Therefore, an application mass ratio of 1:2 was selected for each stabilizer to increase the likelihood of observable chemical changes in structure and morphology of clay minerals.

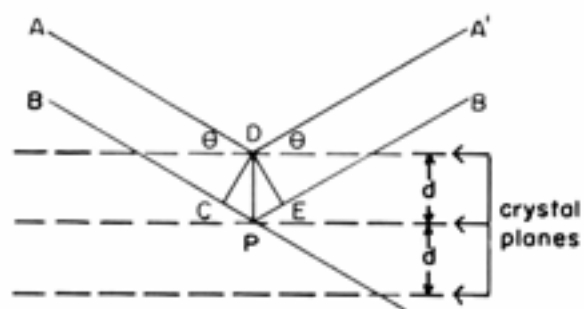


Figure 4-1. Diffraction from crystal planes according to Bragg's Law (from Whittig and Allardice 1986)

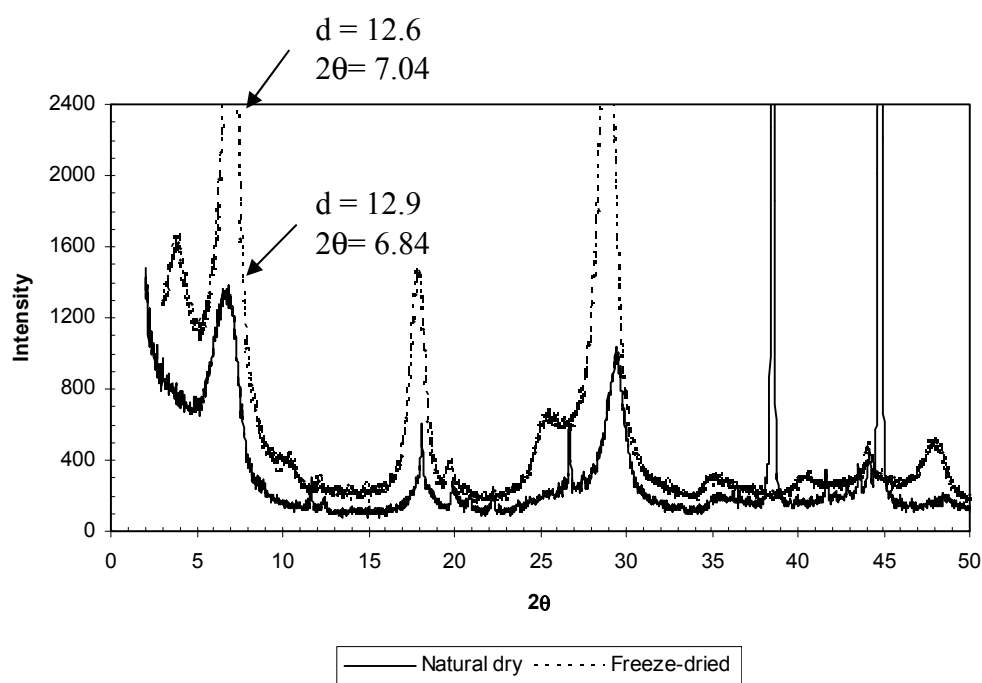


Figure 4-2. Comparison of XRD results for air dried and freeze-dried sodium montmorillonite

CHAPTER 5

METHODS FOR MACRO-CHARACTERIZATION OF STABILIZER EFFECTIVENESS

5.1. INTRODUCTION

In the macro-characterization study standard geotechnical laboratory tests were used to assess how the engineering properties of the test soils were altered by treatment with the liquid stabilizer products. Tests were performed on five soils (the bulk reference clays and the native Texas soils), both untreated and treated with the three selected stabilizer products. A detailed, rational protocol was developed and followed in preparing the soil test specimens. The following engineering properties were then assessed:

- grain size distribution, measured using the hydrometer test method
- Atterberg limits (liquid limit, plastic limit, and plasticity index)
- compaction characteristics, evaluated by comparing the compacted dry density of specimens mixed to the same target water content
- undrained shear strength, measured using unconsolidated-undrained triaxial compression tests
- Free swell potential, determined from one-dimensional swell tests.

All test data are presented in Appendices H through N. The results for the test soils when treated with the ionic, enzyme, and polymer stabilizers are discussed in Chapters 7, 9, and 11, respectively.

5.2. PREPARATION OF SOIL TEST SPECIMENS

Test specimens of untreated and treated soils were prepared by mixing pulverized, air-dry soil with de-ionized water. In this study, treated specimens were prepared following a ten-step protocol, which is outlined in section 5.3. Untreated control specimens were prepared in the same manner, but without the addition of the stabilizer product.

Clearly, test results are influenced by the way the test specimens are prepared. Other laboratory evaluations of soil stabilizers, especially those that failed to show positive effects, have been dismissed for not accurately representing soil conditions in the field. It was thus anticipated that conclusions drawn from this study could be criticized based on the methods used to prepare the test specimens. Hence, a concerted effort was made to clearly define a detailed, rational protocol for preparing untreated and treated soil specimens for the laboratory evaluation of product effectiveness. The ten-step protocol detailed in section 5.3 was developed and followed in preparing all test specimens for the macro-characterization study.

In August 2000 the ten-step protocol was sent to a number of industry representatives and to the Texas Department of Transportation with a request for comments and criticisms. The responses to this request are summarized in Appendix P, together with a discussion of the points raised. Some aspects of the specimen preparation protocol were revised based on the suggestions received. The revised, thirteen-step protocol is given in Appendix Q. Most revisions were minor

and helped to clarify miscellaneous details within the protocol. It is recommended that future studies of this type follow the protocol given in Appendix Q.

In this study all untreated or treated specimens were compacted at the optimum water content for the untreated soil, as given in Tables 2-5 and 5-1. As some stabilizers are reported to affect soil compaction characteristics, it may be better in future studies to determine a separate optimum water content for compaction of the untreated and treated soil samples. The revised protocol in Appendix Q incorporates this suggestion. In this study, however, the same water content was used to prepare all specimens of a given soil, so that the effect of the stabilizer on the measured soil properties could be distinguished from the effects of varying the water content. For the same reason, the samples were maintained at a constant water content during the curing period.

In addition, a seven-day curing period was selected as a reasonable delay to allow reactions between the stabilizer and the soil prior to conducting the evaluation tests. Laboratory assessments of soil stabilizers often include a 28-day cure following treatment; the additional three weeks may, depending on the stabilizer, yield additional changes in the soil properties. However, it is expected that significant changes due to an effective soil treatment should be measurable at seven days.

5.3. SAMPLE PREPARATION PROTOCOL

Four terms are used to describe the proportions of water and chemical stabilizer in a soil. These terms are defined here and shown in Figure 5-1.

IWC = *Initial Water Content* = mass ratio of water to oven-dry solids in the uncompacted soil prior to the addition of the diluted stabilizer chemical.

OWC = *Optimum Water Content* = mass ratio of water to oven-dry soil that yields the maximum dry density of an untreated soil when compacted with a specified compaction effort.

DMR = *Dilution Mass Ratio* = mass ratio of concentrated chemical product to water, used to express the dilution recommended for construction operations. This ratio applies only to the diluted product prior to mixing with the soil and has almost no relevance to the final concentration of product in the treated soil.

AMR = *Application Mass Ratio* = mass ratio of concentrated chemical product to oven-dry soil in the treated soil.

The following ten steps were followed in preparing laboratory test specimens of untreated, control soil specimens and specimens of soil treated with chemical stabilizers. In all cases, only distilled or de-ionized water was used to dilute the stabilizer products or to increase the water content of the test soil. Additional commentary on the selection of these procedural steps is given below.

Step 1. Using a specified compaction test method, determine the optimum water content (OWC) for compaction of the untreated soil.

Step 2. Determine the recommended application mass ratio (AMR) for the stabilizer product.

- Step 3. Dilute the concentrated stabilizer product to the recommended dilution mass ratio (DMR).
- Step 4. Pre-moisten the test soil to an initial water content of $IWC = OWC - (AMR/DMR)$.
- Step 5. Allow the pre-moistened soil to mellow for 16 hours in a sealed container.
- Step 6. Measure out the mass of diluted stabilizer needed to achieve the recommended application mass ratio (AMR) and optimum water content (OWC) in the treated sample.
- Step 7. Thoroughly mix the diluted stabilizer with the soil sample, and then allow to stand for 1 hour in a sealed container.
- Step 8. Compact the soil with the specified compaction method, extrude from the mold, and seal in a container.
- Step 9. Cure the compacted soil in sealed container at room temperature for 7 days.
- Step 10. Trim the sample to an appropriate size for testing, and determine the specimen water content. If the water content is not within acceptable limits for compaction, prepare new specimens using an adjusted initial water content (IWC).

Use of Distilled or De-ionized Water

Dissolved solids in the pore water may alter the soil chemistry and, in some circumstances, could affect the observed test results. Ideally, samples of the water to be used at the project construction site would be used to prepare the laboratory test specimens, but this is rarely practical. Ordinary tap water will typically contain a number of dissolved chemicals that could interact with the stabilizer or soil, so the use of untreated tap water is undesirable. As is generally recommended for geotechnical testing practice, the use of distilled or de-ionized water is recommended here to prevent the introduction of unknown chemical species.

Step 1. Using a specified compaction test method, determine the optimum water content (OWC) for compaction of the untreated soil.

The optimum water content (OWC) for compaction is determined for the untreated soil using an appropriate, standardized compaction test. In this study a modified Proctor compaction test method (ASTM D-1557, AASHTO T-180) was used. Other standardized tests, such as the standard Proctor compaction test method (ASTM D-698, AASHTO T-99) or the TxDOT compaction test methods (Tex-113-E and Tex-114-E), may be more appropriate for a given project. The soil is prepared in accordance with the test specification, which may include screening out oversized particles.

Note that the OWC determined for the untreated soil was used as the target water content for compaction of the treated soil specimens. A separate compaction curve was not determined for the soil when treated with a given stabilizer. Hence, all test specimens, including both untreated control samples and treated samples, should have about the same water content and degree of compaction. Preparing all test specimens in this manner ensures that any observed changes in soil properties can be attributed to the action of the chemical stabilizer and not to substantial differences in the density or fabric of the soil, which would result from different compaction conditions.

Step 2. Determine the recommended application mass ratio (AMR) for the stabilizer product.

The rate of field application recommended by many stabilizer suppliers can be somewhat difficult to translate into an equivalent application rate for preparing laboratory samples. For example, assume 1 gallon of a product is diluted 1 to 500 by volume in water in the field. This diluted product is then sprayed over an area of 5,000 square feet, mechanically mixed with the base material, and compacted to a final thickness of 6 inches. Hence, such a product is applied at a rate of 1 gallon of concentrated product per 2,500 cubic feet of moist, compacted soil. Knowing the density of the concentrated chemical product and the dry density of the compacted soil, it is possible to convert the supplier's recommended application rate to the application mass ratio (AMR) as defined in Figure 5-1.

There are several advantages to expressing the application rate in terms of the application mass ratio (AMR). First, using the AMR simplifies the conversion of recommended field application rates to equivalent values for preparing laboratory test specimens. More importantly, using the AMR clarifies that the critical aspect of determining an appropriate application rate is to consider the ratio of stabilizer chemical to dry soil solids. While the dilution mass ratio (DMR) is relevant for determining how much water to mix with a product prior to use on a construction site, it is really the AMR that expresses how much stabilizer is present in the treated soil. Therefore, AMR is of greater relevance. It is worth noting that conventional lime or cement soil stabilization is also usually specified in terms of lime or cement contents that are computed based on dry soil weights. Finally, using the AMR in combination with the OWC, it is clear how to handle the soil water when computing application rates.

To convert recommended field application rates (e.g., 1 gallon of product diluted in 500 gallons of water, sprayed on 5,000 square feet of soil, and then mixed 6 inches deep), the dry density of the soil is needed. In making these conversions, a representative dry unit weight of about 100 lbs/ft³ was assumed for this study. This represents a typical dry density of a well-compacted clayey soil.

Step 3. Dilute the concentrated stabilizer product to the recommended dilution mass ratio (DMR).

Nontraditional chemical soil stabilizers are typically sold as concentrated liquids that are diluted in water on the project site before application. In this step a sufficient quantity of stabilizer was prepared by diluting the concentrated product in distilled or de-ionized water.

The dilution ratio is usually specified by the supplier on a volumetric basis. For example, the product might be diluted to a ratio of 1 gallon of concentrated chemical per 500 gallons of

water. Knowing the specific gravity or mass density of the chemical, this ratio can be converted to the mass-based DMR, which is more convenient to use in subsequent calculations.

Note that the DMR is *not* the ratio of the chemical product to water in the compacted soil, because the diluted product is added to soil that is already wet with water.

Step 4. Pre-moisten the test soil to an initial water content of $IWC = OWC - (AMR/DMR)$.

Begin with a sufficient quantity of soil for the planned testing program. Screen out oversized particles in accordance with the chosen compaction procedure followed in Step 1. Next, the water content is adjusted to a point dry of the determined optimum water content (OWC) in Step 1. This may involve either air drying the soil over a period of time or spraying distilled or de-ionized water onto the soil as it is thoroughly mixed.

The objective at this step is to mix the soil to an initial water content (IWC) just below the OWC, such that the OWC is attained when the diluted stabilizer is added in Step 7. Recall that the stabilizer chemical, diluted to the DMR, is added to the soil in sufficient quantities to achieve the desired AMR. Adding stabilizer diluted in water will therefore change the water content of the treated soil by this amount:

$$\text{change in water content} = \frac{\text{mass of water added with stabilizer}}{\text{mass of dry soil}}$$

$$\Delta w = \frac{(M_w)_c}{M_s} = \frac{\left(\frac{R}{C} \right) M_c}{DMR} \left(\frac{R}{C} \right) \frac{1}{M_s} = \frac{AMR}{DMR}$$

Hence, if the initial water content (IWC) is set at:

$$IWC = OWC - \frac{AMR}{DMR}$$

then the water content should be equal to the OWC when the diluted chemical is added in Step 7. Note that this calculation assumes no water loss due to evaporation during sample preparation. Depending on laboratory procedures, the IWC may need to be adjusted as discussed under Step 10.

For a typical stabilizer product, the value of (AMR/DMR) is on the order of 3%. Hence, the soil would be pre-moistened to a water content 3% below the OWC at this step.

Step 5. Allow the pre-moistened soil to mellow for 16 hours in a sealed container.

The pre-moistened soil was then sealed in a container and allowed to sit at least 16 hours (overnight) at room temperature. This mellowing period is needed to ensure that the pore water becomes completely and uniformly dispersed into the soil.

Step 6. Measure out the mass of diluted stabilizer needed to achieve the recommended application mass ratio (AMR) and optimum water content (OWC) in the treated sample.

Based on the mass of dry solids (M_s) in the sample, the mass of concentrated chemical (M_c) that must be added to achieve the desired AMR was determined. A sufficient quantity of the diluted stabilizer to obtain the required mass of chemical concentrate was measured out.

If the stabilizer is diluted properly to the DMR in Step 3, and the soil is moistened to the correct IWC in Step 4, then the water content of the treated soil will be equal to the OWC (less any losses due to evaporation).

Step 7. Thoroughly mix the diluted stabilizer with the soil sample, and then allow to stand for 1 hour in a sealed container.

The soil was thoroughly and completely mixed using a mechanical mixer. Care was taken to limit evaporation losses and maintain the desired values of AMR and OWC in the mixed soil.

Immediately following mixing, the sample was sealed in a container and allowed to stand for 1 hour. This standing time is intended to allow the stabilizer chemicals to achieve a more homogeneous diffusion into the soil. Longer standing times were avoided to prevent excessive stabilizer curing prior to compaction. The one-hour delay is also meant to reflect a typical time delay between initial application and mixing of a product and final compaction of a roadbed in the field. The sample was sealed during the standing time to prevent excessive loss of moisture. The one-hour standing time is also required prior to compaction of untreated control samples.

Step 8. Compact the soil with the specified compaction method, extrude from the mold, and seal in a container.

Immediately following the one-hour standing time, the soil was compacted following the same standard procedures used in Step 1. The specimens were then extruded, sealed in containers, and cured according to the procedures in Step 9.

Step 9. Cure the compacted soil in sealed container at room temperature for 7 days.

Compacted samples, including both treated and untreated specimens, were cured at constant water content by placing them in sealed, non-reactive containers (sealed plastic bags). Curing at constant water content was selected to make it possible to discern the effects of a given product on the measured properties of the soil. A constant overall water content eliminates the effect of changing water content on the observed soil strength and stiffness. That is, simply wetting or drying an untreated, unsaturated soil will lead to changes in the measured shear strength in an undrained triaxial test. To observe how much the strength may change due to the presence of the stabilizer, one needs to eliminate variations in water content as a possible cause of these measured changes. This procedure is also believed to effectively represent the curing conditions in a chemically stabilized, compacted roadway subgrade. While the very top of a compacted base material may have free access to air during the curing period, soil just below the surface does not have open ventilation and will remain moist.

Secondly, the soil was cured at room temperature, which is a reasonable and convenient compromise between the extremes of hot or cold temperatures that could be encountered in the field.

Finally, a curing time of seven days was specified to allow sufficient time for the stabilizer product to completely react with the soil. During the curing period, the compacted samples were out of the molds, sealed, and kept at room temperature, as described above. The seven-day cure period is based on the recommendations of the various stabilizer suppliers, is consistent with typical curing periods used in the evaluation of lime and cement soil stabilization, and is convenient for sequencing a laboratory test program.

Step 10. Trim the sample to an appropriate size for testing, and determine the specimen water content. If the water content is not within acceptable limits for compaction, prepare new specimens using an adjusted initial water content (IWC).

At the end of the seven-day curing period, the soil samples were removed from the sealed containers and trimmed to an appropriate size for testing.

The water content of the trimmed specimen was then checked to determine if significant water had been lost to evaporation during sample preparation. This was conveniently evaluated by measuring the water content of the specimen trimmings. The amount of evaporation loss could vary considerably, depending on a number of factors such as the relative humidity and temperature of the laboratory where the soil is mixed.

If the water content of the trimmed specimen was too low, new specimens were prepared using a higher IWC in Step 4. For example, suppose that the compaction specification calls for compacting soil in the field at a water content within $\pm 2\%$ of optimum. If the specimen water content measured in Step 10 was found to be 3% below the OWC (outside the acceptable range), then new specimens should be prepared starting with: $IWC = OWC - (AMR/DMR) + 3\%$.

5.4. MEASUREMENT OF GRAIN SIZE DISTRIBUTION

The grain-size distribution of each untreated and treated soil sample was determined using the hydrometer test method (Figure 5-2). Sieve testing was not feasible, given that all five soils were almost entirely clay- and silt-sized. The hydrometer tests were conducted in accordance with ASTM D 422-63 "Standard Method for Particle-Size Analysis of Soils" (1998a). Sodium hexametaphosphate (Calgon brand water softener) was used as a chemical dispersant with de-ionized water as the solute. A mechanical stirring device (Apparatus A, ASTM D 422-63) was used to mix the sample suspensions. The mass of dispersed soil varied by soil type, depending on the plasticity of the clays. The dry sample mass ranged from 10 g for the sodium montmorillonite to 50 g for the TX Mesquite HS HP and the commercial kaolinite. ASTM 152H hydrometers were employed for the suspended soil readings. The test measurements were corrected to compensate for the dispersing agent and the meniscus error. Measurements taken during testing showed the temperature to be almost constant at $23^\circ \pm 0.5^\circ$ C. Hence, a constant temperature correction factor (K) was used in reducing the data.

The grain size distributions determined from all of the hydrometer tests are plotted in Appendix H. The results are inconclusive. Possible small changes in the gradations of the test soils following treatment cannot be distinguished from the scatter in the test results. The observed scatter may be due to inherent variability between test samples, the sensitivities of the

test method, or operator error. Accordingly, the grain size distribution data will not be discussed further.

5.5. MEASUREMENT OF ATTERBERG LIMITS

The Atterberg limits were determined in accordance with ASTM D 4318-95a "Standard Test Method for Liquid Limit, Plastic Limit, and Plasticity Index of Soils" (1998e). The dry preparation method was used with the untreated soil having been pulverized and air-dried (1% to 10% water content). The soil samples were assumed to be all finer than the No. 40 (425 μm) sieve, as required. A ceramic bowl was used for mixing the soils, and de-ionized water was employed throughout the testing. The treated samples were allowed to mellow for at least 16 hours at the target moisture content prior to testing.

A single, hand-operated liquid limit device (Figure 5-2) was utilized for all tests to avoid introducing device variability. Multipoint liquid limit tests were performed on all samples with a minimum of four points (a combination of blow count and water content) per test; the results are plotted in Figures 2 through 6 in Appendix I. Three plastic limits were performed per test with a goal of all having all tests on the same soil sample within $\pm 1\%$ of one another. The measured Atterberg limits are summarized in Appendix I.

5.6. MEASUREMENT OF COMPACTION CHARACTERISTICS

Compaction tests were performed on the untreated soils using a modified Proctor compaction effort in accordance with ASTM D 1557-91 "Standard Test Method for Laboratory Compaction Characteristics of Soil Using Modified Effort (56,000 ft-lb/ft³, 2,700 kN-m/m³)" (1998b). A 4-inch diameter mold and a mechanically operated rammer were used. The compacted soil was extruded with a hydraulic ram and split longitudinally, and a representative sample was taken for the water content determination.

Moisture-unit weight curves for the five untreated test soils are presented in Figures J-1 through J-5 in Appendix J. The optimum water content (w_{opt}) and maximum dry unit weight (γ_{dmax}) determined for each untreated soil, corresponding to the modified Proctor compaction energy, are summarized in Tables 5-1 and J-1. Separate moisture-unit weight curves were not determined for the soils treated with the three liquid stabilizers.

The measured w_{opt} for compaction of the untreated soil was subsequently used as the target moisture content in preparing all untreated and treated test samples of a particular soil. Following the protocol in section 5.3, test specimens for swell and strength testing were mixed to the target water content, compacted in a 4-inch diameter mold using the mechanical rammer and a modified Proctor compaction energy, extruded with a hydraulic ram, and then trimmed to an appropriate size for testing.

To evaluate the potential effects of a stabilizer product on soil compaction, the compacted density of all untreated and treated soil test specimens were compared. For each soil-stabilizer combination, data are available on seven compacted specimens, which were prepared for swell and strength testing. These data are tabulated and plotted in Appendix K.

5.7. MEASUREMENT OF UNDRAINED SHEAR STRENGTH

To assess the soils' shear strength, unconsolidated-undrained (UU) triaxial compression tests were conducted following ASTM D 2850-95 "Standard Test Method for Unconsolidated-Undrained Triaxial Compression Test on Cohesive Soils" (1998d). Highway subgrade materials are often characterized using unconfined compression tests, but testing in a triaxial cell yields a more reliable measure of strength. This is especially true for fissured, compacted soils where the confining pressure keeps the specimen intact under load.

The triaxial test apparatus is shown in Figure 5-3. An electronic load cell, calibrated against a proving ring, was used to measure the applied axial force. The transducer used to record confining pressure was calibrated using a mercury manometer. In order that specimen volume strains could be determined from changes in the volume of cell fluid, expansion of the triaxial cell was measured over the pressure range used in the tests.

To prepare specimens for testing, the compacted, cured soil samples were quartered using an electric band saw. A trimming frame and blade were then used to form a 1.5-inch-diameter specimen with a height of about 3.75 inches. An initial height-to-diameter ratio of 2.5 to 1 minimized error from end platen friction near failure. Confined inside thin latex membranes, the specimens were then mounted inside the triaxial test cell. At the start of shearing, the load cell readout was zeroed with the piston moving but not in contact with the sample, thereby accounting for friction between the piston and the seal in the test chamber. During shearing, the applied load, axial deformation, and change in cell fluid volume were recorded. At the conclusion of each test, the failed soil specimen was sketched to document the failure mode, then dried and weighed to determine the water content.

Trimmed sample dimensions were measured using a circumferential pi tape and a caliper. The initial cross-sectional area (A_i) was computed from a weighted average of the diameter measured at the top, middle, and bottom of the specimen. The initial sample height (H_i) was taken as the average of measurements taken in three locations. In reducing the raw test data, the height and cross-sectional area of the test specimen at the start of shearing are needed. Because the specimens were unsaturated, some compression of the specimen occurred when the confining pressure was applied. This volume strain ($\epsilon_{v,con}$) is given by:

$$\epsilon_{v,con} = \frac{\Delta V_{buret} - \Delta V_{cell}}{V_i}$$

where ΔV_{buret} is the recorded change in cell fluid volume, ΔV_{cell} is the expansion of the triaxial cell due to the increase in confining pressure, and V_i is the initial volume of the trimmed test specimen ($V_i = A_i \cdot H_i$). Assuming that compression is isotropic, the height (H_o) and cross-sectional area (A_o) of the specimen at the start of shearing are approximately:

$$H_o = H_i \left(1 - \frac{1}{3} \epsilon_{v,con} \right)$$

$$A_o = A_i \left(\frac{1 - \epsilon_{v,con}}{1 - \frac{1}{3} \epsilon_{v,con}} \right)^{2/3}$$

Triaxial tests were conducted on specimens confined under cell pressures (σ_c) of 5, 10, 15, and 20 psi. During the shearing phase, the axial strain of the specimen (ϵ_a) is computed from the measured change in sample height (ΔH):

$$\epsilon_a = \frac{\Delta H}{H_o}$$

Volumetric strains are determined from the change in cell fluid volume indicated by readings in a burette (ΔV_{buret}). These readings are corrected to account for the cell fluid displaced by penetration of the piston (cross-sectional area = a_{piston}) into the cell, so that the volume strain (ϵ_v) is given by:

$$\epsilon_v = \frac{\Delta V_{buret} + (\Delta H * a_{piston})}{H_o * A_o}$$

Compression strains are assumed to be positive.

The deviator stress, equal to twice the maximum shear stress in the sample, is the applied axial load (F_a) divided by the cross-sectional area of the specimen. The area increases during the test as the specimen is axially compressed, so a corrected area (A_c) must be used. Following usual practice, the corrected area of the triaxial specimens was computed assuming a right circular cylindrical shape. This leads to the following equation for computing the deviator stress (σ_d):

$$\sigma_d = \frac{F_a}{A_c} = \frac{F_a(1 - \epsilon_a)}{A_o(1 - \epsilon_v)}$$

Given that the minimum principal stress (σ_3) in the specimen is equal to the applied confining pressure (σ_c), the maximum principal stress is given by $\sigma_1 = \sigma_c + \sigma_d$.

The results from the UU triaxial tests, plotted in terms of the deviator stress and volumetric strain versus axial strain, are presented in Appendix L. Specimen failure was defined as the peak deviator stress or, when no peak was reached, at 15% axial strain. The failure stresses from each test were then plotted (Appendix M) in terms of:

$$p = \frac{1}{2}(\sigma_1 + \sigma_3)$$

$$q = \frac{1}{2}(\sigma_1 - \sigma_3)$$

Linear strength envelopes for each untreated and treated soil were then fit as shown in Appendix M, plots M-1 to M-5. The slope (α) and intercept (d) of the strength envelopes in p-q space are related to the Mohr-Coulomb shear strength parameters (ϕ and c) with the following relationships:

$$\sin \phi = \tan \alpha$$

$$c = d / \cos \phi$$

The shear strength parameters determined in this manner are summarized in Table M-1.

Four UU triaxial tests were conducted on specimens under confining pressures of 5, 10, 15, and 20 psi. This range of pressures was selected to represent the low-pressure levels experienced in highway subgrades. In retrospect, it would have been better to conduct the triaxial tests over a wider range of confining pressure, so that more well-defined strength envelopes could be obtained. Also, because the test specimens were unsaturated, the strength envelopes are inclined ($\phi > 0$); UU triaxial tests will yield a $\phi = 0$ condition only if the soil is saturated. Indeed, higher initial saturation levels gave flatter undrained strength envelopes. For example, the untreated and enzyme-treated kaolinite samples were more than 90% saturated and gave essentially flat strength envelopes. In comparison, the kaolinite samples treated with the ionic and polymer products were only about 85% saturated and exhibited friction angles in excess of 30°. Hence, small variations in the initial properties of the compacted specimens, which did not appear to result from the chemical treatment, can lead to significantly different strength parameters.

Because the shear strength varies with pressure (i.e., the envelopes are inclined), it is somewhat awkward to compare the relative shear strengths of the untreated and treated soils. One cannot simply compare the envelope intercepts (c values), because the strength also depends on the friction angle (ϕ) and confining pressure. It is more convenient to compare the relative strengths of the soil at a common stress level. Here, this comparison was made at an arbitrary normal stress of 100 psi, which was selected to minimize extrapolation of the fitted strength envelopes. A reference shear strength (S_{ref}) was thus computed as:

$$S_{ref} = c + (100 \text{ psi}) \tan \phi$$

where c and ϕ are taken from the fitted strength envelopes (Table M-1).

5.8. MEASUREMENT OF FREE SWELL POTENTIAL

To measure the potential expansiveness of the untreated and treated soils, one-dimensional free swell tests were conducted in accordance with ASTM D 4546-96 "Standard Test Methods for One-Dimensional Swell or Settlement Potential of Cohesive Soils" (1998f). Specimens measuring 2.5 inches in diameter by 0.75 inch thick were tested in the apparatus shown in Figure 5-4. Method A of the ASTM D 4596 standard, involving swelling of an inundated specimen under a nominal seating pressure, was followed.

Soil expansiveness can also be assessed using unconfined specimens subjected to three-dimensional (3-D) swell conditions. Minimal equipment is required to run such tests, which are usually conducted on cylindrical test specimens, with volume changes monitored through periodic measurement of the sample height and diameter. One-dimensional (1-D) swell tests are conducted inside an oedometer ring and require an apparatus for maintaining a constant vertical

seating pressure. While 3-D swell tests may be a valid means for measuring swell potential, 1-D tests were selected for this study for these reasons:

- Volume changes measured in a 1-D test are more accurate and reliable than those measured in a 3-D swell test. Because the sample is confined inside an oedometer ring in a 1-D test, the soil's volume strain is equal to the vertical strain. With a seating pressure on the top platen, vertical deformations can be accurately measured with a dial gage. With a 3-D swell test, measurements of the volume change in an unconfined specimen are less precise because the specimen does not swell uniformly.
- Because the drainage lengths are considerably shorter, a thinner 1-D swell specimen comes to moisture equilibrium much faster than a larger 3-D test specimen. Hence, 1-D swell tests can be completed in much less time.
- Pavement subgrade soils are laterally confined and experience essentially 1-D swelling conditions. Hence, a 1-D swell test is more representative of the field conditions of interest.
- Widely accepted test procedures, embodied in the ASTM standard, are available for 1-D swell tests.

Swell test specimens were trimmed from samples at the target water contents, which were compacted in 4-inch diameter molds using a modified Proctor compaction effort. A trimming frame and blade were used to reduce the diameter of the extruded sample, and a band saw was used to cut the soil into appropriate lengths. The resulting slices were then carefully trimmed into oedometer rings measuring 2.5 inches in diameter by 0.75 inch high. To allow for their much greater expansion, the montmorillonite specimens were trimmed to an initial thickness of 0.40 inch.

The test specimens were then placed in the test apparatus with filter paper and porous stones placed on the top and bottom of the soil. With the weight of the upper platen and stone, and additional pressure from the lever arm of the load frame, a vertical seating pressure of 0.35 psi (2.4 kPa) was applied to the soil. The specimen was inundated with de-ionized water, which could seep into the sample through the top and bottom porous stones. Swelling of the test specimens was then monitored until a well-defined, linear secondary swell response was observed. The dry density of the soil was determined at the conclusion of each test by drying the whole test specimen.

The 1-D free swell data are plotted versus the logarithm of elapsed time in Appendix N. The magnitude of the free swell potential was determined from the test data following the procedure described in ASTM D 4546-96 (1998f). In this construction the end of primary swell is determined by extending intersecting lines through the linear portions of the data in semi-log space.

Table 5-1. Summary of compaction test results from tests on untreated bulk soil samples

<i>Bulk Soil Sample</i>	<i>Maximum Dry Unit Weight (pcf)</i>	<i>Optimum Water Content for Compaction (%)</i>
Kaolinite	98.7	24
Illite	124.5	12
Montmorillonite	96.8	24
TX Bryan HP	115.0	16
TX Mesquite HS HP	112.0	17

Note: All values determined using modified Proctor compaction energy (ASTM D 1557).

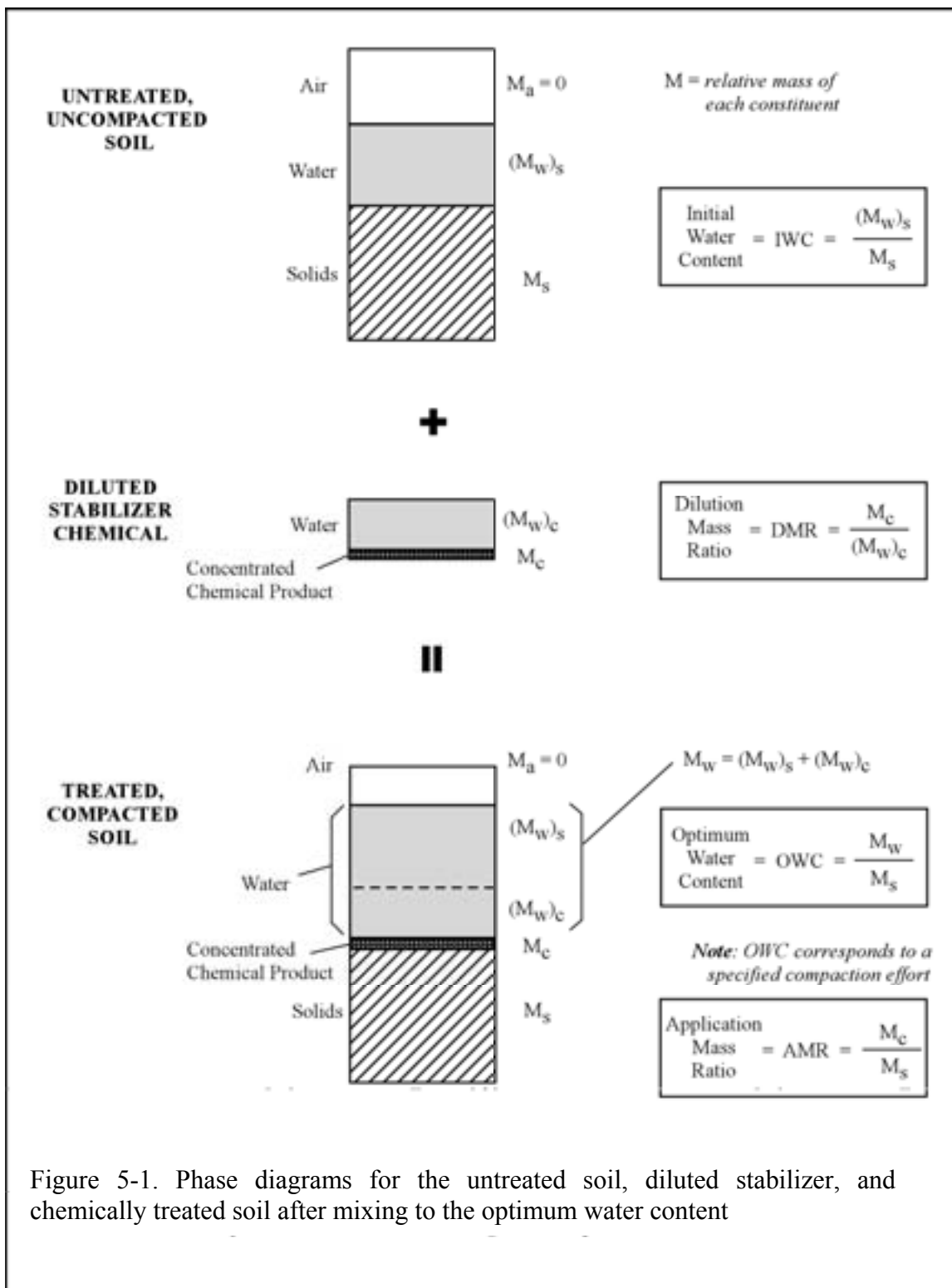


Figure 5-1. Phase diagrams for the untreated soil, diluted stabilizer, and chemically treated soil after mixing to the optimum water content



Figure 5-2. Determination of grain size distribution using the hydrometer test method, and determination of liquid limits using a hand-operated liquid limit device



Figure 5-3. Apparatus used for conducting the unconsolidated-undrained triaxial compression tests



Figure 5-4. Apparatus used for conducting the one-dimensional free swell tests

CHAPTER 6

IONIC STABILIZER: RESULTS FROM STUDY OF STABILIZER MECHANISMS

6.1. OVERVIEW

This chapter presents the results of the clay/ionic stabilizer experiments. The effects of the ionic stabilizer on the clay minerals and natural soils were determined by employing a range of analytical techniques including BET surface area analysis, XRD, SEM/EDS, and ESEM. Specifically, these techniques were employed to test the hypothesized mechanism of clay stabilization by the ionic stabilizer. As stated earlier, ionic stabilizers are believed to work through cation exchange with subsequent alteration in the clay mineral lattice. If the hypothesized mechanism is correct, then changes in mineralogy should be reflected in the XRD analyses, and changes in the CEC and Al:Si ratio should be consistent with a mineral weathering process in which nonexpansive clays are produced. Changes in electron micrographs and external surface area may also be apparent.

The initial tests using SEM/EDS and XRD examined sodium montmorillonite treated with the ionic stabilizer around the manufacturer's application mass ratio of 1:6,000. The observed changes were small, and the testing protocol was adjusted to use an increased application mass ratio of 1:2, which allowed changes to be more obvious and made chemical stabilizer mechanisms more evident. This higher application mass ratio was used to test sodium montmorillonite, kaolinite, illite, Bryan soil, and Mesquite soil.

6.2. RESULTS OF STABILIZER/CLAY EXPERIMENTS CONDUCTED IN THE RANGE OF THE MANUFACTURER'S SUGGESTED APPLICATION MASS RATIOS

Initial soil/stabilizer experiments were conducted on sodium montmorillonite samples treated with the ionic stabilizer in the range of the manufacturer's recommended application mass ratio (AMR) of 1:6,000. The ionic stabilizer was applied to two different fractions of sodium montmorillonite. The first, referred to as "composite samples," contained a measurable quartz component, and the second, referred to as the "montmorillonite fraction," was further centrifuged to obtain a purer sodium montmorillonite sample containing a much smaller quartz fraction. AMRs (mass of stabilizer:mass of dry soil) of 1:1,000, 1:3,000, 1:6,000, and 1:9,000 were applied to both the composite sample and montmorillonite fraction to determine effects of various application mass ratios. The samples were cured for 7 days and then analyzed using SEM, SEM/EDS, and XRD. Scanning electron micrographs for an untreated sample of montmorillonite and a sample treated with the ionic stabilizer at an AMR of 1:6,000 are shown in Figure 6-1. Comparison of the SEM results with a reference spectrum for pure montmorillonite (Figure 6-2b) suggest that the composite samples are somewhat aggregated. It is not possible to identify the flake-like structure in either the treated or untreated samples. It is likely that the montmorillonite is coating quartz particles present in the composite samples as in the reference SEM shown in Figure 6-2a. Nevertheless, it does appear that the treated sample has a morphology different from that of the untreated sample.

To more fully evaluate the differences between the treated and untreated samples, EDS was performed on the samples. Figure 6-3 presents representative EDS spectra obtained for a

single point on scanning electron micrographs of untreated and treated samples of composite montmorillonite. As can be seen in the figure, aluminum (Al), silica (Si), and iron (Fe) peaks are clearly evident in both the untreated and treated composite samples. The presence of both Al and Si in the spectra indicates that a clay particle (as opposed to quartz) was isolated in each sample. The presence of iron is not surprising given that the clay preparation methods did not include an iron removal process because many of these processes can alter the clay structure. In addition, the treated sample also contains sulfur (S). The presence of sulfur is consistent with the presence of ionic stabilizer containing sulfonated limonene. Comparison of the EDS results for the treated and untreated sample indicate that the ratio of Al:Si in the treated sample increased as a result of the treatment. This observation is consistent with the loss of silica during weathering if the end product is similar to kaolinite. However, the results could be confounded by the presence of quartz underlying the montmorillonite, especially given that the depth of penetration of EDS ranges from 1 to 5 microns.

Powder x-ray diffraction (XRD) patterns were collected for untreated and ionic stabilizer treated composite montmorillonite samples to determine whether ionic stabilizer treatment caused changes in clay mineralogy. Data were collected for samples varying in AMR from 1:1,000 to 1:9,000 for the composite samples and are presented in Figure 6-4. Comparison of the XRD patterns indicates that all of the samples are consistent with the reference XRD pattern for montmorillonite; however, for all of the treated samples there is a slight shift in the d-spacing determined by the presence of the peak at a value of approximately $6.5\ 2\theta$. Indeed, comparison of the d-spacings for the first peak in the spectra presented in Table 6-1 shows a reduction in the d-spacing between the untreated and treated samples. However, these lower d-spacings are still consistent with the mineralogy of an expansive montmorillonite sample. Indeed, d-spacings for montmorillonite can range from 9.6 to 18 Å.

The peak at $29\ 2\theta$ disappears after ionic stabilizer treatment at 1:1,000, 1:6,000, and 1:9,000 AMR. Although this peak is representative of montmorillonite as indicated by the reference XRD pattern, it is likely that the disappearance of a peak at this value of 2θ is associated with a change in orientation of the samples rather than a change in mineralogy. However, because this is the only montmorillonite peak affected, it is difficult to prove conclusively.

A characteristic quartz peak observed at $26\ 2\theta$ in all of the samples presented in Figure 6-4 verifies the presence of a quartz fraction. It should be noted that the high relative intensity of the quartz peak is an indication of the strong x-ray absorption characteristics of the peak. Figure 6-5 shows that additional centrifugation was effective in removing the quartz fraction from the montmorillonite. Treatment of this purer fraction led to a much smaller reduction in the d-spacing for an AMR of 1:6,000, as can be seen in Figure 6-5.

Treatment of the composite montmorillonite was also performed using sulfuric acid and the sulfonated limonene prepared in the laboratory. The sulfuric acid and sulfonated limonene were applied at the same concentration and AMR as the ionic stabilizer. The results of these treatments for an AMR of 1:6,000, which are presented in Figure 6-6 and Table 6-1, show a similar decrease in d-spacing for sulfonated limonene, sulfuric acid, and the ionic stabilizer at the recommended AMR of 1:6,000. This suggests that the mode of interaction of sulfonated limonene, sulfuric acid, and the ionic stabilizer with the composite sample provide the same end result of reducing the d-spacing.

The results of these analyses indicate that changes in clay mineralogy may be difficult to assess quantitatively at the suggested manufacturer's AMR of 1:6,000. This is in part due to the

fact that in most natural soils, clay minerals constitute only a fraction of the soil matrix. As a result, much higher application mass ratios of 1:2 were used to enhance the ability to view and study changes in clay and soil morphological and chemical features.

6.3. OVERVIEW OF TESTS AT HIGH APPLICATION RATES

Three well-characterized clays (sodium montmorillonite, kaolinite, and illite) and two natural Texas soils (Bryan and Mesquite) were tested with the ionic stabilizer and sulfuric acid. After characterizing the untreated soil media, each stabilizer was applied to each clay and natural soil using a high application mass ratio (1:2). The testing was performed to evaluate changes in morphology and mineralogy as a result of each chemical stabilizer treatment. The sulfuric acid was also applied to each of the clays and natural soils, at an application mass ratio consistent with the ionic stabilizer, to determine whether high concentrations of protons and sulfate affected the clay properties to the same extent as the ionic stabilizer.

The analytical tests employed to study the clay/stabilizer interactions were BET nitrogen analysis, ESEM, SEM/EDS, XRD, and CEC. The results of these studies are presented in this section according to clay and soil type. Most experiments were conducted with three to twelve replicates (depending on the method), and the figures presented in this section are illustrative of the typical findings. The complete set of results is presented in Appendices C, D, E, and G.

Using results from the BET analysis, pore size distributions were examined for possible changes in the clays and soils after treatment with the stabilizer. This was done to assist in confirming (or disproving) the hypothesized mechanisms of stabilizer interaction with the clay and soil particles. Pore size distributions are provided in the discussion of the BET surface area results for each clay and soil type.

All of the ESEM images presented in this section correspond to a magnification of 7,000 \times and a working distance of 7 to 8 mm. The scale bar at the bottom of the images represents a length of 5 μ m. The ESEM images for both the ionic stabilizer and sulfuric acid treatments for all clay and soil specimens were similar. Therefore the sulfuric acid treated ESEM image was omitted from the images below. However, it is included in Appendix D, along with images taken at a magnification of 200 \times and 14,500 \times .

6.4. XRD RESULTS OF TREATED AND UNTREATED CLAY AND SOIL SAMPLES

X-ray diffraction (XRD) was performed on untreated and treated samples with randomly oriented and oriented specimens. Changes in 2θ (which translate to changes in d-spacing) were determined by evaluating the first peak in the diffractogram (001 peak). Figure 6-7 shows the XRD results for untreated and treated samples, in addition to typical diffractograms for each clay mineral investigated.

Comparison of the diffractograms for the untreated and treated sodium montmorillonite samples with the reference spectrum suggests that sodium montmorillonite is present in all of the samples. No significant differences in the 001 peak were observed following the ionic stabilizer or sulfuric acid treatments of the montmorillonite. However, the peak at approximately 17 2θ disappeared following treatment, and the peak at 29 2θ shifted. In addition, the particular montmorillonite sample contained slight quartz contamination, as shown by the peak at 26 2θ . These results for the ionic stabilizer treatment appear to be somewhat inconsistent with initial results reported in section 6.2, which indicated a slight increase in 2θ for the 001 peak

(corresponding to a decrease in d-spacing) using low AMRs. However, because glycolation tests were not conducted for the low AMR samples, it cannot be determined whether the expansiveness was reduced as a result of treatment with the ionic stabilizer.

Oriented and glycolated samples at high AMRs were prepared and analyzed to further evaluate the 001 peak in untreated and treated samples, both before and after clay layer expansion. The behavior of the clay, when exposed to ethylene glycol, results in a shift of the 001 peak toward a lower 2θ or higher d-spacing (Sarkar 2000). An increase in d-spacing is consistent with expansion of the inner layer. The d-spacing results for randomly oriented, glycolated samples were similar to those expected for montmorillonite. The expected d-spacing value for sodium montmorillonite is 12 Å for randomly oriented samples and 17-18 Å after glycolation. The results for the untreated and treated samples are consistent with expected d-spacings for randomly oriented and glycolated samples, as is shown in Table 6-2. Thus, the ionic stabilizer treatment does not appear to impact the ability of the montmorillonite to expand at the high AMRs used in this part of the research.

The results presented for kaolinite treated samples also do not indicate a change in 2θ (or d-spacing) as a result of treatment. Diffractograms for both untreated and treated samples are consistent with the reference sample. Because kaolinite is a nonexpanding clay, d-spacings will not be affected by glycolation. As a result, glycolated samples were not analyzed.

The location of the 001 peak for the reference illite is located at approximately 8 2θ . The results presented in Figure 6-5 and Table 6-2 indicate that there were no changes in d-spacing as a result of treatment. Oriented and glycolation tests were also performed to determine if changes in d-spacing would occur for oriented samples and to verify the nonexpansive properties of illite, respectively. The d-spacing results for the glycolated samples were similar to those for the randomly oriented samples. The results verify that illite is a nonexpansive clay and that there were no changes in the d-spacing as a result of ionic stabilizer treatment.

Figure 6-8 provides a comparison of untreated and treated samples for the native soils. The effects of glycolation and orientation for the treated Bryan samples and the treated and untreated Mesquite samples are not presented because XRD of treated, glycolated samples proved to be difficult. In both cases, the samples clumped after treatment, making it difficult to separate the clay fraction for further analysis. However, as is indicated in Figure 6-8, the XRD patterns showed no shift in peaks located at 2θ of 7.6 or 11.5. Comparison of the d-spacings for the untreated oriented Bryan sample (15.13 Å) with those for the untreated, glycolated Bryan sample (17.40 Å) indicated that the material contains an expansive fraction, as well as a nonexpansive (illite) component ($2\theta = 8.8$). In addition, treatment with the ionic stabilizer and sulfuric acid decreased the d-spacing of randomly oriented samples from 15.3 Å to 13.9 Å and 13.3 Å, respectively. The d-spacing for the untreated Mesquite soil sample was consistent with the presence of an expansive soil component. However, it was not possible to identify the location of the 001 peak for the treated samples, as is shown in Figure 6-8.

6.5. BET ANALYSIS OF TREATED AND UNTREATED CLAY AND SOIL SAMPLES

BET nitrogen adsorption results for treated and untreated samples are presented in Table 6-3. A comparison between the measured surface area results and those reported by the University of Missouri Source Clays Repository showed good agreement for all of the clay minerals, although surface areas of the treated and untreated illite samples were all slightly higher than the published values. The untreated samples were analyzed as both washed and

unwashed specimens, to determine whether or not washing had an impact on surface area measurements. The results do not suggest a difference in surface area between washed and unwashed samples except for the illite sample, in which there was an increase in surface area between the unwashed and washed samples ($28.4 \text{ m}^2/\text{g}$ and $35.03 \text{ m}^2/\text{g}$, respectively). This increase in surface area may be the result of slight particle fragmentation caused by washing the illite, but the change in surface area was not significant enough to negate the benefits of washing the samples after treatment to remove residual material that would otherwise remain after drying the samples.

Comparison of the surface areas of the treated and untreated samples suggests that the effect of treatment varied among the different soil materials. Treatment of montmorillonite with the ionic stabilizer led to a significant reduction in surface area, whereas treatment of the kaolinite and illite with the ionic stabilizer did not appear to impact the surface area of the clay minerals. The results for the two soils were similar to the montmorillonite sample. In both cases, there was a significant reduction in the surface area of the soils following treatment with the ionic stabilizer; however, the reduction was greater for the sample of Bryan soil.

Treatment with sulfuric acid also produced varied results among the soils. A reduction in surface area was observed for samples of montmorillonite and kaolinite, and an increase in surface area was apparent for both of the soil samples treated with sulfuric acid. There was no effect of sulfuric acid treatment on the illite sample.

Differences between the effect of sulfuric acid and the ionic stabilizer on kaolinite and the soils were not expected based on the proposed mechanism of attack of these chemicals on clay matrices. An increase in surface area can be explained by dissolution and recrystallization of particles to smaller particles or by an increase in the number of accessible pores. Because nitrogen does not penetrate the inner layer of clay particles during a BET analysis, the pores in this case correspond to the pore space between individual clay particles. Thus, in a clay matrix, an increase in surface area resulting from an increase in accessible pores would correspond to altering the spacing between clay particles. A decrease in surface area can be explained either through a particle bridging mechanism, in which particles destabilize and flocculate to form larger particles, or through a pore blockage mechanism, in which the chemicals block access to the pore space between clay particles. For sulfuric acid addition to the samples, the latter mechanism of surface area reduction would be unlikely.

To investigate which of these mechanisms might be responsible for the observed effects, further analyses were conducted. First, an excess of sulfuric acid (20 parts sulfuric acid to 1 part dry soil, in contrast to 1 part sulfuric acid to 2 parts dry soil for regular sulfuric acid treatment) was added to sodium montmorillonite to enhance the rate of weathering. For this treatment, a significant increase in surface area ($83.85 \text{ m}^2/\text{g}$ for the heavy sulfuric acid treatment, as compared with $30.87 \text{ m}^2/\text{g}$ for the untreated clay) was observed, which would be consistent with an increase in the number of particles in the system.

Second, the nitrogen adsorption data were evaluated to determine the pore size distribution for each of these samples. These results are plotted in Figures 6-9 through 6-12. Treatment of the montmorillonite sample with the ionic stabilizer and the sulfuric acid (at an AMR of 1:2) produced similar effects on the pore size distribution. In each case, an increase in pore volume was observed for pores in the 20 to 100 Å range. Similar but more dramatic results (shown in Figure 6-13) were observed for the high sulfuric acid treatment that was used to simulate weathering. For the ionic stabilizer and the high sulfuric acid treatment, the volume of pores less than 20 Å decreased following treatment. Although this reduction was not observed

for the sulfuric acid, a decrease in microporosity (pores less than 10 Å) must have occurred because the surface area of the montmorillonite decreased after treatment. Unfortunately, nitrogen adsorption cannot estimate the volume of pores less than about 15 Å.

The results for kaolinite also showed a shift in the pore size distribution for both the ionic stabilizer and sulfuric acid treatments, although the pore volume in all cases was very small. The pore size distributions shown in Figures 6-9 and 6-10 indicate a shift to smaller pore radii following ionic stabilizer treatments and sulfuric acid. Whereas a large portion of the pore volume is associated with pore radii of 700 Å in the untreated samples, this peak is absent from the ionic stabilizer treated sample and significantly reduced in the sulfuric acid treated sample. Treatment of illite with the ionic stabilizer and the sulfuric acid were similar. In both cases, smaller radii pores (less than 18 Å) were absent from the treated samples.

The pore size distribution results were similar for the two soil samples, as is shown in Figures 6-11 and 6-12. Treatment of the samples with the ionic stabilizer did not lead to a shift in the pore size distribution. In all cases, a peak is observed at approximately 18 Å. However, ionic stabilizer treatment reduced the size of this peak, suggesting fewer particles containing pores of a similar nature are present in the samples. Treatment of the soils with the sulfuric acid did not yield the same reduction in size of this peak in the pore size distribution. Furthermore, an increase in pores of smaller radii was evident, especially for the Bryan soil. This suggests that the sulfuric acid may be creating new micropores in the soil particles. This finding is inconsistent with the results of the montmorillonite results presented above.

6.6. ESEM AND SEM/EDS ANALYSES OF TREATED AND UNTREATED CLAY AND SOIL SAMPLES

ESEM Images

ESEM images for the treated and untreated samples of the clay minerals are presented in Figure 6-14. The sodium montmorillonite images were obtained after 12 days of curing, owing to mechanical servicing of the ESEM instrument. The ESEM images for montmorillonite appear to be similar to the typical SEM shown in Figure 6-2b. However, the ESEM images appear less flaky than the reference SEM, presumably because of moisture in the ESEM samples. Comparison of treated and untreated ESEM images of montmorillonite samples indicates the presence of sharper particle edges after treatment with the ionic stabilizer. This result is consistent with dissolution of the particles.

A typical SEM image of illite is displayed in Figure 6-15. The illite particles appear to contain flaky, platy, geometric layers in this image. However, other literature presents more string-like features. This seems to indicate significant variability among ESEM images. The SEM image in Figure 6-15 was selected because it was most similar to those observed in this study. Indeed, the images obtained in this study (Figure 6-14) appear to be similar to the typical SEM of illite in Figure 6-15. However, the ESEM images appear less flaky and do not have sharp edges like the SEM images in the literature. The ESEM images for treated illite were obtained after 7 days of curing. A comparison of the ESEM images indicates that the ionic stabilizer may lead to particles with sharper edges, as can be observed for montmorillonite.

The ESEM images for kaolinite were obtained after 9 days of curing. The ESEM images in Figure 6-14 appear to be similar to the SEM of kaolinite in the literature, as is shown in Figure 6-15. The ESEM images of kaolinite do not indicate a noticeable difference upon application of

the ionic stabilizers when compared with the untreated sample.

ESEM images for treated and untreated samples of the soils are shown in Figure 6-16. The treated Mesquite and Bryan soils were cured for twelve and seven days, respectively. The ESEM images for the ionic stabilizer treated sample of the Mesquite soil indicates that the particle morphology changed considerably. The ESEM image for the soil treated with the ionic stabilizer is similar to an ESEM image of gypsum ($\text{CaSO}_4 \bullet 2\text{H}_2\text{O}$) obtained from the literature and presented in Figure 6-17. Gypsum is one of the most common types of sulfate containing minerals found in soil environments. The presence of gypsum in this sample is not surprising, given the high sulfate content of the ionic stabilizer. Indeed, similar results were observed with the sulfuric acid treated samples shown in Appendix D.

EDS Results

A more sophisticated technique using SEM coupled with energy dispersive X-ray (EDS) analysis was used to help derive more detailed information regarding changes in particle composition following treatment with the stabilizer. The major goal in this analysis was to evaluate changes in the Al:Si ratios. This ratio is expected to increase if silica is released from the clay as occurs in a natural weathering process; however, if Al is selectively extracted from the clay mineral, a decrease in this ratio would be expected. The peak response in the EDS results can be used to identify the element present, and the intensity (counts/sec) indicates the concentration of that element (Electroscan 1996). EDS results for averages of untreated and treated samples of the clay minerals and soils are presented in Table 6-4. For all of the clay minerals, the Al:Si ratio varied less than 8% between the untreated sample results and data obtained from the University of Missouri Source Clays Repository. The Al:Si ratios were similar for both sulfuric acid and ionic stabilizer treatments of the clay minerals. For all of the clay minerals, the Al:Si ratio decreased following treatment. However, the standard deviations for many of the conditions tested were relatively high. To evaluate whether these decreases were statistically significant, hypothesis testing was conducted using a two-sided Student's t-test, in which retained results suggest the mean values of Al:Si ratio are not significantly different between treated and untreated samples. The test assumed that both sample sets were random and independent with equal population variances.

The results of the hypothesis testing suggests that for montmorillonite the decrease in Al:Si ratio following treatment with either the ionic stabilizer or sulfuric acid was not significant at the 95% confidence level. The decrease in Al:Si ratio following treatment of kaolinite was significant based on rejection of the null hypothesis of equal means at the 95% confidence level (if the confidence level was increased to 99%, the null hypothesis would have been retained). Ionic stabilizer treatment did not yield significant changes in the Al:Si ratios of illite samples; however, treatment with sulfuric acid did lead to a significant reduction at the 95% confidence level (if the confidence level was increased to 98%, the null hypothesis would be retained). A decrease in Al:Si ratio would be consistent with a mechanism in which Al is selectively extracted from the clay mineral. However, the XRD results were not consistent with a major change in clay structure.

Comparison of the Al:Si ratios of untreated and treated soil samples varied among the soils. The Al:Si ratio did not change significantly for the Mesquite soil, whereas a significant reduction in Al:Si ratio was observed for the Bryan soil. Comparison of the EDS spectra between the treated and untreated Bryan soil samples (Figure 6-18) shows a significant sulfur (S)

contribution to the ionic stabilizer treated sample. Indeed, the analyses indicate that the S content of the soil increased from 0.05 to 4.45% following treatment. The sulfur content of the untreated sample (0.05%) compares favorably to the 0.03% result obtained from ICP analysis of a hydrofluoric acid (HF) digestion of the soil. The increase in sulfur content after treatment is consistent with the presence of the sulfur containing ionic stabilizer. The untreated Mesquite soil also contained significant S content, as was indicated both by the HF digestions (1.36% S) and the EDS results (0.2%). The ionic stabilizer and sulfuric acid treated samples of Mesquite soil also contained a very high amount of sulfur (6% to 7% by weight), consistent with the results for the Bryan soil.

Evaluation of SEM images of the Mesquite soil indicated that several SEM images contained sharp fragments with a morphology completely different from any of the materials found in the untreated particles. The trend was also identified in ESEM images. The EDS results of these SEM images representing Mesquite soil treated with ionic stabilizer were compared with EDS results obtained from the concentrated ionic stabilizer (after reacting with NaOH) and untreated Mesquite soil. Sodium hydroxide was added to the concentrated ionic stabilizer to mimic the cation transfer (Na^+) that was suspected to otherwise occur with clay lattice cationic species. A comparison of these EDS results is presented in Figure 6-19.

Because clay fractionation was not performed for the Mesquite soil, many minerals and clay materials are present in the sample. This makes reproducibility difficult, because particles that appear similar in SEM may indeed be different materials. This was also evidenced by a variable occurrence of potassium and calcium in the EDS results.

As evident in the EDS results, the Mesquite soil treated with the ionic stabilizer had very low intensities for aluminum and silica but very high levels of sulfur. The ionic stabilizer in concentrated form contained high levels of sulfur and sodium (the sodium dissociated from NaOH and attached to the sulfate anion). Although it is more difficult to displace calcium than sodium from the soil due to its higher selectivity for clay minerals, high concentrations of hydrogen ions can displace calcium from the inner layer of clays, and chemical weathering is possible in these acidic conditions. Furthermore, if calcium is released from the clay, the Mesquite soil contains all four essential components (water, sulfates, calcium, and aluminum) for formation of highly expansive calcium-alumina-sulfate-hydrate minerals.

6.7. CEC ANALYSIS OF TREATED AND UNTREATED MONTMORILLONITE

Cation exchange capacity (CEC) was measured for untreated and treated samples of montmorillonite at three application mass ratios: 1:3, 1:1,000 and 1:6,000. Three application mass ratios were used to study the effects of the stabilizer over a wide range of concentrations. However, as is evident from the data presented in Table 6-5 and hypothesis testing of the data, there is no impact of the ionic stabilizer on the CEC of the montmorillonite sample at any of the AMRs examined. Indeed, the null hypothesis, which assumed that untreated and treated CEC mean values were equal, was retained for all of the samples at the 95% confidence level. These data provide further support that there are no significant changes in the clay mineralogy due to treatment with the ionic stabilizer.

6.8. SUMMARY

For sodium montmorillonite, BET surface area measurements indicated a substantial

decrease in surface area for the ionic stabilizer treatment. Moreover, ESEM images showed sharper edges on the sodium montmorillonite clay particles following ionic stabilizer treatment. The EDS and XRD results for the ionic stabilizer treatment did not support the proposed mechanism, and no changes in clay chemical structure alteration were observed for the ionic stabilizer treatment at the AMR of 1:2 for sodium montmorillonite.

The kaolinite samples did not experience any changes in clay layers associated with the ionic stabilizer treatment, based on the XRD and EDS Al:Si results. However, this was expected, because hydrogen ions are adsorbed less readily for clays with low cation exchange capacity. Therefore, kaolinite has a resistance to clay structure alteration (Loughnan 1969). A neoformation process is possible in low pH environments, but there was no strong evidence for this process in the ionic treated samples of kaolinite.

Similarly, no clay chemical alteration was expected for the illite treated with the ionic product. In this case, the K^+ ions are held so tightly within the clay interlayer that H^+ replacement is very unlikely. This expectation was supported by the EDS and XRD results, which indicated no chemical change associated with the ionic stabilizer treatment of illite.

The results of the ionic stabilizer treatment for the Bryan soil are conflicting. A decrease in the Al:Si ratio is evident, as expected by the above mechanism of hydrogen transfer to the interlayer and release of clay cations into solution. At such a low pH, aluminum is soluble and could be removed from the clay lattice, resulting in a decrease in the Al:Si ratio. On the other hand, while the XRD results did indicate a change in the d-spacing of the clay, the reduced value of the d-spacing is still consistent with an expansive clay. Although the glycolated XRD diffractogram indicated that untreated Bryan soil contains an expansive clay, it was not possible to analyze glycolated soil samples. Further testing is warranted to assess changes in d-spacing as a result of treatment and glycolation.

The Mesquite soil also contained a smectite-type clay, according to XRD results. However, no chemical changes were observed in either the EDS or XRD analyses. The EDS results indicated no changes in Al:Si ratios as a result of treatment and detected the presence of calcium and potassium in the soil. Based on a comparison of the diffractogram of the ionic treatment of Mesquite soil with well-characterized clay diffractograms, it appears that the Mesquite soil contains gypsum and illite. Gypsum is a very common sulfate mineral found in clay that has the ability to form highly expansive calcium-alumina-sulfate-hydrate minerals in the presence of calcium and water. For this reason, it could be detrimental to apply the ionic stabilizer to Mesquite soil, because the ionic stabilizer might enable expansion of clay materials rather than stabilization.

The Mesquite soil contained impurities and minerals that proved difficult to remove by Stokes' settling procedures. Separation of the clay fraction is essential to understanding the mode of interaction between the ionic stabilizer and clay particles. Therefore, it is difficult to determine the validity of the hypothesized mechanisms of ionic stabilizer treatment for both Bryan and Mesquite soils.

Table 6-1. XRD results of composite and montmorillonite fraction samples

<i>Sample</i>	<i>d-spacing (Å)</i>
Composite Samples	
Untreated	12.4
1:9,000 ionic treated	11.3
1:6,000 ionic treated	11.2
1:1,000 ionic treated	11.1
1:6,000 sulfuric acid	11.15
1:6,000 sulfonated limonene	12.1
Montmorillonite Fraction	
Untreated	12.85
1:6,000 ionic treated	12.77

Table 6-2. Summary of d-spacings and values of 2θ for the 001 peak for untreated and ionic stabilizer and sulfuric acid treated samples of clay minerals and native soils

<i>Sample Description</i>	<i>d-spacing (Å)</i>			<i>2θ</i>		
	<i>Ionic Stabilizer</i>	<i>Sulfuric Acid</i>	<i>Untreated</i>	<i>Ionic Stabilizer</i>	<i>Sulfuric Acid</i>	<i>Untreated</i>
Illite						
Randomly oriented	10.071	10.071	10.094	8.78	8.78	8.76
Glycolated	10.164	10.187	10.14	8.7	8.68	8.72
Oriented	10.187	10.071	10.21	8.68	8.78	8.66
Montmorillonite						
Randomly oriented	12.81	12.45	12.923	6.9	7.1	6.84
Glycolated	17.327	17.126	17.192	5.1	5.16	5.14
Oriented	13.272	14.119	14.929	6.66	6.26	5.92
Kaolinite						
Randomly oriented	7.266	7.173	7.184	12.18	12.34	12.26
Glycolated	NA	NA	NA	NA	NA	NA
Oriented	NA	NA	NA	NA	NA	NA
Bryan Soil						
Randomly oriented	13.85	13.3	15.29	6.38	6.65	5.78
Glycolated	NA	NA	17.40	NA	NA	5.08
Oriented	NA	NA	15.134	NA	NA	5.84

Table 6-3. BET results for ionic stabilizer treated samples of montmorillonite, kaolinite, illite, Bryan soil, and Mesquite soil

<i>Sample Description</i>	<i>BET N₂ Surface Area</i>	
	<i>(m²/g)</i>	<i>St. Dev. (+/-)</i>
Montmorillonite		
Unwashed/untreated	31.79	0.3465
Untreated ^a	30.87	0.2843
Weathered (excess H ₂ SO ₄)	83.85	1.744
Sulfuric acid (H ₂ SO ₄) ^a	16.39	0.1413
Ionic stabilizer ^a	5.009	0.05477
Repository ^b	31.82	0.22
Kaolinite		
Unwashed/untreated	11.05	0.03189
Untreated ^a	11.5	0.06867
Ionic stabilizer ^a	12.02	0.1908
Sulfuric acid (H ₂ SO ₄) ^a	7.991	0.0415
Repository ^b	10.05	
Illite		
Unwashed/untreated	28.4	0.1482
Untreated ^a	35.03	0.6272
Ionic stabilizer ^a	28.42	0.3205
Sulfuric acid (H ₂ SO ₄) ^a	27.86	0.3656
Repository ^b	23.7	
Bryan Soil		
Unwashed/untreated	35.48	0.1119
Untreated ^a	31.93	0.1142
Ionic stabilizer ^a	13.15	0.1118
Sulfuric acid (H ₂ SO ₄) ^a	57.96	0.4773
Mesquite Soil		
Unwashed/untreated	40.45	0.2226
Untreated ^a	40.88	0.2809
Ionic stabilizer ^a	32.09	0.2105
Sulfuric acid (H ₂ SO ₄) ^a	47.43	0.2864

^a Samples were washed, treated, cured, and rinsed through a 0.45 µm cellulose nitrate filter prior to evaluation.

^b Results provided by University of Missouri Repository Source Clay Data Sheet.

Table 6-4. Al:Si ratios and hypothesis testing of EDS results obtained for untreated and ionic stabilizer and sulfuric acid treated samples of clay minerals and native soils

<i>Sample Description</i>	<i>Al:Si</i>					<i>Reject/ Retain Ho</i>
	<i>Ratio (wt %)</i>	<i>Std. Dev (±%) (S_i)</i>	<i># Samples</i>	<i>Calculated t value</i>	<i>Value of t_{0.975}</i>	
Montmorillonite						
Untreated	0.395	0.105	11			
Ionic stabilizer	0.387	0.091	10	0.193	2.093	Retain
Sulfuric acid	0.383	0.091	11	0.291	2.086	Retain
<i>Repository</i>	0.366					
Kaolinite						
Untreated	1.052	0.036	10			
Ionic stabilizer	1.016	0.022	10	2.703	2.101	Reject ^a
Sulfuric acid	1.013	0.029	10	2.693	2.101	Reject ^a
<i>Repository</i>	1.015					
Illite						
Untreated	0.579	0.035	11			
Ionic stabilizer	0.525	0.090	14	1.865	2.069	Retain
Sulfuric acid	0.517	0.084	10	2.242	2.093	Reject ^b
<i>Repository</i>	0.558					
Bryan Soil						
Untreated	0.532	0.031	8			
Ionic stabilizer	0.346	0.125	7	4.078	2.160	Reject
Sulfuric acid	0.405	0.101	7	3.413	2.160	Reject
Mesquite Soil						
Untreated	0.583	0.184	7			
Ionic stabilizer	0.583	0.082	12	0.002	2.110	Retain
Sulfuric acid	0.580	0.088	10	0.049	2.131	Retain

Note: Each treated sample was compared with an untreated sample using the Student's t-test assuming both sample sets are random, independent, and with equal population variances.

^a Ho was not rejected at 99% confidence level.

^b Ho was not rejected at 98% confidence level.

Table 6-5. Cation exchange capacity results for the untreated and ionic treated montmorillonite

<i>Sample Description</i>	<i>Application Mass Ratio</i>	<i>CEC (centimoles/kg)</i>					<i>Reject/ Retain Ho</i>
		<i>Avg.</i>	<i>Std. Dev</i>	<i># Samples</i>	<i>t</i>	<i>t_{0.975}</i>	
Montmorillonite							
Untreated	zero	54.16	6.04	3			
Ionic stabilizer	1:3	48.19	4.34	3	1.390	2.776	Retain
Ionic stabilizer	1:1,000	52.82	3.06	3	0.343	2.776	Retain
Ionic stabilizer	1:6,000	49.46	2.85	3	1.219	2.776	Retain

Note: Each treated sample was compared to untreated sample using the Student's t-test assuming both sample sets are random, independent, and with equal population variances.

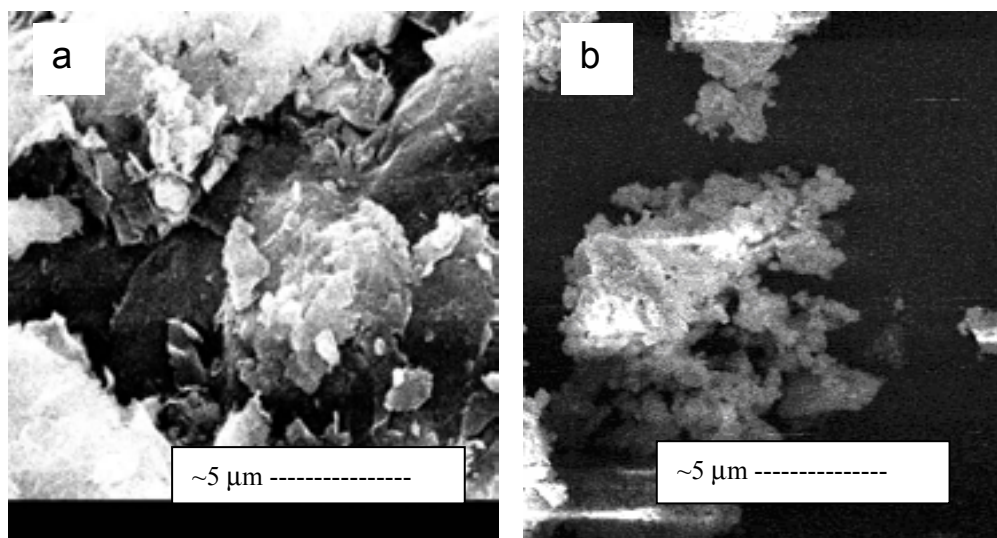


Figure 6-1. SEM images at a magnification of 5,000 \times for (a) untreated and (b) ionic stabilizer (AMR 1:6,000) treated composite samples

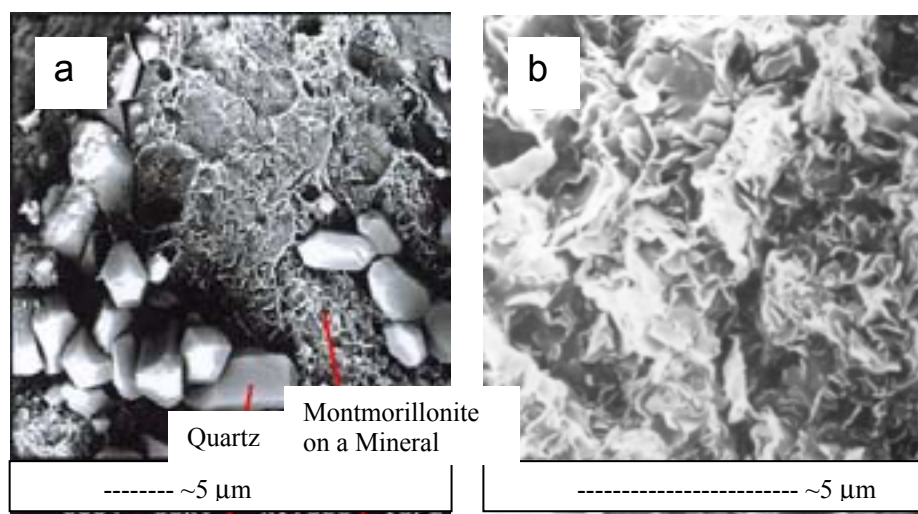


Figure 6-2. Reference SEM images of (a) sodium montmorillonite coating another mineral (adapted from www.glossary.oilfield.slb.com/Files/OGL98037.jpg) and (b) pure montmorillonite (adapted from Keller 1989)

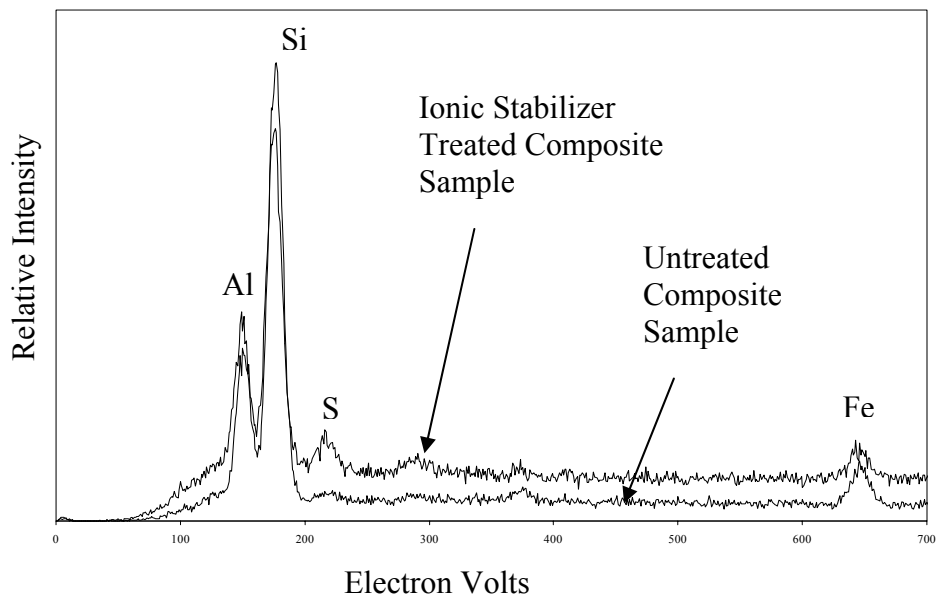


Figure 6-3. Comparison of EDS results for an untreated composite sample and AN ionic stabilizer treated sample (AMR 1:6,000)

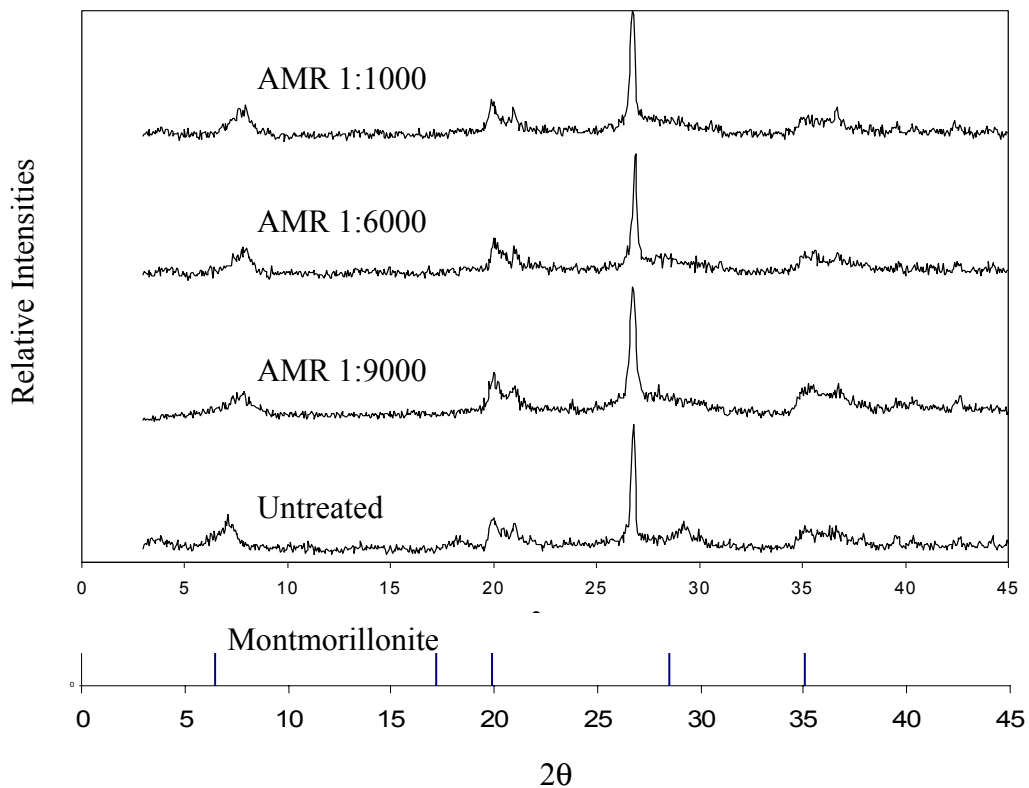


Figure 6-4. Reference XRD pattern for montmorillonite and XRD patterns for montmorillonite composite samples that were untreated and treated with the ionic stabilizer at AMRs of 1:1,000, 1:6,000, and 1:9,000

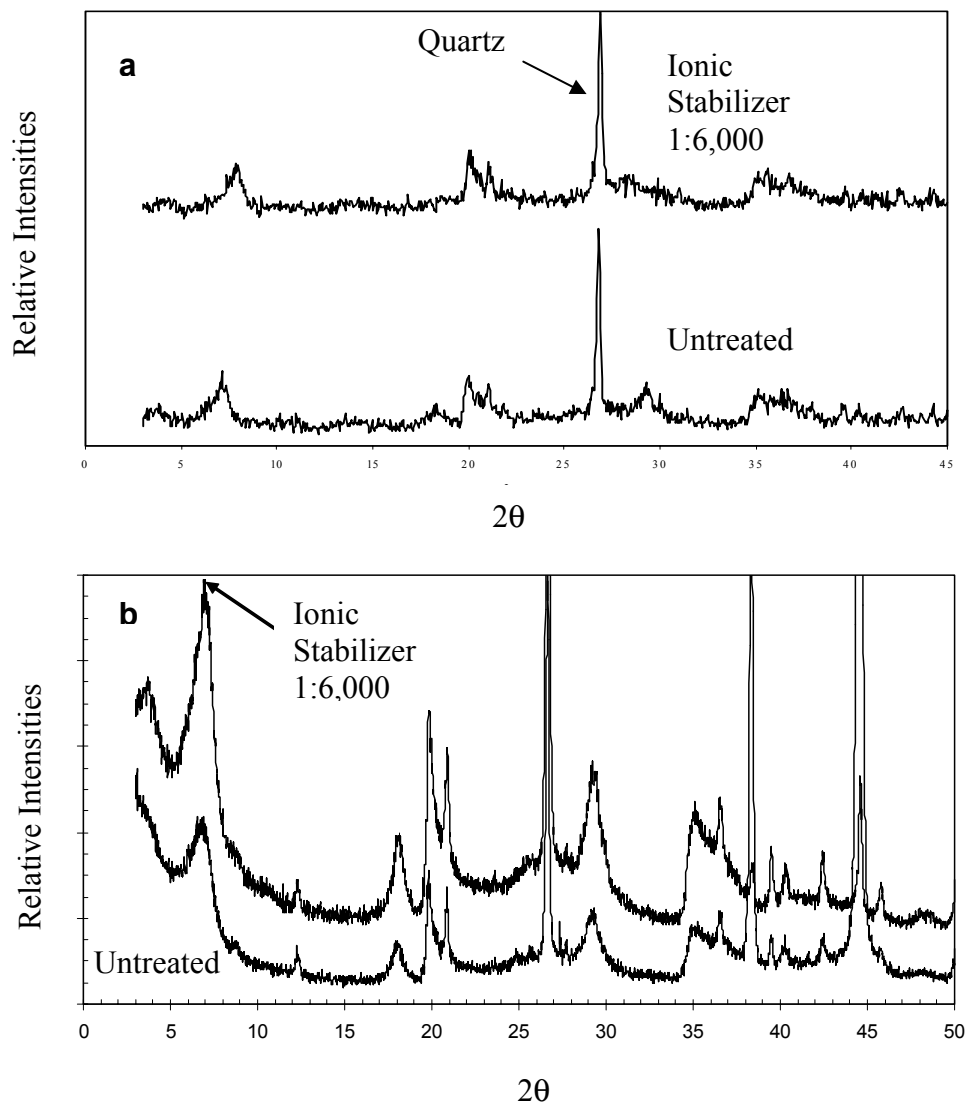


Figure 6-5. X-ray diffraction patterns for (a) composite sample and (b) montmorillonite fraction treated with the ionic stabilizer at the recommended AMR of 1:6,000

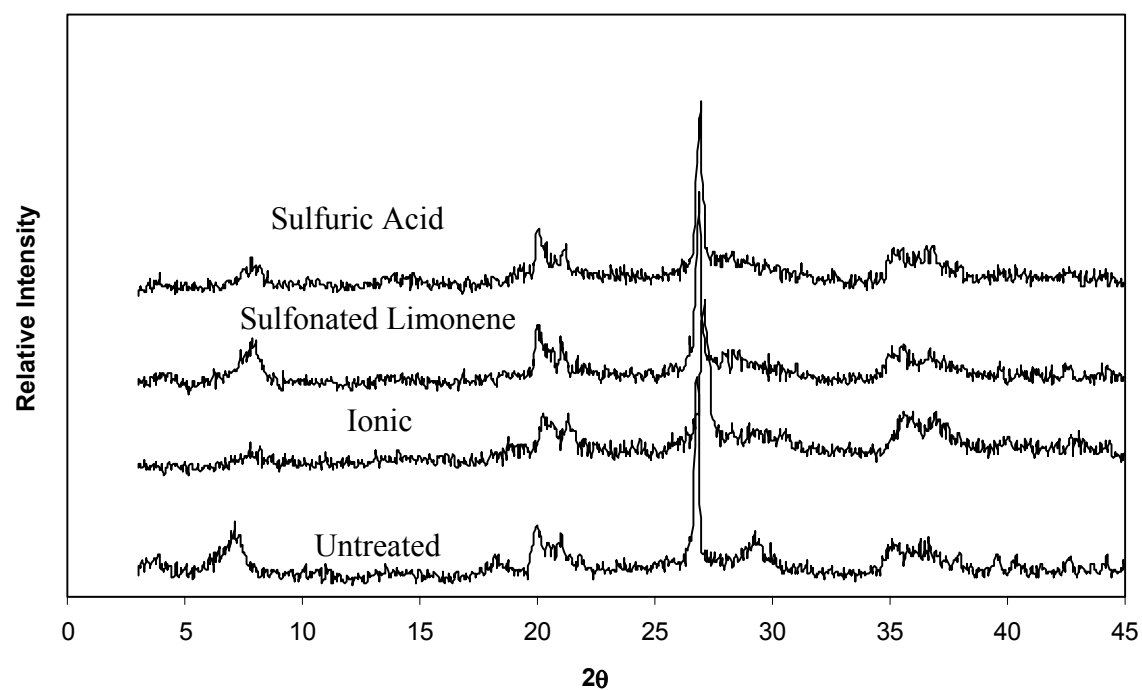


Figure 6-6. X-ray diffraction patterns for freeze-dried composite samples treated at an AMR of 1:6,000 with the ionic stabilizer, sulfonated limonene, and sulfuric acid

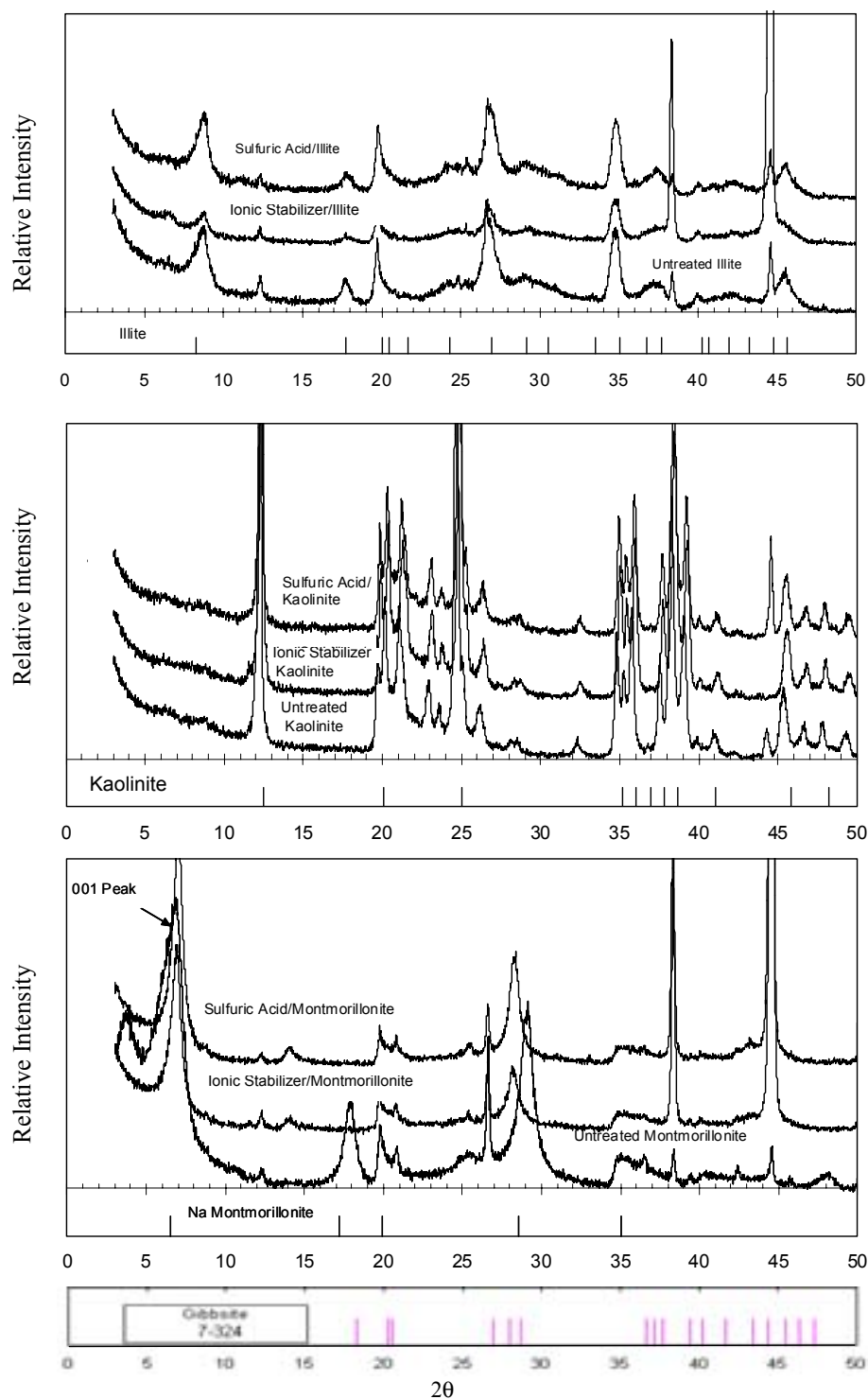


Figure 6-7. X-ray diffraction patterns for untreated and ionic stabilizer and sulfuric acid treated samples of illite, kaolinite, and montmorillonite (reference spectra from Mineral Powder Diffraction File Data Book 1980)

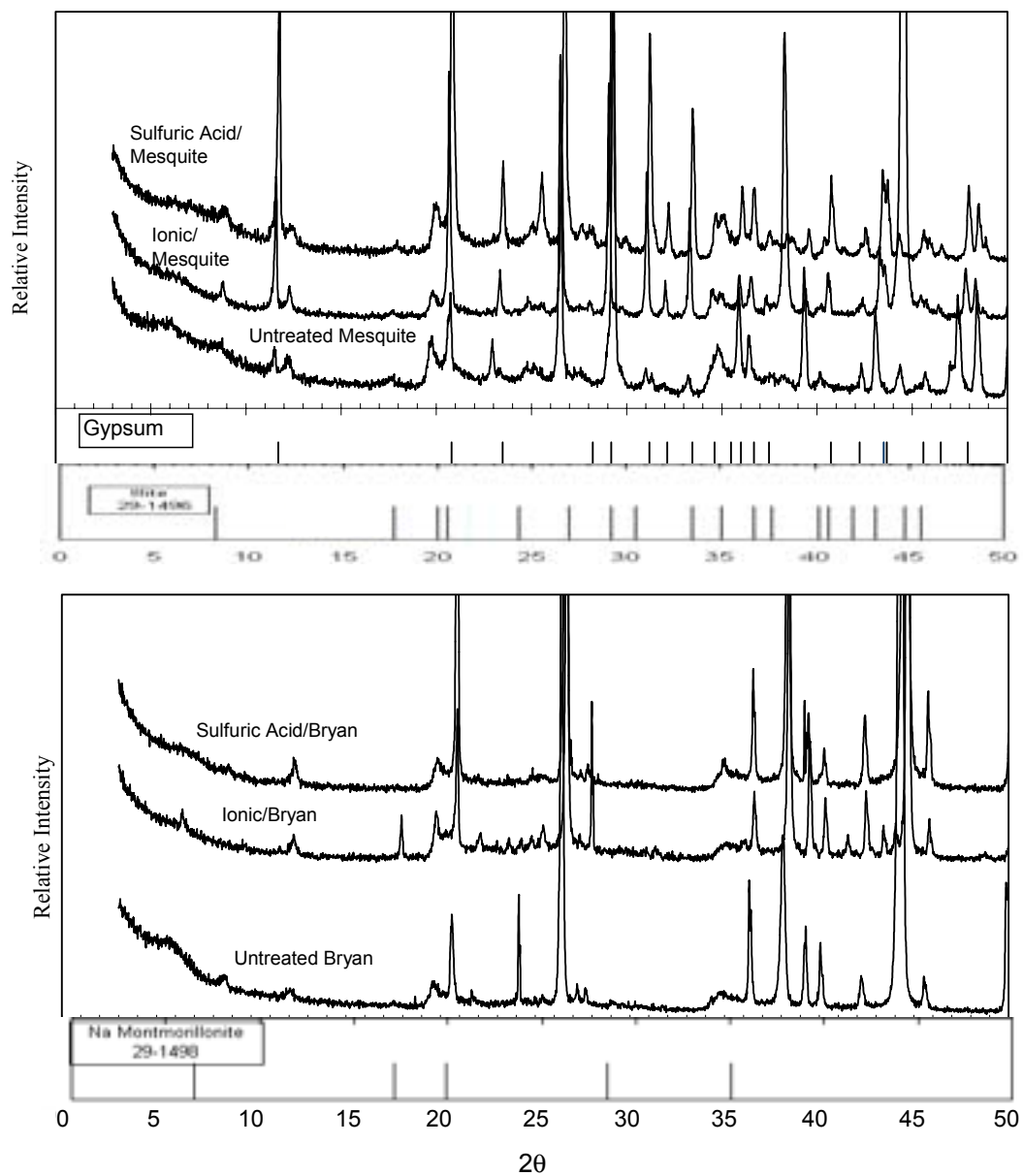


Figure 6-8. X-ray diffraction patterns for untreated and ionic stabilizer and sulfuric acid treated samples of Mesquite and Bryan soils

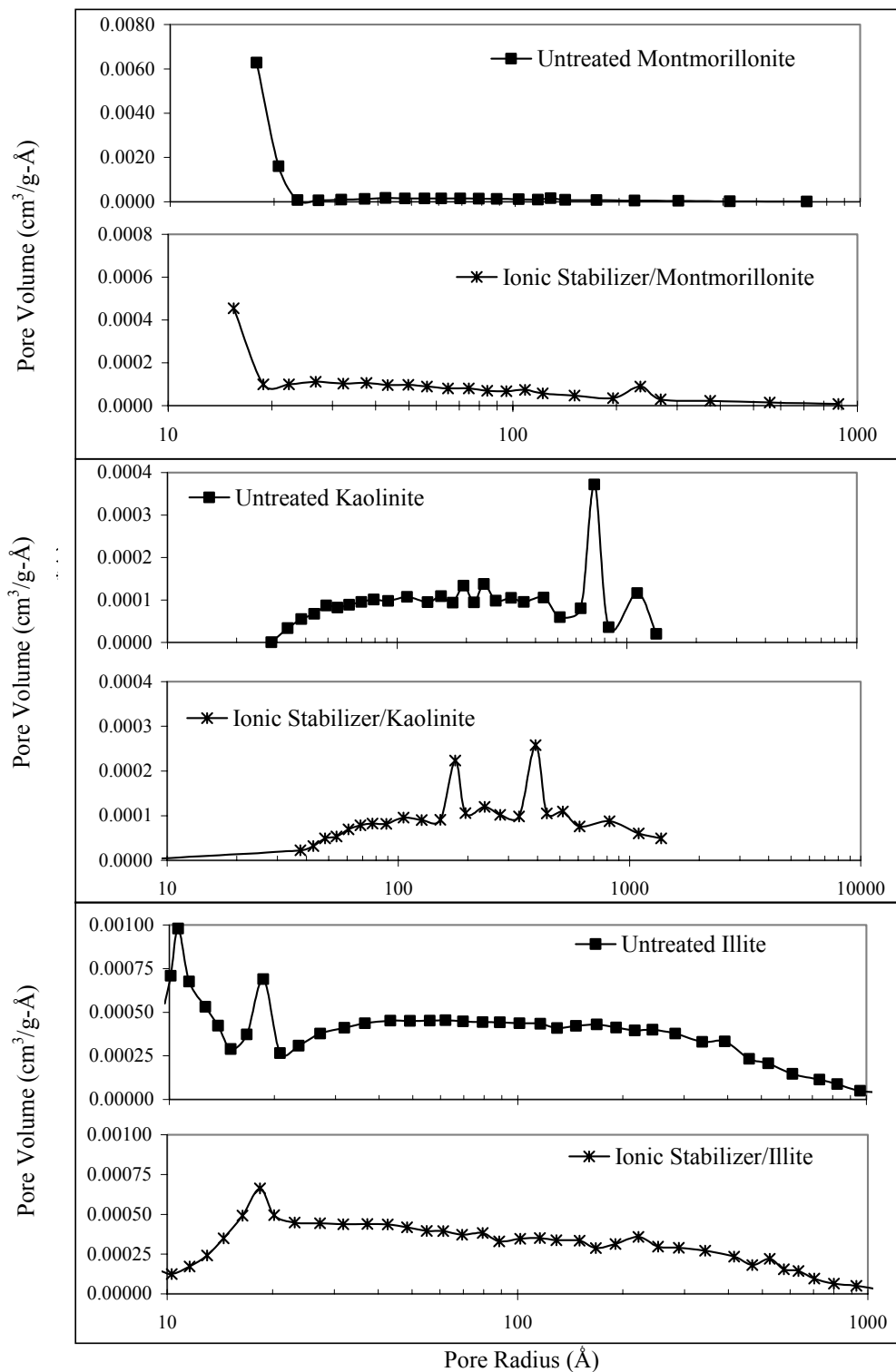


Figure 6-9. Pore size distributions for untreated and ionic stabilizer treated samples of illite, kaolinite, and montmorillonite

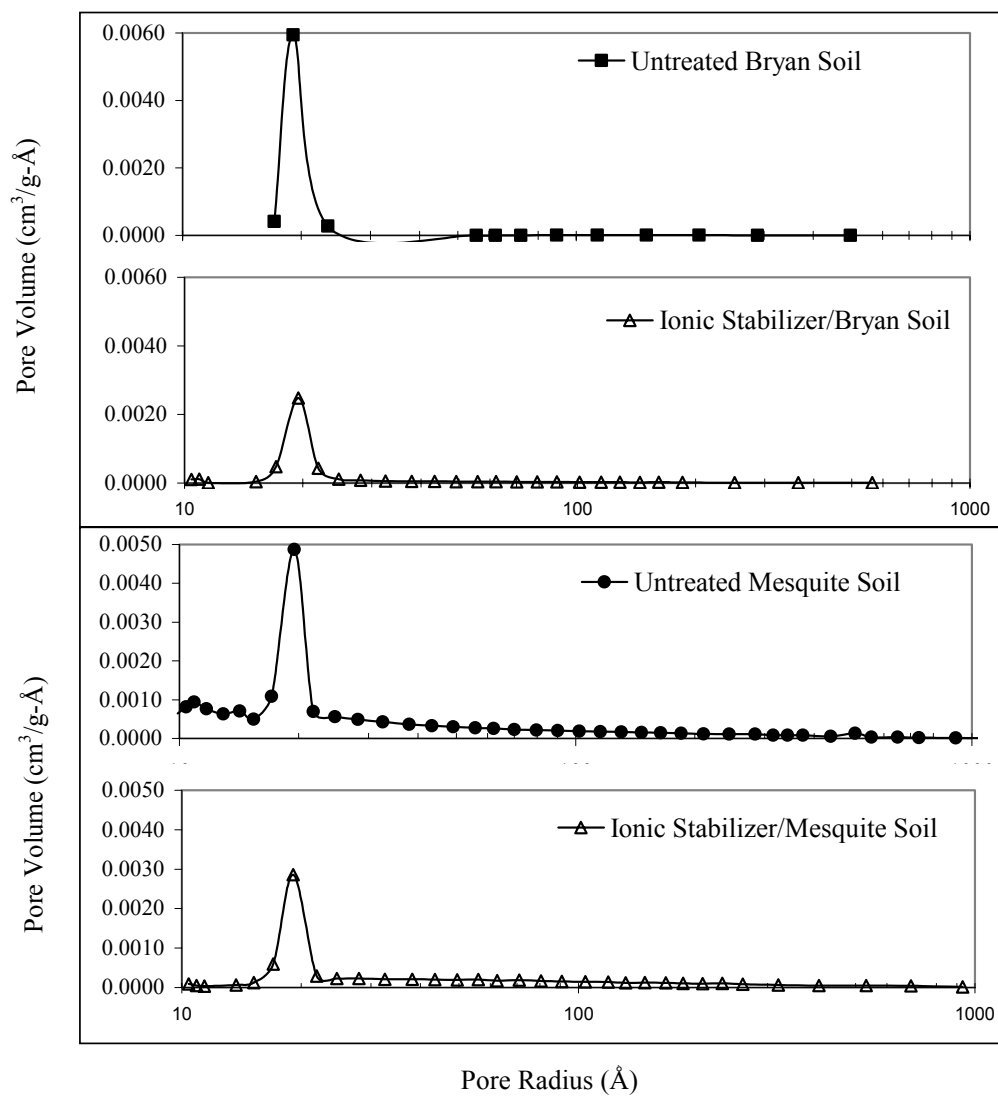


Figure 6-10. Pore size distributions for untreated and ionic stabilizer treated samples of Mesquite and Bryan soil

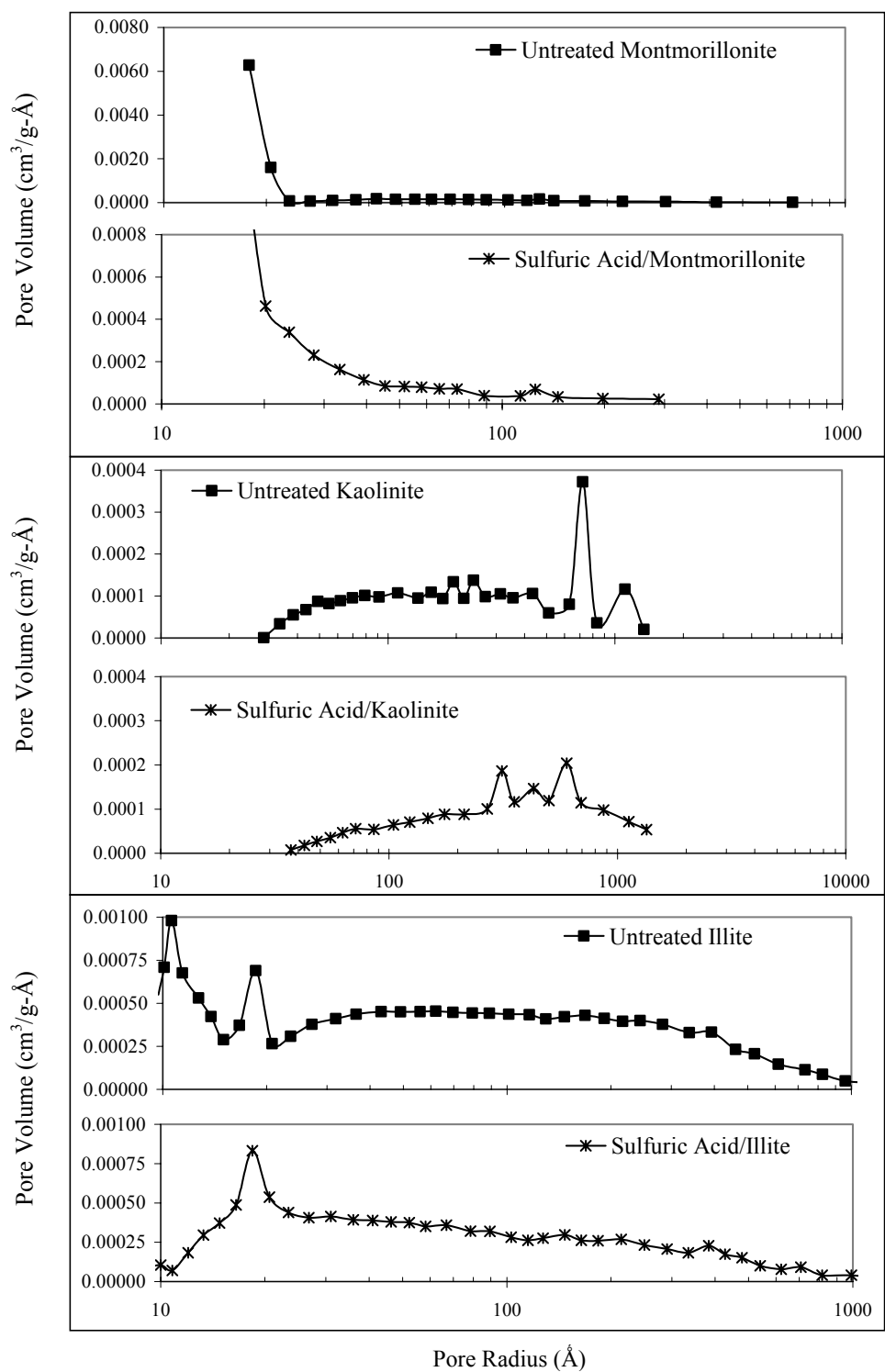


Figure 6-11. Pore size distributions for untreated and sulfuric acid treated samples of illite, kaolinite, and montmorillonite

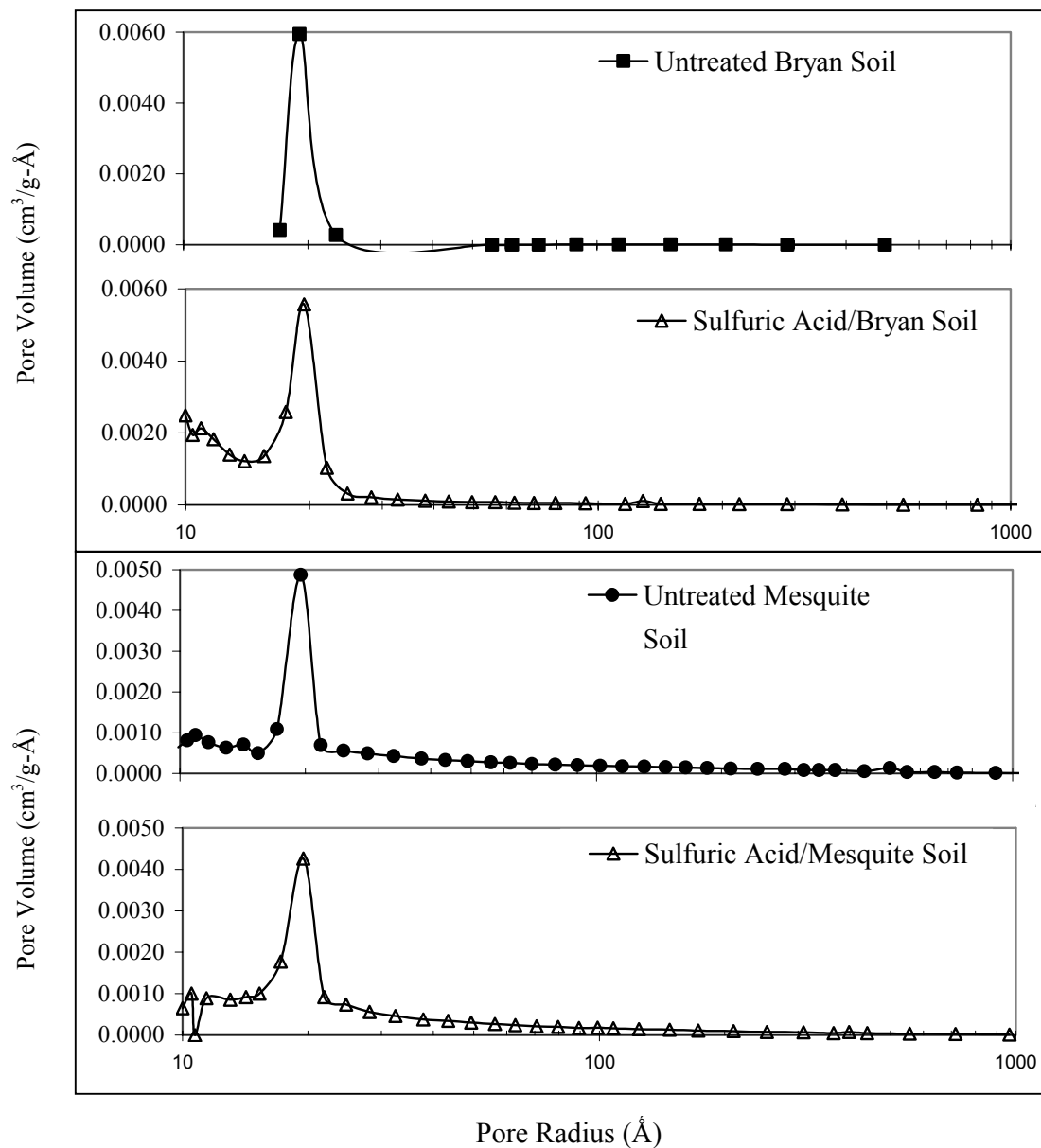


Figure 6-12. Pore size distributions for untreated and sulfuric acid treated samples of Bryan and Mesquite soils

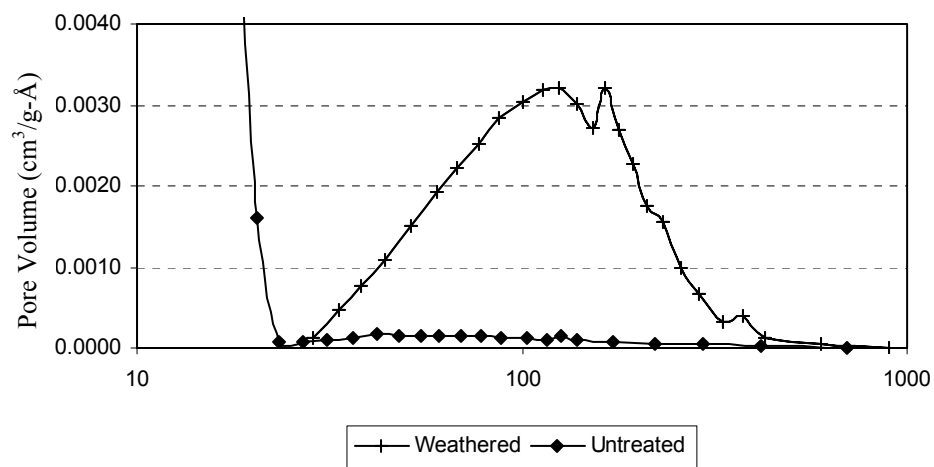


Figure 6-13. Pore size distributions of untreated montmorillonite and of montmorillonite samples treated with an excess of sulfuric acid (weathered)

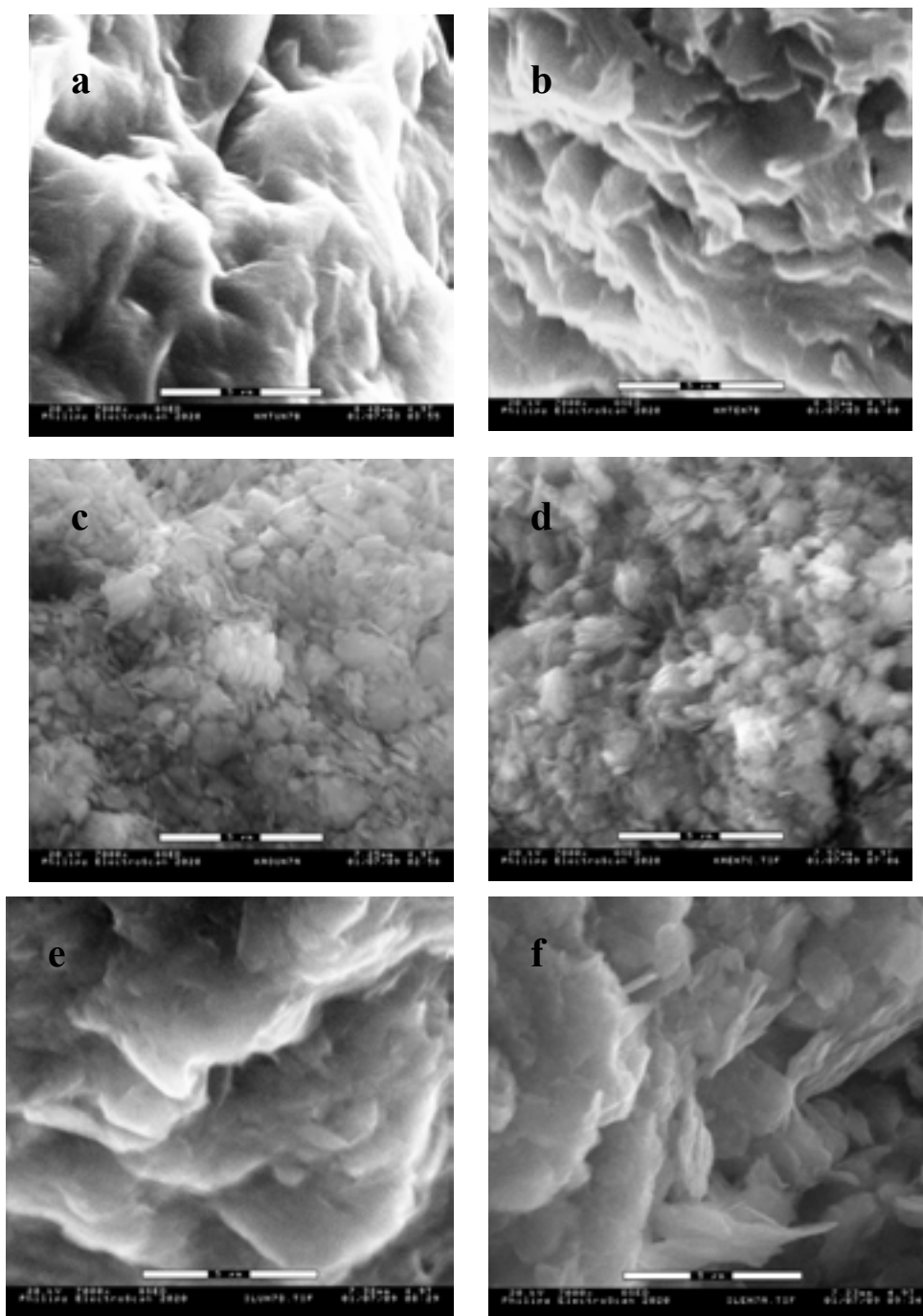


Figure 6-14. ESEM images for ionic stabilizer treated clay minerals at a magnification of 7,000 \times for (a) untreated montmorillonite, (b) ionic stabilizer/montmorillonite treatment, (c) untreated kaolinite, (d) ionic stabilizer/kaolinite treatment, (e) untreated illite sample, and (f) ionic stabilizer/illite treatment (*Note:* scale bar shown on each SEM corresponds to 5 μ m)

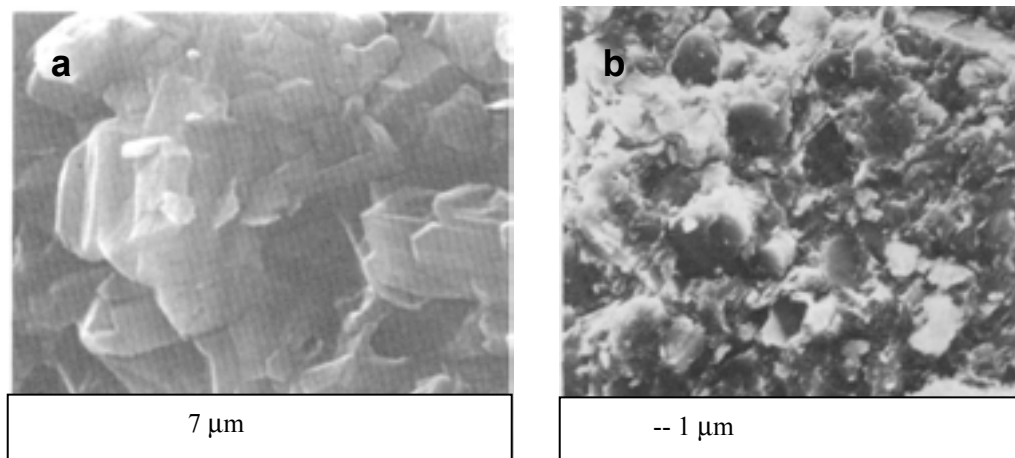


Figure 6-15. Reference SEM images of (a) illite (adapted from Mitchell 1993) and (b) kaolinite (adapted from Keller 1989)

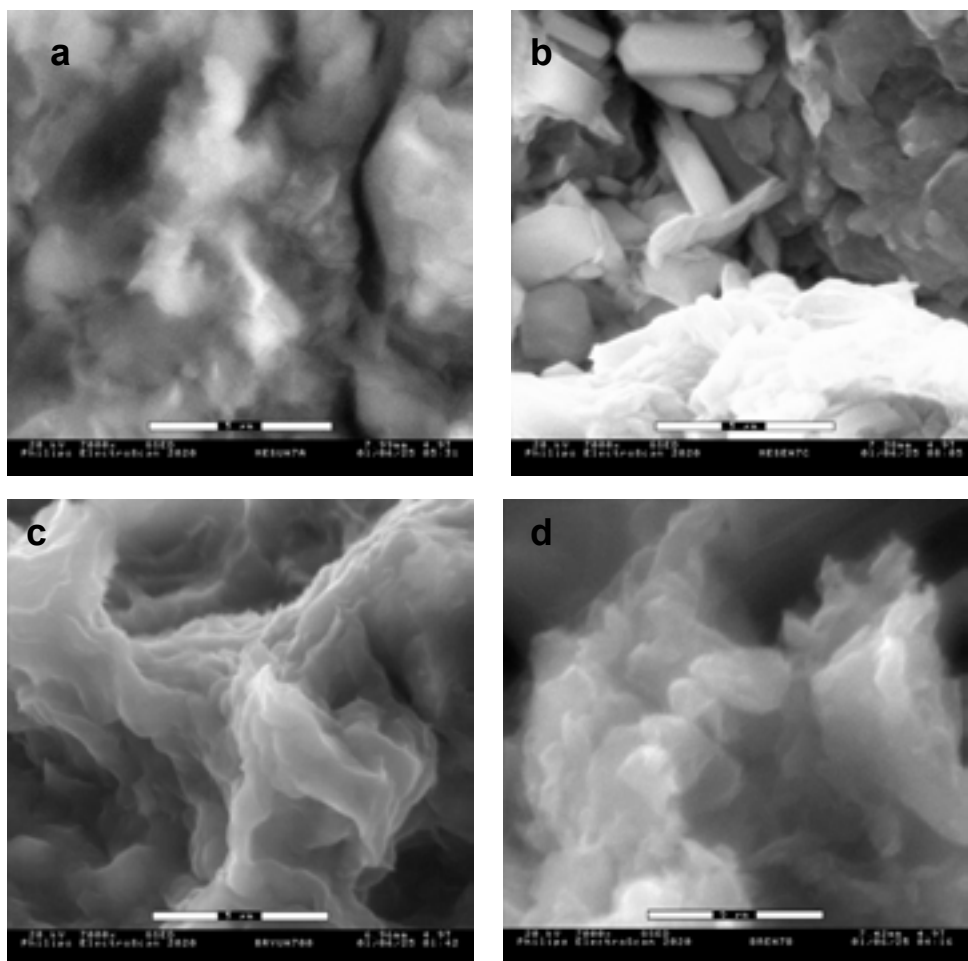


Figure 6-16. ESEM images for ionic stabilizer treated clay minerals at a magnification of 7,000× for (a) untreated Mesquite soil, (b) ionic stabilizer/Mesquite soil treatment, (c) untreated Bryan soil, and (d) ionic stabilizer/Bryan soil treatment (*Note:* scale bar shown on each SEM corresponds to 5 µm)



Figure 6-17. SEM image of gypsum (The Gypsum Project, Wilheims University 1996)

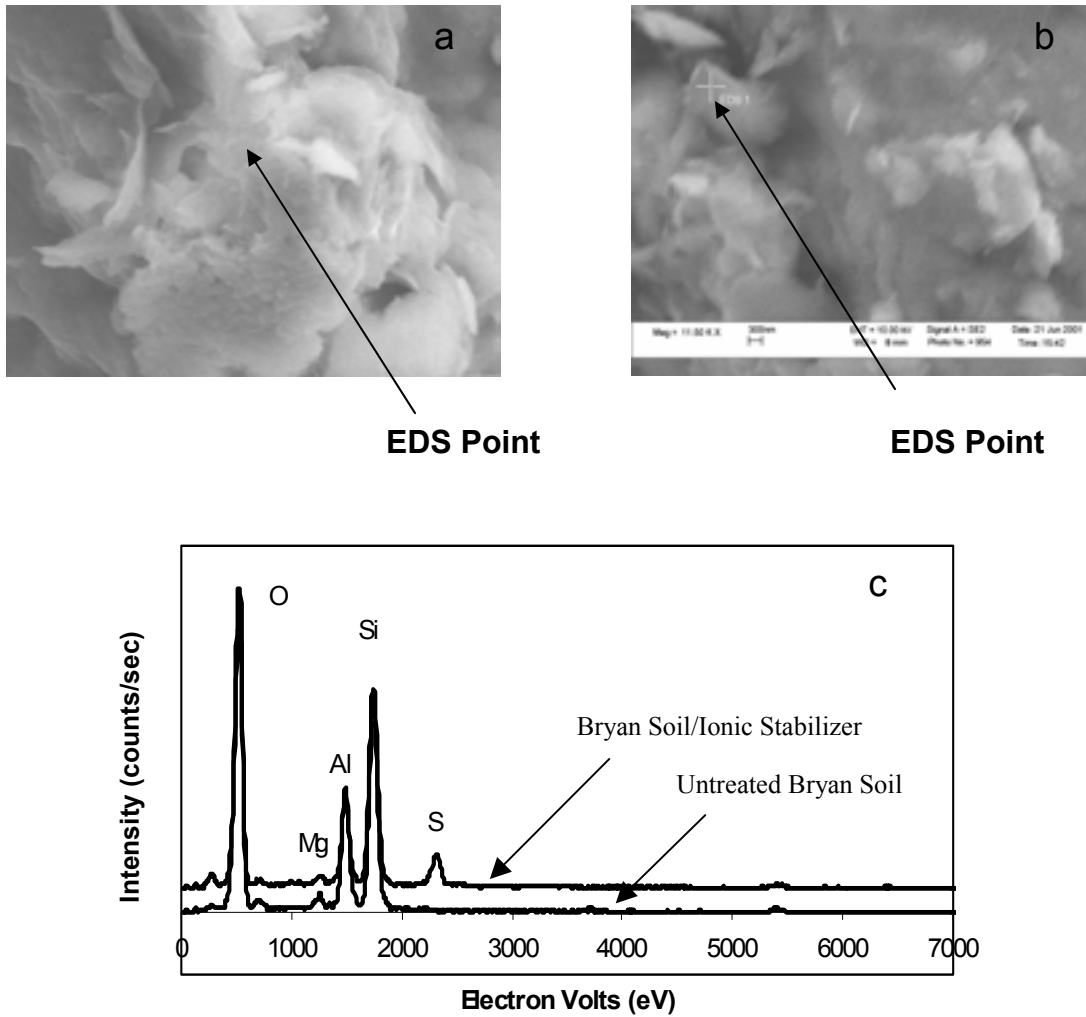


Figure 6-18. SEM/EDS results for untreated and ionic stabilizer treated Bryan soil at a magnification of 11,500 \times including (a) SEM image of untreated Bryan soil with EDS point identified, (b) SEM image of ionic stabilizer treated Bryan soil with EDS point identified, and (c) corresponding EDS spectra for the untreated and treated samples

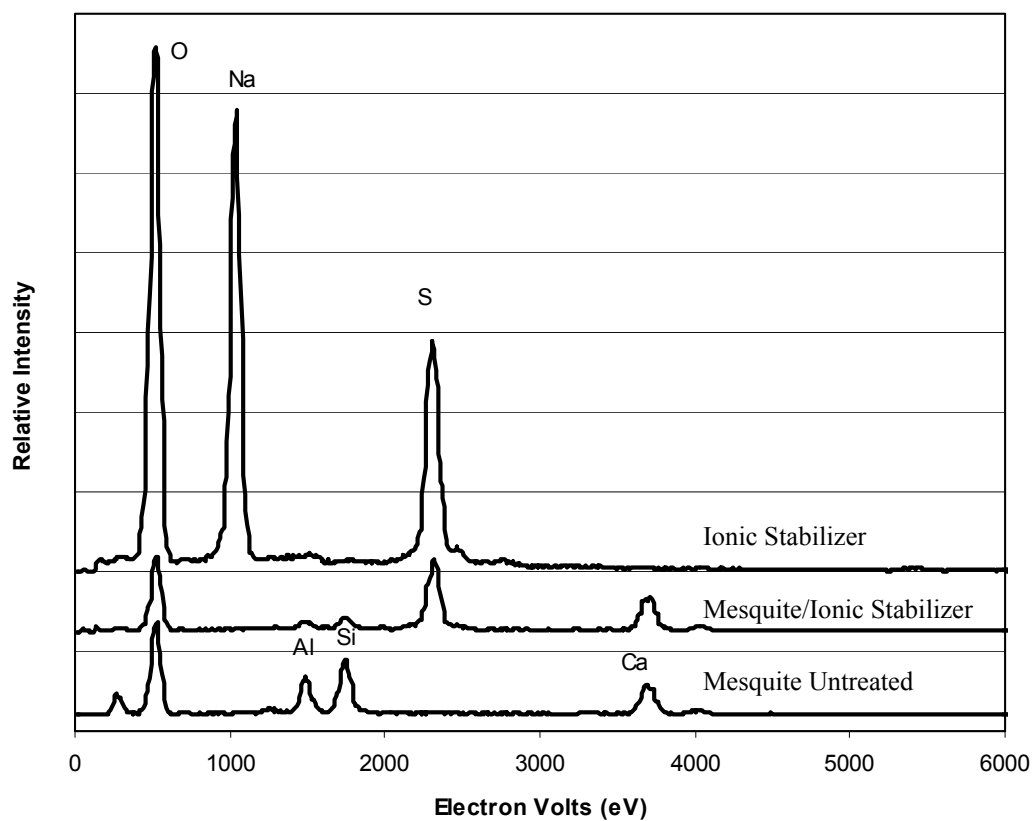


Figure 6-19. EDS results for ionic stabilizer, untreated Mesquite soil, and Mesquite soil treated with the ionic stabilizer

CHAPTER 7

IONIC STABILIZER: RESULTS FROM STUDY OF STABILIZER EFFECTIVENESS

7.1. OVERVIEW

Results from the macro-characterization study of the selected ionic stabilizer are presented in this chapter. Tests were conducted using the two native Texas clays (TX Bryan HP and TX Mesquite HS HP) and the bulk samples of the three reference clays (kaolinite, illite, and montmorillonite). The ionic stabilizer was mixed at the supplier's recommended dilution rate (DMR = 1/176) and applied to the soil at the supplier's recommended application rate (AMR = 1/6,000 = 0.02%). Samples of the untreated and treated soil were prepared following the protocols detailed in section 5.3. Standard geotechnical laboratory tests were conducted as described in Chapter 5.

To evaluate the effects of treating the five soils with the ionic stabilizer, the Atterberg limits, compacted soil density, undrained shear strength, and one-dimensional (1-D) free swell potential of the untreated and treated soils were compared. Overall, no significant, consistent improvement in the engineering properties was observed when these five test soils were treated with the selected ionic stabilizer at the application rate used.

7.2. EFFECT OF THE IONIC STABILIZER ON ATTERBERG LIMITS

The Atterberg limits determined for the untreated and ionic treated soils are summarized in Table 7-1 and are plotted in Figure 7-1. For perspective in considering these data, it is helpful to note the typical variability encountered in measuring Atterberg limits. As indicated in the ASTM D 4318-95a (1998e) standard, determinations of the liquid limit (LL) of a particular soil by a single technician can be expected to vary by 2.4, and determinations by multiple laboratories can vary by 9.9. Similarly, determinations of the plastic limit (PL) by a single technician and multiple laboratories can vary by 2.6 and 10.6, respectively. Hence, much of the difference in LL and PL between the untreated and treated soil samples (Table 7-1 and Figure 7-1) can be attributed to the usual variability encountered in these laboratory measurements. Note that the ASTM criteria listed above was determined from tests on a soil with a LL of 64 (ASTM 1998e); much greater variability can be expected for soils with much higher liquid limits, such as the sodium montmorillonite used in this study.

Focusing on the plasticity index ($PI = LL - PL$) determined for each sample (Table 7-1 and Figure 7-1), treating these soils with the ionic stabilizer does not produce a consistent improvement in soil plasticity. A lower PI was measured following treatment of the TX Mesquite HS HP and bulk montmorillonite samples; however, these changes do not appear to be significant.

7.3. EFFECT OF THE IONIC STABILIZER ON COMPACTED DENSITY

The water content and dry unit weight of the untreated and ionic treated compacted soil samples, which were prepared for triaxial and swell testing, are tabulated in Appendix K and are plotted in Figure 7-2. The target optimum water content and maximum dry unit weight are also

shown for reference; these values, which are summarized in Table 5-1, were determined for the untreated soil using a modified Proctor compaction effort (ASTM D 1557-91 1998b).

In preparing test specimens of each soil, whether treated or untreated, an attempt was made to achieve a moisture content as close as possible to the target optimum. Given that some variation in the water content was unavoidable, it was decided to accept any sample having a moisture content within ± 2 percentage points of the target optimum. Hence, the scatter in the measured water contents about the target optimum in Figure 7-2 represents an acceptable, unavoidable variability among the test specimens. Given the variability in moisture content, as well as additional variability introduced by impact compaction, the variability in the compacted dry unit weights of the various specimens as seen in Figure 7-2 can be expected.

Comparing the compacted dry unit weights of the untreated samples with those of the treated samples in Figure 7-2, it is clear that the addition of the ionic stabilizer did not result in greater soil density or improved soil compaction characteristics.

7.4. EFFECT OF THE IONIC STABILIZER ON SHEAR STRENGTH

Undrained shear strength envelopes, which were fit to the results from the UU triaxial tests on the untreated and ionic treated soil samples, are plotted in Figure 7-3. The differences between the strength envelopes for the untreated and treated bulk illite and montmorillonite are not significant. The slightly lower strength of the treated TX Mesquite HS HP soil can be attributed to the lower compacted density of these specimens, as is evident in Figure 7-2 and Table K-5. Likewise, the more notable difference between the strength envelopes for the untreated and treated TX Bryan HP soil can be attributed to a lower density and higher water content in the treated samples.

Only the bulk kaolinite shows significantly increased shear strength following treatment with the ionic stabilizer product. However, the untreated kaolinite specimens were more than 94% saturated, whereas the treated specimens were about 85% saturated. The relatively high saturation of the untreated samples would result in greater pore pressure generation during shearing and therefore lower undrained shear strength. Hence, the greater strength of the kaolinite following treatment cannot be credited to the addition of the ionic stabilizer product.

The Mohr-Coulomb strength parameters, corresponding to the envelopes plotted in Figure 7-3 and determined as described in section 5.7, are given in Table 7-2. These values were used to compute the reference shear strength (S_{ref}) at the arbitrarily selected normal stress of 100 psi. The resulting values of S_{ref} are plotted in Figure 7-4. Only the bulk kaolinite shows an increase in S_{ref} following treatment with the ionic product; however, the higher strength cannot be ascribed to the stabilizer treatment because of the higher saturation in the untreated test specimens.

7.5. EFFECT OF THE IONIC STABILIZER ON SWELL POTENTIAL

The one-dimensional free swell potential of the untreated and ionic treated soils was measured as described in section 5.8. Three replicate tests were run on each untreated and treated soil sample. The results are plotted in Figure 7-5, where the variability in test results, for samples prepared in an identical manner, is evident.

Note that the bulk kaolinite appears to exhibit substantially more expansion following treatment with the ionic product (more expansiveness was also observed when the kaolinite was

treated with the other two stabilizer products evaluated). This behavior is not linked to readily apparent differences in the test specimens, because both the untreated and treated kaolinite specimens had similar moisture contents. It is possible that the nonexpansive, untreated kaolinite was chemically activated by the ionic stabilizer product and became more expansive. Alternatively, it is possible that some unknown error exists in the test data on the untreated bulk kaolinite.

No reduction in the 1-D free swell potential was observed following treatment of the bulk montmorillonite, TX Bryan HP, and TX Mesquite HS HP soils. Only the bulk illite showed any reduction in swell potential following treatment with the ionic stabilizer product. Inspection of the specimen properties in Table K-2 shows that the treated illite test samples were somewhat wetter than the untreated samples, which could explain the observed reduction in the swell potential of the illite. Hence, no consistent reduction in the expansiveness of the different test soils can be attributed to treatment with the ionic stabilizer product.

Table 7-1. Atterberg limits of the untreated test soils and of those treated with the ionic stabilizer product

<i>Soil Sample</i>		<i>Plastic Limit</i>	<i>Liquid Limit</i>	<i>Plasticity Index</i>
TX Bryan HP	untreated	20	68	48
	ionic treated	15	65	50
TX Mesquite HS HP	untreated	23	60	37
	ionic treated	22	49	27
Kaolinite	untreated	32	51	19
	ionic treated	28	52	24
Illite	untreated	24	44	20
	ionic treated	19	47	28
Montmorillonite	untreated	32	567	535
	ionic treated	36	485	449

Table 7-2. Shear strength parameters for envelopes that were fit to UU triaxial data in Figure 7-3

<i>Soil Sample</i>		<i>c</i> (psi)	<i>φ</i> (deg)
TX Bryan HP	untreated	113	1
	ionic treated	38	13
TX Mesquite HS HP	untreated	71	18
	ionic treated	57	20
Kaolinite	untreated	38	0
	ionic treated	28	35
Illite	untreated	21	51
	ionic treated	39	33
Montmorillonite	untreated	32	51
	ionic treated	79	33

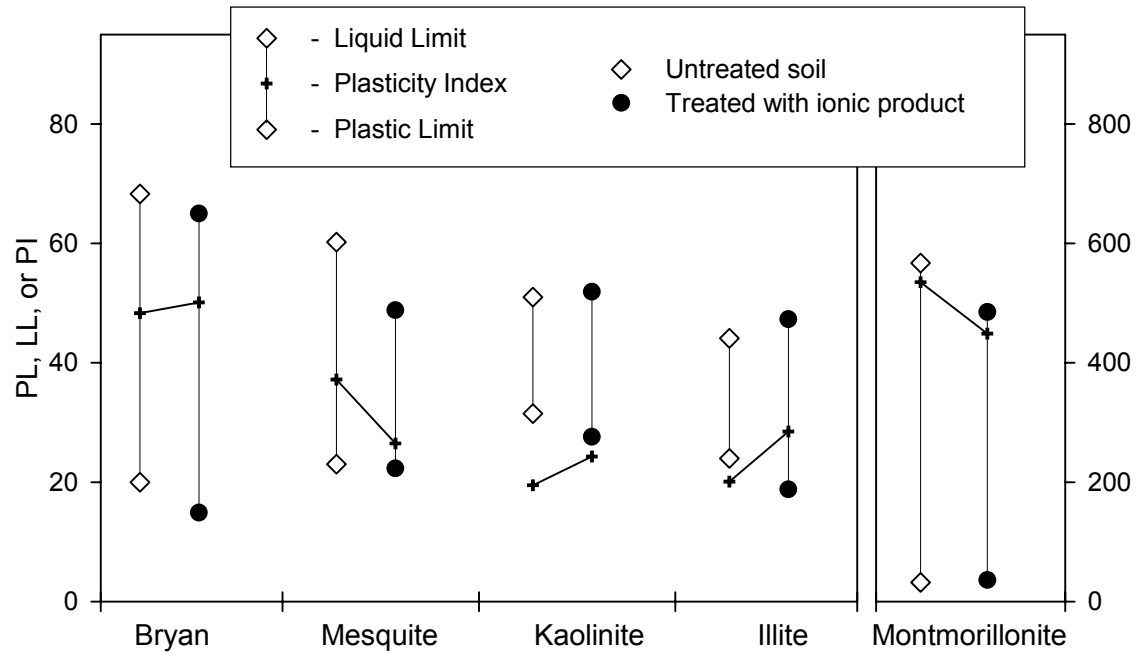


Figure 7-1. Atterberg limits of the untreated test soils and of those treated with the ionic stabilizer product

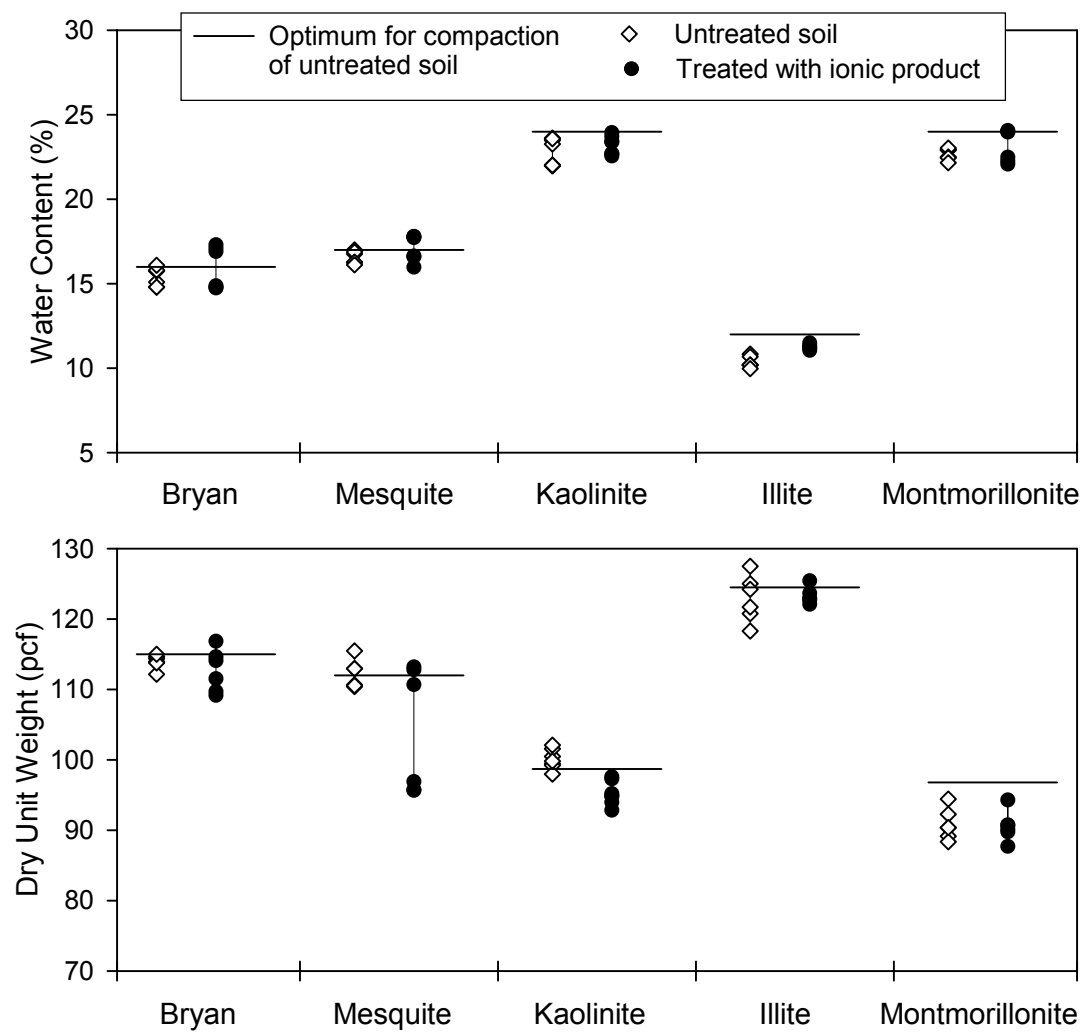


Figure 7-2. Water contents and dry unit weights of the triaxial and swell test soil specimens, both untreated and treated with the ionic stabilizer product

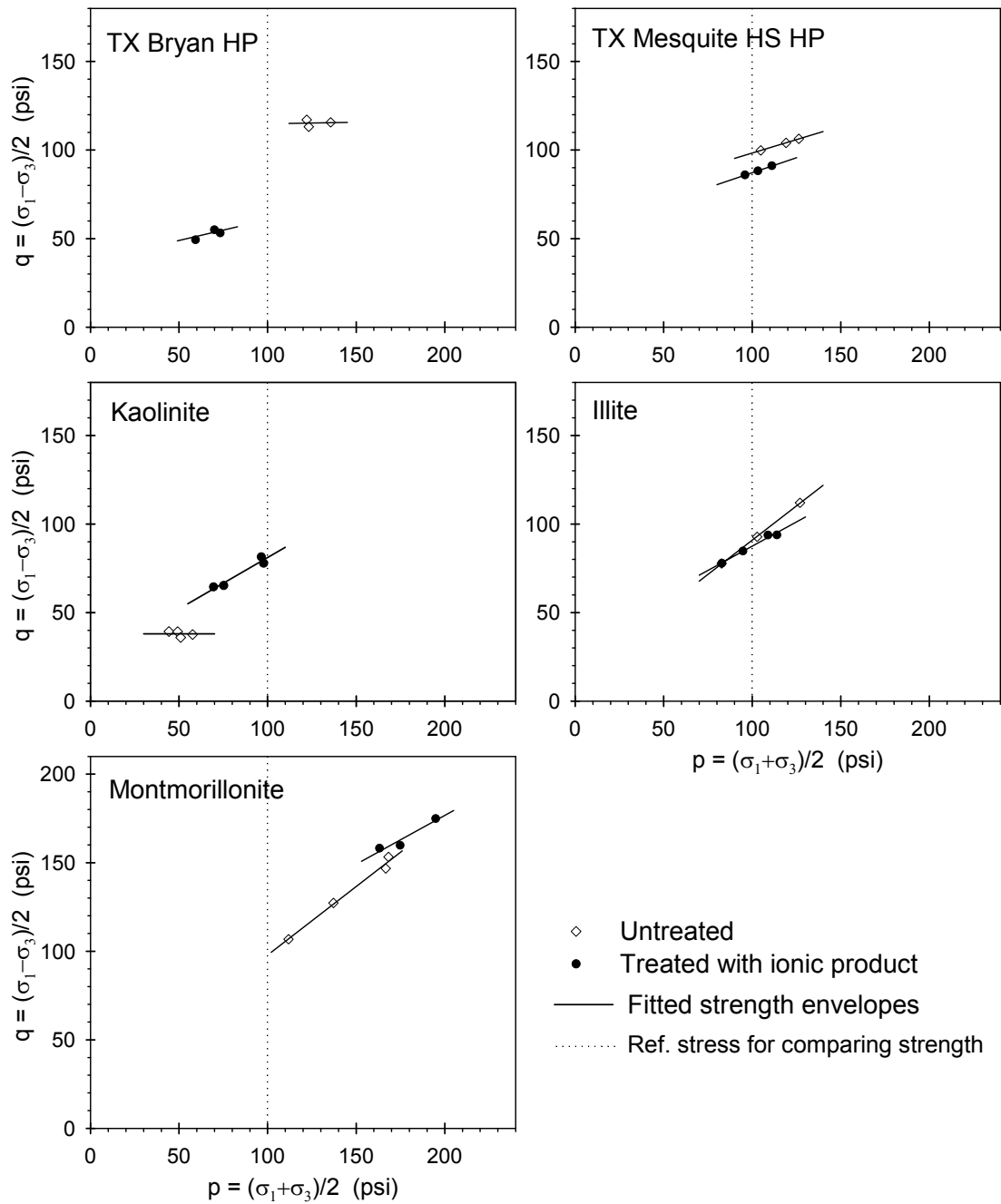


Figure 7-3. Fitted shear strength envelopes from UU triaxial tests on the untreated soils and on the soils treated with the ionic stabilizer product

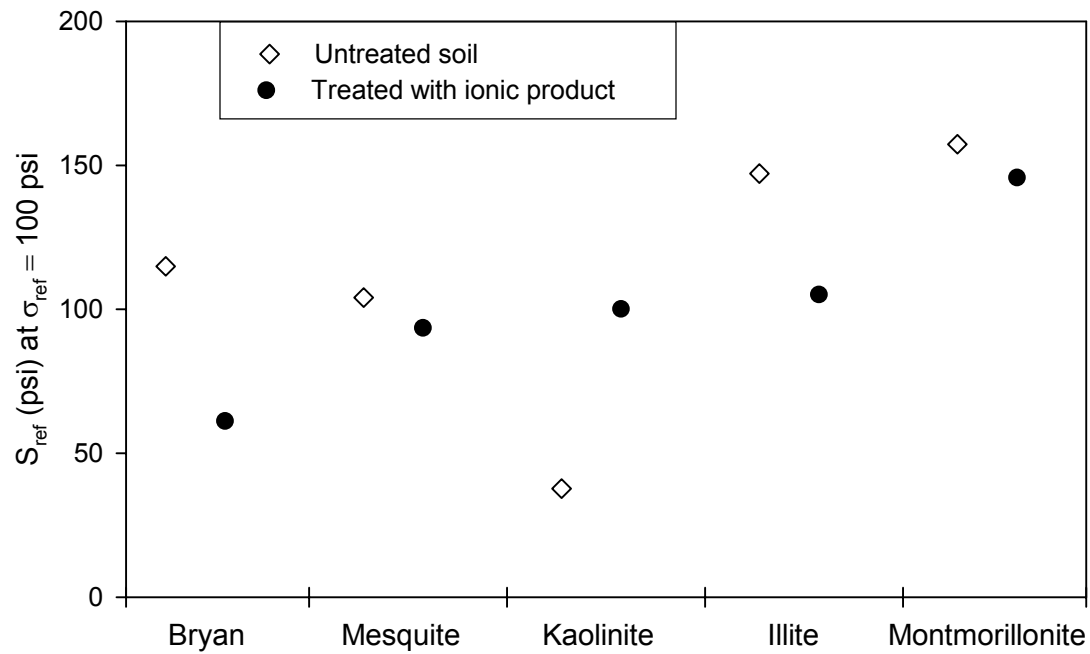


Figure 7-4. Reference shear strengths of the untreated test soils and of those treated with the ionic stabilizer product

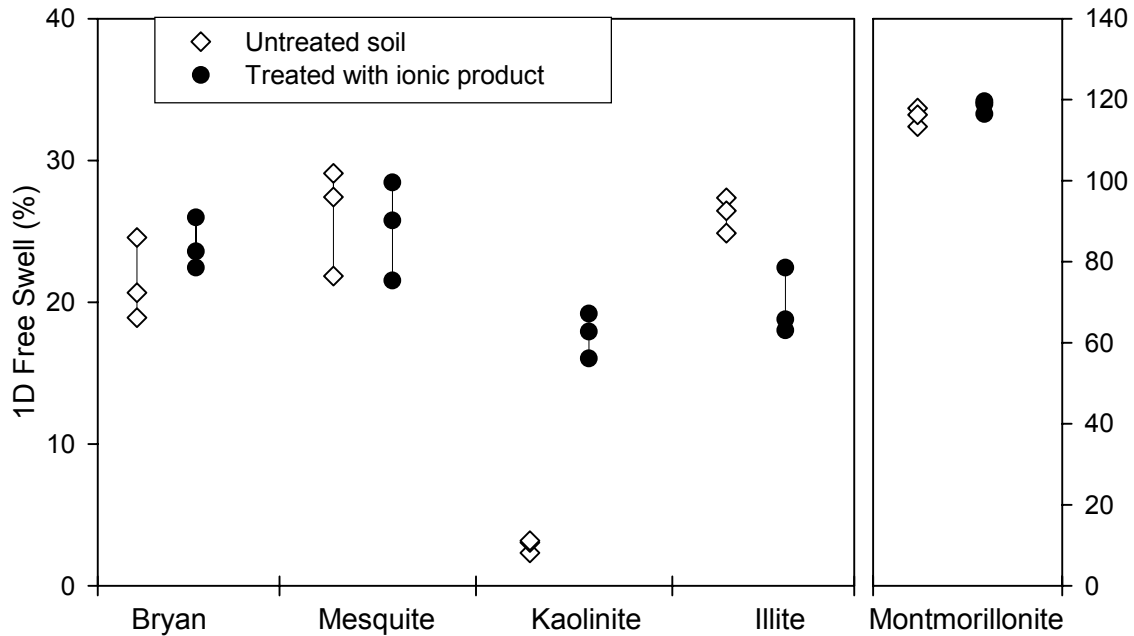


Figure 7-5. One-dimensional free swell of the untreated test soils and of those treated with the ionic stabilizer product

CHAPTER 8

ENZYME STABILIZER: RESULTS FROM STUDY OF STABILIZER MECHANISMS

8.1. OVERVIEW

This chapter presents the results of the clay/enzyme stabilizer experiments. The effects of the enzyme stabilizer on the clay minerals and natural soils were determined by employing a range of analytical techniques including BET surface area analysis, XRD, SEM/EDS, and ESEM. Specifically, these techniques were employed to test the hypothesized mechanism of clay stabilization by the enzyme stabilizer. As stated earlier, enzyme stabilizers are hypothesized to work through adsorption to internal and external regions of the clay mineral (Scholen 1992). Presumably, these enzymes can combine with large organic molecules and adsorb to the clay surfaces, thereby blocking potential cation exchange sites and preventing absorption of moisture and consequent swelling. Ionized water can then form linkages between packed particles to provide a cementation effect. If the hypothesized mechanism is correct, then changes in mineralogy should not be expected in the XRD patterns of treated samples or the Al:Si ratios obtained from SEM/EDS analyses of treated and untreated samples. However, expansive clays should remain in an expansive state (d-spacings should be consistent with those of glycolated samples), which should be reflected in the d-spacing of randomly oriented and oriented samples obtained from the XRD patterns. In addition, adsorption to the external regions of the clay can lead to particle destabilization and flocculation which may lead to a reduction in surface area as reflected in nitrogen BET adsorption data. Changes in electron micrographs may also be apparent.

8.2. XRD RESULTS OF TREATED AND UNTREATED CLAY AND SOIL SAMPLES

X-ray diffraction was performed on untreated and treated samples of the clay minerals with randomly oriented specimens and oriented specimens. Figure 8-1 shows the XRD results for randomly oriented untreated and treated samples of the clay minerals, in addition to reference diffractograms for each clay mineral investigated. As indicated in Chapter 6, comparison of untreated and treated diffractograms with the reference spectrum suggests that the sample XRD patterns are consistent with their respective mineral phases for all three clay minerals. A comparison of the enzyme treated sample with the untreated samples shows that the 001 peak shifted to the left (an increase in d-spacing) and that the montmorillonite peak at 28 2 θ disappeared in the diffractogram for the treated sample. In contrast, the XRD patterns for the kaolinite treated samples and illite treated samples are consistent with the corresponding untreated diffractogram. Indeed, the d-spacings for the treated and untreated samples for kaolinite and illite are nearly identical, as can be seen in Table 8-1.

Oriented and glycolated sample results support the conclusions from the randomly oriented XRD patterns. In the presence of the enzyme stabilizer the d-spacing of the montmorillonite sample is similar to the d-spacing obtained for an untreated glycolated sample. This result suggests that the enzyme has penetrated the inner layer of the montmorillonite and forced it into an expanded state in accordance with the proposed mechanism.

The results presented for illite samples do not indicate a change in 2θ (or d-spacing) as a result of treatment, orientation, or glycolation of the samples. The d-spacings of the treated and untreated glycolated samples were similar to the oriented and randomly oriented samples. As a result, it appears that the enzyme was unable to penetrate the illite inner layer.

Figure 8-2 provides a comparison of untreated and treated samples for the native soils. As was indicated in Chapter 6, effects of glycolation and orientation for the treated Bryan samples and the treated and untreated Mesquite samples are not presented because XRD of the treated glycolated samples was difficult. In both cases, the samples clumped after treatment, making it difficult to separate the clay fraction for further analysis. Comparison of the d-spacings for the untreated oriented Bryan sample (15.13 Å) with the untreated glycolated Bryan sample (17.40 Å) indicated that the material contains an expansive fraction. As a result, the enzyme stabilizer was expected to increase the d-spacing of randomly oriented soil samples. The results presented in Figure 8-2 and Table 8-1 confirm this result. The location of the 001 peak for the treated sample shifted from 5.78 to 4.70 2θ , corresponding to d-spacings of 15.29 Å and 18.80 Å, respectively. Comparison of the Mesquite soil with the reference diffractograms suggests that there are two different types of clay components. The XRD pattern contains peaks that are consistent with both montmorillonite and illite with d-spacings for each component of 10.09 Å and 14.49 Å. These d-spacings correspond to illite and an expanded smectite, respectively. After treatment, the d-spacing of the peak in the untreated diffractogram at 6.10 2θ was not apparent, presumably because of its low intensity. The peak associated with a d-spacing of approximately 10 Å was evident in the treated sample, and it did not shift significantly after treatment, as can be seen in Figure 8-2.

8.3. BET ANALYSIS OF TREATED AND UNTREATED CLAY AND SOIL SAMPLES

BET nitrogen adsorption results for treated and untreated samples are presented in Table 8-2. The nitrogen BET results show a significant reduction in surface area following treatment with the enzyme stabilizer for all of the clay minerals and soils tested. These results suggest that the enzyme stabilizer caused a substantial amount of agglomeration of the soil particles regardless of the nature of the soil material, which again is consistent with the proposed mechanism. However, the percentage decrease in surface area is significantly less for kaolinite than for the other materials.

To evaluate why kaolinite exhibits a smaller decrease in surface area, the pore size distributions for each of these samples are plotted in Figures 8-3 and 8-4. The results clearly show a reduction in the pore volume for all of the samples. In addition, the enzyme virtually eliminates all pores having radii less than about 50 Å. Since many of the kaolinite pores are larger than this value, there is less reduction in the pore volume, which explains why there is a smaller reduction in surface area for kaolinite. The results for kaolinite also showed a shift in the pore size distribution to smaller pore radii. Whereas a large portion of the pore volume is associated with pore radii of 700 Å in the untreated samples, the most predominant peak in the enzyme stabilizer treated sample corresponds to a pore radius of 300 Å.

Thus, the results of the nitrogen adsorption tests for treated clays and soil samples suggest that the enzyme stabilizer is binding clay particles together and restricting access to the pore spaces between particles.

8.4. ESEM AND SEM/EDS ANALYSES OF TREATED AND UNTREATED CLAY AND SOIL SAMPLES

ESEM images for the treated and untreated samples of the clay minerals are presented in Figure 8-5 and 8-6. Comparison of the treated samples with the untreated samples reveals similar changes in the micrographs following treatment. For all of the clay and soils analyzed except possibly the kaolinite, the treated samples appear more aggregated than the corresponding untreated sample, and the clay features are less visible. However, there does not appear to be a change in the composition of the material. These results are consistent with the results of the BET and the XRD analyses.

Energy dispersive x-ray (EDS) analysis was used to confirm the conclusion that the clay composition had not changed. As is shown in Table 8-3, there were no significant changes in the Al:Si ratio following treatment. In all cases, hypothesis testing suggests that changes in Al:Si ratio following treatment were not significant. Indeed, the null hypothesis of equal means at the 95% confidence level was retained in all cases.

8.5. CEC ANALYSIS OF TREATED AND UNTREATED MONTMORILLONITE

Cation exchange capacity (CEC) was measured for untreated and treated samples of montmorillonite at three application mass ratios: 1:4, 1:1,000 and 1:6,000. Three application ratios were used to study the effects of the stabilizer over a wide range of concentrations. However, as is evident from the data presented in Table 8-4 and hypothesis testing of the data, there is no impact of the enzyme stabilizer on the CEC of the montmorillonite sample at any of the AMRs examined. Indeed, the null hypothesis, which assumed that untreated and treated CEC mean values were equal, was retained for all of the samples at the 95% confidence level. These data indicate that the expanded inner layer is still accessible for cation exchange.

8.6. SUMMARY

It has been suggested (Scholen 1992; 1995) that the enzyme stabilizer acts in several ways, including a breakdown of clay minerals with expulsion of water from the double layer, the binding of clay particles by aggregation, internal or external adsorption to clay layers preventing water absorption, or interlayer expansion with subsequent moisture entrapment. The enzyme stabilizer was not applied at the manufacturer's recommended application rates, as in the initial testing of the ionic stabilizer. However, it did indicate a convincing change in d-spacing for montmorillonite at an AMR of 1:2. With the enzyme treatment, the d-spacing was fully expanded, and consequently, the d-spacing did not change significantly after glycolation. This result suggests that upon application of the enzyme to an expansive clay such as sodium montmorillonite, the clay layers fully expand. This is consistent with the mechanism of interlayer expansion with subsequent moisture entrapment.

The surface area results of the enzyme stabilizer treatment showed the largest decrease in surface area of all of the stabilizers tested when compared with the results for untreated samples for all clay and soil types, except kaolinite. For kaolinite, the hypothesized mechanism of providing an adsorbing surface complex on the edges of clay particles was supported by BET results. As with the kaolinite results, the illite surface area measurements, pore size distributions,

ESEM images, and EDX Al:Si ratios suggested external clay particle adsorption rather than chemical alterations by enzyme treatment.

For the Bryan soil, the largest change in surface area was observed for the enzyme treatment. There was no peak in the pore size distribution for the enzyme treatment, and a sharp decrease in pore radius was observed, indicating possible binding of clay particles by aggregation. According to the XRD results, there were no changes in d-spacing resulting from stabilizer treatment.

For the Mesquite soil, the largest decrease in surface area again was for the enzyme treatment. Additionally, the ESEM images were significantly different for the enzyme treated samples when compared with those for the untreated samples. However, the mechanism of enzyme interaction with the Mesquite clay particles is difficult to determine, as a result of the inability to separate the clay fraction from other minerals and impurities, as mentioned earlier.

Table 8-1. Summary of d-spacings and values of 2θ for the 001 peak for untreated and enzyme treated samples of clay minerals and native soils

<i>Sample Description</i>	<i>d-spacing (\AA)</i>		<i>2θ</i>	
	<i>Enzyme Stabilizer</i>	<i>Untreated</i>	<i>Enzyme Stabilizer</i>	<i>Untreated</i>
Illite				
Randomly oriented	10.094	10.094	8.76	8.76
Glycolated	10.164	10.14	8.7	8.72
Oriented	10.071	10.21	8.78	8.66
Montmorillonite				
Randomly oriented	17.397	12.923	5.08	6.84
Glycolated	17.327	17.192	5.1	5.14
Oriented	17.395	14.929	5.08	5.92
Kaolinite				
Randomly oriented	7.161	7.184	12.36	12.32
Glycolated	NA	NA	NA	NA
Oriented	NA	NA	NA	NA
Mesquite Soil				
Randomly oriented	NA	14.49	NA	6.10
Glycolated	NA	NA	NA	NA
Oriented	NA	NA	NA	NA
Bryan Soil				
Randomly oriented	18.80	15.29	4.70	5.78
Glycolated	NA	17.40	NA	5.08
Oriented	NA	15.134	NA	5.84

Table 8-2. BET results for enzyme stabilizer treated samples of montmorillonite, kaolinite, illite, Bryan soil, and Mesquite soil

<i>Sample Description</i>	<i>BET N₂ Surface Area</i>		<i>Difference between Treated and Untreated</i>
	<i>(m²/g)</i>	<i>St. Dev (+/-)</i>	<i>%</i>
Montmorillonite			
Unwashed/untreated	31.79	0.3465	
Untreated ^a	30.87	0.2843	
Enzyme stabilizer ^a	4.06	0.0455	86.85
Repository ^b	31.82	0.22	
Kaolinite			
Unwashed/untreated	11.05	0.0319	
Untreated ^a	11.5	0.0687	
Enzyme stabilizer ^a	8.89	0.1474	22.70
Repository ^b	10.05		
Illite			
Unwashed/untreated	28.4	0.1482	
Untreated ^a	35.03	0.6272	
Enzyme stabilizer ^a	6.35	0.1125	81.87
Repository ^b	23.7		
Bryan Soil			
Unwashed/untreated	35.48	0.1119	
Untreated ^a	31.93	0.1142	
Enzyme stabilizer ^a	0.7875	0.0489	97.53
Mesquite Soil			
Unwashed/untreated	40.45	0.2226	
Untreated ^a	40.88	0.2643	
Enzyme stabilizer ^a	5.376	0.09535	86.85

^a Samples were washed, treated, cured, and rinsed through a 0.45 µm cellulose nitrate filter prior to evaluation.

^b Results provided by University of Missouri Repository Source Clay Data Sheet.

Table 8-3. Al:Si ratios and hypothesis testing of EDS results obtained for untreated and enzyme stabilizer treated samples of clay minerals and native soils

<i>Sample Description</i>	<i>Al:Si</i>					<i>Reject/ Retain Ho</i>
	<i>Ratio (wt %)</i>	<i>Std. Dev (±%) (S_i)</i>	<i># Samples</i>	<i>T</i>	<i>t_{0.975}</i>	
Montmorillonite						
Untreated	0.395	0.105	11			
Enzyme stabilizer	0.379	0.092	12	0.390	2.080	Retain
<i>Repository</i>	0.366					
Kaolinite						
Untreated	1.052	0.036	10			
Enzyme stabilizer	1.042	0.029	10	0.0011	0.726	Retain
<i>Repository</i>	1.015					
Illite						
Untreated	0.579	0.035	11			
Enzyme stabilizer	0.570	0.044	12	0.556	2.080	Retain
<i>Repository</i>	0.558					
Bryan Soil						
Untreated	0.532	0.031	8			
Enzyme stabilizer	0.465	0.125	9	1.456	2.131	Retain
Mesquite Soil						
Untreated	0.583	0.184	7			
Enzyme stabilizer	0.633	0.101	12	-0.770	2.110	Retain

Note: Each treated sample was compared with an untreated sample using the Student's t-test assuming both sample sets are random, independent, and with equal population variances.

Table 8-4. Cation exchange capacity results for the untreated and enzyme treated montmorillonite

<i>Sample Description</i>	<i>Application Mass Ratio</i>	<i>CEC (centimoles/kg)</i>					<i>Reject/ Retain Ho</i>
		<i>Avg.</i>	<i>Std. Dev</i>	<i># Samples</i>	<i>t</i>	<i>t_{0.975}</i>	
Montmorillonite							
Untreated	zero	54.16	6.04	3			
Enzyme stabilizer	1:4	54.83	6.54	3	0.130	2.776	Retain
Enzyme stabilizer	1:1,000	50.73	4.87	3	0.766	2.776	Retain
Enzyme stabilizer	1:6,000	50.44	2.10	3	1.008	2.776	Retain

Note: Each treated sample was compared to untreated sample using the Student's t-test assuming both sample sets are random, independent, and with equal population variances.

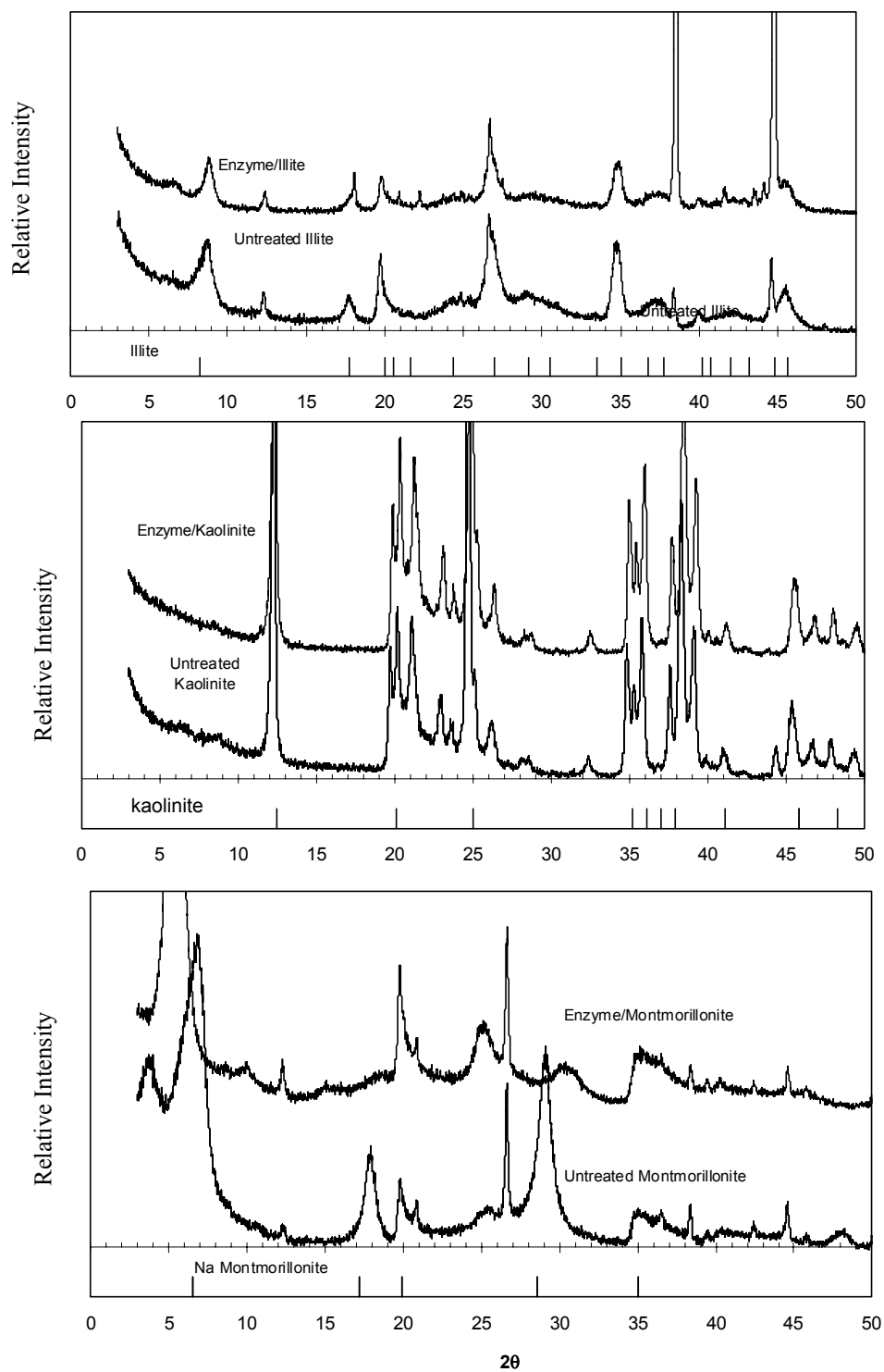
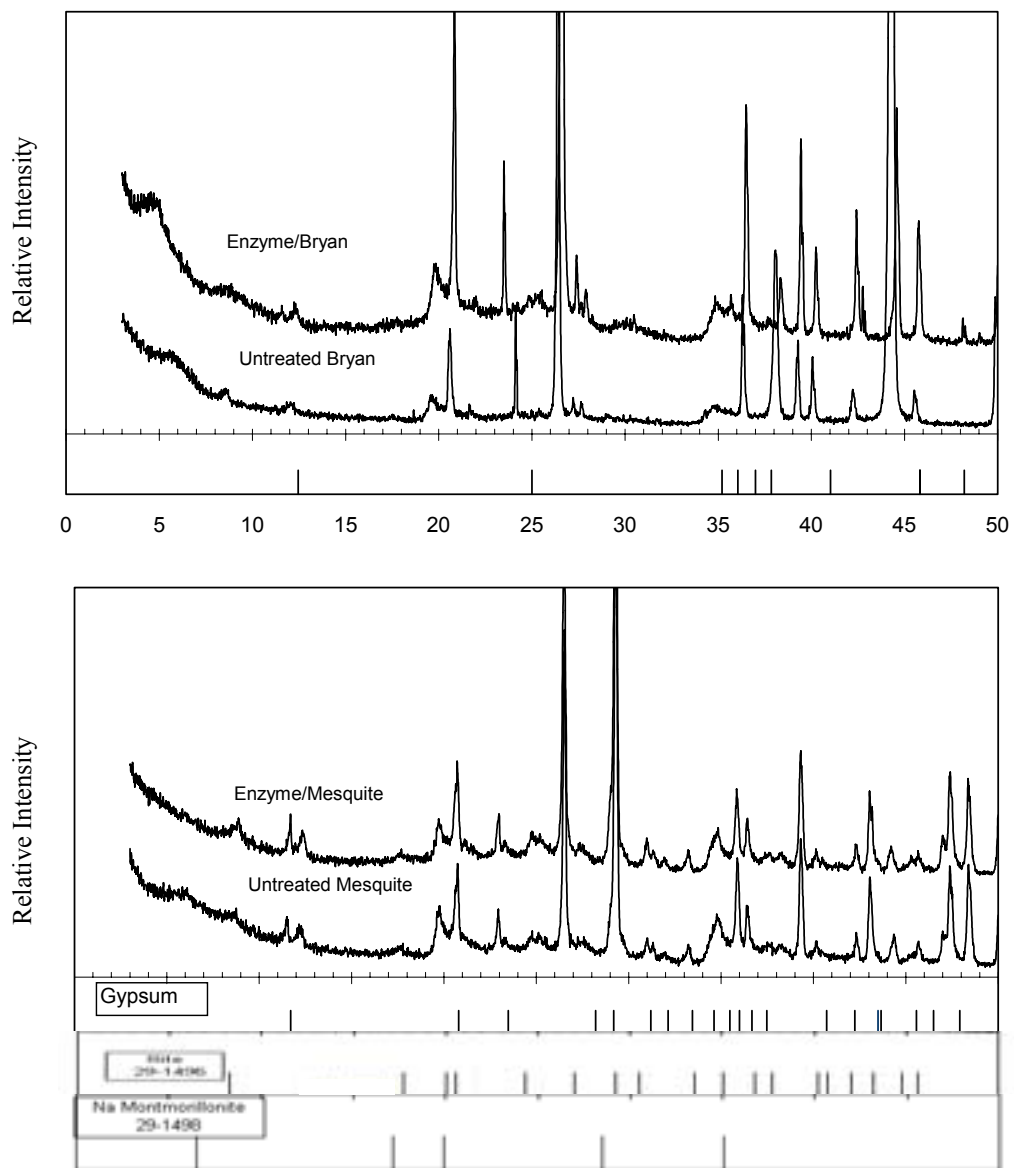


Figure 8-1. XRD patterns of enzyme treated and untreated samples of montmorillonite, illite, and kaolinite



20

Figure 8-2. XRD patterns of enzyme treated and untreated samples of Bryan and Mesquite soil samples

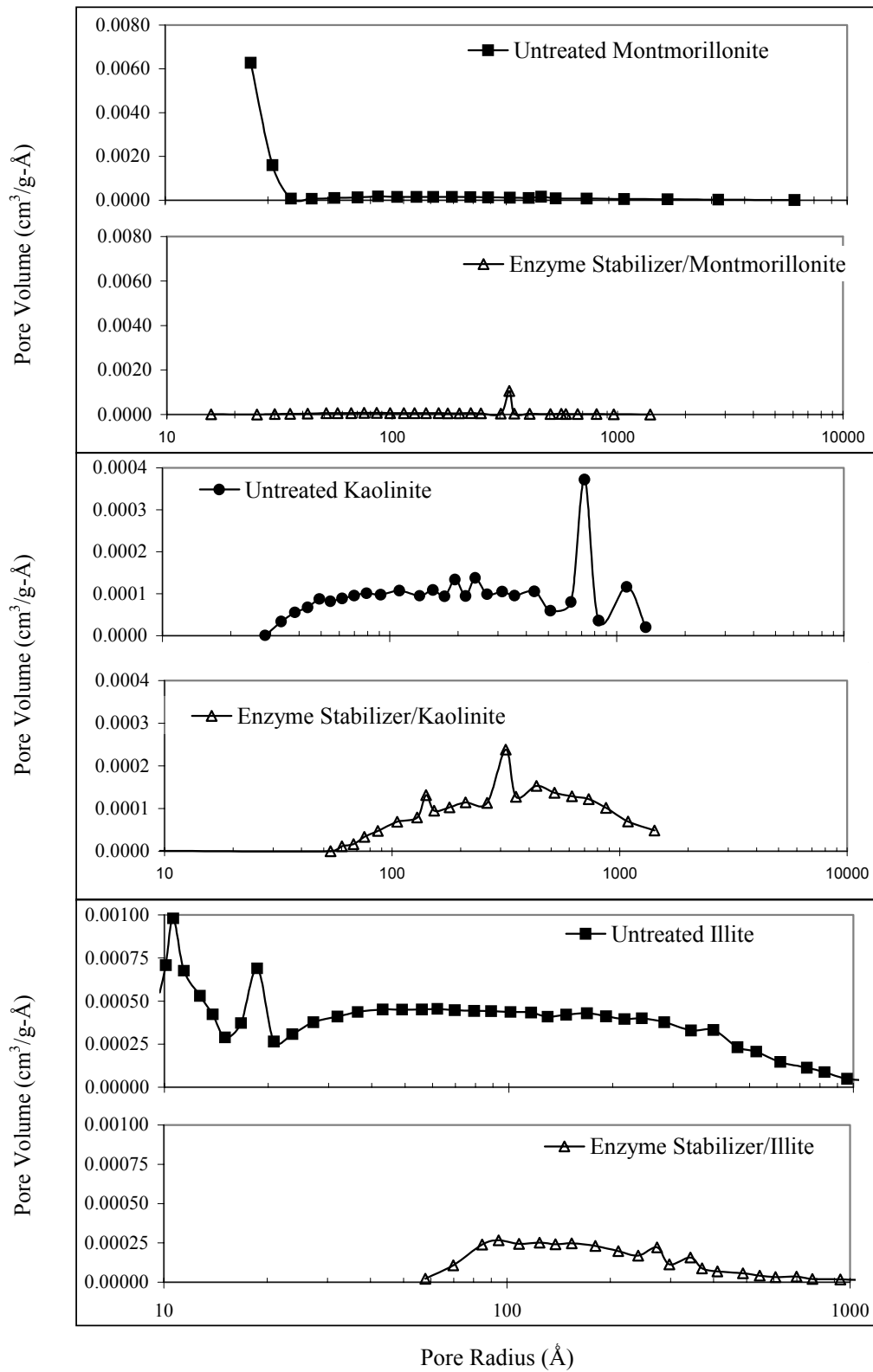


Figure 8-3. Pore size distributions for untreated and enzyme stabilizer treated samples of illite, kaolinite, and montmorillonite

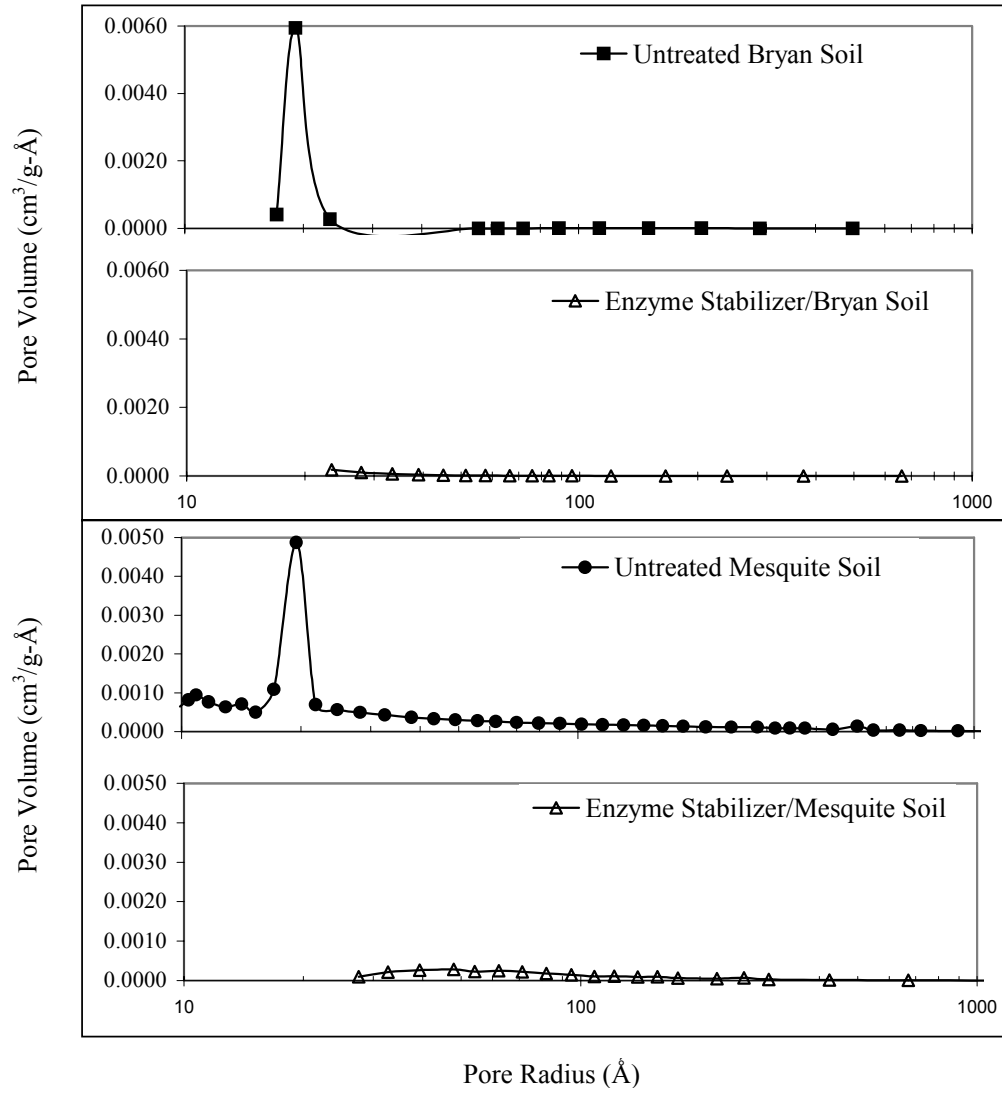


Figure 8-4. Pore size distributions for untreated and enzyme stabilizer treated samples of Bryan and Mesquite soils

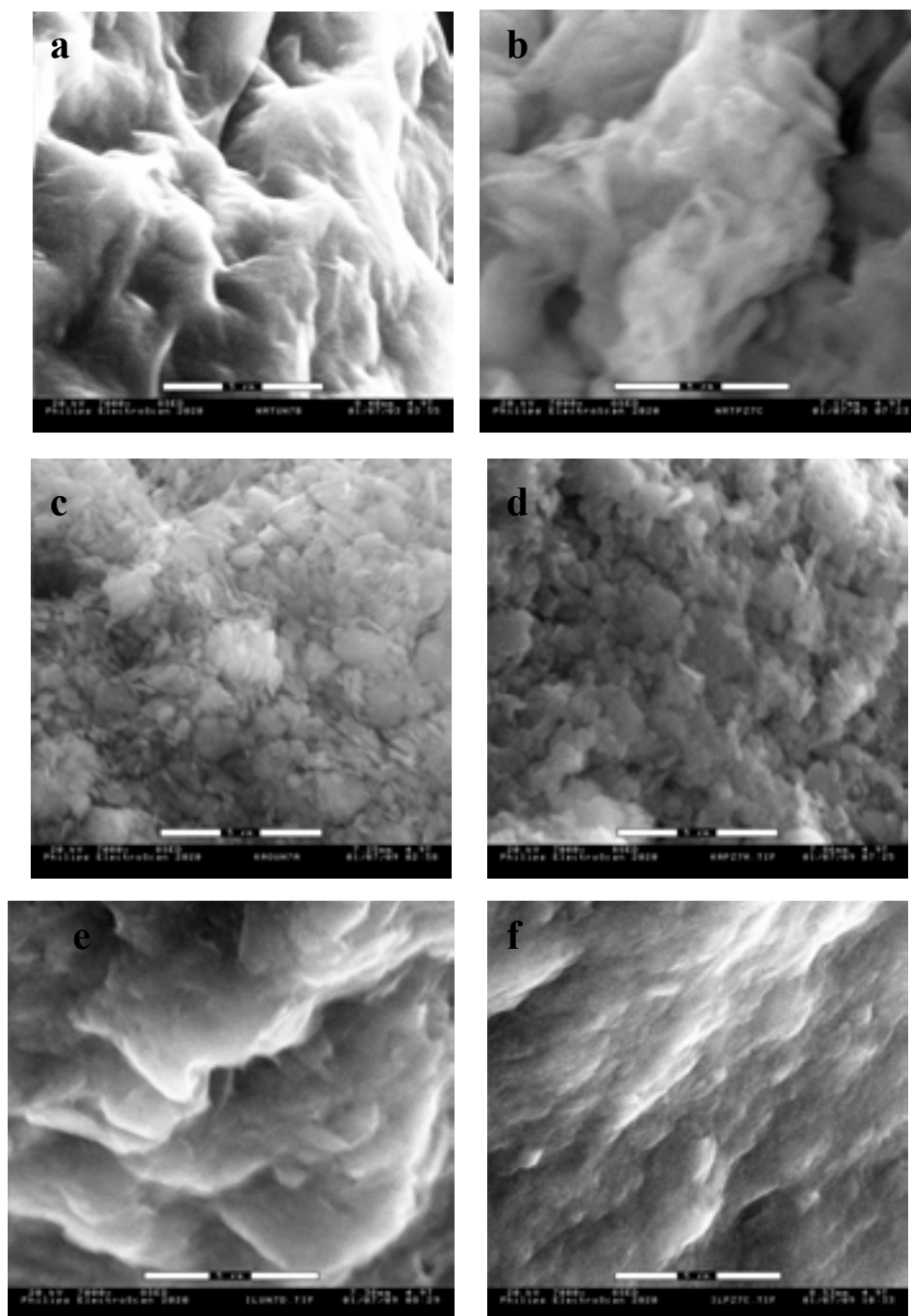


Figure 8-5. ESEM images for enzyme stabilizer treated clay minerals at a magnification of 7,000 \times for (a) untreated montmorillonite, (b) enzyme stabilizer/montmorillonite treatment, (c) untreated kaolinite, (d) enzyme stabilizer/kaolinite treatment, (e) untreated illite sample, and (f) enzyme stabilizer/illite treatment (*Note*: scale bar shown on each SEM corresponds to 5 μm)

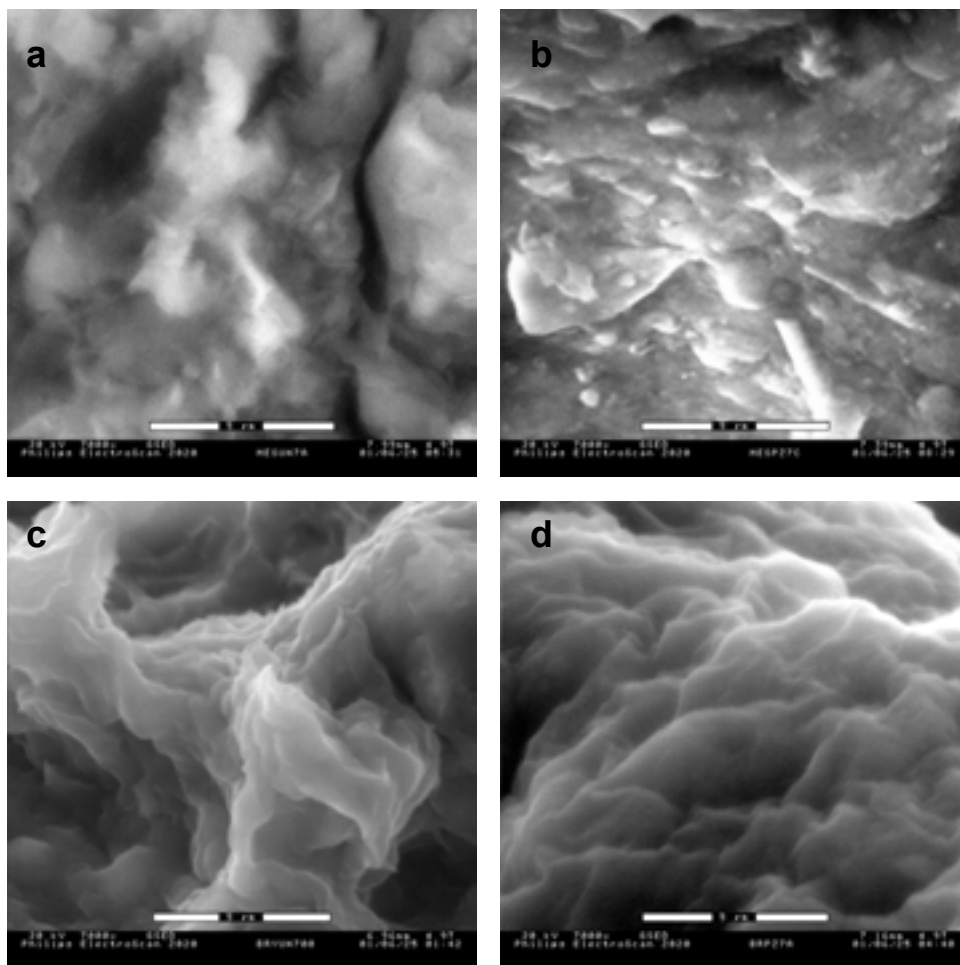


Figure 8-6. ESEM images for enzyme stabilizer treated clay minerals at a magnification of 7,000× for (a) untreated Mesquite soil, (b) enzyme stabilizer/Mesquite soil treatment, (c) untreated Bryan soil, and (d) enzyme stabilizer/Bryan soil treatment (*Note*: scale bar shown on each SEM corresponds to 5 μm)

CHAPTER 9

ENZYME STABILIZER: RESULTS FROM STUDY OF STABILIZER EFFECTIVENESS

9.1 OVERVIEW

Results from the macro-characterization study of the selected enzyme stabilizer are presented in this chapter. Tests were conducted using the two native Texas clays (TX Bryan HP and TX Mesquite HS HP) and the bulk samples of the three reference clays (kaolinite, illite, and montmorillonite). The enzyme stabilizer was mixed at the supplier's recommended dilution rate (DMR = 1/935) and applied to the soil at the supplier's recommended application rate (AMR = 1/50,000 = 0.002%). Samples of the untreated and treated soils were prepared following the protocols detailed in section 5.3. Standard geotechnical laboratory tests were conducted as described in Chapter 5.

To evaluate the effects of treating the five soils with the enzyme stabilizer, the Atterberg limits, compacted soil density, undrained shear strength, and one-dimensional (1-D) free swell potential of the untreated and treated soils were compared. Overall, no significant, consistent improvement in the engineering properties was observed when these five test soils were treated with the selected enzyme stabilizer at the application rate used.

9.2. EFFECT OF THE ENZYME STABILIZER ON ATTERBERG LIMITS

The Atterberg limits determined for the untreated and enzyme treated soils are summarized in Table 9-1 and are plotted in Figure 9-1. For perspective in considering these data, it is helpful to note the typical variability encountered in measuring Atterberg limits. As is indicated in the ASTM D 4318-95a (1998e) standard, determinations of the liquid limit (LL) of a particular soil by a single technician can be expected to vary by 2.4, and determinations by multiple laboratories can vary by 9.9. Similarly, determinations of the plastic limit (PL) by a single technician and multiple laboratories can vary by 2.6 and 10.6, respectively. Hence, much of the difference in LL and PL between the untreated and treated soil samples (Table 9-1 and Figure 9-1) can be attributed to the usual variability encountered in these laboratory measurements. Note that the ASTM criteria listed above was determined from tests on a soil with a LL of 64 (ASTM 1998e); much greater variability can be expected for soils with much higher liquid limits, such as the sodium montmorillonite used in this study.

Focusing on the plasticity index ($PI = LL - PL$) determined for each sample (Table 9-1 and Figure 9-1), treating these soils with the enzyme stabilizer does not produce a consistent improvement in soil plasticity. A lower PI was measured following treatment of the TX Mesquite HS HP sample; however, this change is not significant.

9.3. EFFECT OF THE ENZYME STABILIZER ON COMPACTED DENSITY

The water content and dry unit weight of the untreated and enzyme treated compacted soil samples, which were prepared for triaxial and swell testing, are tabulated in Appendix K and are plotted in Figure 9-2. The target optimum water content and maximum dry unit weight are

also shown for reference; these values, which are summarized in Table 5-1, were determined for the untreated soil using a modified Proctor compaction effort (ASTM D 1557-91 1998b).

In preparing test specimens of each soil, whether treated or untreated, an attempt was made to achieve a moisture content as close as possible to the target optimum. Given that some variation in the water content was unavoidable, it was decided to accept any sample having a moisture content within ± 2 percentage points of the target optimum. Note that several of the treated TX Bryan HP samples were slightly wetter than 2% above the target optimum. The scatter in the measured water contents about the target optimum in Figure 9-2 represents an acceptable, unavoidable variability among the test specimens. Given the variability in moisture content, as well as additional variability introduced by impact compaction, the variability in the compacted dry unit weights of the various specimens as seen in Figure 9-2 can be expected.

Comparing the compacted dry unit weights of the untreated samples with those of the treated samples in Figure 9-2, it is clear that the addition of the enzyme stabilizer did not result in greater soil density or improved soil compaction characteristics.

9.4. EFFECT OF THE ENZYME STABILIZER ON SHEAR STRENGTH

Undrained shear strength envelopes, which were fit to the results from the UU triaxial tests on the untreated and enzyme treated soil samples, are plotted in Figure 9-3. The differences between the strength envelopes for the untreated and treated bulk illite and montmorillonite are not significant. The lower strength of the treated TX Bryan HP soil can be attributed to the higher moisture content and lower compacted density of these specimens, as is evident in Figure 9-2 and Table K-4. Indeed, the TX Bryan HP samples used in the UU triaxial tests had a water content 18.2% to 18.3%, which is slightly more than the allowable upper limit (2% above the optimum water content of 16%) established for forming acceptable test specimens.

Slightly greater shear strengths were measured in the bulk kaolinite and TX Mesquite HS HP samples following treatment with the enzyme stabilizer product. However, the untreated kaolinite specimens were more than 94% saturated, whereas the treated specimens were about 91% saturated. The higher saturation of the untreated samples would result in greater pore pressure generation during shearing and therefore lower undrained shear strength. Likewise, the higher strength of the treated TX Mesquite HS HP soil can be attributed to the lower water content or saturation of these samples. Hence, the greater strength of the kaolinite and TX Mesquite HS HP soils following treatment cannot be credited to the addition of the enzyme stabilizer product.

The Mohr-Coulomb strength parameters, corresponding to the envelopes plotted in Figure 9-3 and determined as described in section 5.7, are given in Table 9-2. These values were used to compute the reference shear strength (S_{ref}) at the arbitrarily selected normal stress of 100 psi. The resulting values of S_{ref} are plotted in Figure 9-4. Both the bulk kaolinite and TX Mesquite HS HP show an increase in S_{ref} following treatment with the enzyme product; however, the higher strengths cannot be ascribed to the stabilizer treatment because of the higher saturation in the untreated test specimens.

9.5. EFFECT OF THE ENZYME STABILIZER ON SWELL POTENTIAL

The one-dimensional free swell potential of the untreated and enzyme treated soils was measured as described in section 5.8. Three replicate tests were run on each untreated and treated

soil sample. The results are plotted in Figure 9-5, where the variability in test results, for samples prepared in an identical manner, is evident.

Note that the bulk kaolinite appears to exhibit more expansion following treatment with the enzyme product (more expansiveness was also observed when the kaolinite was treated with the other two stabilizer products evaluated). This behavior is not linked to readily apparent differences in the test specimens, because both the untreated and treated kaolinite specimens had similar moisture contents. It is possible that the nonexpansive, untreated kaolinite was chemically activated by the enzyme stabilizer product and became more expansive. Alternatively, it is possible that some unknown error exists in the test data on the untreated bulk kaolinite.

No reduction in the 1-D free swell potential was observed following treatment of the TX Mesquite HS HP soil. Small reductions in expansiveness were observed following treatment of the bulk illite and montmorillonite. A more significant reduction in swell potential was seen when the TX Bryan HP soil was treated with the enzyme stabilizer product. Inspection of the specimen properties in Table K-2 shows that the treated TX Bryan HP samples were 1% to 3% wetter than the untreated samples, which could explain the observed reduction in the swell potential of this soil. Hence, no consistent reduction in the expansiveness of the different test soils can be attributed to treatment with the enzyme stabilizer product.

Table 9-1. Atterberg limits of the untreated test soils and of those treated with the enzyme stabilizer product

<i>Soil Sample</i>		<i>Plastic Limit</i>	<i>Liquid Limit</i>	<i>Plasticity Index</i>
TX Bryan HP	untreated	20	68	48
	enzyme treated	15	68	53
TX Mesquite HS HP	untreated	23	60	37
	enzyme treated	19	53	34
Kaolinite	untreated	32	51	19
	enzyme treated	28	49	21
Illite	untreated	24	44	20
	enzyme treated	18	50	32
Montmorillonite	untreated	32	567	535
	enzyme treated	33	612	579

Table 9-2. Shear strength parameters for envelopes that were fit to UU triaxial data in Figure 9-3

<i>Soil Sample</i>		<i>c</i> (<i>psi</i>)	<i>φ</i> (<i>deg</i>)
TX Bryan HP	untreated	113	1
	enzyme treated	37	7
TX Mesquite HS HP	untreated	71	18
	enzyme treated	111	7
Kaolinite	untreated	38	0
	enzyme treated	56	3
Illite	untreated	21	51
	enzyme treated	55	24
Montmorillonite	untreated	32	51
	enzyme treated	101	22

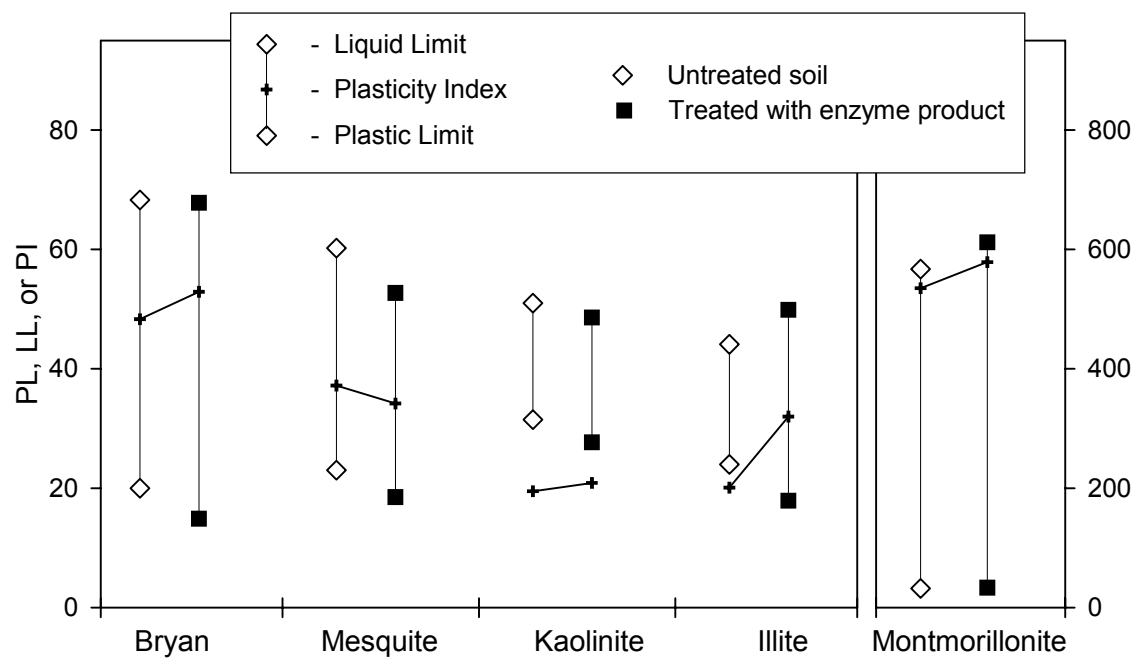


Figure 9-1. Atterberg limits of the untreated test soils and of those treated with the enzyme stabilizer product

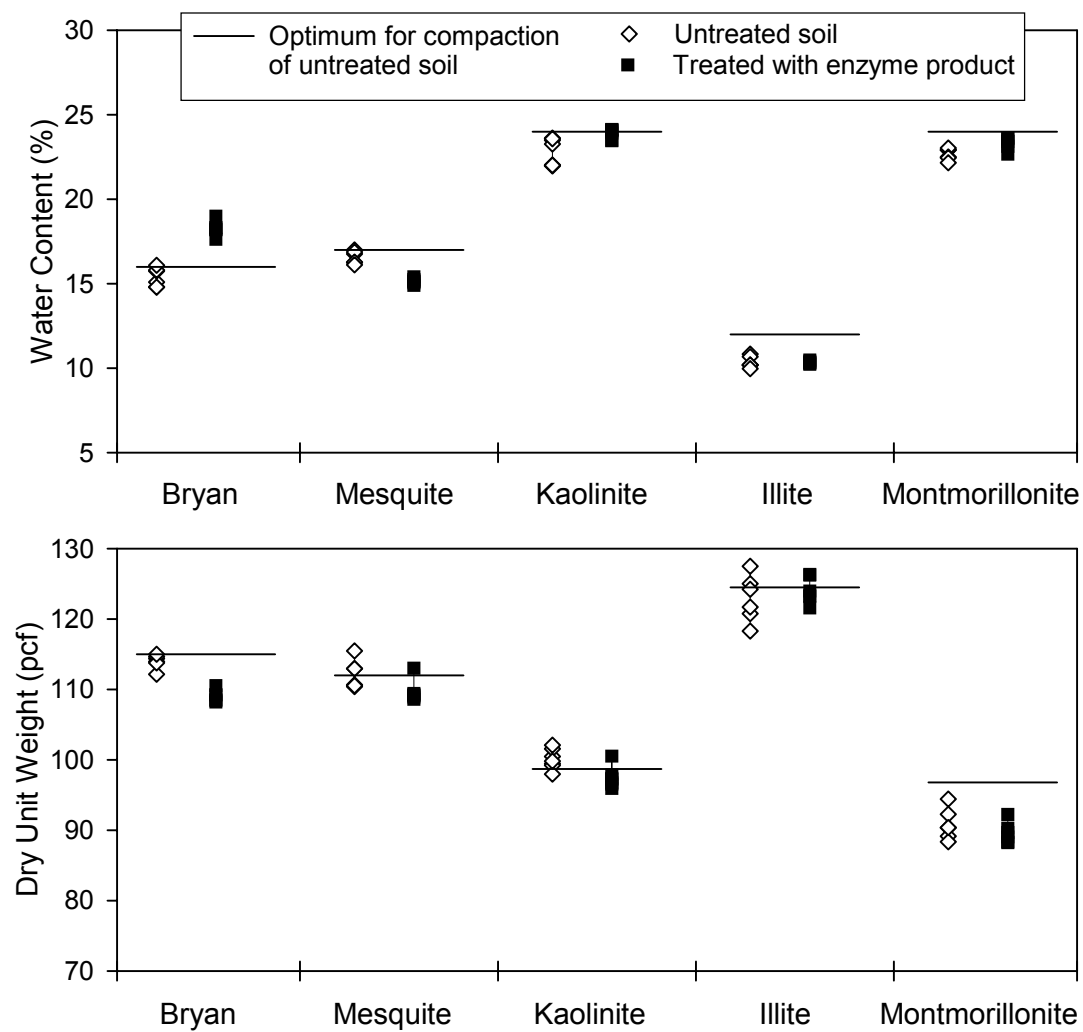


Figure 9-2. Water contents and dry unit weights of the triaxial and swell test soil specimens, both untreated and treated with the enzyme stabilizer product

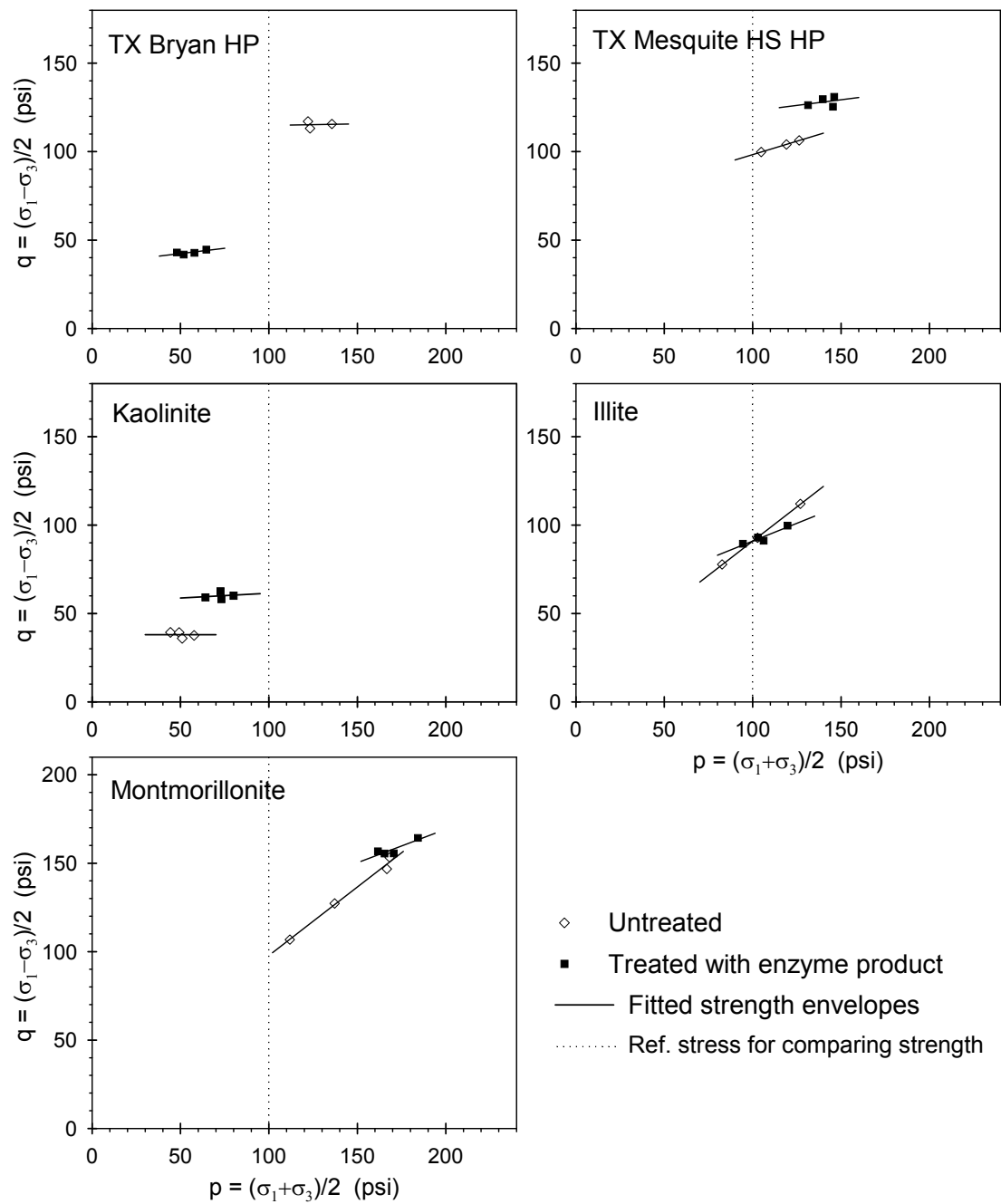


Figure 9-3. Fitted shear strength envelopes from UU triaxial tests on the untreated soils and on the soils treated with the enzyme stabilizer product

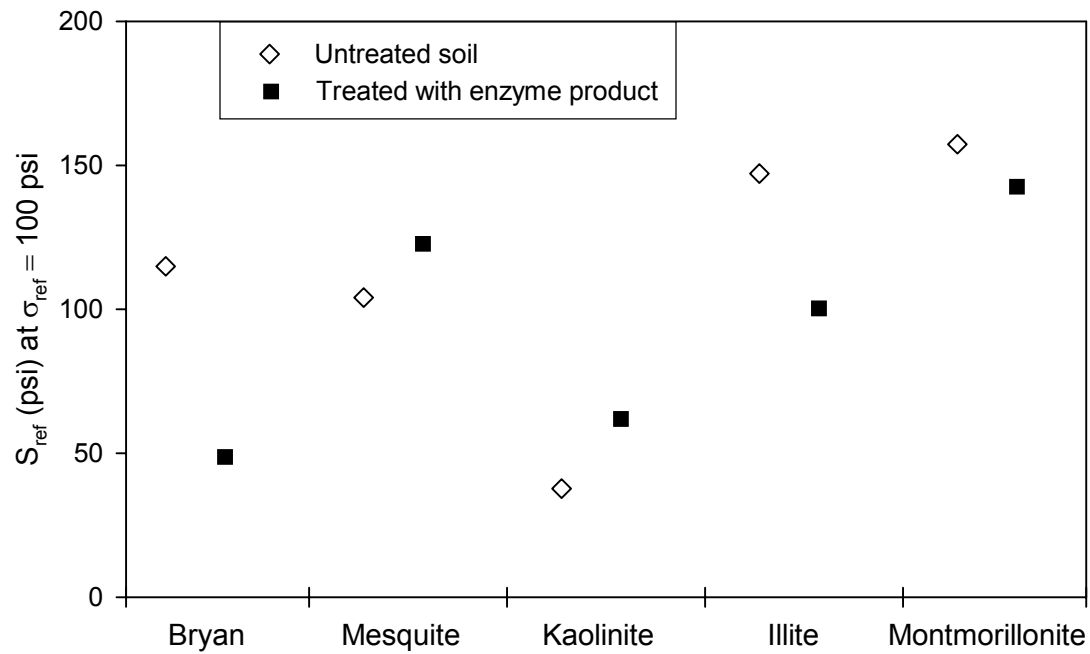


Figure 9-4. Reference shear strengths of the untreated test soils and of those treated with the enzyme stabilizer product

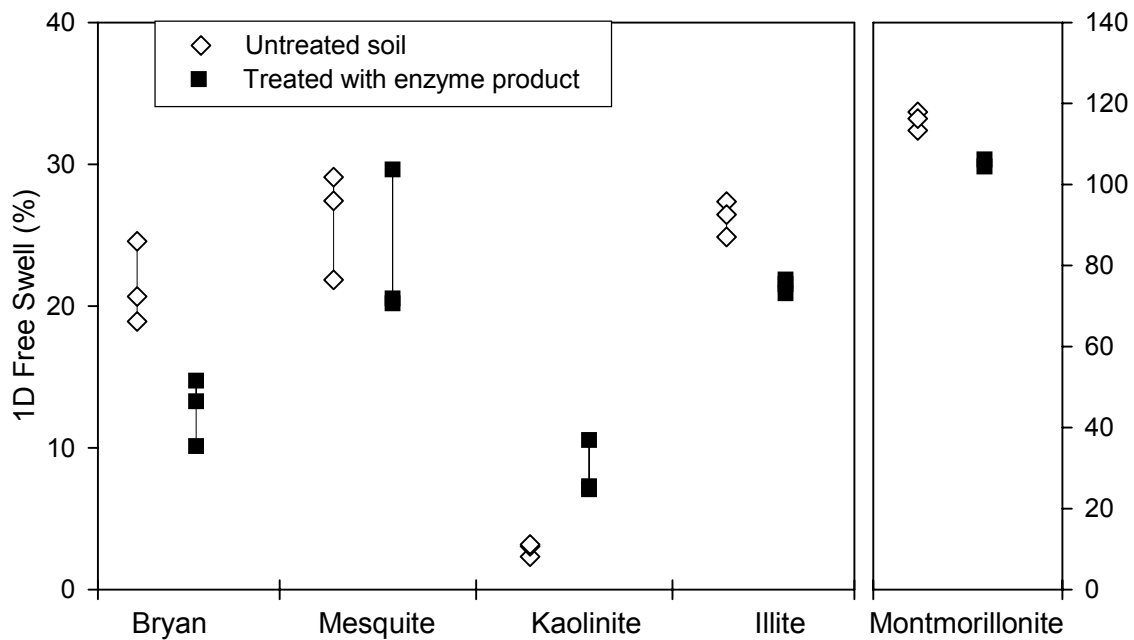


Figure 9-5. One-dimensional free swell of the untreated test soils and of those treated with the enzyme stabilizer product

CHAPTER 10

POLYMER STABILIZER: RESULTS FROM STUDY OF STABILIZER MECHANISMS

10.1. OVERVIEW

This chapter presents the results of the clay/polymer stabilizer experiments. The effects of the polymer stabilizer on the clay minerals and natural soils were determined by employing the same analytical techniques as those used for the two other stabilizers evaluated. The polymer stabilizer used in this research was a sodium silicate based polymer. The polymer stabilization mechanism involves coating the surface of soil particles rather than chemically altering the clay inner layers. The polymer binds to the surface and produces a strongly adhesive, aggregated material (Scholen 1992). If the hypothesized mechanism is correct, then changes in mineralogy should not be expected in the XRD patterns of treated samples unless the application is high enough to coat the soil surface with a silicate phase. At moderate doses, a decrease in the Al:Si ratios of treated samples should be evident in SEM/EDS analyses of treated and untreated samples. In addition, adsorption to the external regions of the clay can lead to particle destabilization and flocculation, which may lead to a reduction in surface area as reflected in nitrogen BET adsorption data. Electron micrographs may reveal the presence of a silicate coating.

10.2. XRD RESULTS OF TREATED AND UNTREATED CLAY AND SOIL SAMPLES

Figure 10-1 shows the XRD results for randomly oriented untreated and treated samples of the clay minerals, in addition to reference diffractograms for each clay mineral investigated. A comparison of the polymer treated sample with the untreated montmorillonite sample shows that the 001 peak shifted to the right (a decrease in d-spacing). Although there was a reduction in the d-spacing of the randomly oriented and oriented samples of treated montmorillonite, the d-spacing of the treated and untreated glycolated samples are similar. This suggests that polymer is not affecting the swelling potential of the clay. The XRD patterns for the treated kaolinite samples and treated illite samples are consistent with the diffractograms of the corresponding untreated samples. Indeed, the d-spacings for the treated and untreated samples for kaolinite and illite are nearly identical, as can be seen in Table 10-1.

Comparison of XRD patterns for randomly oriented samples of untreated and treated Bryan soil, as is shown in Figure 10-2, indicates a reduction in d-spacing. This is illustrated by the shift to the right in the 001 peak at approximately $6\ 2\theta$, owing to the polymer treatment. The reduction in d-spacing is similar to that observed for the montmorillonite sample. Unfortunately, the d-spacing after glycolation of the Bryan sample was not determined. For the Mesquite soil, the resolution of the XRD diffractogram was not sufficient to evaluate whether there was a shift in the d-spacing for the peak at approximately $6\ 2\theta$.

10.3. BET ANALYSIS OF TREATED AND UNTREATED CLAY AND SOIL SAMPLES

Surface areas and pore size distributions were determined using the nitrogen BET method for polymer treated and untreated samples of the clay minerals and soils. The results from these

analyses for treated and untreated samples (Table 10.2 and Figures 10.3 and 10.4) are consistent with the hypothesized aggregation mechanism and suggest that at these high application ratios, the polymer is effective for agglomerating clay particles. Indeed, the nitrogen BET results for treated and untreated samples show a significant reduction in surface area following treatment with the polymer stabilizer for all of the clay minerals and soils tested. The pore size distributions also show a reduction in pores for treated samples, especially for pores having radii less than about 20 Å.

Thus, the results of the nitrogen adsorption tests for treated clays and soil samples suggest that the polymer stabilizer is binding clay particles together and restricting access to the pore spaces between particles.

10.4. ESEM AND SEM/EDS ANALYSES OF TREATED AND UNTREATED CLAY AND SOIL SAMPLES

ESEM images for the treated and untreated samples of the clay minerals are presented in Figures 10-5 and 10-6. Comparison of the treated samples with the untreated samples suggests that the changes in the electron micrographs for the polymer treated samples are similar to the changes observed for the enzyme treated samples. For all of the clay and soils analyzed, the treated samples appear more aggregated than the corresponding untreated sample, and the clay features are less visible. However, there does not appear to be a change in the composition of the material. These results are consistent with the results of the BET and the XRD analyses.

In contrast to the enzyme stabilizer, the EDS analysis indicated that the surface composition had changed after treatment. As shown in Table 10-3, there was a significant reduction in the Al:Si ratio following treatment for the illite, kaolinite, and Bryan soil. Closer examination of the results for the Bryan soil, as shown in Figure 10-7, indicates that there was an increase in the fraction of both Na and Si in the samples. This finding suggests that the decrease in Al:Si ratio was due to the presence of a surface coating of sodium silicate, the primary ingredient of the polymer.

10.5. CEC ANALYSIS OF TREATED AND UNTREATED MONTMORILLONITE

Cation exchange capacity (CEC) was measured for untreated and treated samples of montmorillonite at three application mass ratios: 1:4, 1:1,000 and 1:6,000. As with the other stabilizers, three application ratios were used to study the effects of the stabilizer over a wide range of concentrations. However, as is evident from the data presented in Table 10-4 and hypothesis testing of the data, there is no impact of the polymer stabilizer on the CEC of the montmorillonite sample at any of the AMRs examined. Indeed, the null hypothesis, which assumed that untreated and treated CEC mean values were equal, was retained for all of the samples at the 95% confidence level. These data are consistent with the hypothesized physical aggregation mechanism for this stabilizer.

10.6. SUMMARY

For the polymer stabilizer, the hypothesized mechanism is the “binding of organic and inorganic soil pigments resulting in a strongly adhesive, aggregated product” (Scholen 1992). Furthermore, the polymer stabilizer was alleged to coat the surface of soil particles rather than to

chemically alter the clay inner layers. However, the possibility of forming calcium silicates on the clay surface was present. The results of polymer treatment for all clays and soils tested supported the proposed mechanism of surface coating and aggregation. This was confirmed consistently with all five soil samples by ESEM images and BET analysis. No changes in d-spacing or Al:Si ratio were reported for any of the clay or soil samples, which is expected because of the interaction of the polymer stabilizer and clay by physical rather than chemical means. For kaolinite and illite, the Al:Si ratio for the polymer treated clay decreased when compared with the Al:Si ratio of the untreated clays. This result is as expected if the polymer stabilizer coats the clay particles, because sodium silicate (the active ingredient in the polymer stabilizer) would increase the silica content.

Table 10-1. Summary of d-spacings and values of 2θ for the 001 peak for untreated and polymer treated samples of clay minerals and native soils

<i>Sample Description</i>	<i>d-spacing - Å</i>		<i>2θ</i>	
	<i>Polymer Stabilizer</i>	<i>Untreated</i>	<i>Polymer Stabilizer</i>	<i>Untreated</i>
Illite				
Randomly oriented	10.14	10.094	8.72	8.76
Glycolated	10.21	10.14	8.66	8.72
Oriented	10.234	10.21	8.64	8.66
Montmorillonite				
Randomly oriented	11.978	12.923	7.38	6.84
Glycolated	17.126	17.192	5.16	5.14
Oriented	12.737	14.929	6.94	5.92
Kaolinite				
Randomly oriented	7.278	7.184	12.16	12.32
Glycolated	NA	NA	NA	NA
Oriented	NA	NA	NA	NA
Mesquite Soil				
Randomly oriented	NA	14.49	NA	6.10
Glycolated	NA	NA	NA	NA
Oriented	NA	NA	NA	NA
Bryan Soil				
Randomly oriented	13.90	15.29	6.36	5.78
Glycolated	NA	17.40	NA	5.08
Oriented	NA	15.134	NA	5.84

Table 10-2. BET results for polymer stabilizer treated samples of montmorillonite, kaolinite, illite, Bryan soil, and Mesquite soil

<i>Sample Description</i>	<i>BET N₂ Surface Area</i>	
	<i>(m²/g)</i>	<i>St. Dev (+/-)</i>
Montmorillonite		
Unwashed/untreated	31.79	0.3465
Untreated ^a	30.87	0.2843
Polymer stabilizer ^a	16.42	0.2293
Repository ^b	31.82	0.22
Kaolinite		
Unwashed/untreated	11.05	0.0319
Untreated ^a	11.5	0.0687
Polymer stabilizer ^a	6.64	0.0794
Repository ^b	10.05	
Illite		
Unwashed/untreated	28.4	0.1482
Untreated ^a	35.03	0.6272
Polymer stabilizer ^a	18.8	0.1059
Repository ^b	23.7	
Bryan Soil		
Unwashed/untreated	35.48	0.1119
Untreated ^a	31.93	0.1142
Polymer stabilizer ^a	5.373	0.05477
Mesquite Soil		
Unwashed/untreated	40.45	0.2226
Untreated ^a	40.88	0.2643
Polymer stabilizer ^a	26.48	0.2809

^a Samples were washed, treated, cured, and rinsed through a 0.45 µm cellulose nitrate filter prior to evaluation.

^b Results provided by University of Missouri Repository Source Clay Data Sheet.

Table 10-3. Al:Si ratios determined from EDS results for polymer stabilizer treated samples of montmorillonite, kaolinite, illite, Bryan soil, and Mesquite soil

<i>Sample Description</i>	<i>Al:Si</i>					<i>Reject/ Retain Ho</i>
	<i>Ratio (wt %)</i>	<i>Std. Dev (±%) (S_i)</i>	<i># Samples</i>	<i>T</i>	<i>t_{0.975}</i>	
Montmorillonite						
Untreated	0.395	0.105	11			
Polymer stabilizer	0.338	0.054	12	1.672	2.080	Retain
<i>Repository</i>	0.366					
Kaolinite						
Untreated	1.052	0.036	10			
Polymer stabilizer	0.876	0.054	10	8.575	2.101	Reject
<i>Repository</i>	1.015					
Illite						
Untreated	0.579	0.035	11			
Polymer stabilizer	0.505	0.046	10	4.179	2.093	Reject
<i>Repository</i>	0.558					
Bryan Soil						
Untreated	0.532	0.031	8			
Polymer stabilizer	0.344	0.083	7	5.993	2.160	Reject
Mesquite Soil						
Untreated	0.583	0.184	7			
Polymer stabilizer	0.419	0.195	7	1.622	2.179	Retain

Note: Each treated sample was compared with an untreated sample using the Student's t-test assuming both sample sets are random, independent, and with equal population variances.

Table 10-4. Cation exchange capacity results for the untreated and polymer treated montmorillonite

<i>Sample Description</i>	<i>Application Mass Ratio</i>	<i>CEC (centimoles/kg)</i>					<i>Reject/ Retain Ho</i>
		<i>Avg.</i>	<i>Std. Dev</i>	<i># Samples</i>	<i>t</i>	<i>t_{0.975}</i>	
Montmorillonite							
Untreated	zero	54.16	6.04	3			
Polymer stabilizer	1:4	44.65	4.56	3	2.176	2.776	Retain
Polymer stabilizer	1:1,000	49.92	1.05	3	1.198	2.776	Retain
Polymer stabilizer	1:6,000	51.48	2.20	3	0.722	2.776	Retain

Note: Each treated sample was compared to untreated sample using the Student's t-test assuming both sample sets are random, independent, and with equal population variances.

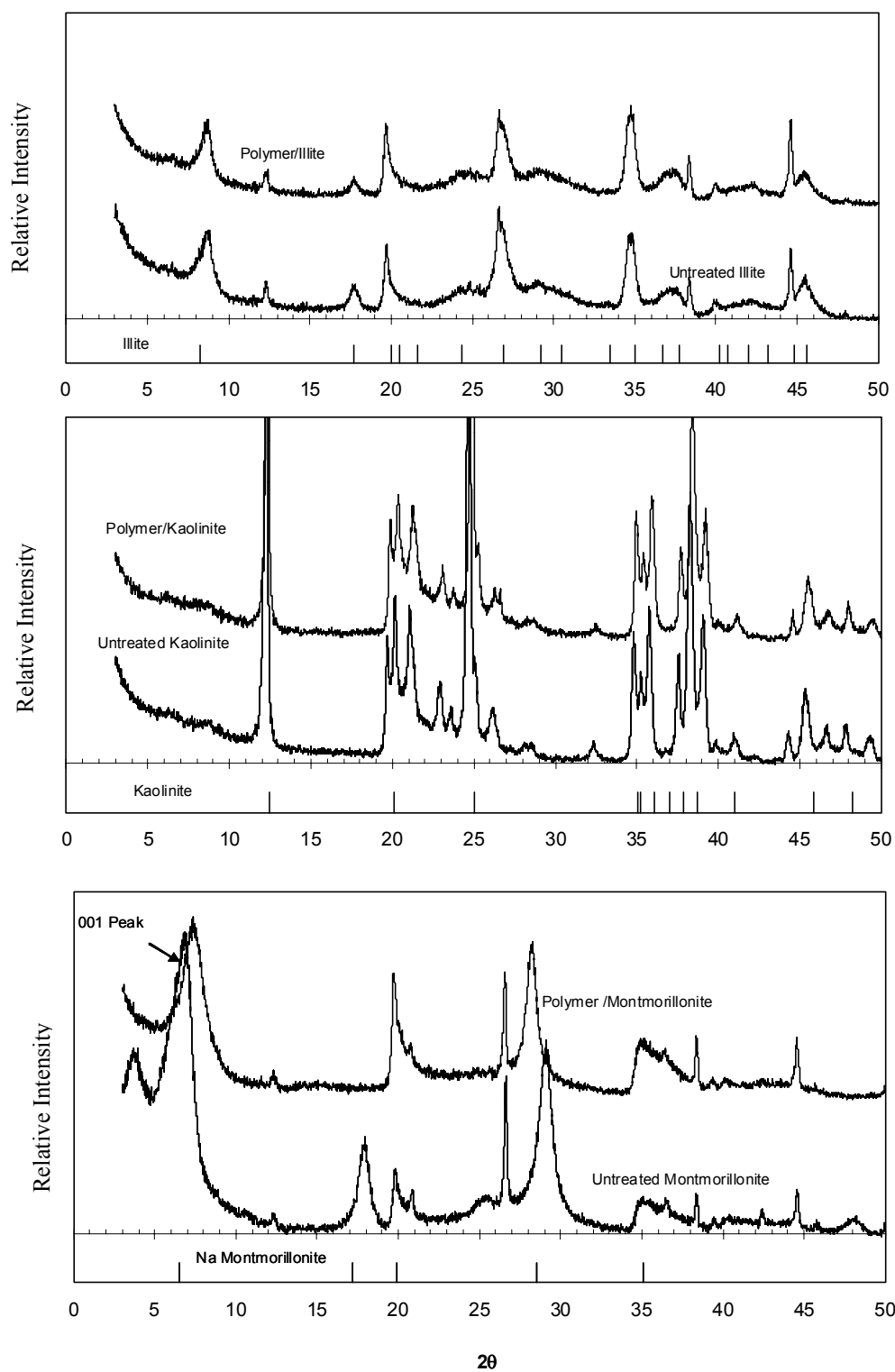


Figure 10-1. XRD patterns of polymer treated and untreated samples of montmorillonite, illite, and kaolinite

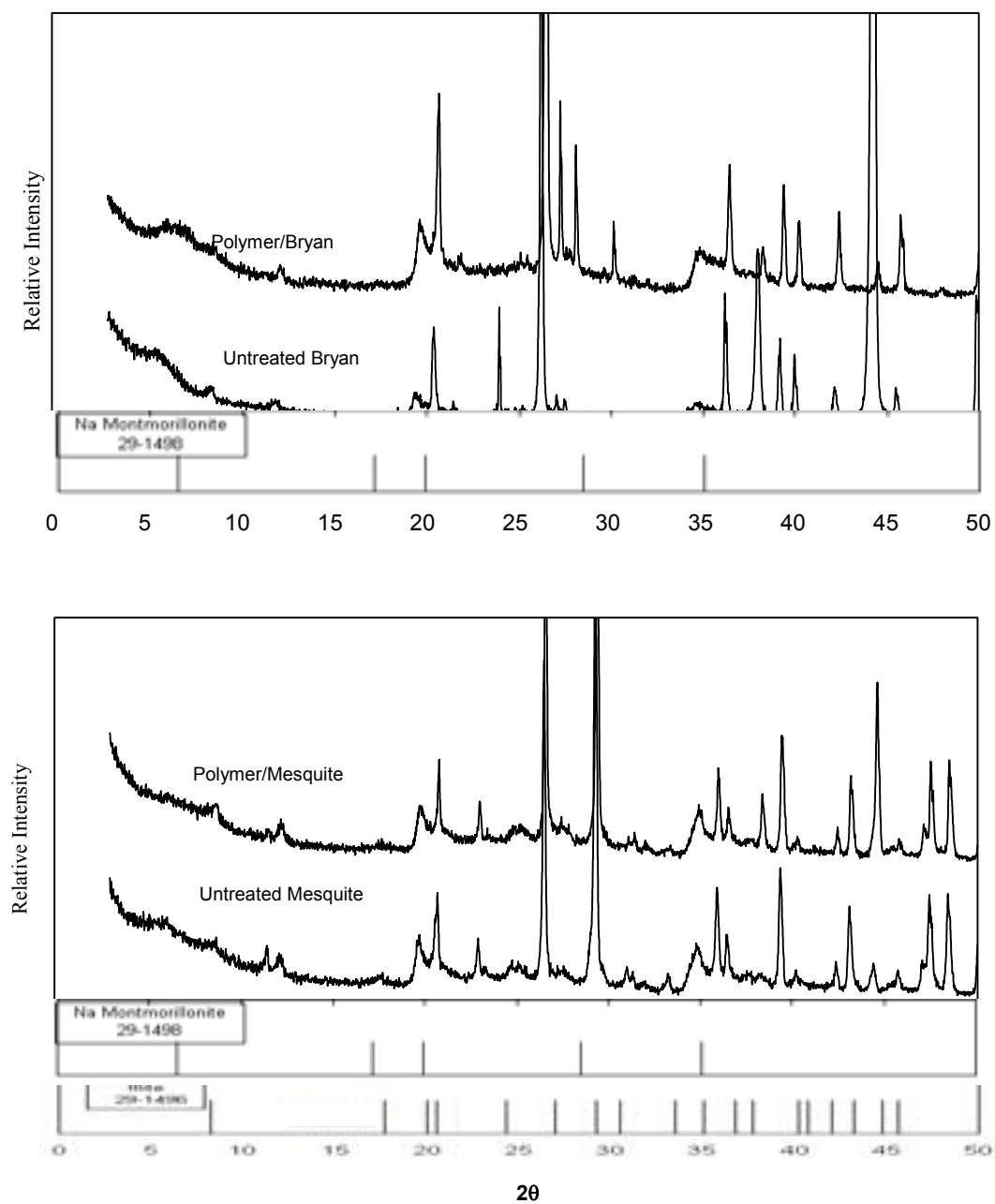


Figure 10-2. XRD patterns of enzyme treated and untreated samples of Bryan and Mesquite soil samples

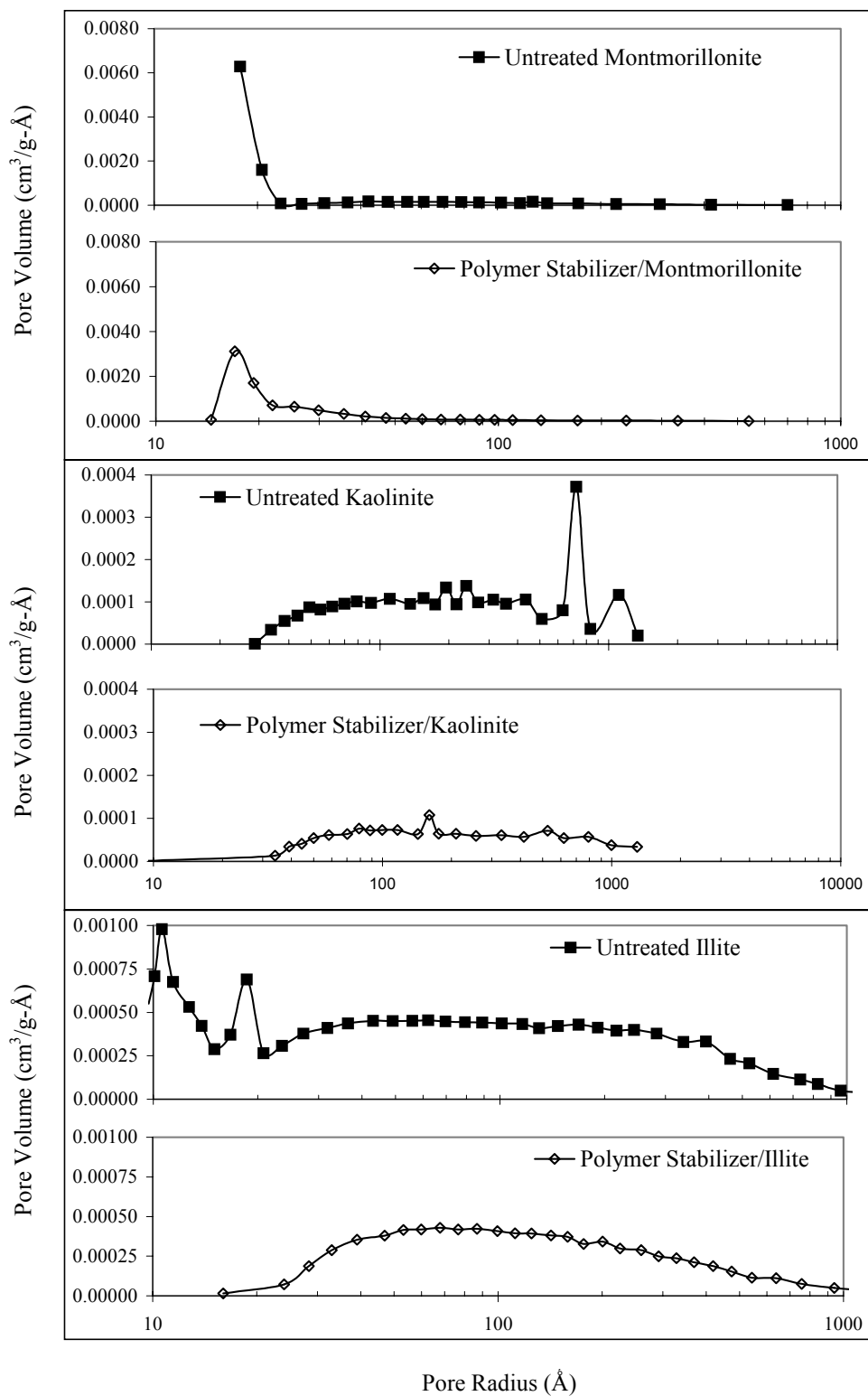


Figure 10-3. Pore size distributions for untreated and polymer stabilizer treated samples of illite, kaolinite, and montmorillonite

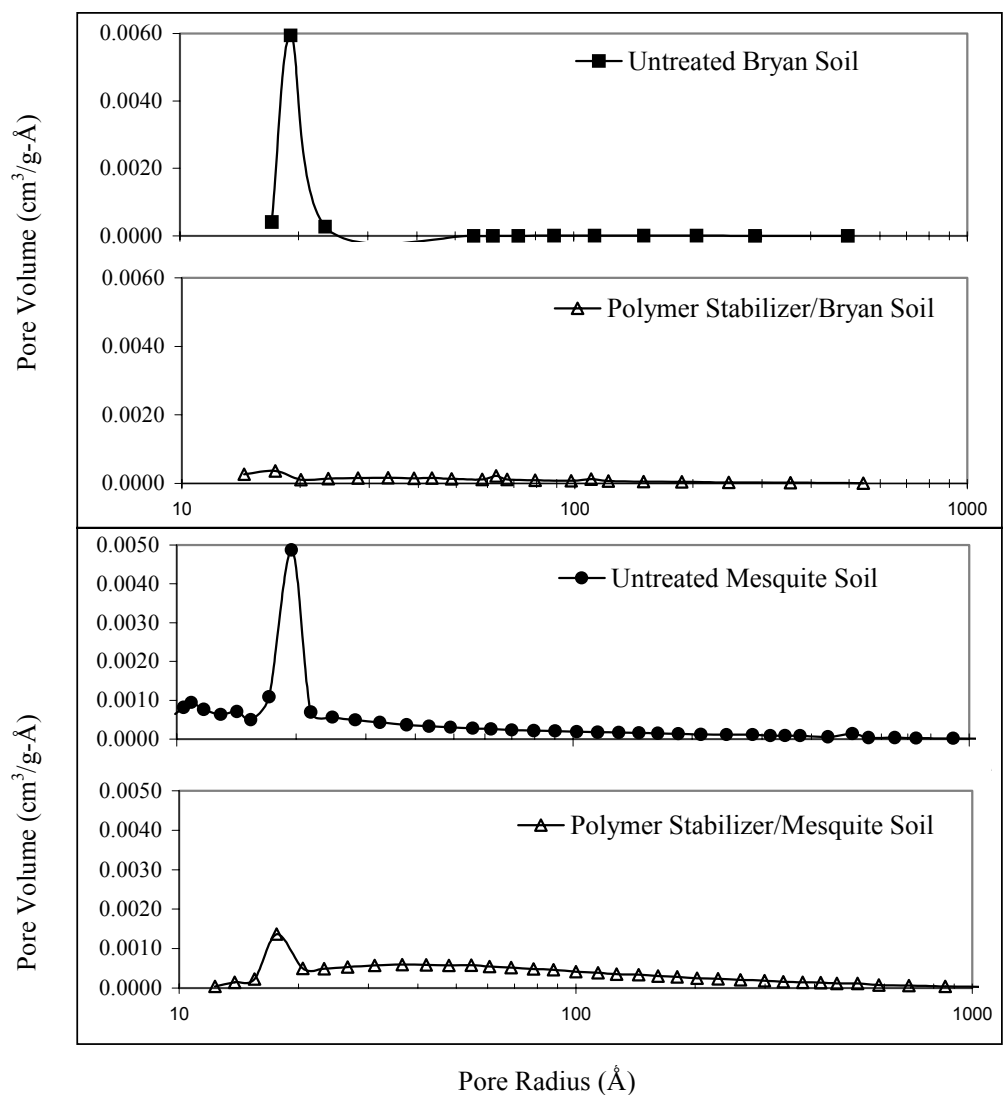


Figure 10-4. Pore size distributions for untreated and polymer stabilizer treated samples of Bryan and Mesquite soils

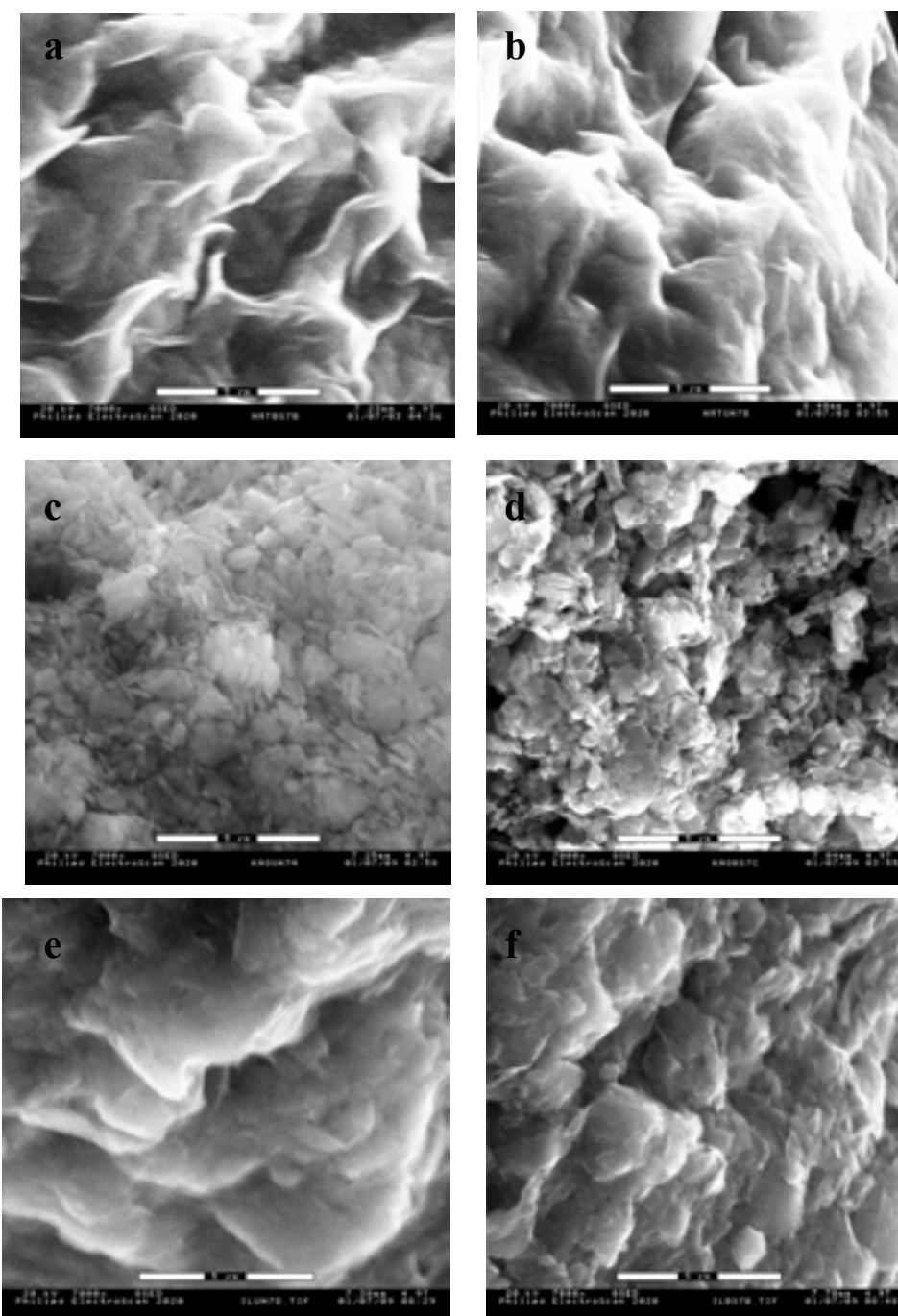


Figure 10-5. ESEM images for polymer stabilizer treated clay minerals at a magnification of 7,000 \times for (a) untreated montmorillonite, (b) polymer stabilizer/montmorillonite treatment, (c) untreated kaolinite, (d) polymer stabilizer/kaolinite treatment, (e) untreated illite sample, and (f) polymer stabilizer/illite treatment (*Note*: scale bar shown on each SEM corresponds to 5 μ m)

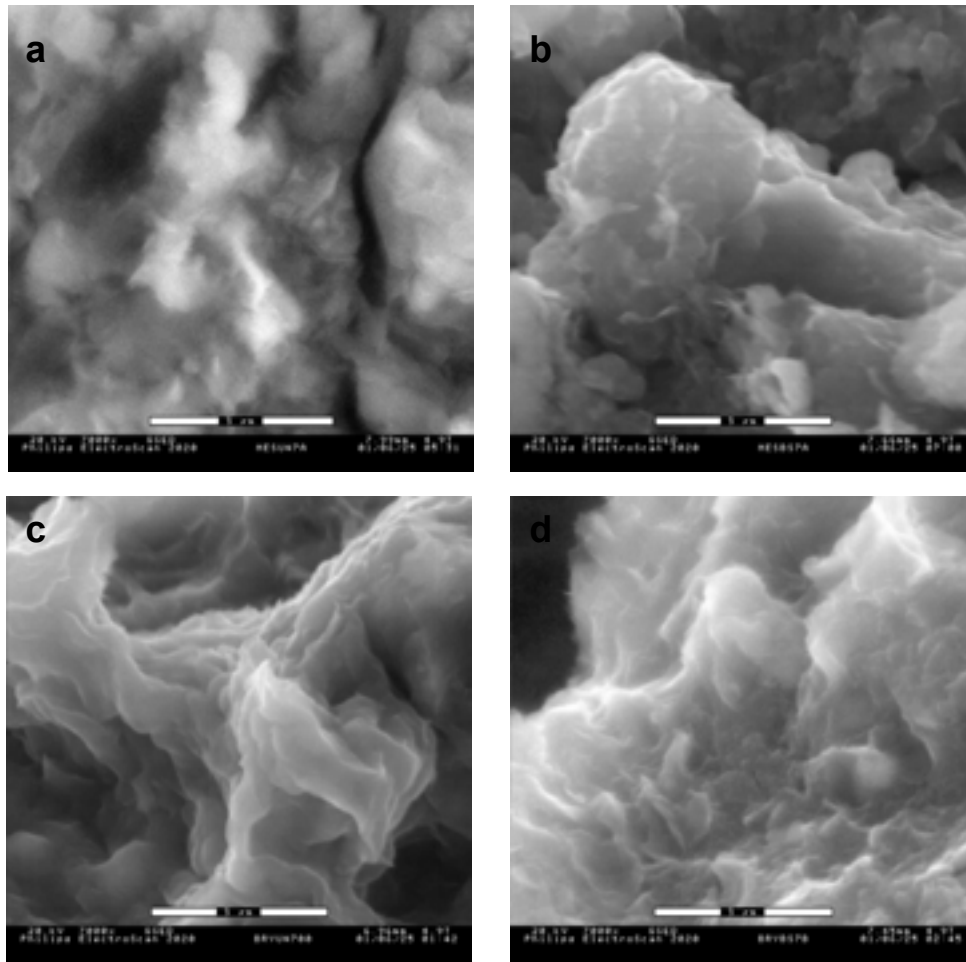


Figure 10-6. ESEM images for polymer stabilizer treated clay minerals at a magnification of 7,000 \times for (a) untreated Mesquite soil, (b) polymer stabilizer/Mesquite soil treatment, (c) untreated Bryan soil, and (d) polymer stabilizer/Bryan soil treatment (*Note*: scale bar shown on each SEM corresponds to 5 μ m)

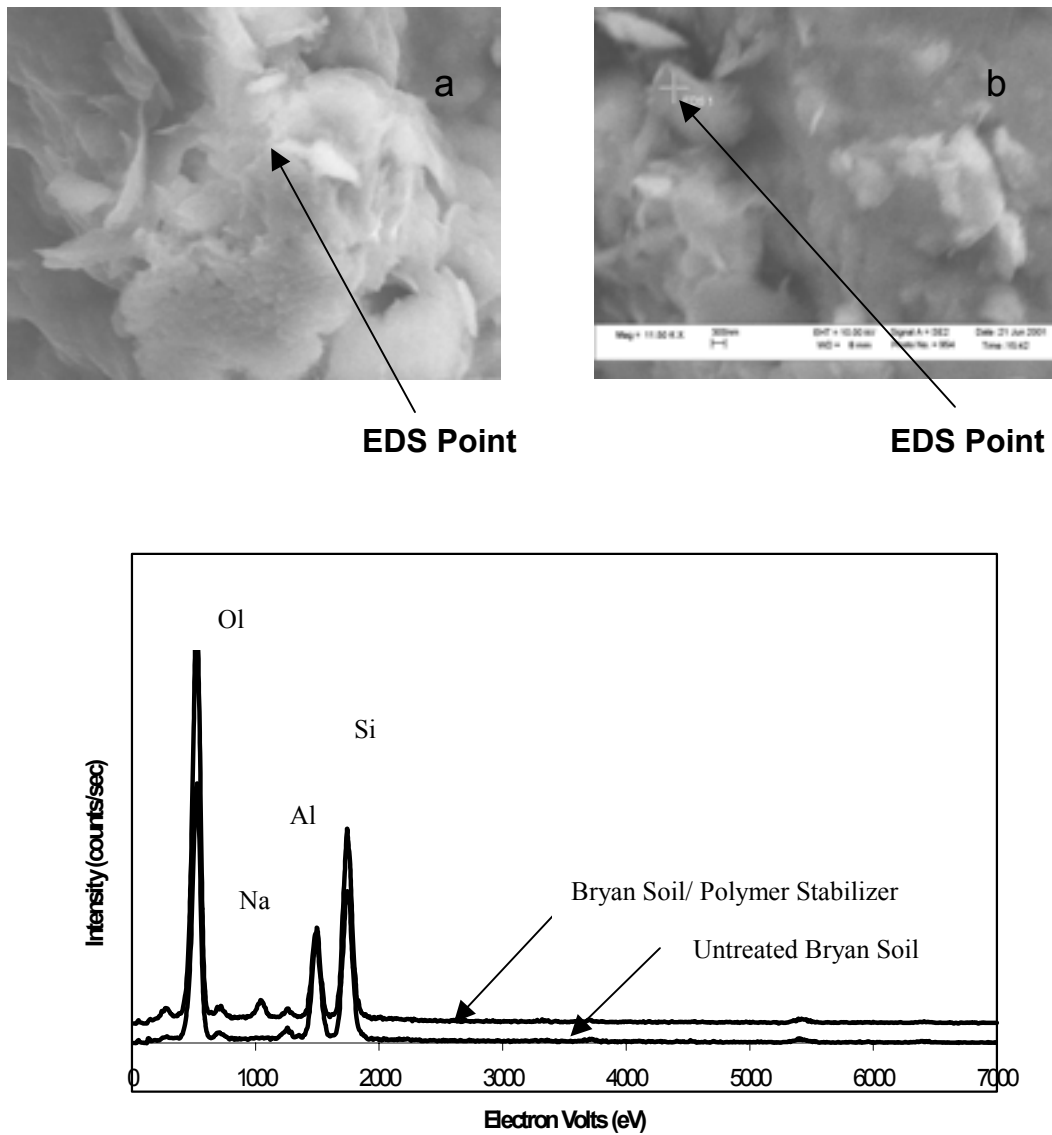


Figure 10-7. SEM/EDS results for untreated and polymer stabilizer treated Bryan soil at a magnification of 11,500 \times including (a) SEM image of untreated Bryan soil with EDS point identified, (b) SEM image of polymer stabilizer treated Bryan soil with EDS point identified, and (c) corresponding EDS spectra for the untreated and treated samples

CHAPTER 11

POLYMER STABILIZER: RESULTS FROM STUDY OF STABILIZER EFFECTIVENESS

11.1 OVERVIEW

Results from the macro-characterization study of the selected polymer stabilizer are presented in this chapter. Tests were conducted using the two native Texas clays (TX Bryan HP and TX Mesquite HS HP) and the bulk samples of the three reference clays (kaolinite, illite, and montmorillonite). The polymer stabilizer was mixed at the supplier's recommended dilution rate (DMR = 1/26) and applied to the soil at the supplier's recommended application rate (AMR = 1/1000 = 0.1%). Samples of the untreated and treated soils were prepared following the protocols detailed in section 5.3. Standard geotechnical laboratory tests were conducted as described in Chapter 5.

To evaluate the effects of treating the five soils with the polymer stabilizer, the Atterberg limits, compacted soil density, undrained shear strength, and one-dimensional (1-D) free swell potential of the untreated and treated soils were compared. Overall, no significant, consistent improvement in the engineering properties was observed when these five test soils were treated with the selected polymer stabilizer at the application rate used.

It is interesting to note that Santoni et al. (2002) found that some polymer products were effective in improving the strength of silty sands. In that study, however, the products were applied at 25 to 50 times the application rates recommended by the suppliers. The polymer product evaluated in this chapter was not investigated by Santoni and her co-workers (personal communication 2002).

11.2. EFFECT OF THE POLYMER STABILIZER ON ATTERBERG LIMITS

The Atterberg limits determined for the untreated and polymer treated soils are summarized in Table 11-1 and are plotted in Figure 11-1. For perspective in considering these data, it is helpful to note the typical variability encountered in measuring Atterberg limits. As indicated in the ASTM D 4318-95a (1998e) standard, determinations of the liquid limit (LL) of a particular soil by a single technician can be expected to vary by 2.4, and determinations by multiple laboratories can vary by 9.9. Similarly, determinations of the plastic limit (PL) by a single technician and multiple laboratories can vary by 2.6 and 10.6, respectively. Hence, much of the differences in LL and PL between the untreated and treated soil samples (Table 11-1 and Figure 11-1) can be attributed to the usual variability encountered in these laboratory measurements. Note that the ASTM criteria listed above was determined from tests on a soil with a LL of 64 (ASTM 1998e); much greater variability can be expected for soils with much higher liquid limits, such as the sodium montmorillonite used in this study.

Focusing on the plasticity index ($PI = LL - PL$) determined for each sample (Table 11-1 and Figure 11-1), treating these soils with the polymer stabilizer does not produce a consistent improvement in soil plasticity. A lower PI was measured following treatment of the TX Mesquite HS HP and bulk montmorillonite samples; however, these changes do not appear to be significant.

11.3. EFFECT OF THE POLYMER STABILIZER ON COMPACTED DENSITY

The water content and dry unit weights of the untreated and polymer treated compacted soil samples, which were prepared for triaxial and swell testing, are tabulated in Appendix K and are plotted in Figure 11-2. The target optimum water content and maximum dry unit weight are also shown for reference; these values, which are summarized in Table 5-1, were determined for the untreated soil using a modified Proctor compaction effort (ASTM D 1557-91 1998b).

In preparing test specimens of each soil, whether treated or untreated, an attempt was made to achieve a moisture content as close as possible to the target optimum. Given that some variation in the water content was unavoidable, it was decided to accept any sample having a moisture content within ± 2 percentage points of the target optimum. Hence, the scatter in the measured water contents about the target optimum in Figure 11-2 represents an acceptable, unavoidable variability among the test specimens. Given the variability in moisture content, as well as additional variability introduced by impact compaction, the variability in the compacted dry unit weights of the various specimens as seen in Figure 11-2 can be expected.

Comparing the compacted dry unit weights of the untreated samples with those of the treated samples in Figure 11-2, it is clear that the addition of the polymer stabilizer did not result in greater soil density or improved soil compaction characteristics.

11.4. EFFECT OF THE POLYMER STABILIZER ON SHEAR STRENGTH

Undrained shear strength envelopes, which were fit to the results from the UU triaxial tests on the untreated and polymer treated soil samples, are plotted in Figure 11-3. The differences between the strength envelopes for untreated and treated TX Mesquite HS HP and the bulk montmorillonite are not significant. The lower strength of the treated bulk illite can be attributed to the higher moisture content of the treated specimens, as is evident in Table K-4. The treated TX Bryan HP specimens also had slightly higher moisture contents than the untreated specimens, leading to a slightly lower strength in the treated soil.

Only the bulk kaolinite shows significantly increased shear strength following treatment with the polymer stabilizer product. However, the untreated kaolinite specimens were more than 94% saturated, and the treated specimens were about 86% saturated. The relatively high saturation of the untreated samples would result in greater pore pressure generation during shearing and therefore lower undrained shear strength. Hence, the greater strength of the kaolinite following treatment cannot be credited to the addition of the polymer stabilizer product.

The Mohr-Coulomb strength parameters, corresponding to the envelopes plotted in Figure 11-3 and determined as described in section 5.7, are given in Table 11-2. These values were used to compute the reference shear strength (S_{ref}) at the arbitrarily selected normal stress of 100 psi. The resulting values of S_{ref} are plotted in Figure 11-4. Only the bulk kaolinite shows an increase in S_{ref} following treatment with the polymer product; however, the higher strength cannot be ascribed to the stabilizer treatment because of the higher saturation in the untreated test specimens.

11.5. EFFECT OF THE POLYMER STABILIZER ON SWELL POTENTIAL

The one-dimensional free swell potential of the untreated and polymer treated soils was measured as described in section 5.8. Three replicate tests were run on each untreated and treated

soil sample. The results are plotted in Figure 11-5, where the variability in test results, for samples prepared in an identical manner, is evident.

Note that the bulk kaolinite appears to exhibit substantially more expansion following treatment with the polymer product (more expansiveness was also observed when the kaolinite was treated with the other two stabilizer products evaluated). This behavior is not linked to readily apparent differences in the test specimens, because both the untreated and treated kaolinite specimens had similar moisture contents. It is possible that the nonexpansive, untreated kaolinite was chemically activated by the polymer stabilizer product and became more expansive. Alternatively, it is possible that some unknown error exists in the test data on the untreated bulk kaolinite.

No reduction in the 1-D free swell potential was observed following treatment of the TX Bryan HP and TX Mesquite HS HP soils. Only the bulk illite and bulk montmorillonite showed reductions in swell potential following treatment with the polymer stabilizer product. Inspection of the specimen properties in Table K-2 shows that the treated illite test samples were about 2% wetter than the untreated samples, which could explain the observed reduction in the swell potential of the illite. Hence, no consistent reduction in the expansiveness of the different test soils can be attributed to treatment with the polymer stabilizer product.

Table 11-1. Atterberg limits of the untreated test soils and of those treated with the polymer stabilizer product

<i>Soil Sample</i>		<i>Plastic Limit</i>	<i>Liquid Limit</i>	<i>Plasticity Index</i>
TX Bryan HP	untreated	20	68	48
	polymer treated	14	62	48
TX Mesquite HS HP	untreated	23	60	37
	polymer treated	20	50	30
Kaolinite	untreated	32	51	19
	polymer treated	27	47	20
Illite	untreated	24	44	20
	polymer treated	18	44	26
Montmorillonite	untreated	32	567	535
	polymer treated	35	547	512

Table 11-2. Shear strength parameters for envelopes that were fit to UU triaxial data in Figure 11-3

<i>Soil Sample</i>		<i>c</i> (psi)	<i>φ</i> (deg)
TX Bryan HP	untreated	113	1
	polymer treated	96	3
TX Mesquite HS HP	untreated	71	18
	polymer treated	94	9
Kaolinite	untreated	38	0
	polymer treated	31	31
Illite	untreated	21	51
	polymer treated	50	14
Montmorillonite	untreated	32	51
	polymer treated	39	49

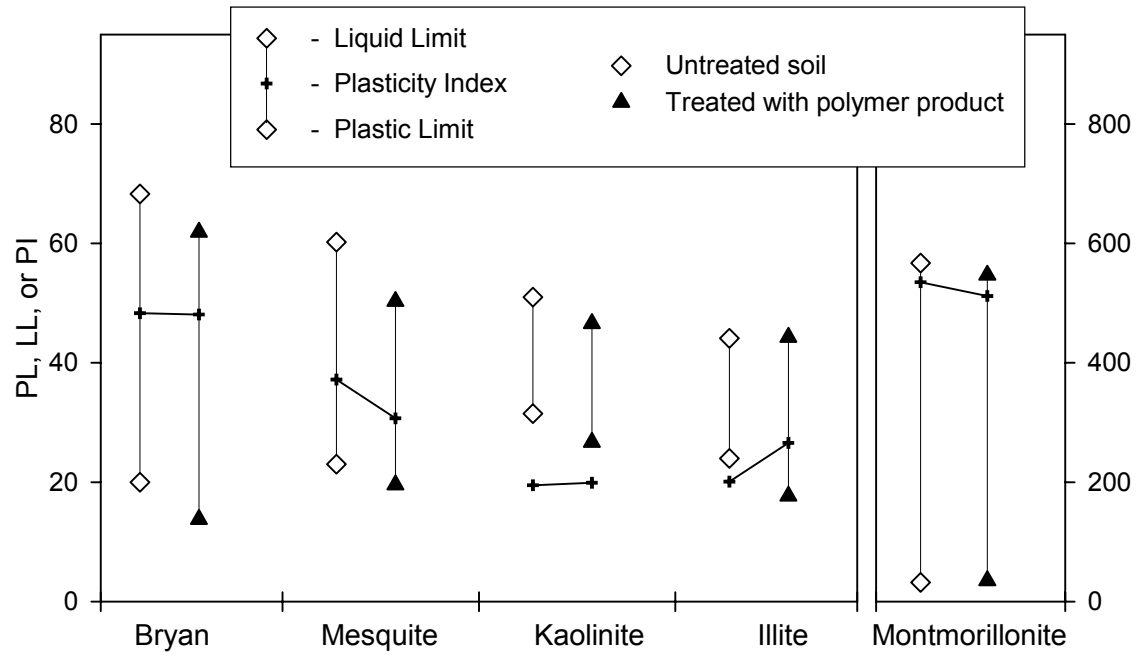


Figure 11-1. Atterberg limits of the untreated test soils and of those treated with the polymer stabilizer product

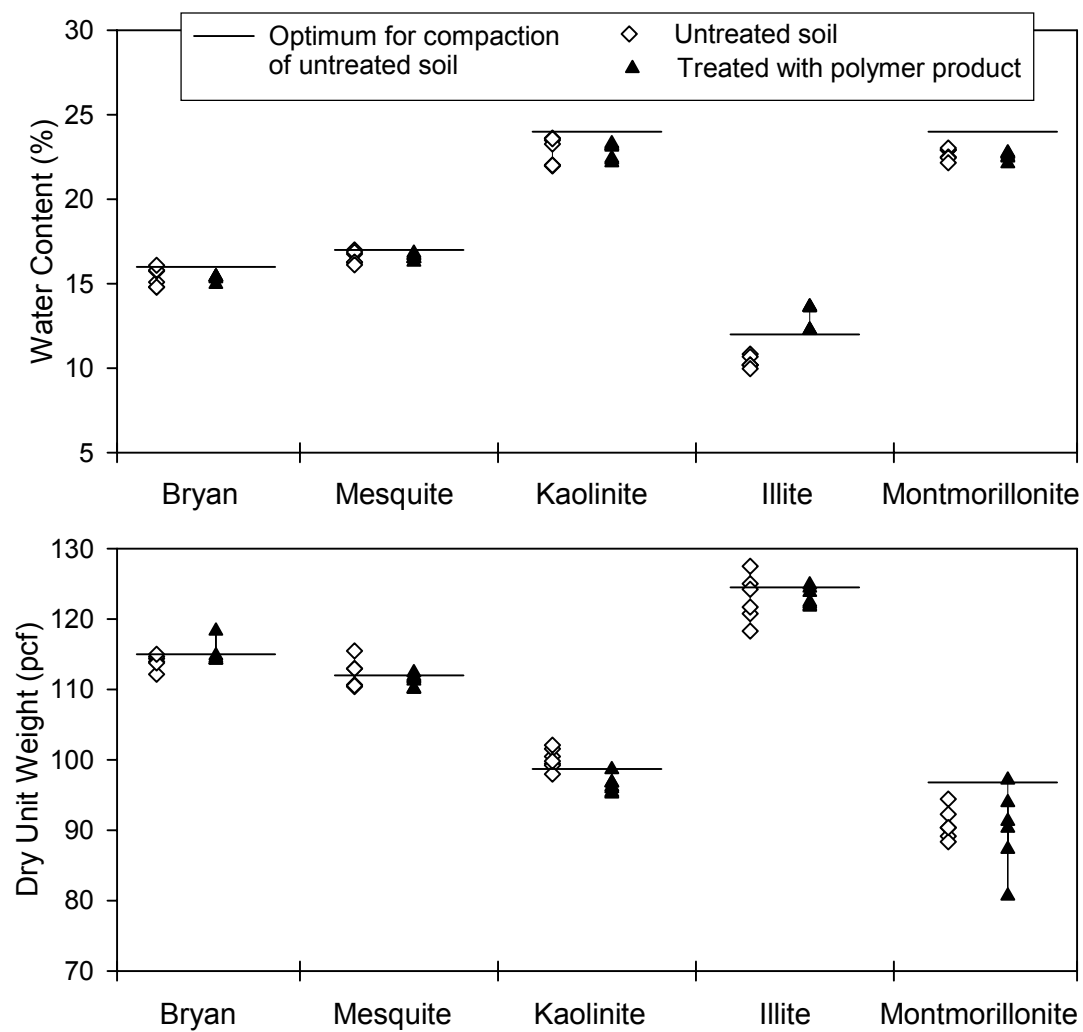


Figure 11-2. Water contents and dry unit weights of the triaxial and swell test soil specimens, both untreated and treated with the polymer stabilizer product

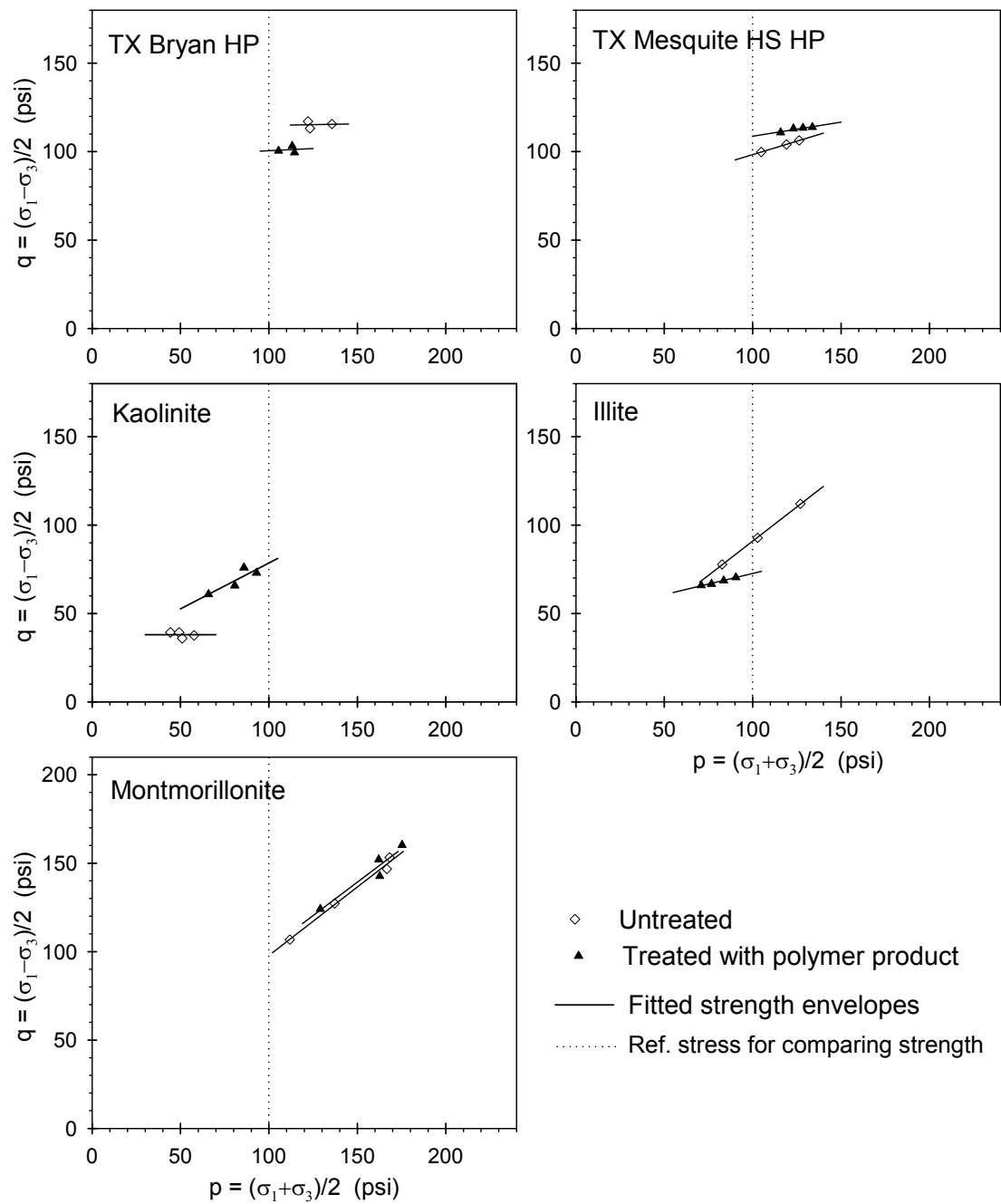


Figure 11-3. Fitted shear strength envelopes from UU triaxial tests on the untreated soils and on the soils treated with the polymer stabilizer product

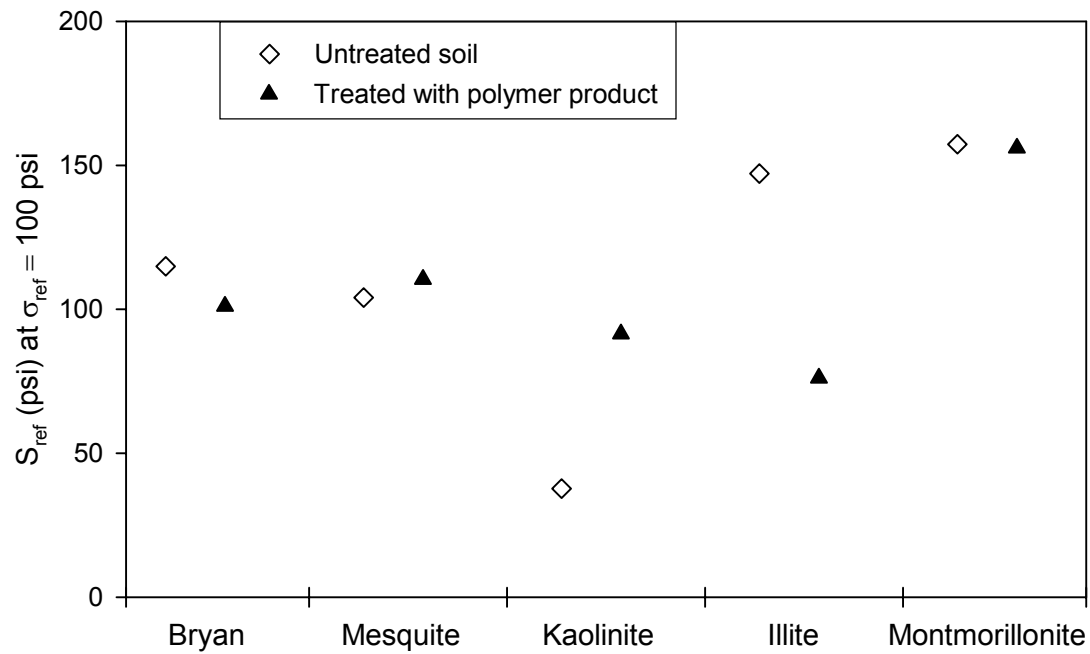


Figure 11-4. Reference shear strengths of the untreated test soils and of those treated with the polymer stabilizer product

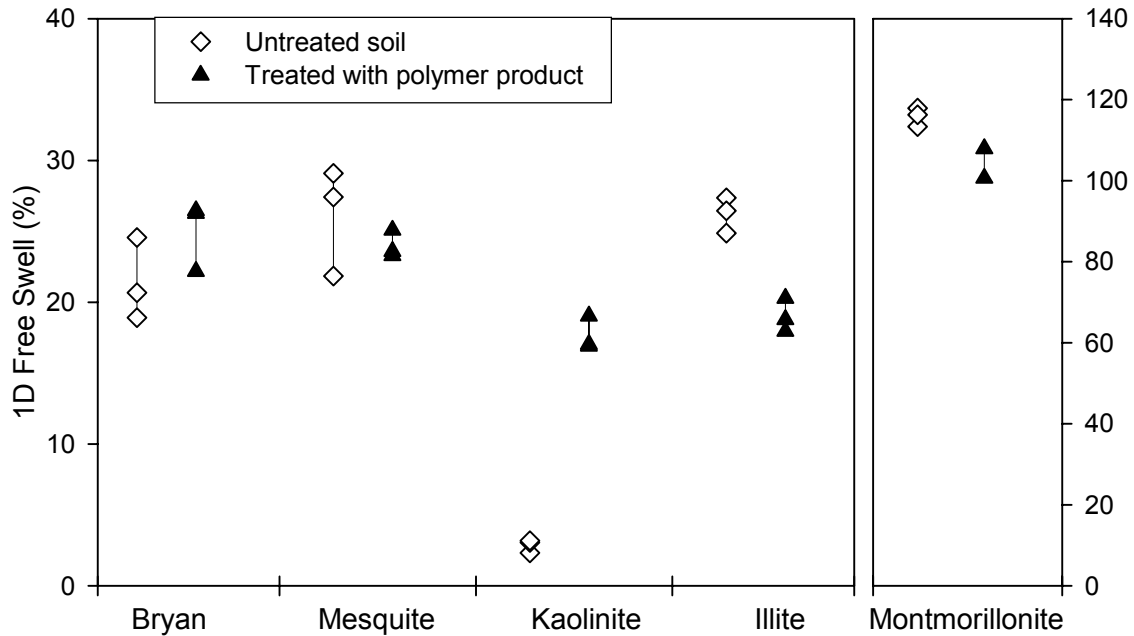


Figure 11-5. One-dimensional free swell of the untreated test soils and of those treated with the polymer stabilizer product

CHAPTER 12

FOLLOW-UP STUDY: EFFECTIVENESS OF STABILIZERS AT HIGH APPLICATION RATES

12.1. OVERVIEW

The macro-characterization studies of the ionic, enzyme, and polymer products (Chapters 7, 9, and 11, respectively) were carried out to determine what effects these products had on the engineering properties of clayey soils. Those test results failed to show a consistent, significant improvement in the properties of the five test soils following treatment with the selected products at the recommended application rates. It is possible that minor improvements in the soil properties were masked by variability among the test specimens and that higher application rates might yield more beneficial results. Hence, an additional study of the stabilizer products was undertaken. Data from this follow-up study, which was outside the scope of planned work for the project, are presented and discussed in this chapter. Some of the supporting test data from the follow-up study are presented in Appendix O.

The same three liquid chemical products (the ionic, enzyme, and polymer products) were evaluated in this follow-up study. Several of the previously used test soils were in short supply, so the additional testing was done on three different clay soils. All three of these test soils were excavated from natural deposits in the Austin, Texas area. To better clarify the potential efficacy of the selected stabilizers, the following changes were made to the previously used macro-characterization methods:

- The stabilizers were mixed with the soil at an application rate ten times that recommended by the product suppliers.
- For comparison, the same soils were treated with 6% hydrated lime and were evaluated.
- The optimum water content for compaction was determined for each soil following treatment with the various stabilizers.
- UU triaxial tests were conducted using a wider range in confining pressure, which allowed for a better definition of the undrained strength envelopes.
- The free swell test specimens were trimmed from individually compacted soil samples, instead of trimming multiple test specimens from a single soil mold.

12.2. TEST SOILS

Samples of three highly plastic soils from the Austin, Texas area were obtained for testing in the follow-up study. These soils are identified as Fire clay, DG (dark gray) Taylor clay, and TG (tan and gray) Taylor clay. The Fire clay was donated by the Elgin Butler Brick Company, which produces this soil from a pit located in Elgin, Texas, about 20 miles east of Austin. Bulk samples of the DG Taylor clay, which had a dark gray color, were hand excavated from the north side of State Highway 290 near Decker Road just east of Austin. The TG Taylor clay, which had tan and gray color variations, was excavated from approximately 10 feet below the ground surface on a soil embankment near the intersection of Martin Luther King Boulevard and State Highway 183 in east Austin.

Taylor clay is the predominant geologic soil formation found east of Austin, Texas. The formation stretches from north of Taylor, Texas, where it gets its name, to as far south as San Marcos, Texas. Taylor clay is well known by pavement and geotechnical engineers in central Texas. Numerous insurance claims from residential homeowners and commercial developers result from the high swelling pressures of Taylor clay and the associated volumetric changes that occur with seasonal moisture changes. Pavement distress, in the form of longitudinal and transverse cracks, is prevalent in all types of pavements constructed on Taylor clay east of I-35 in central Texas.

The test soils and their index properties are listed in Table 12-1. The grain size distribution of each soil was determined using the hydrometer test method (ASTM D 422-63, 1998a). The soils were sieved through a No. 40 sieve, and 40 g of the soil was used for testing. De-ionized water was used with a dispersant, the tests were performed at room temperature (varying from 22.5 to 23.2 °C), and ASTM 151H hydrometers were employed for the suspended soil readings. The results are plotted in Figure 12-1. Hydrometer analyses were conducted only for the untreated soils to better classify the test soils.

12.3. PRODUCT APPLICATION RATES

To determine if higher application rates would yield more significant changes in the soil properties, the stabilizers were evaluated at an application mass ratio (AMR) ten times the application rate recommended by the product suppliers. Increasing the AMR by a factor of ten was arbitrarily chosen to represent a high field application rate. Even higher application rates are feasible, but if the supplier's recommendations are appropriate, then treating the soils at ten times the recommended application rates should cause measurable changes in the soil properties.

To avoid over wetting the soil when the diluted stabilizers were added to the soils at the high application rates, each product was mixed at a higher concentration. Hence, both the dilution mass ratio (DMR) and the application mass ratio (AMR) were increased by a factor of ten. The DMRs and AMRs used in the follow-up study are summarized in Table 12.2.

12.4. TREATMENT WITH HYDRATED LIME

In the follow-up study, tests were also conducted on the soils treated with 6% hydrated lime. This permitted a comparison of the properties of the untreated soil, the soil treated with each of the three liquid chemical products, and the soil treated with a traditional stabilizer (lime). Hydrated lime is widely used for treating subgrade soils throughout the state of Texas and is readily available. In the Austin area, 5% to 8% lime is commonly used to stabilize roadway subgrades.

To determine the appropriate amount of hydrated lime needed to stabilize the test soils, pH-lime series tests (ASTM C 977, 1995) were conducted on each of the three test soils. This standardized test method characterizes a soil's reactivity to lime by measuring the change in pH with the addition of lime. The procedure consists of mixing small amounts of air-dried soil with dry lime at varying percentages, measuring the pH of the mixture using a calibrated glass electrode pH meter, and plotting measured pH as a function of the percentage lime. The optimum amount of lime is determined graphically at the point where the pH stops increasing with the addition of more lime.

Data from the pH-lime series tests are plotted in Figure 12.2. These test results suggest that the optimum lime content for stabilizing these soils varies between 5% and 7%. To maintain a consistent application rate, the soils were all stabilized using 6% lime, which is close to the optimum for all three soils.

12.5. PREPARATION OF TEST SPECIMENS

The test specimens for the follow-up study were prepared in the laboratory from air-dried samples of the three test soils. In preparing both untreated and treated test specimens, the ten-step protocol outlined in Chapter 5, which was used in the rest of the study, was followed with these exceptions:

- The DMR and AMR were ten times higher than the suppliers' recommendations (Table 12.2).
- A standard Proctor compaction energy (ASTM D 698, 2000) was used.
- Samples were compacted at the optimum water content (OWC) as determined for the soil when untreated or treated with each product at the elevated AMR. This change in procedure is included in the revised sample preparation protocol outlined in Appendix Q.

Preparation of Individually Compacted Samples

In the tests conducted at the suppliers' recommended application rates (Chapters 7, 9, and 11), the test specimens were trimmed from one compacted mold of the untreated or treated soil. Consequently, all of the triaxial or free swell test results for a given soil-stabilizer combination represented the soil's behavior at the same water content. That is, all of the untreated samples of one clay had the same water content, whereas of the samples of that clay treated with a particular stabilizer had a different water content. This made it difficult to separate the possible effects of the stabilizer from the effects of small differences in the water contents of the test specimens. For example, triaxial test specimens were trimmed from a single mold of untreated kaolinite that was closer to being saturated than each of the treated kaolinite samples. Although all of the products appeared to cause an increase in the strength of kaolinite, this difference in strength can be attributed to the lower strength of the single compaction mold of wetter, untreated kaolinite.

To alleviate this difficulty in interpreting the test results, individual specimens were trimmed from separate compacted soil molds for most of the tests in the follow-up study. For example, for the free swell tests on the untreated Fire clay, three different compaction molds were prepared and trimmed for testing. The three untreated specimens thus had slightly different water contents, and the measured swell potentials reflected the differences resulting from the typical small variations in compacted laboratory samples. In this manner, the systematic effects of small differences in water content are reduced, and the effects of typical sample variation are reflected in the test results.

A substantial quantity of test soil was needed to prepare these separately compacted soil specimens. For the free swell tests, each specimen was trimmed from an individually compacted soil mold. For the three soils and five treatment combinations (untreated, ionic product, enzyme product, polymer product, and lime), 45 compacted soil molds were prepared to create three swell test specimens of each soil-stabilizer combination. To reduce the amount of soil needed for the overall test program, it was decided that an adequate characterization of the scatter in shear

strength due to sample variations could be obtained from compacting individual test specimens of just the untreated soils. Three different compacted molds were prepared of each of the three untreated test soils (nine untreated molds total), with four triaxial test specimens trimmed out of each compacted mold. For the treated soils, only one compacted mold was prepared (twelve treated samples total for the three soils with four treatments).

Preparation of Triaxial Test Specimens

For the triaxial compression tests (section 12.8), four test specimens were trimmed from a single 4-inch diameter, compacted soil mold. The compacted cylinder of soil was cut lengthwise into quarters using an electric band saw, then each quarter was trimmed into a 1.5 inch-diameter by 3.75 inch-long specimen for testing. This procedure worked satisfactorily for all samples, except for the lime-treated soils and the TG Taylor clay treated with the polymer product. These molds could not be cut cleanly with the band saw, as the soils were hard, brittle, and fractured easily. These samples were thus discarded and an alternative means of forming the triaxial test specimens was developed.

Suitable specimens of the lime-treated soils and the polymer-treated TG Taylor clay were obtained using a split mold and a miniature compactor. The split mold had three pieces that, when held together with a locking ring, formed a 1.5-inch by 3.0-inch cavity in which the soil was compacted. When complete, the split mold was disassembled to obtain a test specimen of the appropriate size without further trimming. The soil was compacted in the split mold using a 0.5-inch diameter tamper rod connected to a small pneumatic piston. Air pressure in the piston, precisely controlled with an air regulator, limited the maximum force that could be applied with the tamping rod. To use the tamper, the rod was pressed into the soil until the soil resistance generated an upward force sufficient to overcome the regulated pressure in the piston. In this manner, the tamper produced a repeatable tamping force.

As suggested in the literature (ASTM 1970; Head 1992), the split mold samples were compacted using five lifts with ten tamps per lift. The tamper air pressure was selected to produce test specimens with similar dry densities as those obtained using the standard Proctor compaction method. A trial test series, using untreated Fire clay as the control soil, was used to determine the appropriate setting for the tamper air pressure. The control soil was wetted to the optimum water content, and samples were prepared at tamper air pressures of 5, 20, 30, and 40 psi. The resulting dry unit weights of the untreated Fire clay are plotted in Figure 12.3. The $\gamma_{d,max}$ obtained in the standard Proctor compaction test (Table 12-1) for this soil is 101.5 pcf. The same dry unit weight was obtained in the split mold device when the pneumatic tamper was set at 30 psi. Hence, all subsequent samples prepared in the split mold apparatus were formed with the air pressure set at 30 psi.

Because the split mold samples had similar densities and water contents, it is assumed that the shear strength of these samples could be compared to the strengths of specimens prepared using standard Proctor compaction. However, a somewhat different soil structure will result from static compaction with the pneumatic tamper, as compared with impact compaction, and this could have affected the measured strengths.

12.6. STABILIZER EFFECTS ON ATTERBERG LIMITS

Atterberg limits were determined in accordance with ASTM D 4318 (1998e). Liquid limits were determined using the multipoint (Method A) procedure with the wet preparation option. To reduce variability, each test was conducted using the same grooving tool and liquid limit device, with the device resting on the same laboratory bench. Soil for the plastic limit tests was gathered from the soil prepared for the liquid limit tests. The soil was placed between plaster plates, which absorb water more uniformly than air drying, to expedite drying of the samples to near the plastic limit. Rubber gloves were worn when rolling out the treated soil, so rubber gloves were also worn when rolling out the untreated samples. The treated samples used to measure the Atterberg limits were prepared and cured in a compacted state for 7 days in the same manner as the other treated test specimens.

The measured Atterberg limits are summarized in Table 12-3 and are plotted in Figure 12-4. Following treatment with the liquid stabilizers, the measured changes in the liquid limits, plastic limits, and plasticity indices of the three test soils were minimal. Note that the expected variability in the test results from a single operator are on the order of about 2.5 for the liquid limit and plastic limit (ASTM 1998e), and that some additional variability can be expected due to variations in the bulk samples of these naturally occurring soils. With a few exceptions, the differences in the measured Atterberg limits fall within the expected test variability. Furthermore, no consistent trend is observed in the changes in the index values following treatment with the three liquid products. As can be seen in Figure 12-4, treatment of the soils with hydrated lime led to substantial changes in the liquid and plastic limits of all three soils. Except for the TG Taylor clay, the plasticity indices were not as dramatically affected by the addition of lime. The trends in Figure 12-4 clearly demonstrate that lime had a more substantial effect on these natural clay soils than the three liquid stabilizers, even though the liquids were used at application rates ten times the suppliers' recommendations.

Additional evidence of the effects of the various treatments was noticed while conducting the Atterberg limit tests. The texture, consistency, and workability of the soils treated with the liquid products were similar to those of the untreated soils. Significant visual changes were noted while processing the lime treated soils, which dried very quickly. A small portion of the lime treated soil was allowed to dry for three hours, at which time the soil could be broken into small, hard pieces resembling sand and small gravel.

12.7. STABILIZER EFFECTS ON COMPACTION CHARACTERISTICS

Moisture-unit weight relationships for the compacted untreated and treated soils were determined using a standard Proctor compaction effort (ASTM D 698, 2000). At least five samples were prepared, with at least one sample both wet and dry of the optimum water content. An automatic, belt-driven rammer was used in lieu of a manual compaction hammer. The results of these tests are plotted in Figures O.1 through O.3 in Appendix O. Examination of these plots clearly shows that treating these three soils with 6% hydrated lime had a more substantial impact on the compaction characteristics than the addition of the three liquid stabilizers at the elevated application rates.

The optimum water content (w_{opt}) and maximum dry unit weight (γ_{dmax}) of the various soil-stabilizer combinations are summarized in Table 12-4. The w_{opt} of the soils following treatment with the three liquid stabilizers did not change more than 3%; smaller changes were

observed in the Fire clay and the TG Taylor clay. In nearly all cases, the γ_{dmax} of the soils treated with the liquid stabilizers was within 1 pcf of that for the untreated soil. Excluding the polymer treated DG Taylor clay, all of the results were within the expected single-operator variability of 1.7 pcf (ASTM D 698, 2000). In contrast, the hydrated lime changed the w_{opt} by 2.5% to 4.0% and decreased the γ_{dmax} by 3.5 to 5.9 pcf.

The optimum water contents determined from the compaction tests (Table 12-4) were the target values used in preparing all subsequent test specimens. The dry unit weights and water contents of all specimens prepared for triaxial and swell testing are plotted in Figure 12-5. The short horizontal lines in this figure indicate the target optimum water content and maximum dry unit weight determined from the compaction tests on the given soil-stabilizer combination. The water contents of the triaxial test specimens were generally uniform, because three test specimens were trimmed from a single compacted sample. The swell test specimens were individually trimmed from different compacted samples, so the resulting water contents were not as uniform as in the triaxial specimens.

Overall, the three liquid stabilizers applied at rates ten times the recommended application rates did not have a significant impact on the compaction characteristics of the three test soils. In contrast, the addition of 6% hydrated lime noticeably changed the optimum water content and maximum dry unit weight of the compacted soils.

12.8. STABILIZER EFFECTS ON SHEAR STRENGTH

The undrained shear strength of the test soils was evaluated by conducting unconsolidated-undrained (UU) triaxial compression tests (ASTM D 2850, 1998d). Tests were conducted at an axial strain rate of one percent per minute with confining pressures between 5 and 80 psi. Failure was defined as the peak axial stress; when no peak was achieved during testing, failure was assumed at 20% axial strain. The triaxial data are plotted in Figures O-4 through O-7 in Appendix O.

To characterize and fit strength envelopes, the peak failure stresses were plotted in p - q space, where $p = (\sigma_1 + \sigma_3)/2$ and $q = (\sigma_1 - \sigma_3)/2$, as was described in Chapter 5. The p - q plots for the untreated and treated soils in the follow-up study are plotted in Figure 12-6. From these plots, it is clear that the addition of hydrated lime caused a substantial increase in the undrained strength of the three test soils, with significant increases in ϕ (friction angle, or slope of the strength envelope). In contrast, the measured strengths of the soils treated with the three liquid stabilizers mostly fell within the scatter of the strengths of the untreated soils.

Linear strength envelopes were fit to the p - q data, and then equivalent strength parameters (c and ϕ) were determined as described in section 5.7. The resulting strength parameters are summarized in Table 12-5, along with the saturation of the test samples. For the Fire clay, the liquid stabilizers caused small reductions in c , whereas the ionic and polymer products caused small increases in ϕ . The measured ϕ of Fire clay treated with the enzyme product was essentially zero. Minor improvements in the shear strength, in terms of increases in c and ϕ , were generally observed for the DG Taylor clay and TG Taylor clay following treatment with the three liquid stabilizers. These changes are all minor when compared with the effect of treating the soils with hydrated lime. In all cases, treating the soils with lime caused small increases in c . More significantly, lime increased the friction angles of the Fire clay, DG Taylor clay, and TG Taylor clay by 12.0°, 25.5°, and 13.8°, respectively. These increases in ϕ are

substantial and indicate a significant improvement in the undrained shear strength of three test soils following treatment with lime.

Given differences in both c and ϕ for the fitted strength envelopes, it is convenient to compare the soil strengths using the reference shear strength (S_{ref}), which is the shear strength at a total normal stress of 100 psi (section 5.7). As is plotted in Figure 12-7, the values of S_{ref} show slight, insignificant changes following treatment with the liquid stabilizers. In comparison, the dramatic changes in strength following lime treatment are readily apparent.

12.9. STABILIZER EFFECTS ON SWELL POTENTIAL

One-dimensional free swell tests were performed in accordance with Method A of ASTM D 4546 (1998f). Three remolded samples were prepared near the optimum water contents for each soil-stabilizer combination, with a single test specimen trimmed from each compacted sample. Using a trimming guide, thin slices of soil were removed with care. Samples with gaps between the inside wall of the ring and the outer edge of the test specimen were discarded, because soil expansion into such gaps would invalidate the test results. After the ring was slid completely through the sample, the top and bottom of the specimen were trimmed off with a sharp straight edge. A vertical seating pressure of 20 lb/ft² was then applied, the sample was inundated with water, and the soil was allowed to swell fully, which took four to seven days. The test results are plotted in Figures O-8 through O-10 in Appendix O.

The swell potential of a specimen is the total measured primary swell (ASTM D 4546, 1998f) divided by the initial sample height of 0.75 in. Comparing the individual test results is difficult because the samples were remolded at different moisture contents to achieve the optimum water content for a given treatment. Because a given soil matrix will have some water absorption capacity, starting at a higher water content will mean less water is absorbed and less expansion will be measured. Hence, for otherwise identical soil samples, the swell potential should decrease with higher initial water contents. The free swell potentials of the soils tested in the follow-up study were thus plotted against the initial specimen water contents as shown in Figure 12-8. As expected, there is an inverse relationship between initial water content and sample expansion in nearly all cases.

The swell potential of the untreated Fire clay specimens ranged from 9.5% to 11.7% for initial water contents ranging from 19.8% to 18.4%, respectively. The optimum water contents for the liquid treated samples were 0.7% to 1.7% higher than those for the untreated soil, so the initial water contents of the treated test specimens were higher. Considering the data trends in Figure 12-8, the Fire clay appears to be slightly more expansive when treated with the liquid stabilizers at a given water content. The Fire clay samples treated with hydrated lime had water contents 2% to 4% greater than the untreated soil, so that the lower swell potential measured for the lime treated soil is partially the result of the elevated initial water contents. However, the three lime treated samples were compacted about 1% dry of the optimum water content, so more swell would be expected in these particular test specimens. On this basis, treatment with hydrated lime can be seen to have significantly reduced the expansiveness of Fire clay.

The swell potential of the untreated DG Taylor clay ranged from 5.6% to 6.5% for specimens with initial water contents ranging from 27.6% to 25.9%, respectively. The measured swell potentials of the soils treated with the liquid stabilizers generally fell within the scatter for the untreated soil, although the data are within a fairly narrow range. Moreover, the optimum water contents for the liquid treated samples are 2.2% to 2.5% higher than those for the untreated

soil, so the initial water contents of the treated test specimens are typically higher. Although less swelling might be expected, the trends of the data suggest that slightly more expansion occurred in the samples treated with the three liquid stabilizers at a given water content. In contrast, the soils treated with hydrated lime at much lower initial water contents produced swell potentials of approximately one percent. These results conclusively demonstrate that lime treatment substantially reduced the swell potential of the DG Taylor clay.

Unlike the other two test soils, a small reduction in the swell potential was observed (Figure 12-8) when the TG Taylor clay was treated with two of the liquid products. At a water content of about 22.5%, treating the TG Taylor clay with the ionic and enzyme products resulted in a swell potential that was 1% to 3% lower. The measured swell of the polymer treated soil was within the trend for the untreated soil. In contrast, treating the TG Taylor clay with hydrated lime reduced the swell potential to about one percent. Some of this reduction may be attributed to the higher initial water content of the lime treated specimens, given the higher optimum water content for compaction. However, at the completion of the swell tests, the lime treated samples of the TG Taylor clay were hard and brittle with a gritty texture, providing physical evidence that the soil was significantly altered by the lime treatment.

Table 12-1. Index properties of soils used in the follow-up study

Soil	USCS Classification ^a	Clay-Size Fraction ^b (%)	Atterberg Limits ^c			Compaction ^d	
			PL	LL	PI	OWC (%)	γ_{dmax} (pcf)
Fire Clay	Fat Clay (CH)	57	17	57	40	19.5	101.5
DG Taylor Clay	Fat Clay (CH)	63	20	76	56	26.0	90.0
TG Taylor Clay	Fat Clay (CH)	61	18	82	64	25.2	92.4

^a Unified Soil Classification System (ASTM D 2487, 1998c).

^b Percent finer by weight than 0.005 mm (ASTM D422-63, 1998a).

^c Plastic limit, liquid limit, and plasticity index (ASTM D 4318, 1998e).

^d Optimum water content (OWC) and maximum dry unit weight (γ_{dmax}) for compaction with a standard Proctor effort (ASTM D 698, 2000).

Table 12-2. Dilution and application rates used in the follow-up study

<i>Stabilizer Type</i>		<i>Ionic</i>	<i>Enzyme</i>	<i>Polymer</i>	<i>Lime</i>
Suppliers' Recommendations	Dilution Mass Ratio (DMR)	$\frac{1}{176}$	$\frac{1}{935}$	$\frac{1}{26}$	--
	Application Mass Ratio (AMR) ^a	$\frac{1}{6,000}$	$\frac{1}{50,000}$	$\frac{1}{1,000}$	--
	Application Rate (% per dry weight of soil) ^a	0.02 %	0.002 %	0.1 %	--
Rates Used in Follow-up Study (this chapter only)	Dilution Mass Ratio (DMR)	$\frac{1}{17.6}$	$\frac{1}{93.5}$	$\frac{1}{2.6}$	--
	Application Mass Ratio (AMR) ^a	$\frac{1}{600}$	$\frac{1}{5,000}$	$\frac{1}{100}$	$\frac{1}{16.7}$
	Application Rate (% per dry weight of soil) ^a	0.2 %	0.02 %	1.0 %	6.0 %

^a Computed assuming a typical soil dry unit weight of 100 pcf (16 kN/m³).

Table 12-3. Atterberg limits of the untreated and treated test soils from the follow-up study

<i>Soil Sample</i>		<i>Plastic Limit</i>	<i>Liquid Limit</i>	<i>Plasticity Index</i>
Fire Clay	untreated	17	57	40
	ionic treated	19	61	42
	enzyme treated	18	58	40
	polymer treated	17	58	41
	lime treated	35	81	46
DG Taylor Clay	untreated	20	76	56
	ionic treated	26	77	51
	enzyme treated	28	82	54
	polymer treated	24	80	56
	lime treated	52	100	48
TG Taylor Clay	untreated	18	82	64
	ionic treated	23	82	59
	enzyme treated	21	79	58
	polymer treated	20	80	60
	lime treated	57	98	41

Table 12-4. Results from standard Proctor compaction tests (ASTM D 698) on the untreated and treated test soils in the follow-up study

<i>Soil Sample</i>		<i>Optimum Water Content (%)</i>	<i>Maximum Dry Unit Weight (pcf)</i>
Fire Clay	untreated	19.5	101.5
	ionic treated	20.7	102.4
	enzyme treated	21.2	102.3
	polymer treated	20.2	102.5
	lime treated	23.4	96.8
DG Taylor Clay	untreated	26.0	90.0
	ionic treated	28.2	89.7
	enzyme treated	29.0	88.7
	polymer treated	28.5	87.5
	lime treated	23.5	86.5
TG Taylor Clay	untreated	25.2	92.4
	ionic treated	24.0	92.8
	enzyme treated	25.3	92.6
	polymer treated	23.6	92.1
	lime treated	28.3	86.5

Table 12-5. Shear strength parameters for envelopes fitted to UU triaxial data on the untreated and treated test soils in the follow-up study

<i>Soil Sample</i>		<i>c</i> (psi)	ϕ (deg)	<i>Saturation of</i> <i>Test Specimens</i> (%)
Fire Clay	untreated	21.3	1.7	76 – 92
	ionic treated	17.2	2.3	89 – 90
	enzyme treated	18.1	0.1	90 – 90
	polymer treated	20.1	2.9	83 – 86
	lime treated	24.3	13.7	86 – 89
DG Taylor Clay	untreated	16.2	3.0	83 – 86
	ionic treated	17.7	5.2	84 – 86
	enzyme treated	16.6	5.3	86 – 90
	polymer treated	18.9	2.6	88 – 90
	lime treated	19.5	28.5	80 – 85
TG Taylor Clay	untreated	20.9	7.6	70 – 81
	ionic treated	20.1	10.1	68 – 69
	enzyme treated	20.8	9.4	71 – 73
	polymer treated	24.3	9.2	82 – 83
	lime treated	23.8	21.4	79 – 83

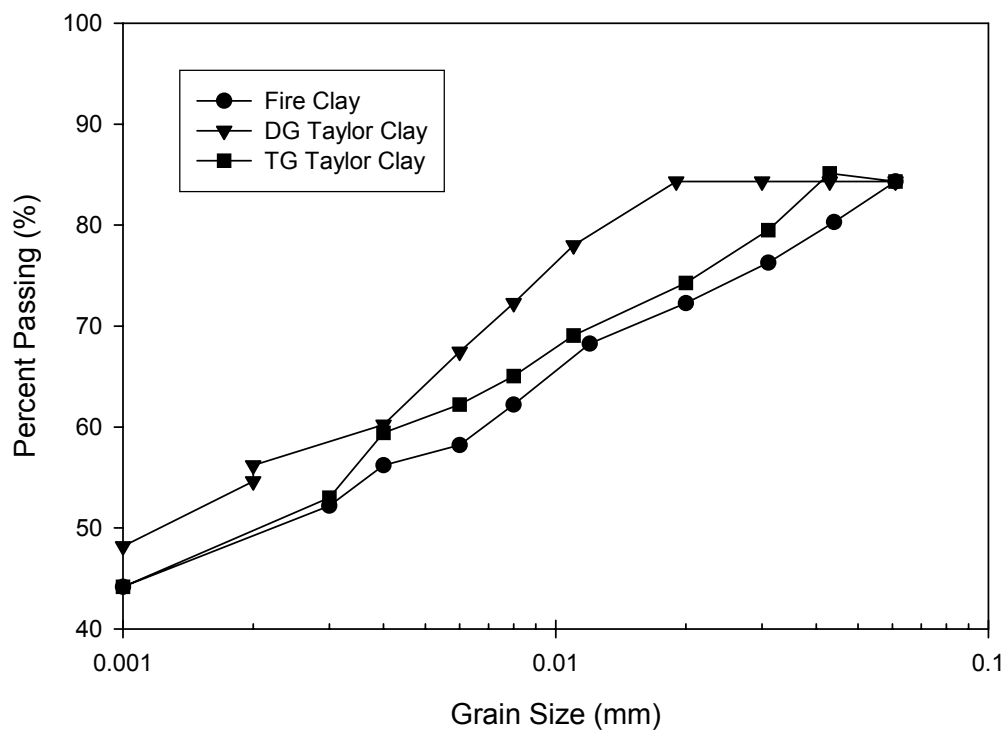


Figure 12-1. Grain size distribution of the untreated test soils, as determined by the hydrometer test method

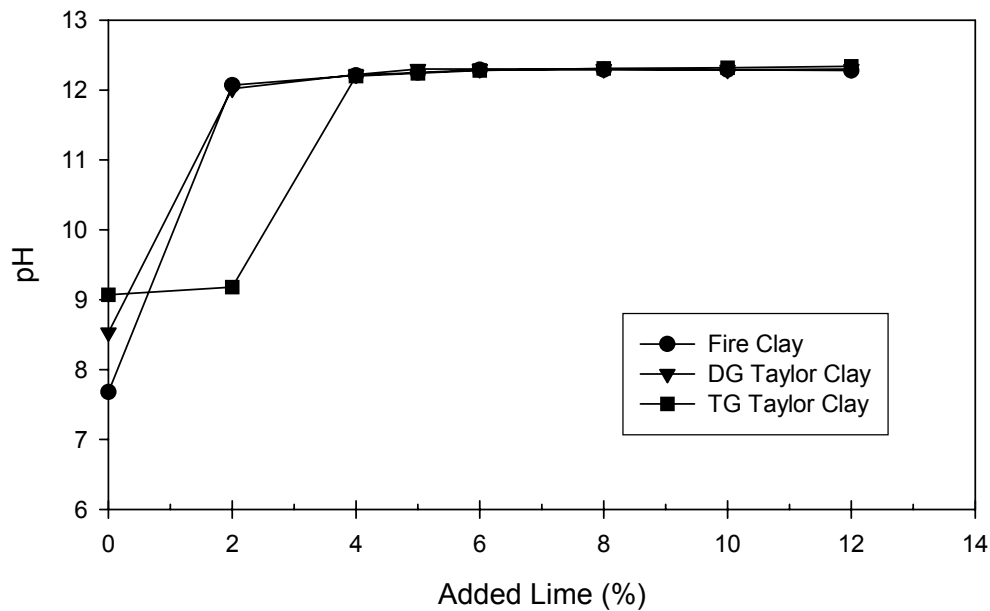


Figure 12-2. Results from pH-lime series tests (ASTM C 977, 1995) on the three test soils

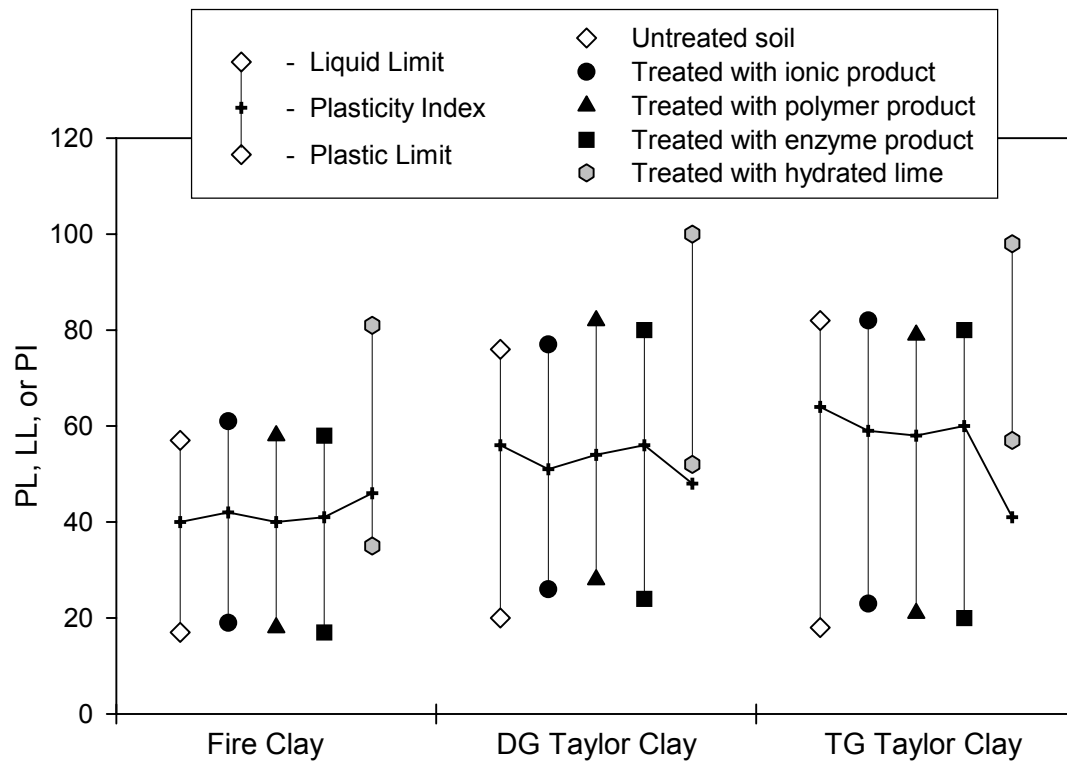


Figure 12-3. Results from trial tests with a pneumatic tamper on untreated Fire clay

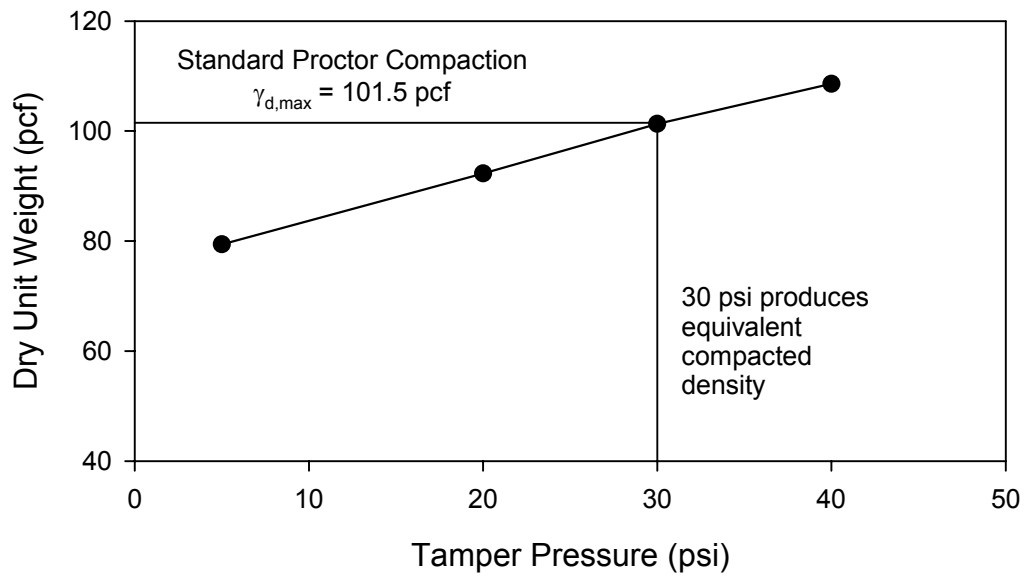


Figure 12-4. Atterberg limits for the untreated and treated test soils in the follow-up study

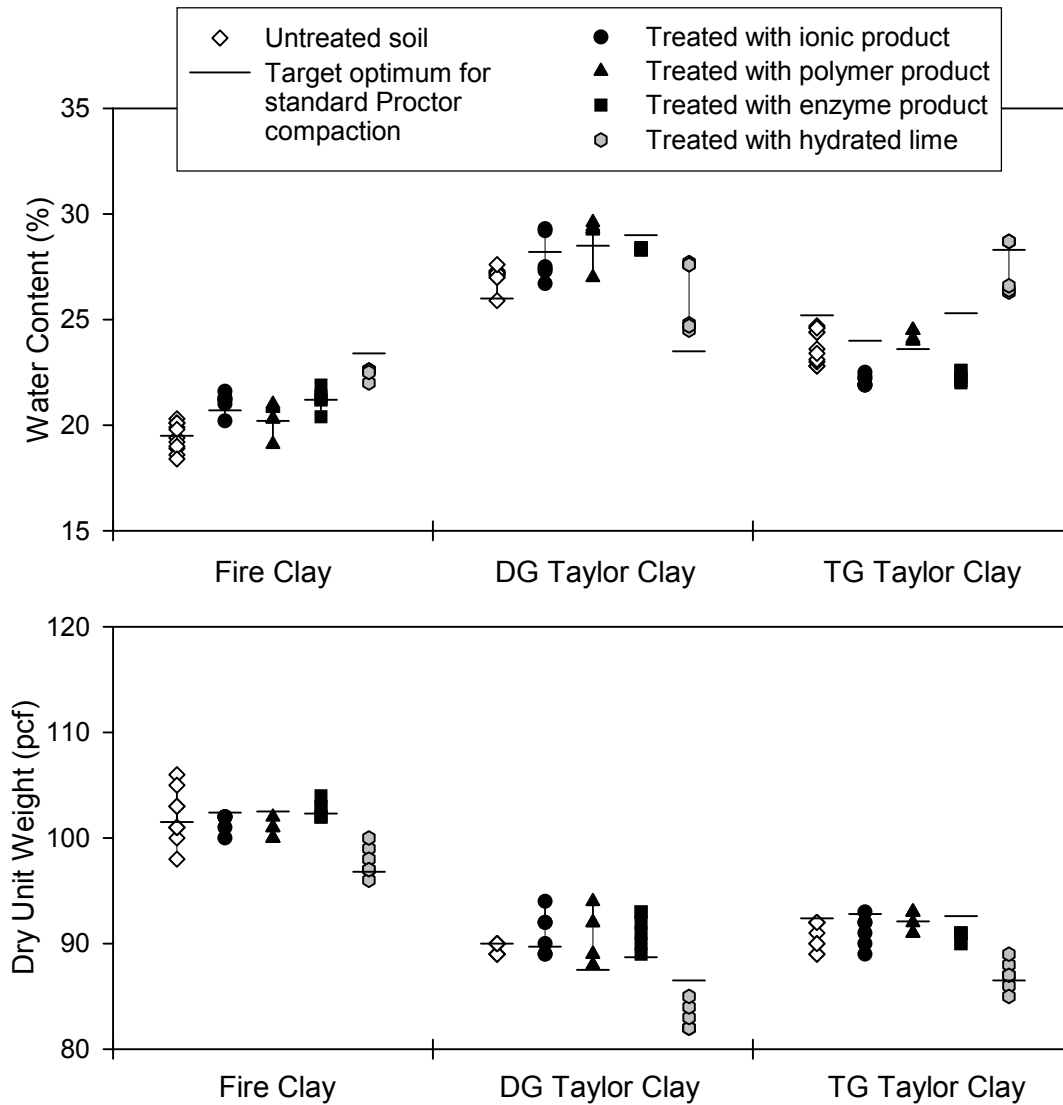


Figure 12-5. Moisture contents and dry unit weights of all compacted test specimens prepared for the follow-up study

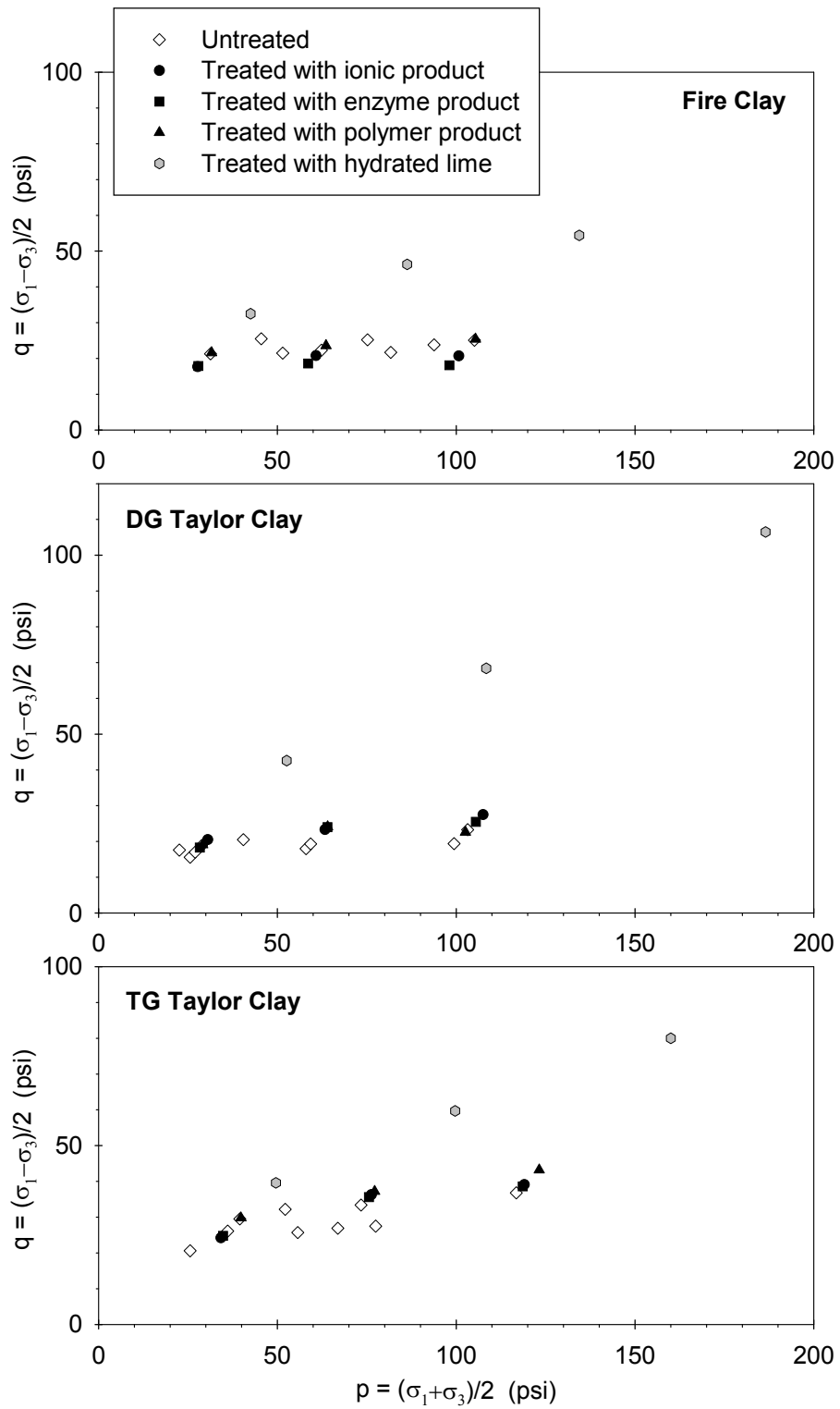


Figure 12-6. Shear strengths of untreated and treated specimens measured in UU triaxial tests in the follow-up study

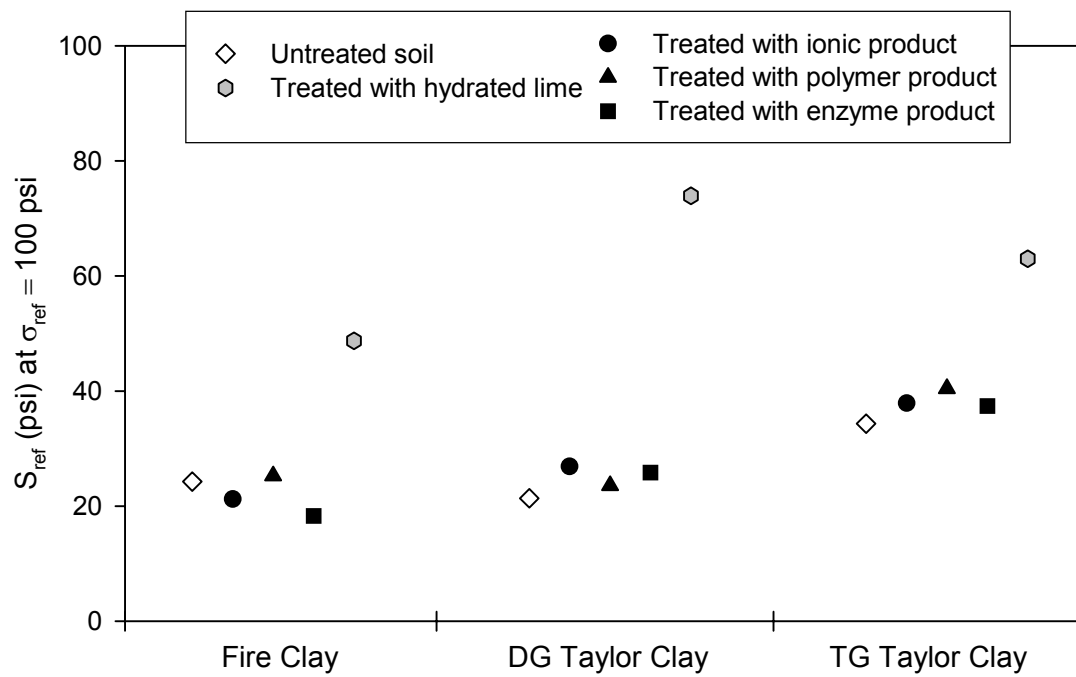


Figure 12-7. Comparison of reference shear strengths, as determined from fitted strength envelopes, for untreated and treated soils in the follow-up study

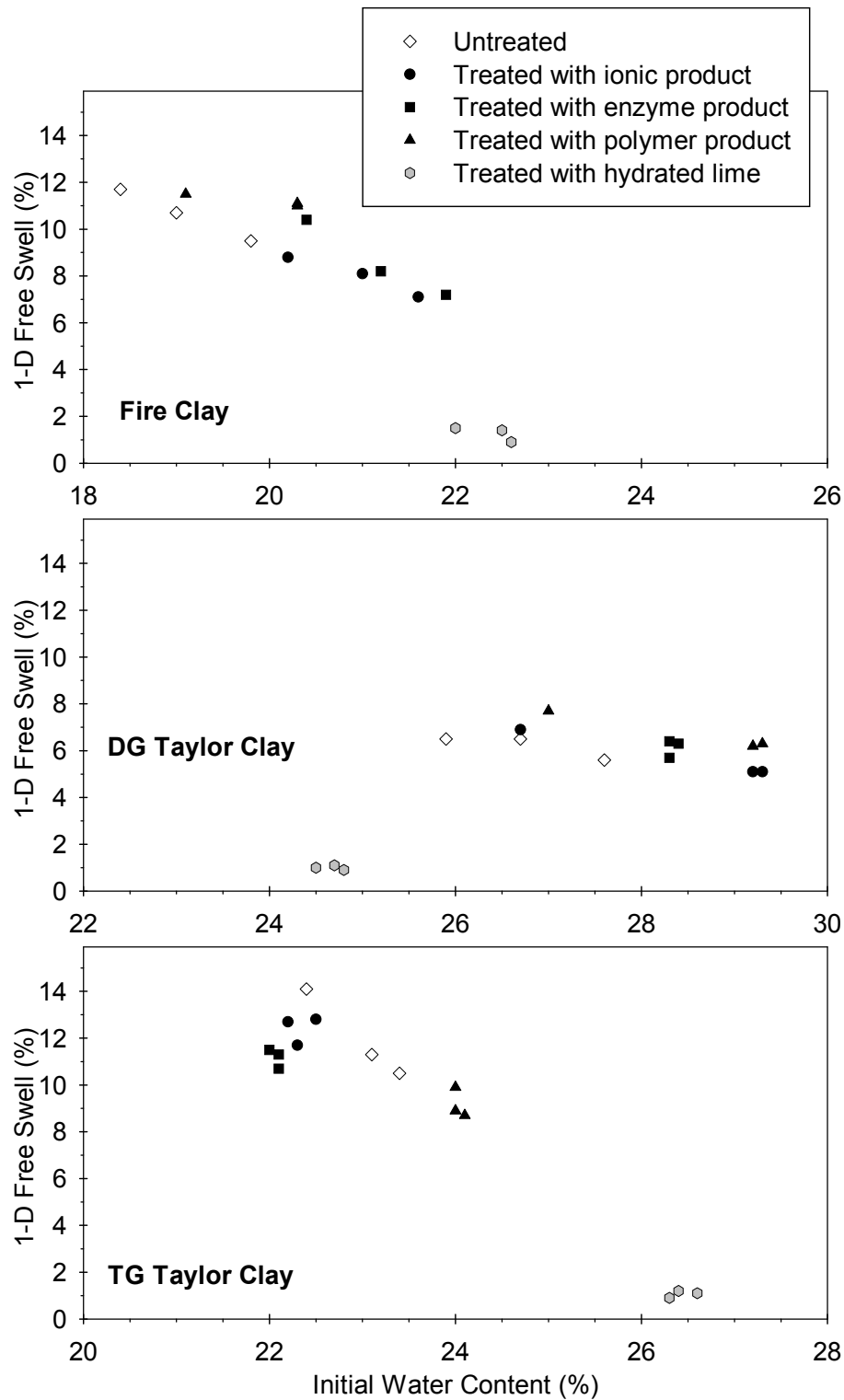


Figure 12-8. Results from 1-D free swell tests on the untreated and treated soils in the follow-up study

CHAPTER 13

SUMMARY AND CONCLUSIONS

13.1. OVERVIEW OF STUDY

Liquid chemical products are marketed by a number of companies for stabilizing pavement base and subgrade soils. If effective, these products could be used as alternatives for treating sulfate-rich soils, which are susceptible to excessive heaving when treated with traditional, calcium-based stabilizers such as lime, cement, and fly ash. However, the chemical composition, reaction mechanisms, and engineering performance of these liquid products are not well understood. The primary objective of this study was to investigate and identify the mechanisms by which clay soils are modified or altered by these liquid chemical agents.

Three representative commercial products were selected for study: an ionic product, an enzyme product, and a polymer product. No effort was made to compile a comprehensive list or classification of available products. Rather, these three products were selected to represent what appear to be the most common types of liquid chemical soil modifiers. The chemical composition of each selected product was characterized using standard chemical test methods.

The three products were then reacted with three reference clays (kaolinite, illite, and montmorillonite) to elucidate the effects of each stabilizer on nonexpansive to highly expansive clay minerals. The same three liquid chemical products were also used to treat five fat clays (CH) from Texas, one with a high sulfate content. Data from tests on multiple soils were used to see whether consistent, significant effects could be attributed to the chemical treatment.

In the “micro-characterization” study, the mechanisms of soil modification at the particle level were studied using physical-chemical analyses of untreated and treated soil samples. Very high product application rates were used so that possible soil modifications could be observed. Findings from this part of the study suggest that the evaluated products may modify the chemical properties of the soil either by agglomerating the clay particles, fully expanding the clay interlayer, or by altering the Al:Si ratios of the clay minerals.

In a paired “macro-characterization” study, standard geotechnical laboratory tests were performed on untreated and treated compacted soil specimens. A specific, multistep protocol was developed and carefully followed in the preparation of the test specimens. Tests were performed to measure the Atterberg limits, compaction characteristics, undrained shear strength, and free swell potential of the untreated and treated test soils. The products were mixed with the reference clays and two of the native Texas soils at the suppliers’ recommended application rates. These tests failed to show significant, consistent changes in the engineering properties of the test soils following treatment with the three selected products at the application rates used.

In a follow-up to the macro-characterization study, the same products were used at ten times the recommended application rates to treat three high-plasticity natural clays. For comparison, these soils were also treated with 6% hydrated lime. Even at the high application rates, the liquid chemical products failed to show consistent, significant improvements in the soil properties.

The findings of this study clearly point to the need to conduct standard laboratory tests, prior to using these products in field applications, to prove the effectiveness of the treatment on a particular soil type at a given chemical application rate. Although effective liquid chemical soil stabilizers may exist, it seems prudent to view supplier claims with skepticism until the

performance of such products can be clearly quantified through objective laboratory testing or controlled field trials.

13.2. MICRO-CHARACTERIZATION OF STABILIZER MECHANISMS

Each of the selected products was evaluated to determine whether chemical changes in clay or soil properties were consistent with the hypothesized mechanisms of stabilization. To this end, a variety of techniques were applied to initially characterize the stabilizer products and then to compare physical/chemical properties of the clays and soils prior to and following treatment. In most cases, extremely high application rates were used to enhance the likelihood of changes in the clay minerals and soil materials following treatment with the stabilizers.

The main ingredient of the ionic stabilizer was sulfonated limonene. The hypothesized mechanism for the ionic stabilizer was cation exchange with subsequent alteration in the clay mineral lattice. It was hypothesized that the sulfonated limonene could preferentially extract aluminum from a clay mineral. However, even at the high application ratios employed in this research, significant changes in clay mineralogy based on XRD or ESEM were not apparent, and decreases in the Al:Si ratio were not significant in many cases.

The results of the ionic stabilizer treatment for the soils were conflicting. For the Bryan soil, a decrease in the Al:Si ratio was evident, as expected by the above mechanism of hydrogen transfer to the interlayer and release of clay cations into solution. On the other hand, although the XRD results did indicate a change in the d-spacing of the clay, the reduced value of the d-spacing was still consistent with an expansive clay. Although the glycolated XRD diffractogram indicated that untreated Bryan soil contains an expansive clay, it was not possible to analyze glycolated soil samples. The Mesquite soil also contained a smectite-type clay, according to XRD results. However, no chemical changes were observed in either the EDS or XRD analyses. The EDS results indicated no changes in Al:Si ratios as a result of treatment, and they detected the presence of calcium and potassium in the soil. Based on a comparison of the diffractogram of the ionic treatment of Mesquite soil with well-characterized clay diffractograms, it appears that the Mesquite soil contains gypsum and illite. Gypsum is a very common sulfate mineral found in clay that has the ability to form highly expansive calcium-alumina-sulfate-hydrate minerals in the presence of calcium and water. For this reason, it could be detrimental to apply the ionic stabilizer to Mesquite soil, because the ionic stabilizer might enable expansion of clay materials rather than stabilization.

The principal ingredient identified for the enzyme stabilizer was polyethylene glycol. It is unlikely that the polyethylene glycol is the activating ingredient; however, polyethylene glycol is used as a protein/enzyme deactivator. It is likely that the active ingredient is microbiological in nature, which is why it wasn't identified through our testing. The enzyme stabilizer is reported to act in several ways, including the breakdown of clay minerals with expulsion of water from the double layer, the binding of clay particles by aggregation, internal or external adsorption to clay layers preventing water absorption, or interlayer expansion with subsequent moisture entrapment (Scholen 1992; 1995). The results of the testing at high application ratios were consistent with interlayer expansion, as was evidenced by the XRD results from treated and untreated samples of the clay minerals. In addition, the surface area results of the enzyme stabilizer treatment showed the largest decrease in surface area of all of the stabilizers tested when compared with the untreated results for all clay and soil types, except kaolinite. For the nonexpanding clay minerals, the hypothesized mechanism of providing an adsorbing surface complex on the edges of clay

particles was supported by surface area measurements, pore size distributions, ESEM images, and EDX Al:Si ratios. Even though it was not possible to fully compare treated and untreated XRD samples of the soils, other assessment techniques such as ESEM, EDX, and BET nitrogen analyses were consistent with the results from the clay mineral studies.

Sodium silicate was identified as the principal component of the polymer stabilizer. The hypothesized mechanism involved formation of a strongly adhesive, aggregated material. Furthermore, the polymer stabilizer was alleged to coat the surface of soil particles rather than chemically altering the clay inner layers. The results of polymer treatment for all clays and soils tested supported the proposed mechanism of surface coating and aggregation. This was confirmed consistently with all five clay mineral and soil samples by ESEM images and BET analysis. No changes in d-spacing or Al:Si ratio were reported for any of the clay or soil samples, which is as expected because of the interaction of the polymer stabilizer and clay by physical rather than chemical means. For kaolinite and illite, the Al:Si ratio of the polymer treated clay decreased when compared with the Al:Si ratio of the untreated clays. This result is as expected for a silicate-based polymer that coats the particle surfaces.

13.3. MACRO-CHARACTERIZATION OF STABILIZER EFFICACY

To evaluate the potential effectiveness of the selected liquid chemical products for stabilizing pavement subgrade materials, standard geotechnical laboratory tests were conducted with the test soils. A specific, multistep protocol was carefully followed in preparing the compacted test specimens, which were allowed to cure for seven days at constant water content prior to testing. The protocol was sent to a number of TxDOT and industry representatives to solicit comments. Subsequent to the laboratory testing work, a revised sample preparation protocol was prepared to clarify a number of minor issues and reflect the suggestions received. The revised protocol, given in Appendix Q, is recommended for future studies of this type.

In the first part of the macro-characterization study, the treated samples were mixed with the stabilizer chemicals at an application mass ratio (AMR) equivalent to the suppliers' recommendations for field applications. Atterberg limits, compacted unit weight, undrained shear strength, and free swell potential were measured and compared for the untreated and treated soils. Overall, no marked changes in these engineering properties were observed following chemical treatment in these tests. Although individual cases can be identified in which a certain product appeared to improve a property of a particular soil, no consistent trend was observed. It is possible that higher application rates, in excess of the supplier recommendations, might produce more significant, beneficial effects.

Some difficulty in comparing these results arose from variations in the compacted test samples. That is, small differences in the initial water contents of various specimens led to discernible variations in their measured strength and expansiveness; in many cases, this effect appeared to be more significant than the effects of the chemical treatments. The difficulty in separating these effects was made worse in this part of the study by trimming all of the triaxial or swell specimens of a particular soil, whether untreated or treated, from one mold of compacted soil. For example, all four of the untreated triaxial specimens of kaolinite were trimmed from one cylinder of compacted soil. It would have been better to trim multiple test specimens from different compacted molds of the same soil, which would make it easier to distinguish the effects of the treatment from the typical variation in the properties of laboratory compacted soil samples.

A follow-up macro-characterization study was undertaken to investigate some of these issues. Given a shortage of the original test soils, three different native Texas clays (all high plasticity, fat clays) were obtained for testing. In the follow-up study, the same three liquid chemical products were mixed with the soils at ten times the suppliers' recommended application rates. These high application rates were arbitrarily chosen to amplify any potential effects of the products on the engineering properties of the test soils. For comparison, additional tests were run on the same soils following treatment with 6% hydrated lime. In addition, many more individually compacted soil specimens were tested so that the results would more accurately reflect the typical variability in laboratory compacted test specimens. The lime caused marked improvements in the soil properties, with substantially increased shear strength and decreased expansiveness. However, even at the high application rates, the liquid chemical products failed to produce significant, consistent improvements in the properties of the three test soils.

Although evidence of the physical-chemical reactions of the three products was obtained in the micro-characterization study, those tests were conducted at extremely high application rates (50% by mass). Those rates would not be economical or practical in the field. Tests in the macro-characterization study at the suppliers' recommended application rates (0.002% to 0.1% by mass) and at ten times the recommended rates failed to show significant improvements in the engineering properties of the soils tested.

Laboratory testing of chemical soil stabilizers is sometimes criticized for not accurately simulating field conditions or predicting soil improvements that are reported in the field. However, lacking well-documented field case studies, laboratory testing is clearly justified. Moreover, substantial improvements in field performance should translate into noticeable changes in the soil properties measured in the laboratory. If laboratory tests indicate that a particular product does yield significant soil improvement, the next logical question to address is how much improvement in the soil's properties is needed to justify field application of the product. Laboratory testing may then be used as a basis for determining optimal field application rates.

CHAPTER 14

RECOMMENDATIONS

This study investigated the reaction mechanisms and effectiveness of three representative liquid chemical products that are marketed for treating pavement base and subgrade soils. The products were reacted with three reference clays and five native Texas clays at the suppliers' recommended application rates and at much higher application rates. Although some evidence of the reactions between the chemicals and the soils was obtained, consistent, significant improvements in the engineering properties of the soils were not observed. The findings of this study clearly point to the need to conduct standard laboratory tests, prior to using these products in field applications, to prove the effectiveness of the treatment on a particular soil type at a given chemical application rate. Although effective liquid chemical soil stabilizers may exist, it seems prudent to view supplier claims with skepticism until the performance of such products can be clearly quantified through objective laboratory testing or controlled field trials.

Specific recommendations for conducting future evaluations of nontraditional soil stabilizers include the following:

- (1) Potential suppliers of chemical soil stabilizers should provide independent, objective data on the performance of their products. Testimonials from other users should be considered inadequate and unreliable for demonstrating effectiveness.
- (2) Application rates should be expressed in a consistent manner, such as the application mass ratio (AMR, defined as the mass of concentrated chemical product per mass of oven-dry soil). The application rate, and not the degree of dilution in water, is the key parameter for expressing how much product should be applied to the soil.
- (3) The application rate needed for obtaining the desired performance is likely to depend on the specific characteristics of the soil to be treated, including the clay content and nature of the clay mineral. Hence, before using these chemical products, an appropriate product application rate should be determined for the project-specific soils.
- (4) This study did not attempt to determine how much improvement in the engineering properties of a soil is needed to justify the application of a soil stabilizer. More research may be needed to provide guidance on what minimum engineering properties are desired for pavement applications.
- (5) Laboratory investigations of the effectiveness of chemical soil treatments should include multiple tests on identically prepared specimens, with tests on both the untreated soil and soil treated over an appropriate range of application ratios. Standard, accepted test methods should be followed to measure the engineering properties of interest.
- (6) Initial estimates of the appropriate application ratios can be determined through micro-characterization studies of treated and untreated samples. X-ray diffraction (oriented and gylcolated samples) and BET surface area analysis were found to be the most useful for assessing changes in soil characteristics.

- (7) The results from laboratory tests on chemically treated soils will depend on how the test specimens are prepared. Variations in water content and compaction can lead to measurable differences in the soil properties that obscure the possible effects of a chemical additive. A rational protocol for specimen preparation, which includes control of specimen water content and a seven-day cure at constant moisture, was developed in this study with input from TxDOT and industry representatives. This recommended specimen preparation protocol is detailed in Appendix Q.
- (8) In this study, the test specimens were prepared using ASTM standard impact compaction methods (standard and modified Proctor compaction efforts). Other standard impact compaction methods for soils would also be appropriate. To reduce the variations in the test data, it may be possible to produce more uniform, repeatable test specimens using static compaction methods.
- (9) The shear strength of treated soils should be evaluated using standard test methods. In this study, soils strengths were evaluated using unconsolidated-undrained triaxial compression tests following ASTM standard methods. Other standardized test methods for measuring soil strength may also be appropriate. However, unconfined compression tests are not recommended.
- (10) The expansiveness or potential swell of treated soils should be evaluated using standard test methods. In this study, one-dimensional free swell potential under a nominal seating pressure was measured using ASTM standard methods. Other standardized test methods measuring expansiveness, including three-dimensional swell tests on unconfined specimens, may also be appropriate.
- (11) Pavement performance is closely related to the stiffness of the underlying base and subgrade materials. Tests to measure the stiffness of untreated and treated soils, such as resilient modulus tests, should be considered.
- (12) If a stabilizer product under consideration shows favorable results in a laboratory study, field tests may be warranted. Field tests of soil stabilizers in pavement base or subgrade layers must include untreated control sections and quantitative measurements of performance.
- (13) For products that are found to produce significant improvements in soil properties, additional studies will be needed to assess the permanence and long-term effectiveness of the product.

REFERENCES

- ACI Committee 230 (1990). "State-of-the-Art Report on Soil Cement." *ACI Materials Journal*, Vol. 87, No. 4, American Concrete Institute, pp. 395-417.
- American Society for Testing and Materials, Committee D-18 (1970). "Special Procedures for Testing Soil and Rock for Engineering Properties." Special Technical Publication 479, 5th ed., ASTM, Philadelphia, Pennsylvania.
- American Society for Testing and Materials (1995). "Standard Specification for Quicklime and Hydrated Lime for Soil Stabilization." ASTM C 977-95, *1995 Annual Book of ASTM Standards*, Easton, Maryland.
- American Society for Testing and Materials (1998a). "Standard Test Method for Particle-Size Analysis of Soils." ASTM D 422-63 (Reapproved 1990), *1998 Annual Book of ASTM Standards*, West Conshohocken, Pennsylvania.
- American Society for Testing and Materials (1998b). "Standard Test Method for Laboratory Compaction Characteristics of Soil Using Modified Effort (56,000 ft-lb/ft³, 2,700 kN-m/m³)." ASTM D 1557-91, *1998 Annual Book of ASTM Standards*, West Conshohocken, Pennsylvania.
- American Society for Testing and Materials (1998c). "Standard Test Method for Classification of Soils for Engineering Purposes (Unified Soil Classification System)." ASTM D 2487-93, *1998 Annual Book of ASTM Standards*, West Conshohocken, Pennsylvania.
- American Society for Testing and Materials (1998d). "Standard Test Method for Unconsolidated-Undrained Triaxial Compression Test on Cohesive Soils." ASTM D 2850-95, *1998 Annual Book of ASTM Standards*, West Conshohocken, Pennsylvania.
- American Society for Testing and Materials (1998e). "Standard Test Method for Liquid Limit, Plastic Limit, and Plasticity Index of Soils." ASTM D 4318-95a, *1998 Annual Book of ASTM Standards*, West Conshohocken, Pennsylvania.
- American Society for Testing and Materials (1998f). "Standard Test Methods for One-Dimensional Swell or Settlement Potential of Cohesive Soils." ASTM D 4546-96, *1998 Annual Book of ASTM Standards*, West Conshohocken, Pennsylvania.
- American Society for Testing and Materials (2000). "Standard Test Methods for Laboratory Compaction Characteristics of Soils Using Standard Effort (12,400 ft-lbf/ft³ (600 kN-m/m³)." ASTM D 698-00a, *2000 Annual Book of ASTM Standards*, West Conshohocken, Pennsylvania.
- Dermatas, D. (1995). "Ettringite-Induced Swelling in Soils: State-of-the-Art." *Applied Mechanics Review*, Vol. 48, No. 10, pp. 659-673.

- ElectroScan Corporation (1996). *Environmental Scanning Electron Microscopy: An Introduction to ESEM®*. Robert Johnson Associates, Wilmington, Massachusetts.
- Gregg, S. J., and Sing, K. S. W. (1982). *Adsorption, Surface Area and Porosity* (2nd ed.). Academic Press Publishers, London.
- Grim, R. E. (1968). *Clay Mineralogy* (2nd ed.). McGraw-Hill, New York.
- Gypsum Project (The), Wilheims University (1996). Retrieved from <http://www.uni-muenster.de/Mineralogie/individuelle%20Forschungsvorhaben/brandt/gypsum.html>
- Head, K. H. (1992). *Manual of Soil Laboratory Testing: Volume 1, Soil Classification and Compaction Test* (2nd ed.). Wiley and Sons, New York.
- Hunter, D. (1988). "Lime-Induced Heave in Sulfate-Bearing Clay Soils." *Journal of Geotechnical Engineering*, Vol. 114, No. 2, ASCE, pp. 150-167.
- Inada, Y., Matsushima, A., Hiroto, M., Nishimura, H., and Kodera, Y. (1995). "Chemical Modification of Proteins with Polyethylene Glycols." *Advances in Biochemical Engineering/Biotechnology*, Vol. 52, Springer-Verlag, Berlin-Heidelberg.
- Joint Depts. of the Army and Air Force, USA (1994). *Soil Stabilization for Pavements*. TM 5-822-14/AFJMAN 32-1019, Washington, D. C., October 25.
- Juma, N. G. (1998). "The Pedosphere and its Dynamics: Mineralogy, 6.3 Clay Crystals." Retrieved October 19, 1998, from <http://www.soils.rr.ualberta.ca/pedosphere/content/section06/page03.cfm>.
- Keller, W. D. (1989). "Scanning Electron Micrographs of Clay Minerals Formed by Weathering and other Genetic Processes." *Weathering Processes*, Vol. 1, Theophrastus Publications, S.A., Greece.
- Klute, A. (1986). *Methods of Soil Analysis: Part 1, Physical and Mineralogical Methods* (SSA Book Series: 5). Soil Science Society of America, Inc., Madison, Wisconsin.
- Kota, P. B. V. S., Hazlett, D., and Perrin, L. (1996). "Sulfate-Bearing Soils: Problems with Calcium-Based Stabilizers." *Transportation Research Record 1546*, TRB, National Research Council, Washington, D. C., pp. 62-69.
- Loughnan, F. C. (1969). *Chemical Weathering of the Silicate Materials*. American Elsevier Publishing Company, Inc., New York.
- McBride, M. B. (1994). *Environmental Chemistry of Soils*. Oxford University Press, Inc., New York.

- Meyers, J. F., Pichumani, R., and Kapples, B. S. (1976). *Fly Ash as a Construction Material for Highways: A Manual*. Report No. FHWA-IP-76-16, FHWA, Washington, D. C., May, 198 pages.
- Mineral Powder Diffraction File Data Book (1980). *Joint Committee on Powder Diffraction Standards in Cooperation with American Society for Testing and Materials*. JCPDS International Centre for Diffraction Data, Newtown, Pennsylvania.
- Mitchell, J. K. (1986). "Practical Problems from Surprising Soil Behavior." *Journal of Geotechnical Engineering*, Vol. 112, No. 3, ASCE, pp. 259-289.
- Mitchell, J. K. (1993). *Fundamentals of Soil Behavior* (2nd ed.). John Wiley and Sons, Inc., New York.
- Mitchell, J. K., and Dermatas, D. (1992). "Clay Soil Heave Caused by Lime-Sulfate Reactions." *Innovations and Uses for Lime, STP 1135*, ASTM, Philadelphia, Pennsylvania, pp. 41-64.
- Moore, D. M., and Reynolds, R. C. (1997). *X-Ray Diffraction and the Identification and Analysis of Clay Minerals* (2nd ed.). Oxford University Press, New York.
- Olson, R. E. (1974). "Shearing Strengths of Kaolinite, Illite, and Montmorillonite." *Journal of Soil Mechanics and Foundations Div.*, ASCE, Vol. 100, No. GT11, pp. 1215-1229.
- Olson, R. E., and Mesri, G. (1970). "Mechanisms Controlling Compressibility of Clays." *Journal of Soil Mechanics and Foundations Div.*, ASCE, Vol. 96, No. SM6, pp. 1863-1878.
- Petry, T. M. (1997). "Performance-Based Testing of Chemical Stabilizers." *Transportation Research Record 1589*, TRB, National Research Council, Washington, D. C., pp. 36-41.
- Petry, T. M., and Das, B. (2001). "Evaluation of Chemical Modifiers/Stabilizers for Chemically Active Soils – Clays." *Transportation Research Record 1757*, TRB, National Research Council, Washington, D.C., pp. 43-49.
- Randolph, R. B. (1997). "Earth Materials Catalyst Stabilization for Road Bases, Road Shoulders, Unpaved Roads, and Transportation Earthworks." *Transportation Research Record 1589*, TRB, National Research Council, Washington, D. C., pp. 58-63.
- Rollings, R. S., Burkes, J. P., and Rollings, M. P. (1999). "Sulfate Attack on Cement-Stabilized Sand." *Journal of Geotechnical and Geoenvironmental Engineering*, Vol. 125, No. 5, ASCE, pp. 364-372.
- Santoni, R. L., Tingle, J. S., and Webster, S. L. (2002). "Stabilization of Silty-Sand with Nontraditional Additives." *Transportation Research Record 1787*, Paper No. 02-3756, Transportation Research Board, Washington, D. C., pp. 61-70.
- Sarkar, S. L., Herbert, B. E., and Scharlin, R. J. (2000). "Injection Stabilization of Expansive

- Clays Using a Hydrogen Ion Exchange Chemical.” *Advances in Unsaturated Geotechnics, Proceedings of Geo-Denver 2000*. ASCE, GSP No. 99, August, pp. 487-516.
- Sawyer, C. N., and McCarty, P. L. (1978). *Chemistry for Environmental Engineering*. McGraw-Hill, New York.
- Scholen, D. E. (1992). *Non-Standard Stabilizers*. Report No. FHWA-FLP-92-011, FHWA, Washington, D. C., July, 113 pages.
- Scholen, D. E. (1995). “Stabilizer Mechanisms in Nonstandard Stabilizers.” *Proceedings of 6th International Conference on Low-Volume Roads*, Vol. 2, TRB, National Academy Press, Washington, D. C., pp. 252-260.
- Sherwood, P. T. (1962). “Effects of Sulfates on Cement and Lime Stabilized Soils.” *Highways Research Board Bulletin 353*, pp. 98-107.
- Transportation Research Board Committee on Lime and Lime-Fly Ash Stabilization (1987). “Lime Stabilization: Reactions, Properties, Design, and Construction.” *State of the Art Report 5*, TRB, National Research Council, Washington, D. C., 59 pages.
- Uchino, T., Sakka, T., Hotta, K., and Iwasaki, M. (1988). “Attenuated Total Reflectance Fourier-Transform Infrared Spectra of Hydrated Sodium Silicate Glass.” *Journal of American Ceramic Society*, Vol. 72, No. 11, pp. 2173-2175.
- United States Environmental Protection Agency (2002). "SW-846, Test Methods for Evaluating Solid Waste, Physical/Chemical Methods." Retrieved from <http://www.epa.gov/epaoswer/hazwaste/test/main.htm>.
- Whittig, L. D., and Allardice, W. R. (1986). *X-Ray Diffraction Techniques*. American Society of Agronomy, Madison, Wisconsin.